## AD NUMBER

AD903971

## NEW LIMITATION CHANGE

TO

Approved for public release, distribution unlimited

FROM

Distribution authorized to U.S. Gov't. agencies only; Test and Evaluation; 13 Oct 1972. Other requests shall be referred to U.S. Army, Frankford Arsenal Attn:SMUFA-L3300, Philadelphia, PA 19137.

## AUTHORITY

FA, D/A ltr, 9 Oct 1974

Litton

DATA SYSTEMS

# FINAL REPORT
# SUPPLEMENT TO PARAMETRIC STUDY OF ADVANCED FORWARD AREA AIR DEFENSE WEAPON SYSTEM (AFAADS)
## VOLUME III, EFFECTIVENESS

15 September 1972



Submitted to:
U. S. Army, Frankford Arsenal SMUFA-L3300
Bridge and Tacony Streets
Philadelphia, Pennsylvania 19137

Prepared Under Contract: DAAG05-70-C-0328

Prepared by:
Data Systems Division
Litton Systems, Inc.
8000 Woodley Avenue
Van Nuys, California 91409

TD 20871

# ACKNOWLEDGEMENTS

Litton is happy to acknowledge the excellent guidance provided on this contract by Mr. Walter Ryba, contract technical supervisor, and the substantive contributions made by Mr. Stanley Goodman in the simulation development.

# FOREWORD

This report describes the research effort of the Data Systems Division of Litton Industries, Inc. under Supplemental Agreement 2 to Contract DAAG05-70-C-0328, with the U.S. Army, Frankford Arsenal. The objective was to provide additional analytic and simulation effort in support of the parametric analysis of predicted fire air defense weapon systems.

The report is presented in three volumes. Volume I, Analysis, by Herbert K. Weiss, reports the analysis effort and the simulation results. Volume II, Simulation Model, by Martin P. Ginsberg, describes the Litton Air Defense Simulation, designed by Mr. Ginsberg. The results of the simulation are included in Volume I. Volume III, Effectiveness, by Herbert K. Weiss, reports on methods of evaluating overall system effectiveness.

In the present report, frequent reference is made to the Final Report on the original contract. The previous report, titled Final Report, A Parametric Study of Advanced Forward Area Air Defense Weapon System (AFAADS) (two volumes), dated 2 October 1970, Revised Edition 1971, is referred to throughout this report as the "AFAADS-I Report."

# TABLE OF CONTENTS

TABLE OF CONTENTS (Continued)

## TABLE OF CONTENTS (Continued)

## LIST OF ILLUSTRATIONS

## LIST OF ILLUSTRATIONS (Continued)

## LIST OF TABLES

# SECTION 1
# INTRODUCTION

## 1.1 AFAADS SYSTEM EFFECTIVENESS MODEL

This report is concerned with the estimation of the effectiveness of systems for defense against low altitude air attack. The estimation and evaluation process involves many factors, of which only a part are amenable to modelling, mathematical analysis and computer simulation. The factors which must be evaluated by military judgement are at least as important as those which may be compared analytically.

The object of system modelling is to provide a means for analyzing those system characteristics which, within reasonable expenditures of time and effort, may be compared analytically, thus reducing the number of factors which must be evaluated by judgement in making decisions. In the last several decades the ability of system modelling to thus support the decision maker has progressively improved. However as models become more complex they reach a point (often exceeded in practice) beyond which the marginal improvement in validity of representation is small compared with the increase in complexity of the model.

Modelling does have the unique advantage that if the analyst does his job well, he is forced to accumulate a great deal of relevant real life information from which to derive his model parameters. This information, the identification of significant system parameters, and the general structuring of the problem can be as helpful to the decision maker as the model results themselves.

Although this report is directed to effectiveness modelling of predicted fire (unguided weapon) systems for defense against low altitude attack, most of the concepts and methodology apply to guided missile systems for operation in the same altitude region, as well.

# SECTION 2
# SUMMARY

The effectiveness model for evaluation of predicted fire air defense systems, as developed in this report, consists of a series of sub-models, each of which can be worked through analytically. Neither the time nor the resources allocated to this effort allowed consideration of development of a computer simulation at this time, although the sub-models can be computerized and probably improved thereby.

## 2.1 PRINCIPAL SUBMODELS

There are four principal submodels which perform the following functions:

a. *Battlefield Day Model.* From this model one obtains the availability/dependability (RAM) estimates of a system under evaluation.

b. *Raid Model.* From this model one obtains the effect of enemy extended strike patterns and tactics on the fire versus reload cycle of the weapon system.

c. *Engagement Model.* From this model (which may be used in conjunction with the Litton engagement simulation) one obtains estimates of desired weapon firing time to enter model (2) and estimates of damage and destruction to the attacking aircraft and defended target to enter model (4).

d. *Overall Effectiveness Model.* The results of a, b, and c are combined into an overall effectiveness estimate. It is argued however, that rather than attempt to obtain a single effectiveness number over all possible enemy attack options, the evaluation should recognize that enemy options will be influenced by defense effectiveness, and so a set of results should be displayed showing defense effectiveness and cost to the enemy for enemy options arranged in order of increasing cost to him.

The procedural flow of an analysis is outlined in Figure 2-1.

The present study does not undertake to develop costing methods. It is suggested however, that RAM objectives for a system should be set independently of overall effectiveness objectives, on the grounds that a system with low availability will never be a good military choice, even though its effectiveness when working is so high that its availability x effectiveness is superior to that of a competitive system with high availability and lower effectiveness. On this basis, it is suggested that in the complete cost and effectiveness evaluation of a system, it should be assigned the costs of whatever maintenance support is required to attain some specified (high) availability level. The comparative effectiveness of two systems will then be in the ratio of 'all up' effectiveness, but the cost of ownership will vary with the difficulty of attaining the specified availability level.

In this report, numerical values have been used to illustrate the use of the models, and parameter values have been chosen to be roughly representative. However, no great effort has been made to choose most probable values, and those associated with particular equipment types are subject to errors of source or interpretation. In addition no attempt has been made to use the same parameters across all examples.

The numerical exercises snould therefore be considered as illustrative of how the models can be used, rather than as definitive comparisons of system types.

## 2.2 OVERVIEW OF THE REPORT

The functions and missions of air defense systems are described as a preliminary to model development in Sections 3 through 6. It is pointed out in Section 5 that any system development should be paralleled throughout its life cycle by model development both to provide a concise, up to date, representation of expected or actual system capability, and to provide the data on which to base evaluations of new systems.

A comprehensive summary and review of the design and performance characteristics of predicted fire air defense systems is provided in Section 7. This has the purpose of indicating trends in system characteristics, and indicating what range of parameters may be included in model development.

Section 8 identifies the description of a typical 'Battlefield Day' as an essential step in system evaluation. The Battlefield Day provides a basis for relating availability and dependability estimates to tactical and operational conditions, and in particular, identifies tactical system states.

Subdivision of a complete system into subsystems for further analysis is described in Section 9. This subdivision assists in designating system operational states, and the alternate operational modes which may be considered.

Methods for computing system availability and dependability are developed in Section 10. It is shown that by combining the tactical states of the Battlefield Day and the operational states in which the system may have various levels of capability, the product of the availability/dependability matrices of the WSEAIC scheme is obtained. That is, for the combat substate, a vector is derived, defining the probability that the system will be in each of its possible operational states during combat.

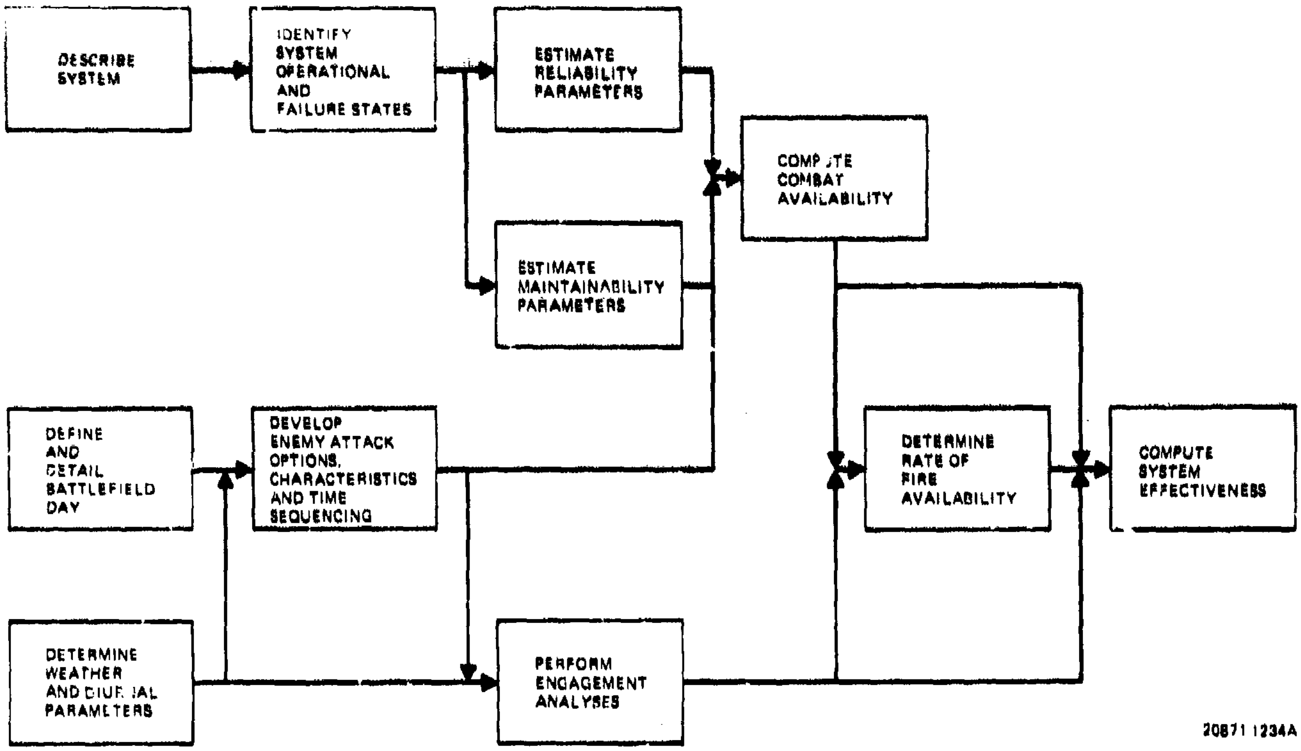


Figure 2-1. Procedural Flow of Effectiveness Analysis

In this section the argument is presented that the analysis can be greatly simplified on the assumption that no system will be acceptable for combat use unless it has a high availability. If it has a high availability, multiple failure modes will have a low probability, compared with single failure modes. If only single failure modes need be considered the analysis simplifies by several orders of magnitude, and relatively simple methods of computation are adequate.

Reload times for most modern predicted fire systems are long compared with the time required to exhaust the ammunition load at the weapon's maximum rate of fire. How important reload time is depends on the enemy attack pattern and time sequencing. The state space models of Section 9 and 10 are extended in Section 11 to include reload rate versus rate of fire and a few engagement parameters in order to examine these factors. The result is an estimate of the probability that the weapon will be in an ammunition availability state during an engagement. However this sub-model is too crude in the form presented for detailed engagement analysis.

Engagement analysis is developed as a separate sub-model in Section 12. A number of simple graphs and nomograms are provided for initial estimates of target exposure range, visual detection range, and for projectile exterior and terminal ballistics. Two simple analytic engagement models are developed, one for evaluation of the defense fire unit against a dive bombing target, and one for its effectiveness against a passing jinking target. It is pointed out that the Litton simulation for predicted fire systems has a comprehensive capability for engagement analysis allowing evaluation of a wide variety of prediction algorithms, weapon and projectile characteristics, target types and paths. Some simulation results are introduced to show consistency with the simple but more limited analytic models.

There is no reason that the analytic models of this report cannot be included in a computer simulation, and it would be interesting, and probably desirable to do this. However predicted fire systems development leading to prototype demonstration, in the opinion of the present writer, should not be delayed pending the completion of additional studies, analyses, and simulation developments.

Combination of the sub-model results to obtain an overall measure of effectiveness if developed in Section 13. It is emphasized that enemy attack options will vary with defense capability, so that analyses must consider the defense capability against a range of attacker's options. A defense can be effective if it denies an enemy the utilization of his most numerous and least expensive aircraft, and munitions types, even if by its presence it prevents attack and so destroys no aircraft, or if is relatively ineffective against a smaller

number of much more expensive enemy aircraft with costly sophisticated weapons.

Section 13 argues that instead of averaging defense effectiveness over all possible attack modes and conditions, the presentation of results should show effectivenss against a set of enemy attack options of progressively increased cost. At each level the damage inflicted by the enemy and to the enemy would be compared.

The use of air defense weapons against ground targets is discussed in Section 14. It is argued that although this capability should be provided as far as possible, it should not be allowed to prejudice the defense capability against air targets, and should be a consideration, but not a decisive factor in system selection.

A deficiency in the models presented, as in the case of most weapons evaluation models is that it has not been possible to compare them against real data to determine whether they capture the essential parametric interrelationships of the systems they purport to represent. The deficiency will not be eliminated by computer simulation. The lack of data for verification will, however, be remedied if the suggestions of Section 3 on 'Life Cycle Modelling' are followed.

# SECTION 3
# FUNCTIONS OF LOW ALTITUDE AIR DEFENSE SYSTEM

The functions performed by the predicted fire systems considered in this report are relatively simple. They are shown in Figure 3-1. The systems must acquire and fire effectively at enemy aircraft. When assigned to the protection of other combat units on the move they must have mobility equal to that of the supported units. Their capability at night or in inclement weather must bear some correspondence to the enemy capability to attack effectively under the same conditions. They must have satisfactory reliability, resistance to enemy countermeasures, and the maintenance burden associated with them must be acceptable. On occasion they may be required to engage enemy ground targets.

It is assumed that the predicted fire systems here considered operate as a part of a larger air defense system complex which includes manned interceptor aircraft and area defense surface to air missile artillery capable of reaching to very high altitudes. The operation of the low altitude defense systems is an integrated part of the complete air defense complex, with which it is coordinated, with which it must communicate, and from which it receives command, control, and alerting instructions. The low level coverage of the area missile defense is an important factor in determining the altitude and range coverage desired of the predicted fire weapons.

At the time of writing, however, the information received from the air defense net by short range fire units is limited, and the early warning information received by Vulcan and Chaparrel type weapons from FAAR radars and displayed on TADD devices is relatively coarse grain. Once a target appears within range of the low altitude defense firing section, the section operates autonomously within the established doctrine of fire.

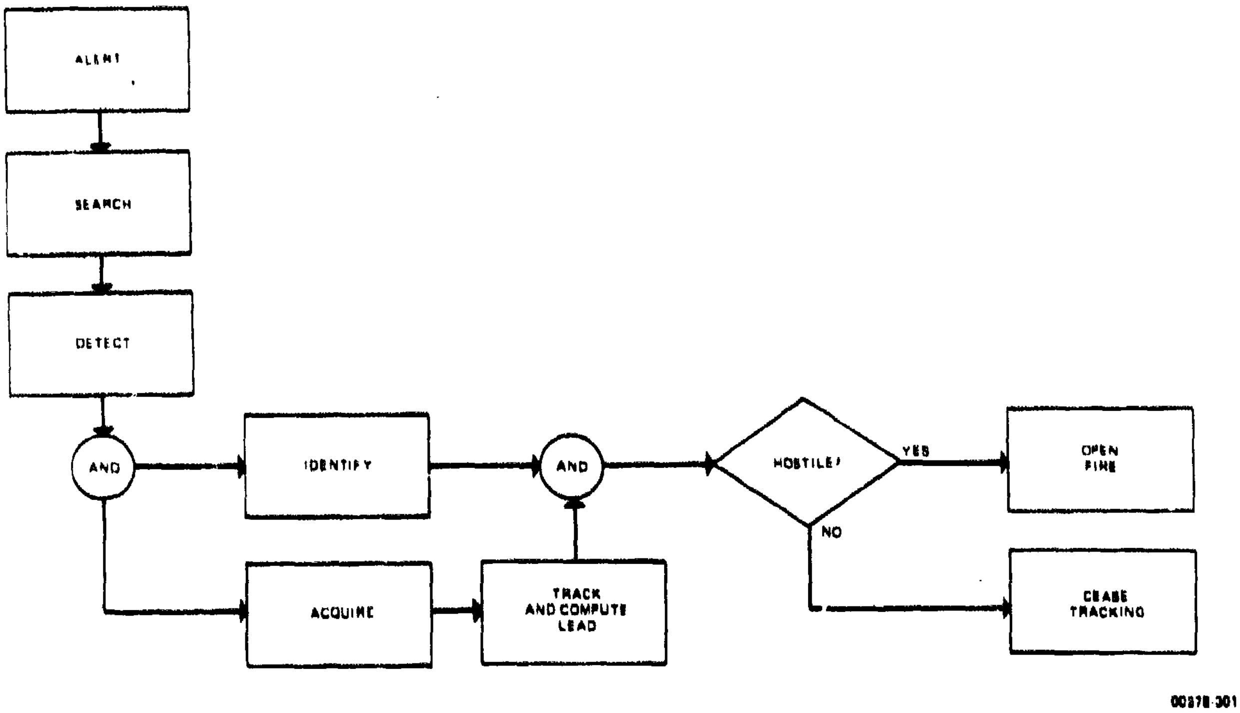


Figure 3-1. Functions Performed by Predicted Fire Air Defense System

## SECTION 4
## GENERAL APPROACH TO MODEL DEVELOPMENT

For any military system to come into being, there must be both a mission which it is required to perform, and a means for performing the mission. The means may be a 'system' consisting of equipment, manpower, and operational procedures. The modelling therefore begins with the definition of the mission and the alternate means of accomplishing it.

The description of the system includes the functional relationships among system elements and characteristic performance parameters. At this stage the parameters imply effectiveness, but are not yet interrelated to explicate how they contribute individually and together to overall system effectiveness. Such parameters may include fire unit weight and dimensions, gun rate of fire, muzzle velocity and caliber, projectile type, fuzing and filler, vehicle power/weight ratio, etc. More complex but critical descriptors include the prediction algorithms of the fire control system, the transfer functions of the gun and tracker servos, and the interrelationship of the operator capability with the functions he is required to perform.

The most important phase of model development is the attempt to integrate these performance parameters into a measure of system ability to perform its mission. This measure has, by convention, come to be called 'capability'.

Capability, however, is not achieved unless the system works when it is needed. The major achievement of the WSEAIC line of model development to date has been the systematization of considerations of system reliability, maintainability and availability, (RAM), in a generic form in which they can be quantified and combined with capability measures to provide overall estimates of system effectiveness.

When the RAM elements are used to estimate the probability that the system will be operable when required to perform a mission, at a random point in time, the result is called 'availability'. When they are used to estimate the probability that the system will function successfully during a mission the estimates are called 'dependability'.

The distinction between 'availability' and 'dependability' is sharpest when a system such as an aircraft is under evaluation. Then 'availability' refers to the state between missions, when the system is relatively unstressed, and repairs and maintenance can be carried out. 'Dependability' then refers to the state during a mission, which may be of extended length, compared with system component failure rates, and during which only limited repairs may be performed.

In the case of a ground based air defense system, 'missions' occur at the enemy's option, and are characterized by individually brief durations of combat, during which the system is highly stressed, and by varying intervals between combats, or engagements, during which there may or may not be time to perform repair and maintenance. These interactions tend to cause the distinction between 'availability' and 'dependability' to be less well defined.

In the present report, an attempt has been made to include both combat and non-combat states in a stochastic model, the solution of which gives the probability of state availabilities during combat and during non-combat directly.

# SECTION 5
# LIFE CYCLE OF THE DEFENSE SYSTEM AND LIFE CYCLE OF THE MODELLING PROCESS

The information available for system modelling, and the amount of detail which should reasonably be incorporated in the model depend on the life cycle phase of the system or systems under consideration. The use for which the model is intended will also depend on the phase.

The relationship of model elements to phase of system life is indicated in Table V-1.

It would seem useful to maintain a continuous modelling activity associated with each system throughout the system life cycle. This is apparently being done more frequently with time, as opposed to past efforts consisting of ad hoc systems analysis with little continuity, activated by crises and terminated when the fire was put out.

Aside from the advantages indicated in the table, of assisting in program management, such a sustained effort, coordinated among parallel system developments, provides a continuously improving body of data which facilitates and improves the validity of analyses of new systems.

The parallel development of system and model is indicated in Figure 5-1. The process forces the model to progressively conform more closely to an accurate description of the real system performance. This interaction may be valuable insurance against the retention of erroneous model concepts and their propagation into evaluations of new systems.

**Table V-1. Tasks Required to Evaluate System Effectiveness and Application by Phase of System Life**

| Task | Phase of System Life | | | |
|---|---|---|---|---|
| | Conceptual | Definition | Acquisition | Operational |
| Mission Definition | Derived from established need or requirement. Broad range of threat, descriptive environment. | Added detail to assist system design, specific threat and environment. | Change only for unforeseen technical or threat changes. | Change only for unforeseen technical or threat changes. |
| System Description | Block diagram with major system elements, simplified mission description. | To major hardware end items; modes of operation; mission time line (geodesic). | Complete detail to piece part identification available; operations plan and maintenance task analysis available. | Complete descriptive information on all hardware, procedures, operation and maintenance schedules, logistics plans available. |
| Specification of Figures of Merit | Overall figure(s) of merit for complete system. | A, D, C elements defined at least at system levels with conditions and units of measurement. | A, D, C elements defined at systems, subsystems, equipment, module, piece part levels. | No change except to evaluate system in new environment or against new threat. |
| Identification of Accountable Factors | Define to system functional block diagram level. Initial rough estimates. | Define to principal end items; skill levels of personnel, maintenance policies, environment. | Define to module or part level, detail support and operating environments, identify new factors based on experience during development. | Identify changes in accountable factor list based on operating experience. |
| Model Construction | Comparatively simple model. | Detail to principal system hardware elements; submodels for subsystems, submodels for matrix and vector elements. | Increased detail to level required for program control, design changes management decisions. | Detail relaxed and/or aggregated to match information from Army and other service supporting systems. |
| Data Acquisition | • Generic data.<br>• Results from similar systems.<br>• Basic physical laws. | • More intensive exploitation of sources in prior phase. | • Proofing and category tests at system and equipment levels.<br>• Extensive in-process tests of assemblies and parts. | • Actual operating, failure and maintenance data. |
| Parameter Estimates | Predicted | Predicted | Refined from incoming data. | From actual system data. |
| Model Exercise | Sufficient exercise to determine probability of major improvement over alternate operations (or not). | Lively exercise in configuration optimization and major element choice. | Exhausting exercise to maintain effectiveness assurance control over system design and production. | Intermittent exercise to monitor status, support product improvement studies. |
| Applications | • Decision to proceed to definition phase. | • Choice of major system elements.<br>• Choice of configuration.<br>• Optimization of configuration. | • Subsystem tradeoffs<br>• Component and part tradeoffs<br>• Suboptimizations<br>• Measure achievement of specified overall effectiveness<br>• Form basis for program management action. | • Design changes<br>• Product improvement<br>• Modification of support/logistics<br>• Force structure decisions<br>• Determination of obsolescence against changing threat. |

20871-597A

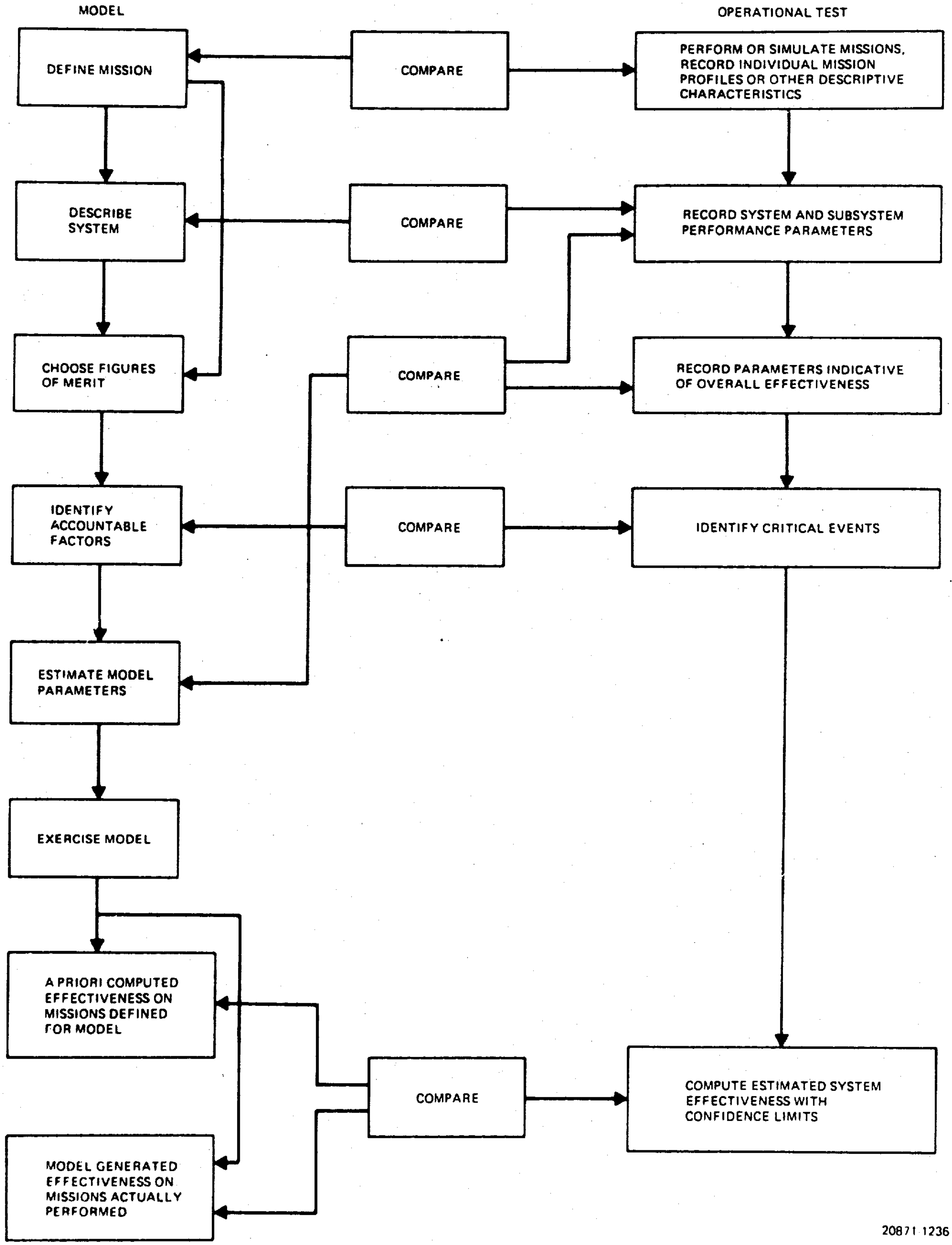


Figure 5-1. Comparison of Model to Operational Data

# SECTION 6
# MISSIONS OF AIR DEFENSE SYSTEMS

## 6.1 OVERALL AIR DEFENSE MISSION

The overall air defense mission is to destroy hostile aircraft and missiles, or to nullify or reduce their effectiveness. In forward area air defense, the air defense forces have the objective of limiting the effectiveness of enemy air efforts to a level permitting freedom of action of friendly forces of all types.

The overall air defense system is composed of a mix of manned interceptors and ground-based air defense artillery weapons.

The ground-based air defense may be composed of several weapon system types including ground to air missiles and predicted fire systems (guns or unguided rockets).

## 6.2 MISSIONS OF LOW ALTITUDE AIR DEFENSE SYSTEMS

Low altitude air defense systems may include both guided missiles (such as Chaparral) and automatic weapons (such as Vulcan). These may be categorized as 'guided missile systems' and 'predicted fire systems'. The latter category then includes predicted fire unguided rocket systems such as Javelot.

The missions of predicted fire systems may be further detailed as:

a. *Limited area defense.*

b. *Vital area defense.*

c. *Small unit defense.* This includes defense in position and on the move.

d. *Ground support.* Use of predicted fire air defense weapons against ground targets is a secondary mission.

## 6.3 INTERRELATIONSHIPS AMONG AIR DEFENSE SYSTEM COMPONENTS

The function of manned interceptors and area defense surface to air missiles is to project the air defense to high altitude and over enemy dominated terrain.

Terrain variations limit the area coverage of a long range surface to air missile fire unit against very low flying aircraft, and low altitude air defense systems provide a complementary capability to complete the defense coverage economically. In addition they allow augmentation of the overall defense effectiveness in the immediate vicinity of vital areas and ground units exposed to enemy air attack while in motion.

## 6.4 ORGANIZATION

Organizations of typical air defense organizations as well as more detailed discussion of missions and interactions with threat characteristics were presented in the AFAADS-I report, to which reference is made.

# SECTION 7
# GENERAL CHARACTERISTICS OF PREDICTED FIRE AIR DEFENSE SYSTEMS

To provide a context for system evaluation a brief review of trends in threat characteristics, and predicted fire unit characteristics is informative in defining the range of conditions and relevant parameters for consideration in the evaluation.

The discussion of defense system trends is based on a comparison against threat changes. It provides a basis for a judgemental answer to the question, 'Has the defense capability kept up with the increase in threat capability?'

## 7.1 CHANGES IN THE THREAT

Some of the changes in the threat presented to low altitude air defense systems over the years are the following:

a. *Target speed.* Aircraft speed has increased steadily with time, although the increase at low altitude has been less rapid than the increase at high altitude. Some targets flying in excess of Mach 1 can be reasonably expected.

b. *Terrain following.* 'Contour chasing' has always been a tactic for postponing detection by the defense until the defense reaction time exceeds the target exposure time. As speed increases, terrain following requires automatic equipment in the aircraft, but in addition to shortening the exposure time, conformity to terrain causes the aircraft to fly an irregular and less predictable flight path.

c. *'Free maneuver' bombsights.* Fire control for unguided air launched munitions is available which allows the aircraft to maneuver moderately during the approach, with a very short interval of constrained flight to match the sight index at weapon release.

d. *Night and all-weather attack capability.* Sensors are available to allow the aircraft to locate and attack its target at night and in bad weather when the target cannot be acquired visually. In addition, bombing under remote control of a ground radar has been available since World War II.

e. *Stand-off Weapons.* Air to surface weapons with various forms of terminal guidance are available, which allow the aircraft to launch outside the effective defense zone of local defenses, or, at most, to make a minimal penetration of the defense. In recent months, air to surface weapons with terminal guidance have demonstrated accuracies in combat operations in Southeast Asia which suggest that they may represent the lowest cost method of destroying small, hard targets such as bridges by air attack, even in the absence of air defense.

f. *Use of Helicopters and VTOL Aircraft.* The low speed of the helicopter allows it to approach using maximum terrain cover, hover for release of weapon and withdraw quickly, with minimum exposure. The difficulty of detecting its approach from a ground site approaches the difficulty of detecting the approach of a ground vehicle. The VTOL type of aircraft may introduce similar problems for the defense.

g. *Reduction in aircraft vulnerability to hits.* Very high speed aircraft are designed for higher stresses than low speed aircraft. Although it is known that even the fastest modern aircraft have (rarely) been brought down by rifle fire, it is conjectured that on the average the probability that a hit of a specified caliber will bring down an aircraft has decreased slowly over the years. It could be reduced even more drastically by special attention in the design stage to vulnerability.

Note that all of the 'improvements' which make the threat more difficult to deal with tend to increase the cost of the aircraft and its munitions. In the absence of air defense the enemy can use relatively inexpensive delivery vehicles and munitions. Since it is unlikely that his full force will have all-weather and other expensive capabilities, a local air defense can restrict his attack options.

## 7.2 TRENDS IN PERFORMANCE OF PREDICTED FIRE SYSTEMS

Some of the most conspicuous descriptors of antiaircraft gun systems are:

a. Caliber.

b. Rate of fire.

c. Number of guns on mount.

d. Muzzle velocity.

e. Time of flight to specified range (or range to sonic projectile velocity).

f. Angular tracking error.

g. Range tracking error.

h. Maximum angular velocity of tracking/gun laying.

i. Maximum angular acceleration of tracking/gun laying.

j. Tracking sensor types and characteristics.

k. Prediction error against 'typical target' (a very ill-defined index).

l. Type of mount (towed, self-propelled).

m. Principal tracking mode (manual or automatic).

n. Fire Control Computation

(1) Inputs used.

(2) Data smoothing, prediction and other computational algorithms.

o. Method of surveillance, and initial target detection.

p. Type of IFF.

q. Fire unit weight (in firing position, in travel position).

r. Transport or tow vehicle (wheels or tracks).

s. Stabilization.

The way in which some of these descriptors have varied with time in response to the changing threat is sketched below. In addition, the interrelationship with threat capability is indicated. A simple combat situation is used for reference.

To avoid dealing in generalities, data on specific predicted fire systems is presented where it is available. The data is put in tabular form so that the reader can fill in missing entries, or correct those which may have been erroneously given in sources available to the writer.

### 7.2.1 Tactical Situation

Consider the idealized situation of Figure 7-1, which depicts an aircraft flying a low level pass over a defended target using a 'laydown', or retro-fired weapon, or conducting a strafing attack. This type of attack is considered by one analyst to be the only one possible for a manned aircraft in a European combat environment where

'The British view on both dive and toss bombing is that both methods are too dangerous for use in Europe as any aircraft that gains any height at all will almost certainly be shot down. Their policy for a European war is therefore to use the laydown method whenever possible.'[1]

The objective of the defense is to destroy the aircraft before it reaches the point of munitions release.

We consider this generic type of engagement in a historical context, with the maximum aircraft speed increasing progressively over the years.

### 7.2.2 Angular Velocity and Acceleration Requirements

To maintain its capability against ever faster targets, the ability of the defending fire unit to track and aim its weapons is associated with increasing requirements for maximum angular velocity and acceleration. If the minimum crossing range is kept constant, the maximum angular velocity is proportional to target velocity, and the maximum angular acceleration is proportional to velocity squared. The torque required to rotate the mount is proportional to angular acceleration (inertia) and angular velocity squared (friction), hence to target velocity squared. The power to drive the mount is proportional to torque multiplied by angular velocity, hence to target velocity cubed.

The power required by the aircraft to achieve a given sea level velocity increases about as its velocity cubed at least to about Mach 0.9. Over the years reduction in aircraft drag coefficient has tended to counterbalance the effect of drag rise at sonic speeds, so that in fact as maximum sea level velocity has increased, aircraft power has increased as about the cube of velocity.

It is interesting that the antiaircraft fire unit must therefore have a peak power capability for tracking directly related to the propulsive power of its target.

The ability of manually powered mounts to provide this power has long been passed. Table VII-1 provides a brief comparison of some obsolescent and current power driven antiaircraft gun mounts.[8,9] Note in particular the 120°/second maximum angular traverse velocity of the modern Oerlikon twin-35 mm turret.

### 7.2.3 Reaction Time

Referring to the situation figure, it is assumed that the target exposure distance $X_e$, and the distance from first exposure to weapon release are terrain dependent. It is also assumed that the provision of terrain following radar and control equipment in the aircraft have allowed it to fly at increasing speed without increasing its minimum altitude above terrain.

Any extension of the detection, identification and acquisition interval will shorten the firing interval. However, human reaction times have not shortened over the years. The shortening of this phase of system reaction time has been approached by:

a. Provision of a separate surveillance radar and a device on the fire unit designating target azimuth and range to the human operator (U.S. Vulcan/FAAR radar with TADD).

b. Surveillance radar on the fire unit with automatic target detection, threat evaluation and turret positioning in azimuth with subsequent acquisition and tracking visually by the gunner. (French twin 30-mm turret on AMX chassis with Oeil Noir radar.)

c. Provision of a surveillance radar on the mount with automatic detection (if desired) and alarm, IFF, and automatic acquisition of the target by

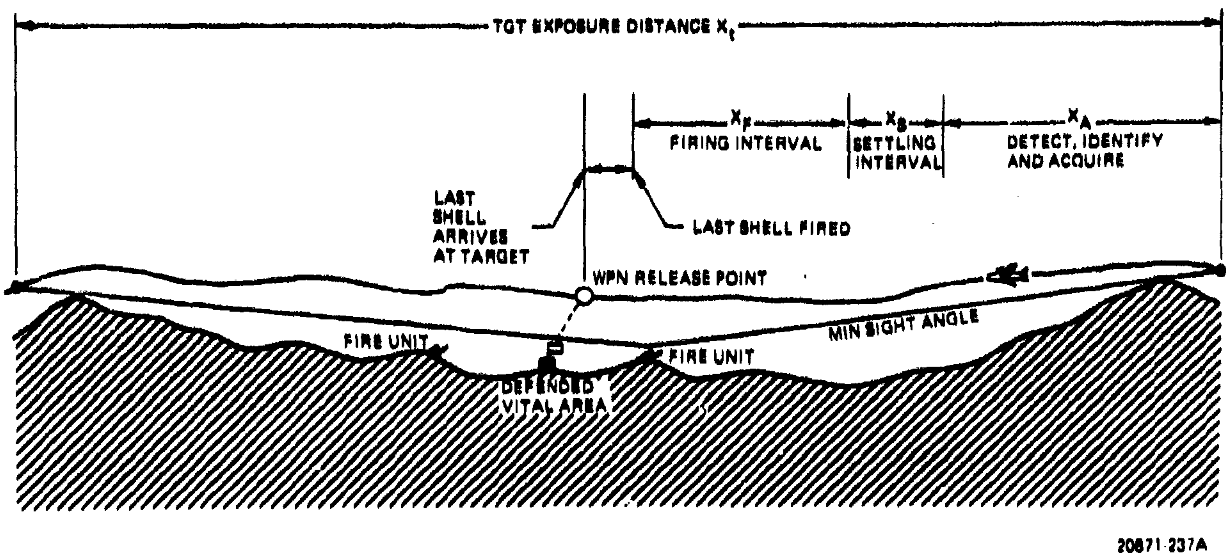


Figure 7-1. Event Sequence in Defense Against Laydown or Retro Weapon Delivery

an on-mount tracking radar. (Swiss Oerlikon/Contraves 5PFZ systems.)

d. Off carriage vehicle or vehicles with search and track radars fire control to direct several guns at the same target. (Netherlands: Signall L4/5 system; French: Eldorado-Mirador system; Swiss: Skyguard, successor to Superfledermaus.)

e. Separate vehicle with surveillance radar, track while scan capability on 12 targets, IFF, automatic track initiation option, automatic threat evaluation and assignment to best sited fire unit, and automatic target acquisition by radar on assigned fire unit (automatic/manual modes in all cases). (French Crotale. This surveillance unit is intended for use with missile fire units but the problem is identical for predicted fire weapon target acquisition.)

Reaction time from target appearance to acquisition by the tracker of the fire unit should shorten generally as one moves down this list. However, many current systems such as the British Falcon and the light Rheinmetall twin 20-mm, and some of the light Hispano Suiza mounts perform the detection, identification and acquisition process with the Mk I eyeball and the relatively invariant time required will cause the acquisition interval to seriously encroach on the firing interval for these weapons.

### 7.2.4 Volume of Fire

For a given firing distance, the maximum number of rounds that can be fired depends on the ratio of rate of fire to target speed. To a limited degree an additional increase in rate of fire will compensate for a shortening of the firing distance caused by insufficient reduction in target acquisition time.

Figure 7-2 compares rate of fire on antiaircraft automatic weapons and guns plotted against caliber, with two bands identifying World War II designs and current designs. For single tube weapons available rate of fire in a given caliber has increased at about the same rate as maximum sea level speed of fixed wing aircraft.

In addition, the Gatling design allows a compact installation with weight and space savings over a multiple gun installation of the same caliber and total rate of fire. The Mauser revolver mechanism (not plotted) delivers with two tubes a performance between that shown for the 6 barrel Gatlings and the single tube weapons. At present it is used only in aircraft installations.

In general, increase in available rate of fire in any given caliber has at least matched the increase in maximum aircraft velocity at low altitude.

Table VII-1. Angular Velocity and Acceleration Capabilities of Fire Units

| Vintage | Obsolescent | | Current Army | | | | Current Navy | | |
|---|---|---|---|---|---|---|---|---|---|
| Designation | M45 | M42 Duster | Vulcan | Rheinmetall RH 202 Mk 2 | Bofors | Falcon (British) Vickers/Hispano | British Hispano | Swiss GDM-A | Bofors |
| Mount | towed | SP | towed | towed | SP | SP | turret | turret | turret |
| Weapon | quad 0.50 | twin 40 mm | 20 mm Gatling | twin 20 mm | twin 40 mm | twin 30 mm | twin 30 mm | twin 35 mm | single 40 mm |
| Maximum Angular Velocity (deg/sec) | | | | | | | | | |
| Azimuth | 60 | 40 | 60 | 100 | 85 | 80 slew<br>40 track | 90 | 120 | 85 |
| Elevation | 60 | 25 | 45 | 55 | 45 | 40 | 60 | 100 | 45 |
| Maximum Angular Acceleration (deg/sec$^2$) | | | | | | | | | |
| Azimuth | | | 160 | | | 120 | | 160 | |
| Elevation | | | 160 | | | 120 | | 130 | |
| Power Requirement (KW) | | | 0.5 | | | | 10 max<br>2-4 av | 50 | 5 |
| Weight of Mount (kg) (firing position for towed mounts) | 1100 | | 1350 | 1450 | | | 1700 | 4800 | 1500-2700 |

20871-598

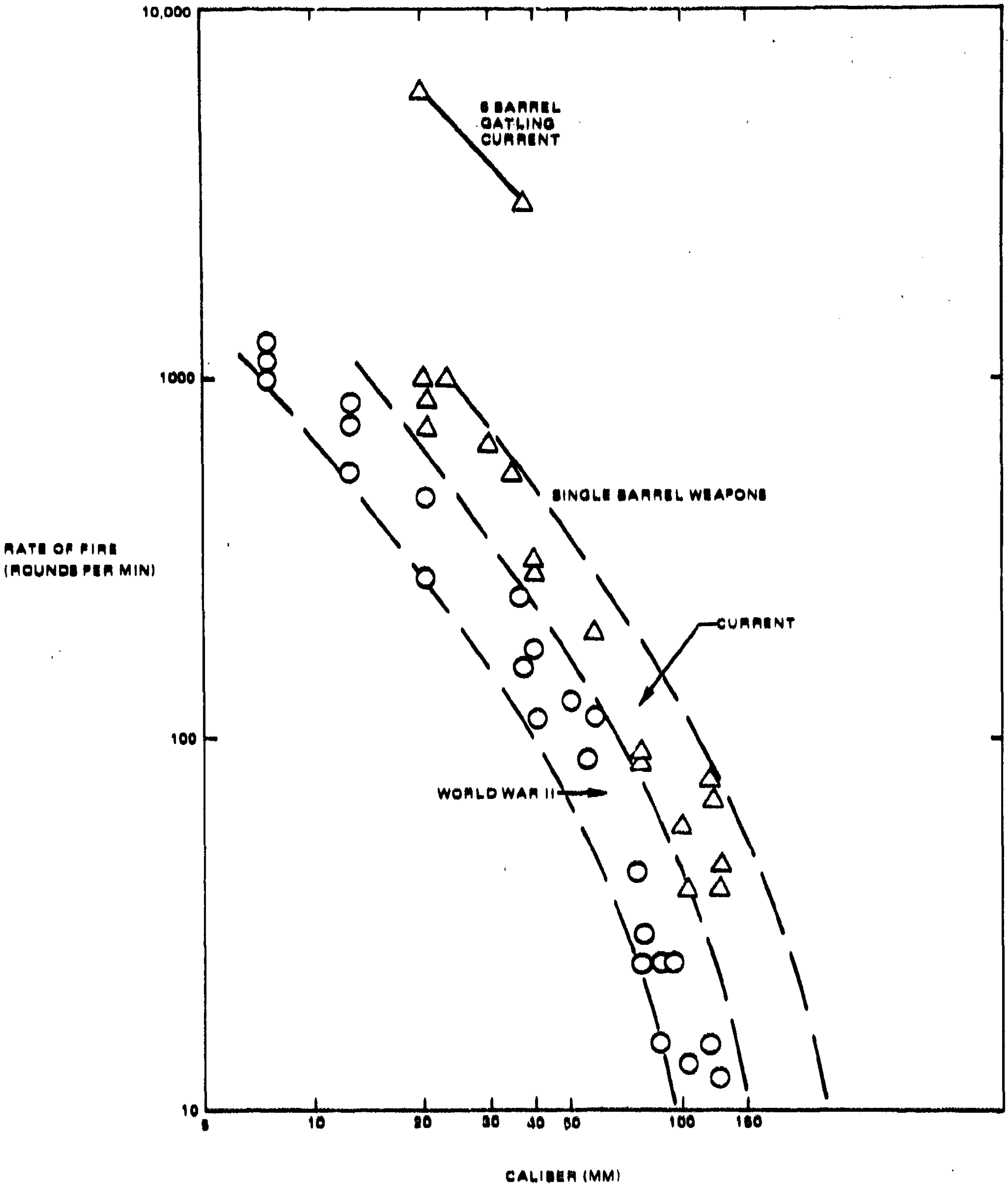


Figure 7-2. Rate of Fire Versus Caliber for Antiaircraft Guns

A problem generated by high rate of fire, however, is that of reload time for the ammunition feed system. This is discussed at length later in the report. Under sustained, multiple attacks with short intervals between attackers, reload time substantially reduces the firing rate averaged over many attacks. It appears that much of the gain in maximum rate of fire has been negated by a less than proportionate increase in rate of reloading.

### 7.2.5 Accuracy of Fire

The weapon characteristic with the highest payoff in terms of effectiveness is almost invariably accuracy. It is difficult to observe trends in accuracy because of the classification usually associated with this parameter and the consequent difficulty in locating and collecting data. Using this as an excuse we begin with information from the distant (and unclassified past) to observe that the antiaircraft predicted fire systems have in fact, over the years, been able to maintain and improve their accuracy with time against ever faster targets, provided only that in each era they used the best available technology.

Predicted fire requires present position data to begin with. Optical tracking has always been a means (in the early days the only means) of getting angular data, and subject to visibility limitations it has been good to excellent, except in those regions where high angular velocities and accelerations exceed the operator's ability. Range was obtained from multistation angular tracking in the beginning[4] (Figure 7-3) then from stereoscopic or coincidence optical range finders[4] (Figure 7-4) and in World War II by radar (Figures 7-5, 7-6), which also provided angular information that quickly became satisfactory as a fire control input.

With time fuzed ammunition, range errors were much more important than with impact or VT fuzes. The optical range finders developed range measurement errors of from 1 to 2% of range. Using this information however, against 100 mph targets in 1930, the predicted fire systems of that era developed vector errors of burst location of from 1.1 to 3.6% of range as shown in Table VII-2[11]. The adequacy of the fire control computation itself is indicated by the fact that azimuth error averaged from 4 to 10 mils.

In the same era, U.S. tests summarized in Table VII-3 indicated a mean absolute angular error of about 7 mils against 100 mph targets. The Aberdeen estimates were originally derived by tabulating absolute errors in firing azimuth and elevation against angular velocity and fitting a linear relation[4]. The maximum recorded angular velocity was about 32 mils per second. Target speed is believed to have been about 50 yards/sec, (100 mph). For an average shell speed of about 2000 f/s, maximum lead would have been about 75 mils, and so the above rate errors correspond roughly to 7 mils at midpoint, and less at angles off midpoint.

By World War II, both proving ground and combat data indicated that predicted fire systems could achieve 'standard angular errors' of about 6 mils at 5000 yards increasing both below and above that range as shown in Figure 7-7[3]. British data taken against the V-1 flying bomb indicated performance at the same range of from 9 to 14 mils. Errors at very long ranges against freely maneuvering targets were, of course, very large.

Figure 7-7 shows the 'standard angular error' in mils versus range of some of the best World War II medium antiaircraft gun systems. The data for the Army 90-mm and 120-mm weapons were derived from Artillery School firings at Fort Bliss at the close of the war, and the Navy data is estimated from 'splash' records of firings in combat in defense against Kamikaze aircraft.

Figure 7-8 shows data in comparable form for British systems. Firings against the V-1 'Flying Bomb' were with SCR-584 radar tracking, the No. 10 Predictor, and the British 3.7 inch Gun. The estimated curves were developed by an operational research group for defense planning with the 3.7 inch gun aginst conventional bombers. Note the very large errors recorded from ground plan plots of errors observed in firings with the 5.25-inch gun, GL-IIIB radar and No. 10 Predictor against freely maneuvering 'tip and run' raiders after the Battle of Britain.

In most of the plotted curves there is a tendency for the mil error to vary inversely with slant range at short ranges, so that the error in linear measure (such as yards) tends to be independent of range.

This appears to be a characteristic of the problem. When the target is close, both man and radar tend to wander over an area proportional to the target size. The error will increase at a far greater rate at short ranges if it is also associated with high angular derivatives of tracking. However, this source of degradation (minimal in the WW-II curves) can be minimized by regenerative tracking systems. Although planned for Vigilante, such regenerative assist is not now included in any U.S. Army design but is indicated to be used in the Super-Fledermaus, and possibly the Eldorado/Mirador equipment.

The convergence of optical tracking error to a linear magnitude at extremely short range and low angular tracking derivatives is demonstrated in Figure 7-9 developed from gun camera data on fighters in tail attacks on WW-II bombers[5]. The ordinate is the radius of the circle containing 50% of the measurements.

An impression of the improvement of angular tracking capability with time more indicative of short range capability is displayed in Figure 7-10. These are estimated for a target dimension of 20 meters perpendicular to the line of sight, and imply some data process-

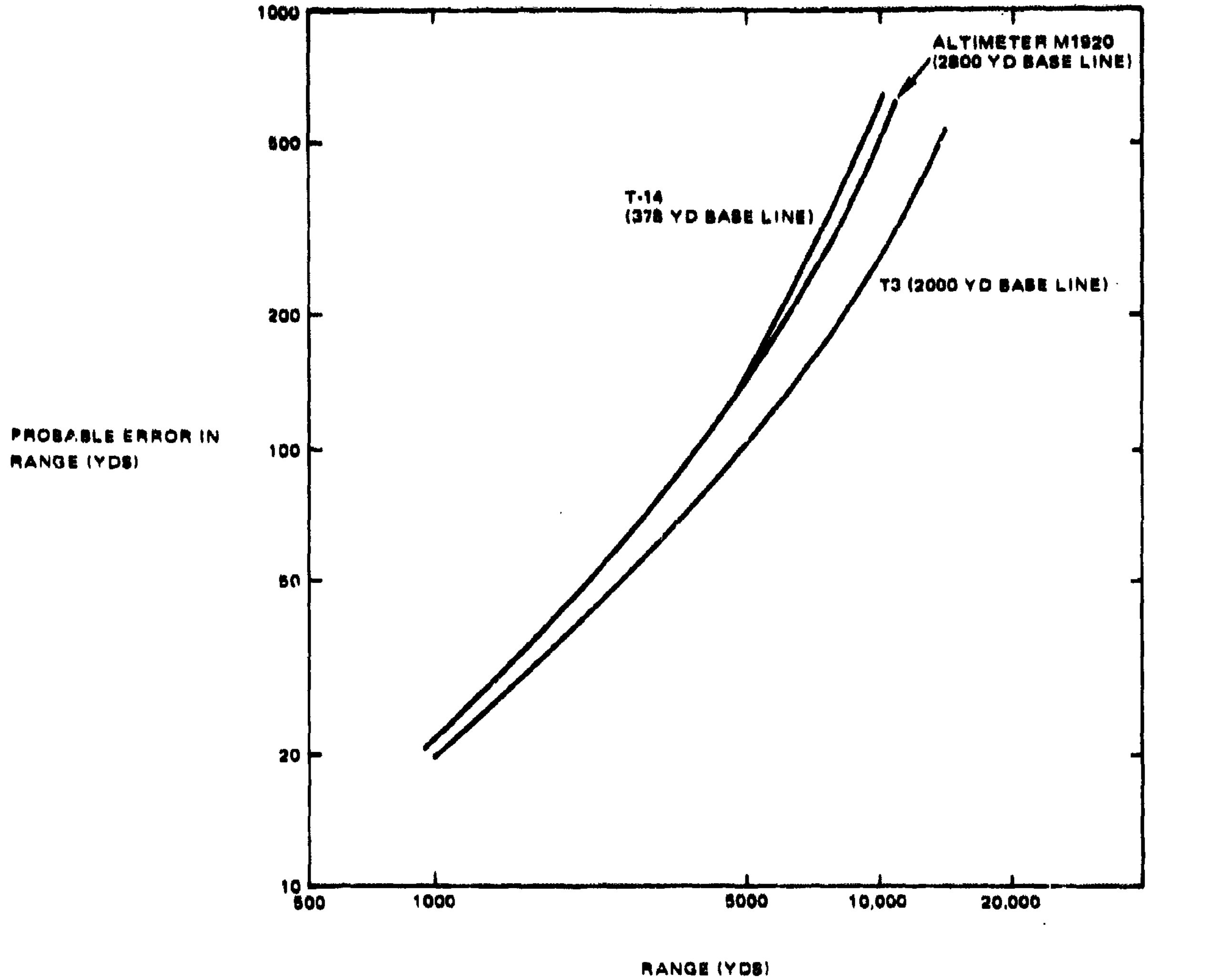


Figure 7-3. Errors of Multistation Optical Range Finding Systems (1937)

ing, the efficiency of which depends on the band width of the sensor error spectrum.

Operational accuracies of current systems can probably be found in the classified literature and will not be listed here. However, it may be noted that for antiaircraft fire, Vulcan has intentional artificial dispersion with a pattern 18 mils by 6 mils.

The published accuracy of the Swiss Super-Fledermaus is[8]

> '50% aiming error in tactical operation against fast flying jet aircraft less than 3 mils' (Complete system)

A report on the ARGO NA9 Fire Control system[8] for the Italian Navy states 'with a target approaching at speeds up to 1340 mph and an angular velocity of 6°/sec the average miss distance at ranges between 1000 and 4500 meters is of the order of 8 meters.' This corresponds to about 4 mils.

It seems reasonable to infer that using the best current technology a predicted fire system can be designed to perform against a target which is not deliberately evading with a CEP of no more than 3 mils at long ranges, or 3 yards at short ranges (i.e., better than 3 mils or 3 yards, whichever is least, range), and that, in fact, some current systems may already have this capability.

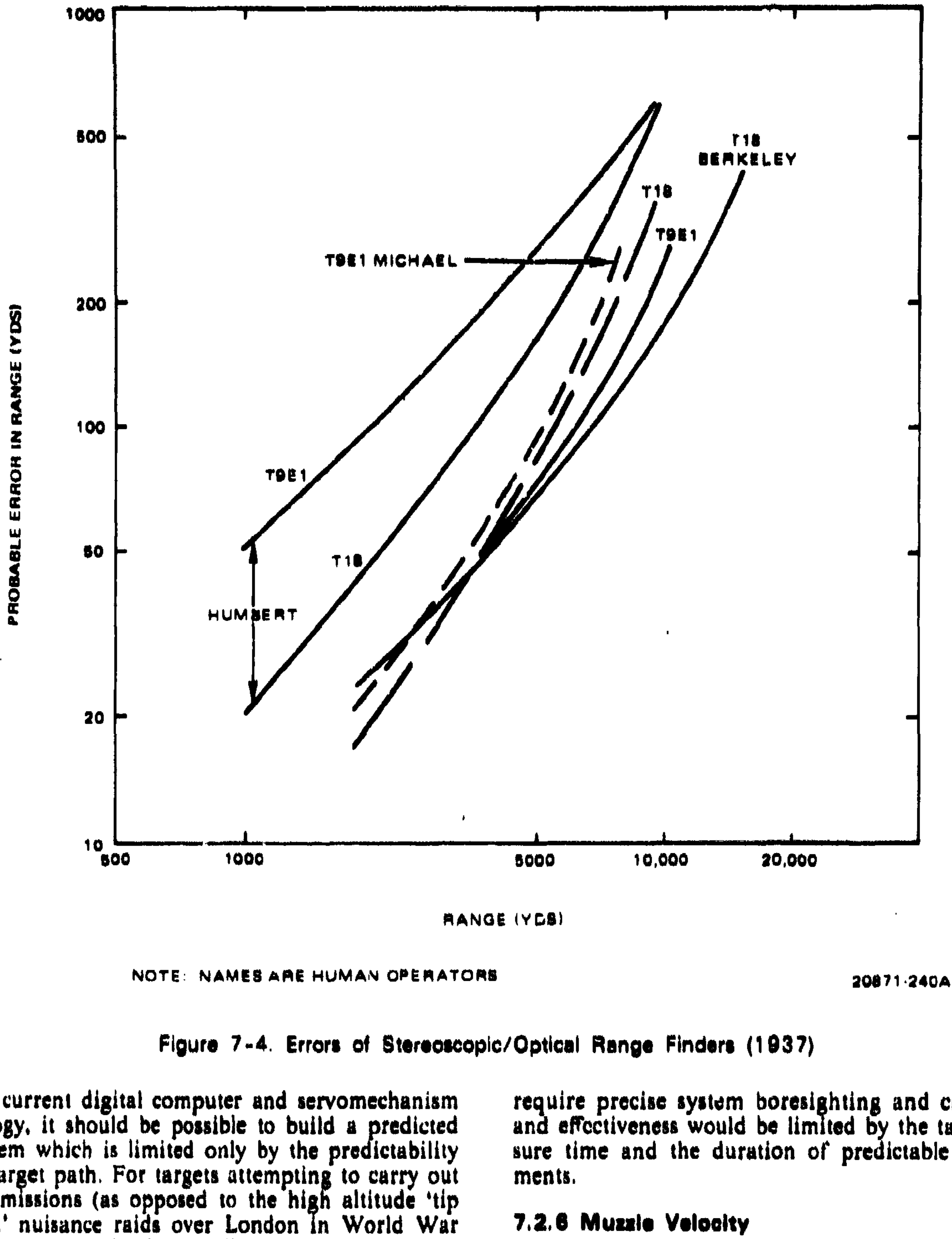


Figure 7-4. Errors of Stereoscopic/Optical Range Finders (1937)

With current digital computer and servomechanism technology, it should be possible to build a predicted fire system which is limited only by the predictability of the target path. For targets attempting to carry out tactical missions (as opposed to the high altitude 'tip and run' nuisance raids over London in World War II), this predictability is usefully high. Unfortunately no statistical data on targets on attack paths is at hand for display at this point.

An attempt has been made in Figure 7-11 to compare the growth in accuracy of predicted fire systems against targets which are neither intentionally 'jinking' nor attempting to fly a precise unaccelerated path. The curve represented by the 'best 1972 technology' would require precise system boresighting and calibration, and effectiveness would be limited by the target exposure time and the duration of predictable path segments.

### 7.2.6 Muzzle Velocity

Improvement in weapon muzzle velocity is a high payoff area for predicted fire weapons, provided that it is associated with excellent present position tracking information.

An approximate expression relating the variance of prediction error resulting from tracking error to variance of tracking error is

$$\sigma_p^2 = \sigma_t^2 \left[1 + 2t_p/T_s + 2(t_p/T_s)^2\right]$$

where

$t_p$ = time of flight

$T_s$ = data smoothing time. (7.1)

This is an upper limit. It should always be possible to do better than this.

Referring again to the situation representation of Figure 7-1, to keep the solution settling distance $X_s$ from expanding as target speed increases, settling time must be reduced in inverse proportion to target velocity. From the above equation, this can be accomplished without degradation of prediction error only if time of flight is shortened in the same proportion.

Although available muzzle velocity has increased steadily with time, its growth has not been proportional to target velocity. The trends are shown in Figure 7-12. Antiaircraft guns had muzzle velocities of about 2600 f/s as early as WW I. The highest current muzzle velocity is that of the Oerlikon 35-mm gun which is 3870 f/s.[8]

The possibility of firing sub-caliber projectiles at hypervelocities was explored intensively for large caliber antiaircraft guns during and subsequent to WW II but the development was terminated with the advent of the guided missile.

The maximum lead angle required of a predicted fire system occurs near minimum slant range and is given by

$$\sin\Delta = v/v_a \qquad (7.2)$$

where v is target velocity, and $v_a$ is average projectile velocity. The maximum lead angle required has increased steadily with time.

Since prediction error against a maneuvering target can increase with time of flight much more rapidly than the linear function indicated above for a non-maneuvering target, the payoff against even mild maneuvers for increased muzzle velocity is expected to be significant, as shown later in this report. The continued improvement of fire control systems in the aircraft itself will allow progressive freedom of maneuver even in delivering unguided munitions and this can best be countered by increased muzzle velocity, in the case of predicted fire weapons.

Consequently, it appears that a principal deficiency in improvement of antiaircraft gun capability with time has been the relatively slow increase in available muzzle velocity.

### 7.2.7 Exterior Ballistics

The ability of projectile designers to develop projectiles with excellent exterior ballistics has improved over the years, although this achievement is more difficult to display simply than in the case of maximum rate of fire, for example. Nevertheless this section attempts to summarize this improvement.

The design region in which the projectile designer can operate is limited, in the case of spinning projectiles, by the interactions of requirements that the projectile be stable, yet orient itself properly along a curving trajectory, with the projectile mass distribution and shape.

Rather undesirable exterior ballistic characteristics are sometime obtained when a projectile originally designed for some other application is used in an antiaircraft role to save ammunition development costs.

Exterior ballistic data from a number of sources[8,9] have been assembled in Table VII-4 to show time of flight versus slant range where available. The functional relationship between these quantities and quadrant elevation is not displayed. For a first order approximation, for most antiaircraft trajectories the reduction of air density with altitude and the projectile acceleration caused by gravity partly compensate for each other, so that except for very long ranges the elevation effect is second order.

For a given muzzle velocity, trajectory data tends to scale with the function $w_p/iC^2$; where $w_p$ = projectile weight, C = projectile caliber, and i = a form factor depending on shape. Hence, to allow data for a wide range of projectile calibers to be compared on a simple chart, time of flight and slant range have been divided by $w_p/iC^2$.

If projectiles were geometrically scaled with caliber, this term would be proportional to caliber. The degree to which projectiles depart from homologous scaling is indicated by the ratio $w_p/C^3$, and this index varies principally with the fraction of projectile weight devoted to high explosive or incendiary filler, and to a lesser degree with projectile shape. A rule of thumb estimate can be obtained from

$$\rho = (w_p/C^3)(10^4) \;;\; w_p \text{ in pounds, C in millimeters} \qquad (7.3)$$

$$\rho \cong 0.39\,(1 - 1.6\,f) \;;\; f = \text{fraction of weight devoted to filler} \qquad (7.4)$$

Since the supersonic drag coefficient decreases with increasing Mach number, the percent loss in projectile

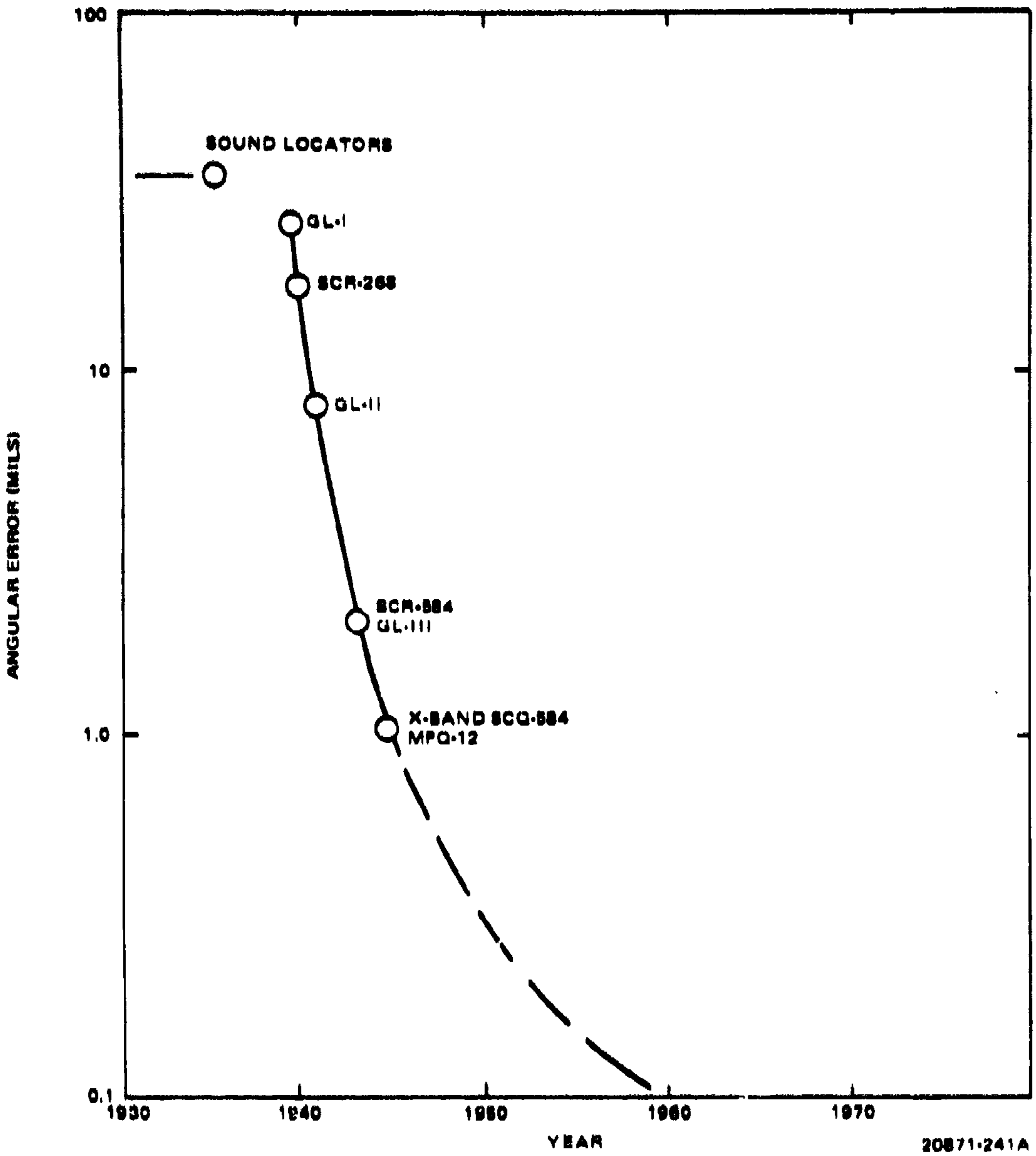


Figure 7-5. Reduction in Radar Angular Tracking Error with Time

velocity to a given range is slightly less for high muzzle velocities than for low. In the following comparison, the graphs are not normalized for this effect, but it should be kept in mind.

Normalization of the tabulated data is done in a form suggested by the simple expressions for square law drag, for which

$$V_r/V_o = e^{-k_1 D/(\rho C)} \tag{7.5}$$

$$k_1 V_o t_p/(\rho C) = e^{k_1 D/(\rho C)} - 1 \tag{7.6}$$

Where $V_r$ = projectile remaining velocity, $t_p$ = time of flight, D = slant range, and $k_1$ is a numerical constant, and $V_o$ = muzzle velocity.

Figure 7-13 compares remaining velocity as a fraction of initial velocity for several projectiles. This data

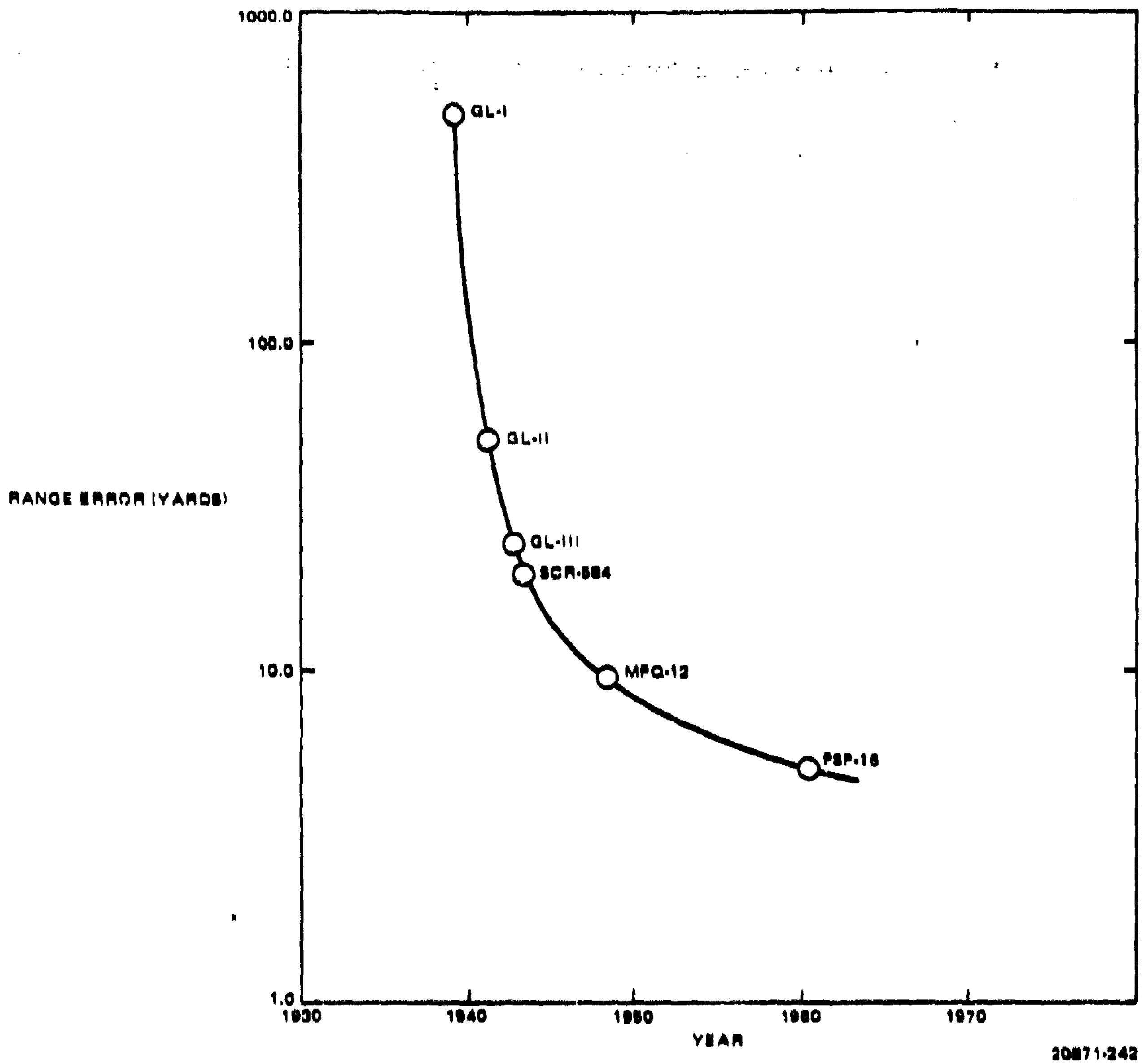


Figure 7-8. Reduction in Radar Range Error with Time

was replotted from graphs furnished by Frankford Arsenal. A portion of the very large difference between the Hispano Suiza and the M61 20-mm rounds in the original graphs is explained by the lighter weight of the M61. A small part of the remaining difference in Figure 7-13 may be explained by the higher muzzle velocity of the HS round, but the remainder suggests poorer than average shape, and possibly stability of the M61.

The very large difference between the original Vigilante round and that estimated in a design study of a new round is almost completely attributable to better shape (boat-tail) and omission of the rotating band.

The 35-mm Oerlikon round appears to have the best ballistics of any past or current antiaircraft projectile.

Time of flight and range are compared for those projectiles for which data is given in Table VII-4, in Figure 7-14. It is clear that for well designed projectiles, the time of flight/slant range relationship is almost completely determined by muzzle velocity, caliber and projectile weight, but that careful attention to drag may yield an additional 10 to 20% reduction in time of flight to ranges given approximately by

Range (kilometers) = Caliber (mm)/10

Table VII-2. Antiaircraft Firing Test Results at Toulon, France, 2-3 February 1932

| Fire Control | Gamma – Juhasz | | Schneider | | |
|---|---|---|---|---|---|
| Range Band (meters) or mean | Vector Error (meters) | Vector Error (% of range) | Vector Error (meters) | Vector Error (% of range) | Azimuth Error (Mils) |
| 2500-4300 | | | 88 | 2.6 | 5.3 |
| 2500 | 90 | 3.6 | | | |
| 3800-4600 | | | 63 | 1.5 | 9.5 |
| 4200 | 95 | 2.3 | | | |
| 4200-4800 | | | 112 | 2.5 | 4.2 |
| 4500 | 50 | 1.1 | | | |
| 5000-5600 | | | 133 | 2.5 | 5.3 |
| 5400 | 80 | 1.5 | | | |

NOTES: Target speed was "up to 50 meters/sec" (110 mph).

Target altitude was "up to 3000 meters".

20871-599

Table VII-3. Antiaircraft Fire Control Equipment Test Results at Aberdeen Proving Ground, 1933

| Director (Computer) | Mean Fractional Error in Angular Velocity |
|---|---|
| R. A. Corrector | 0.097 |
| T-8 (Sperry) | 0.099 |
| M1 (Vickers) | 0.101 |
| M1A1 (Vickers) | 0.123 |
| M2 (Sperry) | 0.166 |

20871-600

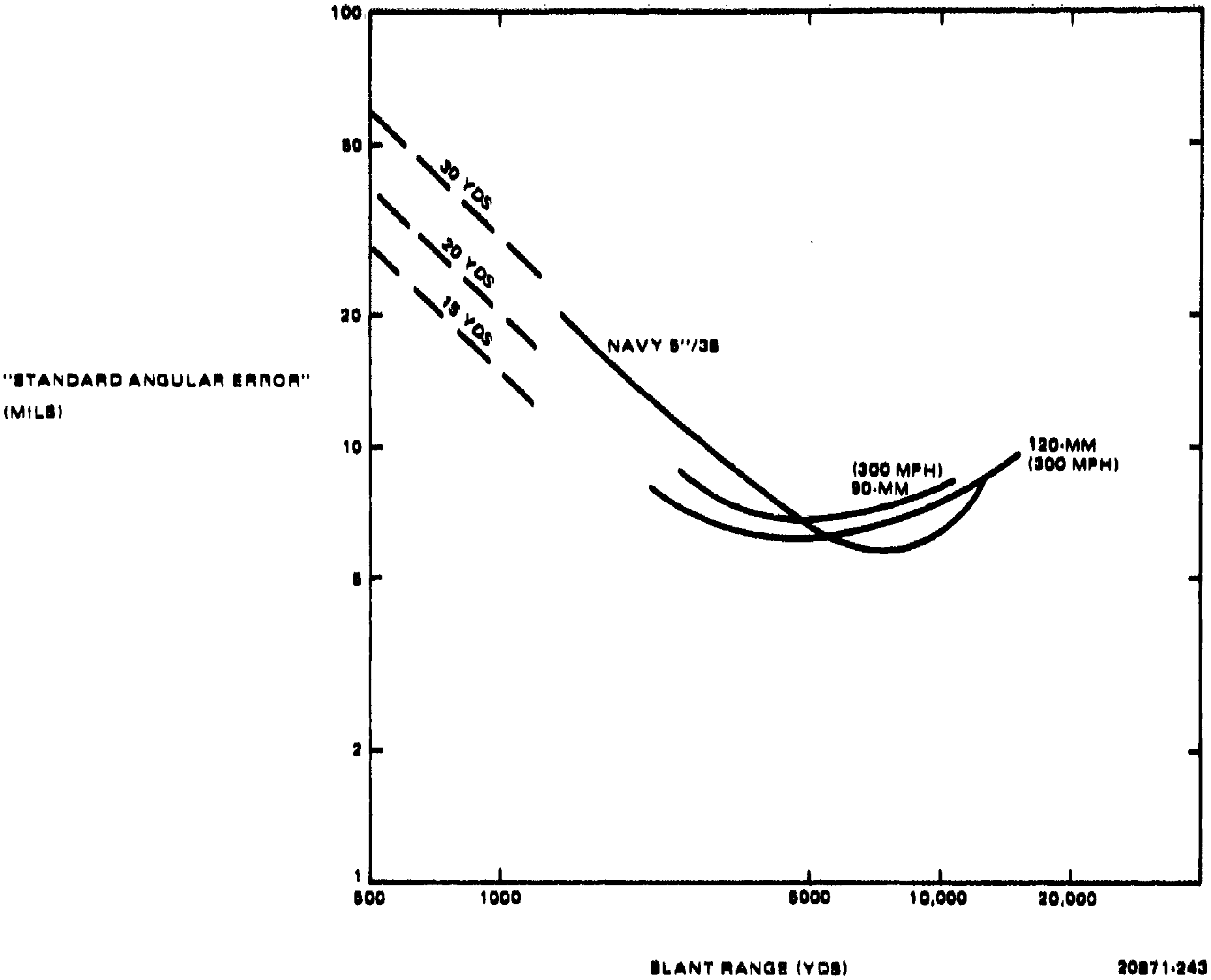


Figure 7-7. U.S. Antiaircraft Gun Performance, WW-II Period

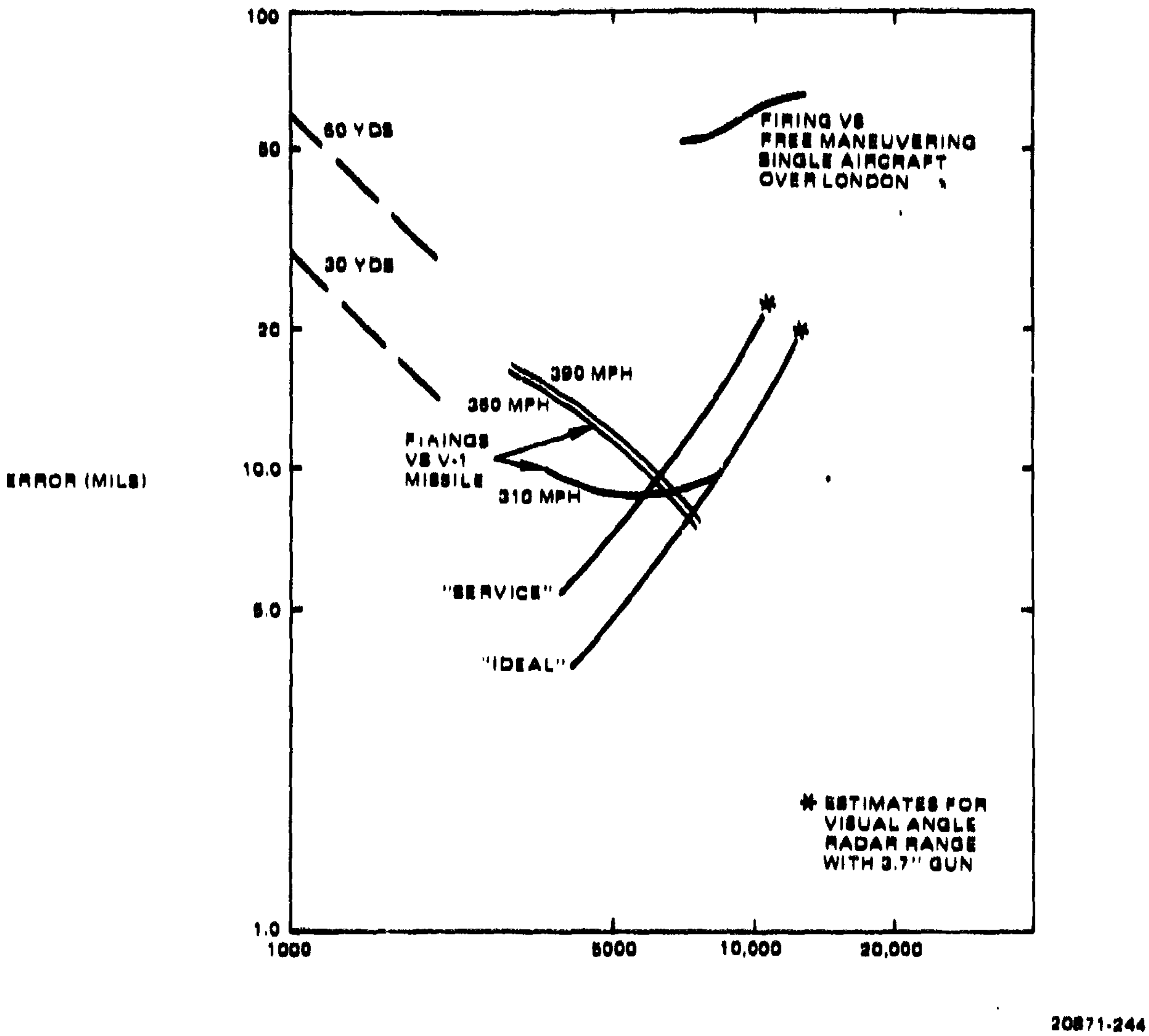


Figure 7-8. U.K. Antiaircraft Gun Performance, WW-II Period

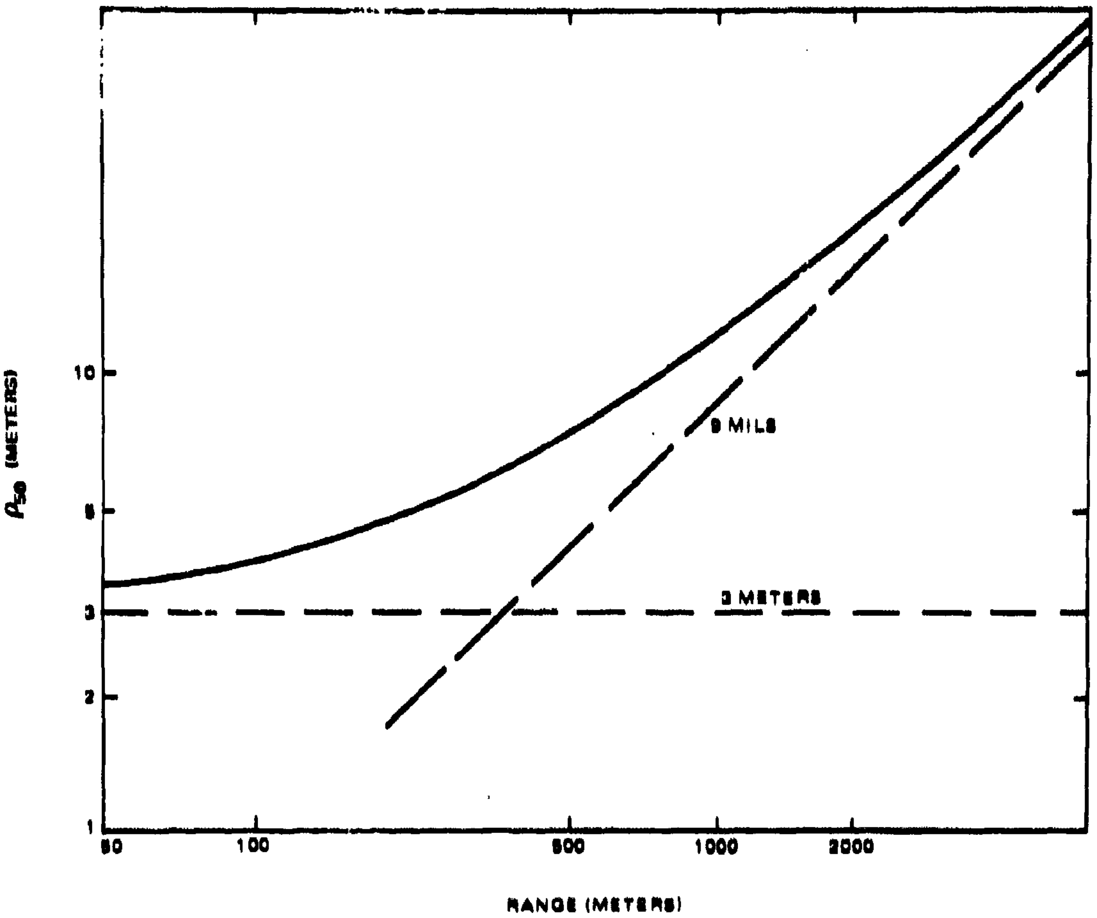


20871-245A

Figure 7-9. Aiming Accuracy versus Range for Fighter Aircraft (WW-II)

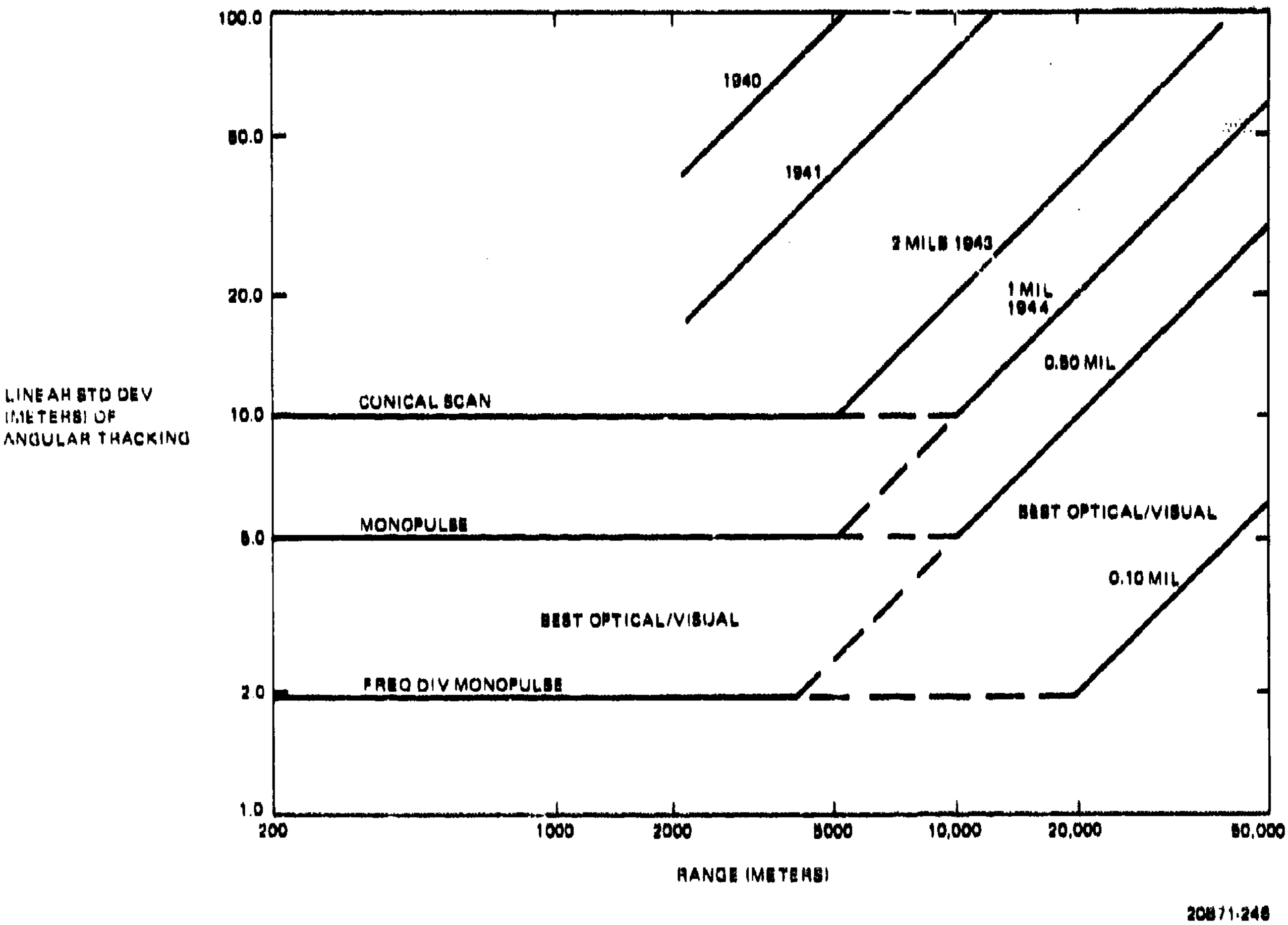


Figure 7-10. Radar Angular Tracking Error in Linear Measure at Target (Meters) versus Range

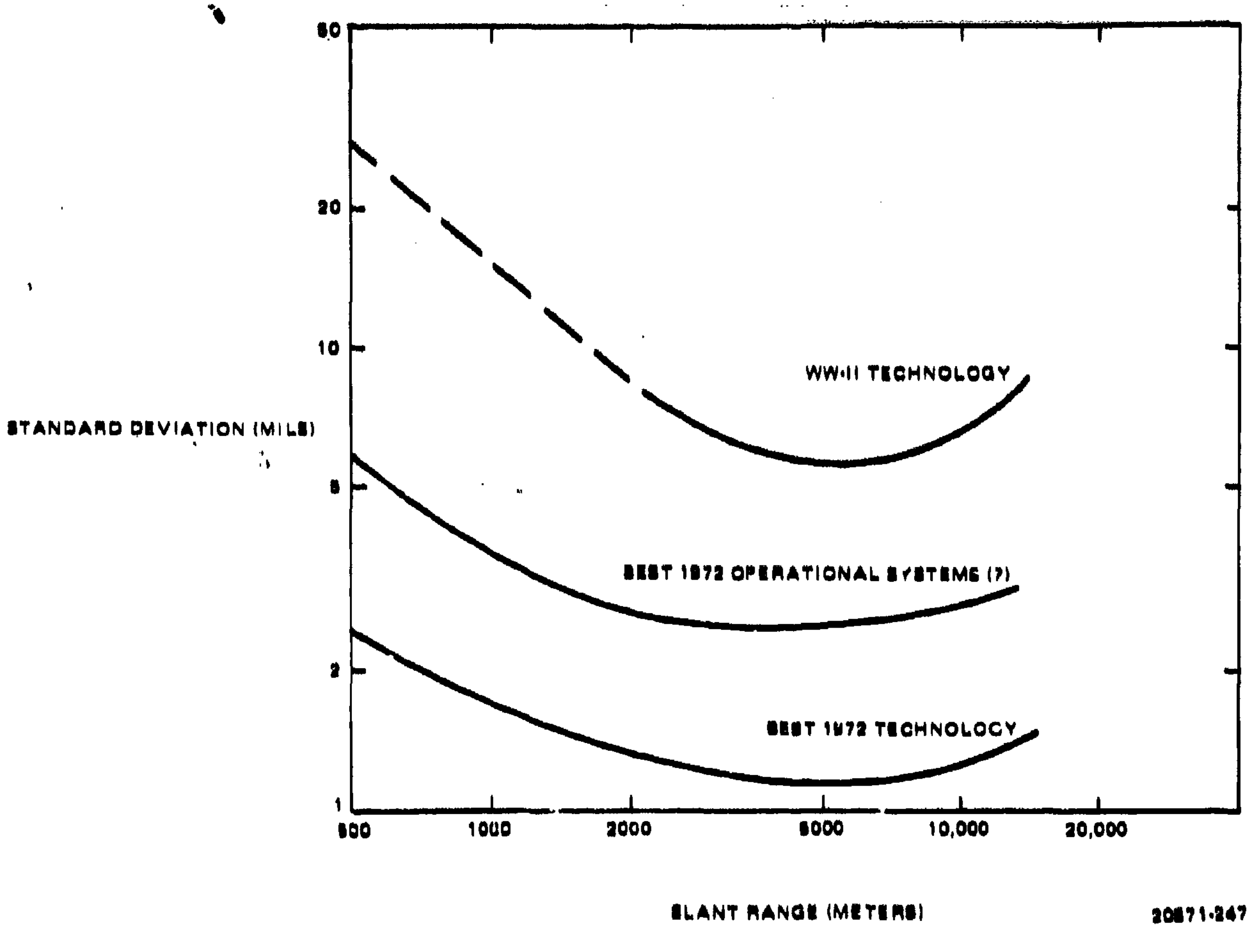


Figure 7-11. Estimated Growth in Accuracy of Predicted Fire Systems

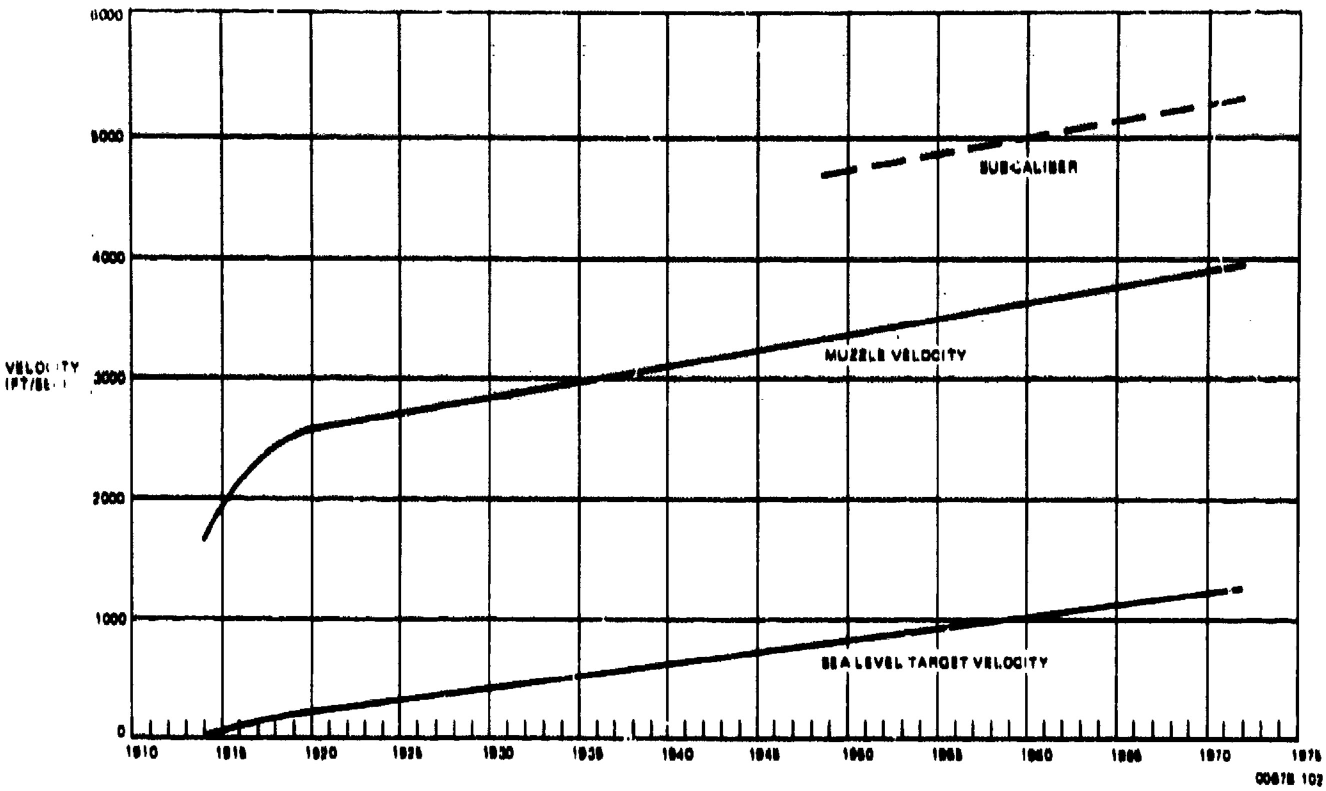


Figure 7-12. Increase in Target and Gun Velocity with Time

Table VII-4. Exterior Ballistic Data

| Caliber | Weapon or Proj. Model | Muzzle Velocity (meters/sec) | Projectile Weight (lbs) | Proj. Wt/Cal$^3$ (Lb/mm$^3$ x 10) | Time of Flight (sec) | Range (meters) |
|---|---|---|---|---|---|---|
| 20 mm | AME 621 | 1030 | 0.22 | 0.275 | 1.45 | 1000 |
| | RH 202 | 1070 | 0.268 | 0.335 | 1.4 | 1200 |
| | | | | | 3.4 | 2000 |
| | HS 820 | 1070 | 0.268 | 0.335 | | |
| | M61 | 1020 | 0.218 | 0.273 | | |
| 30 mm | HS 831 | 1070 | 0.93 | 0.345 | 1.07 | 1000 |
| | | | | | 4.51 | 3048 |
| 35 mm | Oerlikon L/90 | 1175 | 1.20 | 0.280 | | |
| 37 mm | Vigilante | 910 | 1.65 | 0.327 | 4.00 | 2414 |
| | | | | | 6.00 | 3109 |
| | | | | | 8.00 | 3694 |
| | | 1090 | 1.60 | 0.317 | 2.00 | 1792 |
| | | | | | 4.00 | 3072 |
| | | | | | 6.00 | 4023 |
| | | | | | 8.00 | 4755 |
| 40 mm | M2A1 | 875 | 1.96 | 0.307 | 2.0 | 1380 |
| | L/70 Bofors | 1005 | 2.15 | 0.335 | 2.4 | 2000 |
| | | | | | 8.0 | 4670 |
| 57 mm | L/70 Bofors | 1025 | 5.3 | 0.287 | 3.8 | 3000 |
| 76 mm | L/50 Bofors | 825 | 13.0 | 0.298 | 13.0 | 6000 |
| 88 mm | German WW-II | 820 | 19.8 | 0.290 | 6.52 | 4000 |
| | | | | | 11.62 | 6000 |
| | | | | | 18.22 | 8000 |
| | | | | | 26.22 | 10,000 |
| 90 mm | M2, WW-II | 855 | 23.4 | 0.320 | 3.9 | 2740 |
| | | | | | 7.2 | 4560 |
| | | | | | 20.2 | 9140 |
| | | | | | 28.0 | 11,000 |
| 120 mm | M1A3, WW-II | 945 | 50.0 | 0.289 | 3.5 | 2740 |
| | | | | | 6.0 | 4560 |
| | | | | | 12.5 | 8200 |
| | | | | | 16.5 | 10,100 |
| | | | | | 21.1 | 11,900 |
| | | | | | 26.8 | 13,700 |
| | | | | | 29.8 | 14,600 |
| | L/46 Bofors | 800 | 46.3 | 0.268 | 21.7 | 10,000 |
| | L/50 Bofors | 900 | 46.3 | 0.268 | 19.0 | 10,000 |

20871-601

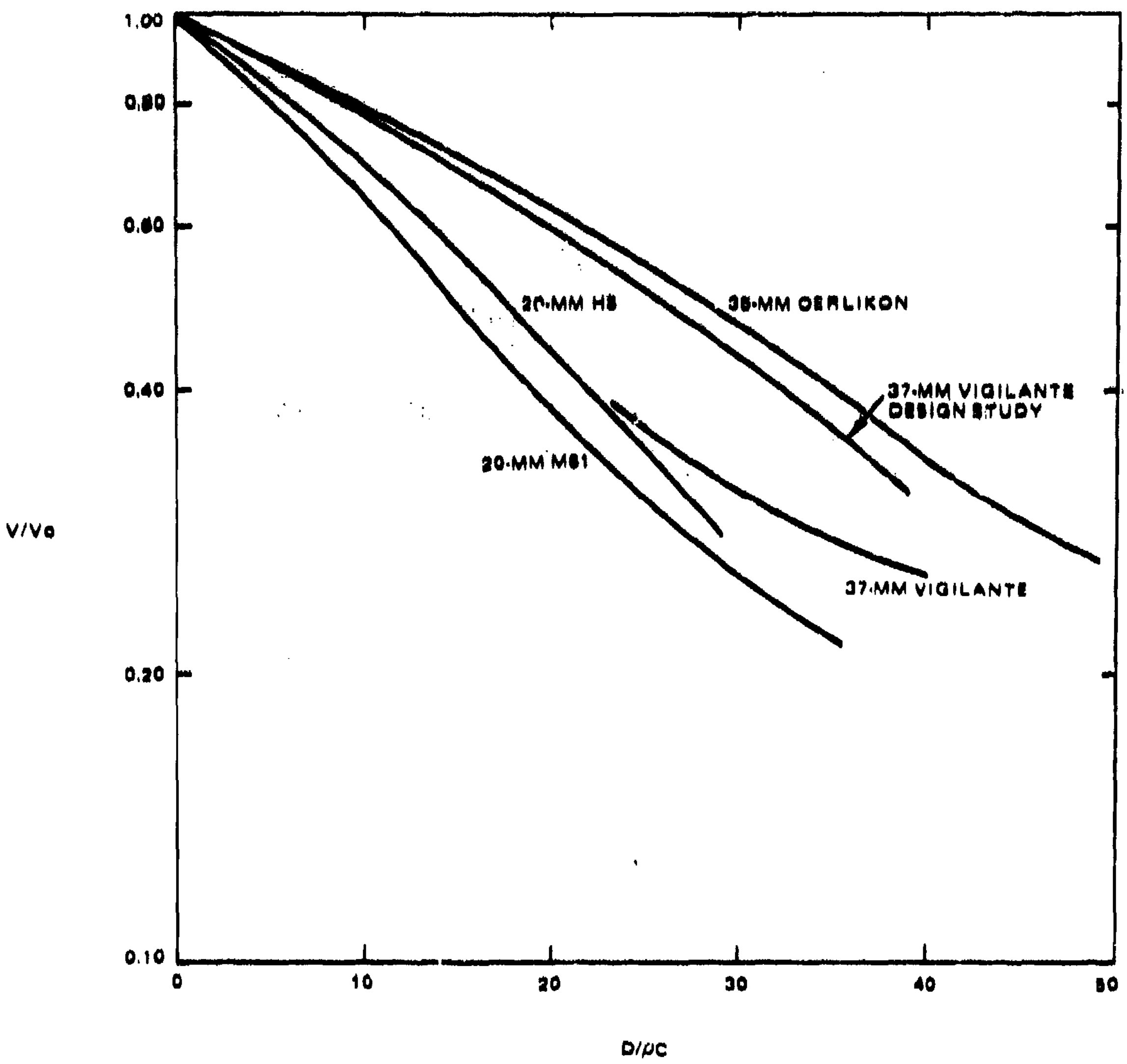


Figure 7-13. Fraction of Initial Velocity Versus Range Index

The filler weight of the Oerlikon projectile is not on hand, but the value of $w_p/C^3$ for this round suggests that it may carry over 20% of high explosive by weight. This would produce a higher terminal effectiveness than that of the Vigilante round, and the fact that the Oerlikon projectile is fired at a muzzle velocity of 1160 meters per second (from an L/90 gun) suggests careful attention to the joint gun/projectile interior ballistics and stresses.

### 7.2.8 Antiaircraft Gun System Development in the United States

The thin record of development of antiaircraft gun systems in the United States is sketched in Figure 7-15, for the period subsequent to World War II. Funding has been minimal probably because surface to air missiles seemed to give promise of greatly exceeding gun performance. During this period, U.S. grounds forces were not exposed to significant air threats in Korea or Southeast Aisa and so there has been no combat verification of the effectiveness of U.S. surface to air missiles. In both wars, however, enemy antiaircraft guns inflicted significant attrition on U.S. high performance aircraft, and over North Vietnam losses

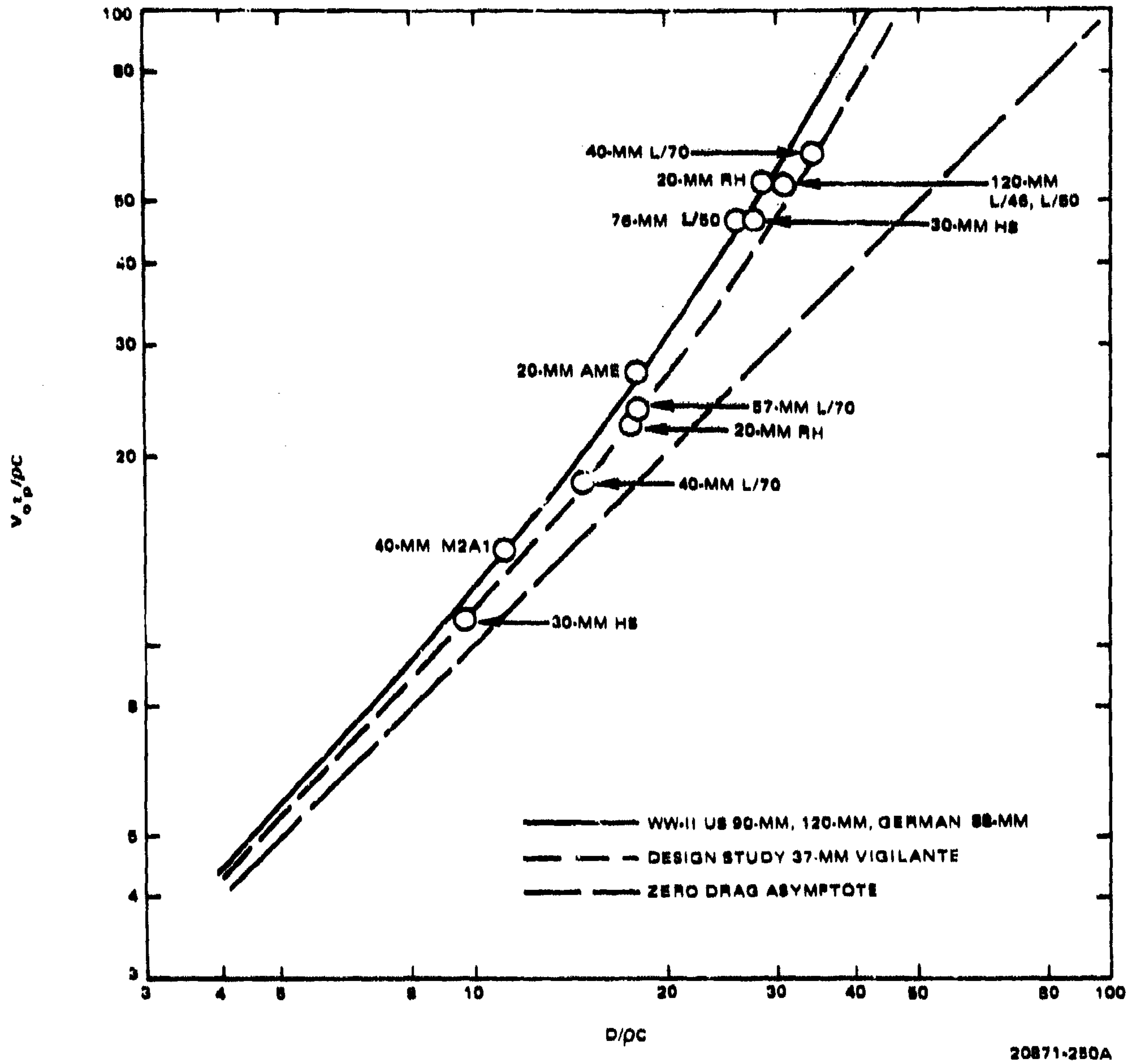


Figure 7-14. Comparison of Time of Flight Versus Slant Range Characteristics

of U.S. aircraft to antiaircraft predicted fire weapons have greatly exceeded losses to both enemy fighters and surface to air missiles. The record has been presented in other reports in this series.

### 7.2.9 Characteristics of Current Predicted Fire Air Defense Systems

In order to provide some realism for the analyses developed in the present report, characteristics of current U.S. and foreign predicted fire air defense systems have been extracted from unclassified sources[8,9] and Field Manuals, and are presented in Table VII-5 for towed fire units, and in Table VII-6 for self-propelled fire units.

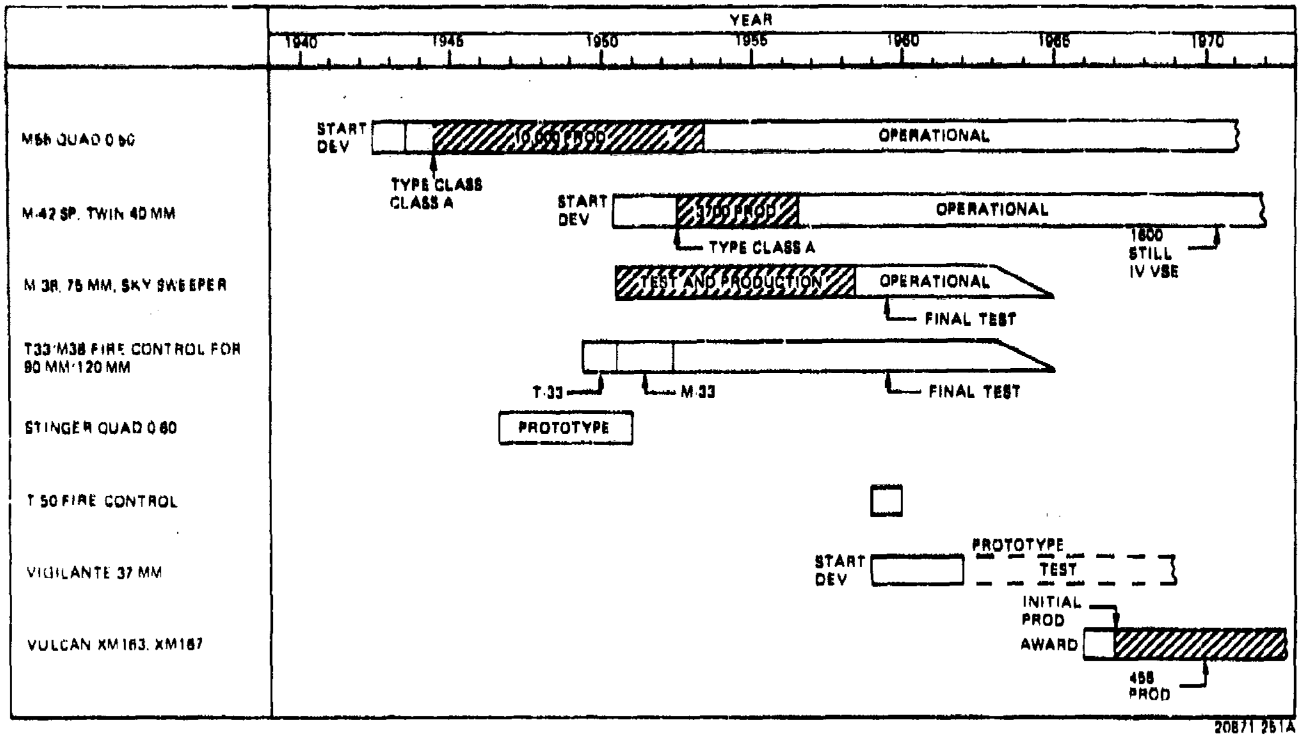


Figure 7-15. U.S. Army Antiaircraft Gun System Phasing

| Designation | M55 | Vulcan XM-167 | Rheinmetall RH 202 Mk 2 | Hispano Suiza HSS 669 | Hispano Suiza (Geneva) | Hispano Suiza HSS 820/665 | Hisp... HS... |
|---|---|---|---|---|---|---|---|
| Weapon | Quad 0.50 | 6-bbl 20 mm Gatling | Twin 20 mm | Single 20 mm | Twin 34 mm (40 mm) | Three 20 mm | Single |
| Rate of Fire (rpm) | 4 x 550 | 3000 | 2 x 1000 | 1000 | 2 x 500 | 3 x 1000 | 650 |
| Muzzle Velocity (f/s) | 2800 | 3400 | 3540 | 3450 | 3280 | 3450 | 3550 |
| Ammo on Mount | 280/gun | 300 on mount<br>3700 on prime mover | 270/gun | 75 (box)<br>50 (drum)<br>10 (clips) | 50/gun | 3 drums (50 each)<br>Link/box on outer guns (120 each) | Box o<br>5 rou |
| Time to Reload | | 7 min (1 min/100 rnds) | | | | | |
| Tube Life | | 2500 rnds/bbl | | | | | |
| Time to Change Tubes | | 6 tubes in 5 min | | | | | |
| Proj. Weight (lb) | 0.10 | 0.218 | 0.268 | 0.268 | | 0.268 | 0.93 |
| Carriage (tow) | M20; 4-wheel | 2-wheel | 2-wheel | | 2-wheel | | 2-whe |
| Weight (travel (lb) | 2950 | 3150 | 4600 | | 7930 (8380) | | |
| Weight (firing) (lb) | 2400 | | 3200 | | | | |
| Crew | | 4 | 3 | | | | |
| Prime Mover | 2-1/2 ton 6x6 truck (tow or transport) | 1-1/4 ton truck M561, M715 | Truck with 5500 lb. tow capacity | | Truck | | |
| Max. Speed | Tow: 10 mph road<br>5 mph cross country<br>Transport: Prime mover limit | Limited by tow vehicle: up to 45 mph | | | | | |
| Time to Convert Travel to Fire Mode | | | | | | | |
| Gun Drive | Electric/V-belt | Electric | Hydrostatic | Two hand-wheels | Electric | Hydraulic | Hydra |
| Power Source | On mount gasoline engine generator | On mount 1.5 KW, 24 volt gasoline engine generator | On mount air cooled gasoline engine | | Off carriage | On mount Wankel engine | On mo<br>Wanke |
| Power Requirement | | 0.5 KW | | | | | |
| Back-up Mode | Batteries | Batteries | Handwheels | | | | |
| e min/max (0) | -10/+90 | -5/+80 | -5/+83 | -10/+80 | | -5/+83 | -5/+83 |
| Ȧ/ė max (0/sec) | 60/60 | 60/45 | 100/55 | | 100/50 | | |
| Ä/ë max (0/sec$^2$) | | 160/160 | | | | | |
| D (meters) | | 200-5000 | | | | | |
| Ḋ (meters/sec) | | 10-320 | | | | | |

Table VII-5. Characteristics of Towed Weapons (Sheet 1 of 2)

| Hispano Suiza HSS 669 | Hispano Suiza (Geneva) | Hispano Suiza HSS 820/665 | Hispano Suiza HSS 661 | Hispano Suiza | Oerlikon/ Bührle | Bofors | Vigilante | Skysweeper M38 |
|---|---|---|---|---|---|---|---|---|
| Single 20 mm | Twin 34 mm (40 mm) | Three 20 mm | Single 30 mm | Quad 30 mm | Twin 35 mm | Single L/70 40 mm | 6-bbl 37 mm Gatling | Single 75mm |
| 1000 | 2 x 500 | 3 x 1000 | 650 | 4 x 650 | 2 x 550 | 300 | 3000 | 45 |
| 3450 | 3280 | 3450 | 3550 | 3545 | 3850 | 3280 (3900 with APDS) | 3000/(3600 Improved) | 2825 |
| 75 (box)<br>50 (drum)<br>10 (clips) | 50/gun | 3 drums (50 each)<br>Link/box on outer guns (120 each) | Box of 8 clips<br>5 rounds/clip | 360 | | | 144 (192 max) | |
| | | | | | | | 2.5 min/ magazine | |
| 0.268 | | 0.268 | 0.93 | 0.93 | 1.20 | 2.15 | 1.65 | 13.0 |
| | 2-wheel | | 2-wheel | | 4-wheel | 4-wheel | 5-wheel | 4-wheel |
| | 7930 (8380) | | | 11,100 | | 11,600 | | |
| | | | | 10,120 | 9300 | 10,100 | | 20,000 |
| | | | | | 3 | 6 | | |
| | Truck | | | | | | | Cargo Tractor 27-T |
| | | | | | 1-1/2 min | | | 5 min |
| Two hand-wheels | Electric | Hydraulic | Hydraulic | | | Hydraulic | Hydraulic | Hydraulic |
| | Off carriage | On mount<br>Wankel engine | On mount<br>Wankel engine | | 1 motor generator per mount | On mount<br>gasoline engine generator | | |
| | | | | | | | 108 hp (max)<br>42 hp (average) | |
| | | | | | | Handwheels | | |
| -10/+80 | | -5/+83 | -5/+83 | | | -5/+90 | -5/+85 | +6/+85 |
| | 100/50 | | | | | 85/45 | | |
| | | | | | | 135/127 | | |
| | | | | | | | | 22,000 |

20871-602A

2

| Designation | M55 | Vulcan XM-167 | Rheinmetall RH 202 Mk 2 | Hispano Suiza HSS 669 | Hispano Suiza (Geneva) | Hispano Suiza HSS 820/665 |
|---|---|---|---|---|---|---|
| Primary Fire Control (Air Targets) | On carriage | On carriage | On carriage | On carriage | Off carriage | On carriage |
| Type | M18 Optical fixed reticle reflex sight | Optical disturbed reticle lead computing gyrosight (max. lead angle 25°) | Optical computing sight (analog) | Optical HSS Kern 722 | | Optical Galileo P-36 |
| Angular data | Optical | Optical | Optical | Optical | | Optical |
| Range Data | None | Radar | Estimated and Regenerated | | | |
| Backup On-carriage Fire Control | None | | | | | |
| Fire Control (Ground Targets) | | 6X Telescope Night vision sight | Telescope | 5X Telescope | | |
| Gunners Control Type | Rate, Handlebar | Rate, Handlebar | Joystick with computer regen. rates | | | |
| Alerting Info Display | None | TADD | | | | |

Table VII-5. Characteristics of Towed Weapons (Sheet 2 of 2)

| ...netall ...Mk 2 | Hispano Suiza HSS 669 | Hispano Suiza (Geneva) | Hispano Suiza HSS 820/665 | Hispano Suiza HSS 661 | Hispano Suiza | Oerlikon/ Bührle | Bofors | Vigilante | Skysweeper M38 |
|---|---|---|---|---|---|---|---|---|---|
| ...e | On carriage | Off carriage | On carriage | On carriage | | Off carriage | Off carriage | On carriage | On carriage |
| ...mputing ...og) | Optical HSS Kern 722 | | Optical Galileo P-36 | Galileo P-36 | | Superfleder-maus 2 guns/ fire control system | L4/5 Dutch or Delswic VII 3 guns/fire control system | Sperry Electro-Mechanical Analog | Sperry Electro-Mechanical Analog |
| | Optical | | Optical | Optical | | | | | Radar |
| ... and ...ed | | | | | | | | | Radar (1) Automatic (1) Manual |
| | | | | | | | Joystick local control and fixed sight | | Optical with aided manual control |
| | 5X Telescope | | | | | | | | Telescope |
| ...vith ...regen. | | | | | | | | | |

20871-1602

2

Table VII-6. Self

| Designation | U.S. Vulcan XM-163 | Swiss Oerlikon | French AMX D.C.A. 30 | British Falcon Vickers-Hispano | Swiss (German) Oerlikon/Contraves 5 PFZ-B | Swiss (Netherlands) Oerlikon/Contrav 5 PFZ-C |
|---|---|---|---|---|---|---|
| Weapon | 20 mm 6 tube Gatling gun M61A1 | Quad 20 mm | Twin 30 mm HSS 831L | Twin 30 mm HSS 831L | Twin 35 mm Oerlikon L/90 KDA | Twin 35 mm KDA |
| Rate of Fire | 3000 | | 2 x 650 | 2 x 650 | 2 x 550 | 2 x 550 |
| Muzzle Velocity (F/S) | 3250 | | 3550 | 3540 | 3850 HG 3950 AP | 3850 HG 3950 AP |
| Ammo on Mount | 1000 in drum 800 stored linkless feed | | 300 rounds/gun linked | 310 rounds/gun | 330/gun | 330/gun |
| Time to Reload | 3 min plus 200 rpm | | | | 20 min | 20 min |
| Tube Life | 20,000/barrel 145,000/gun | | | | | |
| Time to Change Tubes | 5 min for 6 tubes | | | | | |
| Carriage (Self Propelled) | Tracked XM 741 (Mod M113A1 chassis) | Tracked (AMX chassis) | Tracked AMX 13 AMX 30 | Tracked (Abbot) | Tracked (Leopard chassis) | Tracked (Leopard chassis) |
| Weight (lbs) | 26,000 | | 31,000 | 35,000 | 80,000 (?) | 80,000 (?) |
| Crew | 4 | | 3 | 3 | 2 | 2 |
| Horsepower | | | 312 700 | 211/213 | | |
| Ground Pressure (PSI) | | | | 11.6 psi | | |
| Range (miles) | 300 | | | 240 (roads) | | |
| Max Speed (MPH) | 40 | | 36 40 | 30 (roads) | | |
| Turret Weight (lbs) | 2900 | | SAMM 3401A, Turret 13,200 | | | |
| Gun Drive | Electric | | Electro-hydraulic | Electric metadyne | | |
| Auxiliary Power | | | | None | Separate diesel engine and generator | Separate diesel engine and generator |
| Power Requirement | 0.5 KW | | | | | |
| Back-up Mode | Batteries | | | None | | |
| e min/max | -5/+80 | | -8/+85 | -10/+85 | -8/+87 | -8/+87 |
| A/e min ($^{\circ}$/sec) | 60/45 | | | 80 slow 45 track /40 | 90/50 | 90/50 |
| A/e max ($^{\circ}$/sec$^2$) | 160/160 | | | 120/120 | | |
| D (meters) | 200-500 | | 1500-3800 (Regen: 500-1500) | Estimated | | |
| D (meters/sec) | 10-320 | | 50-320 | Not applicable | | |
| Artificial Dispersion | 6 x 18 mils | | | | | |

Table VII-6. Self Propelled Weapon System Characteristics (Sheet 1 of 2)

| British Falcon Vickers-Hispano | Swiss (German) Oerlikon/Contraves 5 PFZ-B | Swiss (Netherlands) Oerlikon/Contraves 5 PFZ-C | U.S. M42 Duster | Sweden Bofors | French Thomson-CSF Javelot | Soviet ZSU-23-4 | Soviet ZSU-57 |
|---|---|---|---|---|---|---|---|
| win 30 mm<br>S 831L | Twin 35 mm<br>Oerlikon L/90 KDA | Twin 35 mm<br>KDA | Twin 40 mm<br>M2A1 L/60 | Twin 40-mm<br>L/70 | Unguided 40 mm rockets | Quad 23 mm | Twin 57 mm |
| x 650 | 2 x 550 | 2 x 550 | 2 x 120 | 2 x 325 | | 4 x 1000 | 2 x 120 |
| 340 | 3850 HG<br>3950 AP | 3850 HG<br>3950 AP | 2870 | 3280 | | 2950 | 3280 |
| 0 rounds/gun | 330/gun | 330/gun | 240 rounds/gun in 4 round clips | 425 | | | |
| | 20 min | 20 min | Not Applicable | | | | |
| | | | 12,000 | | | | |
| | | | 3 min (after 60 rnd are fired because of heating) | | | | |
| acked<br>bbot) | Tracked<br>(Leopard chassis) | Tracked<br>(Leopard chassis) | Tracked | Tracked | Tracked | Tracked<br>(PT-76 tank chassis) | Tracked |
| 000 | 80,000 (?) | 80,000 (?) | 49,500 | 70,000 | | 33,600 | 67,200 |
| | 2 | 2 | 5 | 3 | | | |
| /213 | | | 500 | 240 gasoline<br>330 gas turbine | | | T-54 tank engine |
| psi | | | | | | | |
| (roads) | | | 100 | | | | |
| (roads) | | | 25 cross country<br>45 roads | 37 | | | |
| | | | M4E1: 6900 | | | | |
| tric metadyne | | | Hydraulic | | | | |
| e | Separate diesel engine and generator | Separate diesel engine and generator | One cylinder engine-generator | | | | |
| | | | Manual | | | | |
| +85 | -8/+87 | -8/+87 | Power -3/+85<br>Manual -5/+87 | -5/+85 | | 0/+85 | +2/+87 |
| w /40<br>ack<br>120 | 90/50 | 90/50 | 40/25 4/4 | 85/45 | | | |
| ated | | | Not applicable | 20,000 | | | |
| applicable | | | Not applicable | | | | |

20871-603A



2

Table VII

| Designation | U.S. Vulcan XM-163 | Swiss Oerlikon | French AMX D.C.A. 30 | British Falcon Vickers-Hispano | Swiss (German) Oerlikon/Contrans 5 PFZ-B | Sw (Nethe Oerlikon/ 5 PF |
|---|---|---|---|---|---|---|
| Surveillance Sensor | Visual | Visual | Oeil Noir radar RD VC-IA TCSF | Visual | Siemens MPDR-12 Ka Band | Signaal Ka |
| Automatic Threat Evaluation | No | | Yes | | | |
| Alerting Info (Remote) | TADD(RAID) | | | | Via digital radio link and display on PPI | Via digital and display |
| Tracking Sensor | | | Radar azimuth acquisition | | | |
| Angle | Visual | Visual | Visual | Periscopic visual 1 x 50° field | Albiswerk Ka pulse doppler visual alternate | Signaal do visual alter |
| Range | Radar (Lockheed) | Radar | Radar Reg range (500-1500 meters) | Estimated | Radar | Radar |
| Computer | M61 lead computing sight max lead 25° | | Sagem sight, analog computer | Computing sight | | |
| Backup | | | | | Alternate "emergency" computer on mount | Alternate "emergenc computer |
| IFF | | | | | Siemens MSR 400 | Siemens M |
| Gunner's Control | Rate | | | Joystick | | |
| Fire Control Versus Ground Targets | 6X telescope night vision sight | | Two APX M250 periscopic binocular sights | Periscope 6X; 10° field | | |
| Muzzle Velocity Measurement | | | | | On mount | On mount |
| Stabilization | None | | | Turret | Optical sight | Optical si |

Table VII-6. Self Propelled Weapon System Characteristics (Sheet 2 of 2)

| British Falcon Vickers-Hispano | Swiss (German) Oerlikon/Contrane 5 PFZ-B | Swiss (Netherlands) Oerlikon/Contrane 5 PFZ-C | U.S. M42 Duster | Sweden Bofors | French Thomson-CSF Javelot | Soviet ZSU-23-4 | Soviet ZSU-57 |
|---|---|---|---|---|---|---|---|
| Visual | Siemens MPDR-12 Ka Band | Signaal Ka Band | Visual | | Radar | | |
| | | | No | | | | |
| | Via digital radio link and display on PPI | Via digital radio link and display on PPI | | | | | |
| Periscopic visual 1 x 50° field | Albiswerk Ka pulse doppler visual alternate | Signaal doppler Ka visual alternate | Visual | | Radar | | |
| Estimated | Radar | Radar | Not applicable | | | | |
| Computing sight | | | M38 computing sight. Course and speed estimated | | Digital computer | | |
| | Alternate "emergency" computer on mount | Alternate "emergency" computer on mount | Ring sight | | | | |
| | Siemens MSR 400 | Siemens MSR 400 | | | | | |
| Joystick | | | Rate | | | | |
| Periscope 6X; 10° field | | | | | | | |
| | On mount | On mount | | | | | |
| Turret | Optical sight | Optical sight | None | | | | |

20871-1603

2

# SECTION 8
# MISSION DESCRIPTION: THE BATTLEFIELD DAY

To provide a structure in which to bring together the system performance characteristics for evaluation, it is helpful to have a systematic arrangement of the probable activity states of the system.

A useful approach is via the specification of a 'Battlefield Day'. A Battlefield Day, which may in fact include several 24 hour consecutive intervals, is a skeletonized scenario which has the objective of insuring that the system under evaluation is considered and assessed with respect to each of a number of functions that it must perform when it becomes operational.

## 8.1 DEVELOPMENT OF ELEMENTS OF BATTLEFIELD DAY

A definitive Battlefield Day must be developed by experienced military personnel, however a hypothetical description is provided at this point for illustration.

The time span includes both day and night. The movement schedule includes cross country movements, movement on roads, and periods in fixed position. The system activity states include alert status, engagement of enemy aircraft and enemy ground targets, and periods of no activity (passive).

In each activity state the system components which are activated must be specified. This specification is used to determine failure rates. It may be expected that failure rates for a given component will vary depending on whether the component is being subjected to shock and vibration associated with vehicle movement, whether it is activated in an alert condition in a position state, or whether it is subjected to shock and vibration of gun firing during an engagement.

It appears possible in the interests of simplification of the analysis to use the Battlefield Day primarily for generating the system 'availability' estimates and to perform the 'capability' analyses of combat engagements separately. That is, the system fires during the Battlefield Day, but only the effects of the firing on availability, and possibly 'dependability' are assessed at this point of the analysis.

Availability and dependability thus obtained are then used in the overall effectiveness computation including engagement details as presented later.

This procedure allows most of the effects of weather on the fire control system to be treated in the engagement model. It may however be desired to include weather in the Battlefield Day to assess its effect on vehicle movement and fail and repair rates.

Figure 8-1 shows elements of a Battlefield Day graphically.

There are two approaches to using a Battlefield Day. One is to take a deterministic specification of when events occur, as implied by Figure 8-1, assume that the system begins the day with all components operating, and determine its survival probability at the end of the 'day'. The second approach, which leads directly to availability estimates is to assume that the days are repeated over and over until the system reaches a steady state from which the state probabilities can be determined. In the latter case it is helpful to specify the mean duration of each tactical activity state and its recurrence rate in statistical terms. This may require taking liberties with the deterministic nature of day and night, when it is felt that these are critical parameters.

In general, if one performs the analysis by computer simulation, the approximations needed for a manageable manual computation can be avoided. The following developments assume however, that a first sizing of the problem without use of a computer is more desirable than the avoidance of simplifying approximations.

## 8.2 SYSTEM MOVEMENT AND TACTICAL ACTIVITY STATES

Beginning with the Battlefield Day, we may arrange the system activity and operational states in mutually exclusive sets and sub sets. The movement and positional phases are separated, since they impose different stresses on the system. This set of states is shown in Figure 8-2.

Next we subdivide the movement and position states into three identical subsets each as follows, as shown in Figure 8-3.

a. *Combat:* Enemy targets have been detected by the defense and one or more of the fire units in operational condition is attempting to acquire a target and open fire, or is actually firing.

b. *Alert:* Enemy targets are expected, all operational fire units are in a ready state with power on. Surveillance modes are operational.

c. *Passive:* No enemy targets are expected, and scheduled system maintenance and repairs can be carried out.

The complete system is stressed most highly in the combat mode, moderately in the alert mode, and is under minimal stress in the passive mode. Only in the passive state is there complete freedom to repair malfunctions. In the combat state repair would probably be limited to actions requiring very short time to complete, such as relieving a gun jam. In the alert

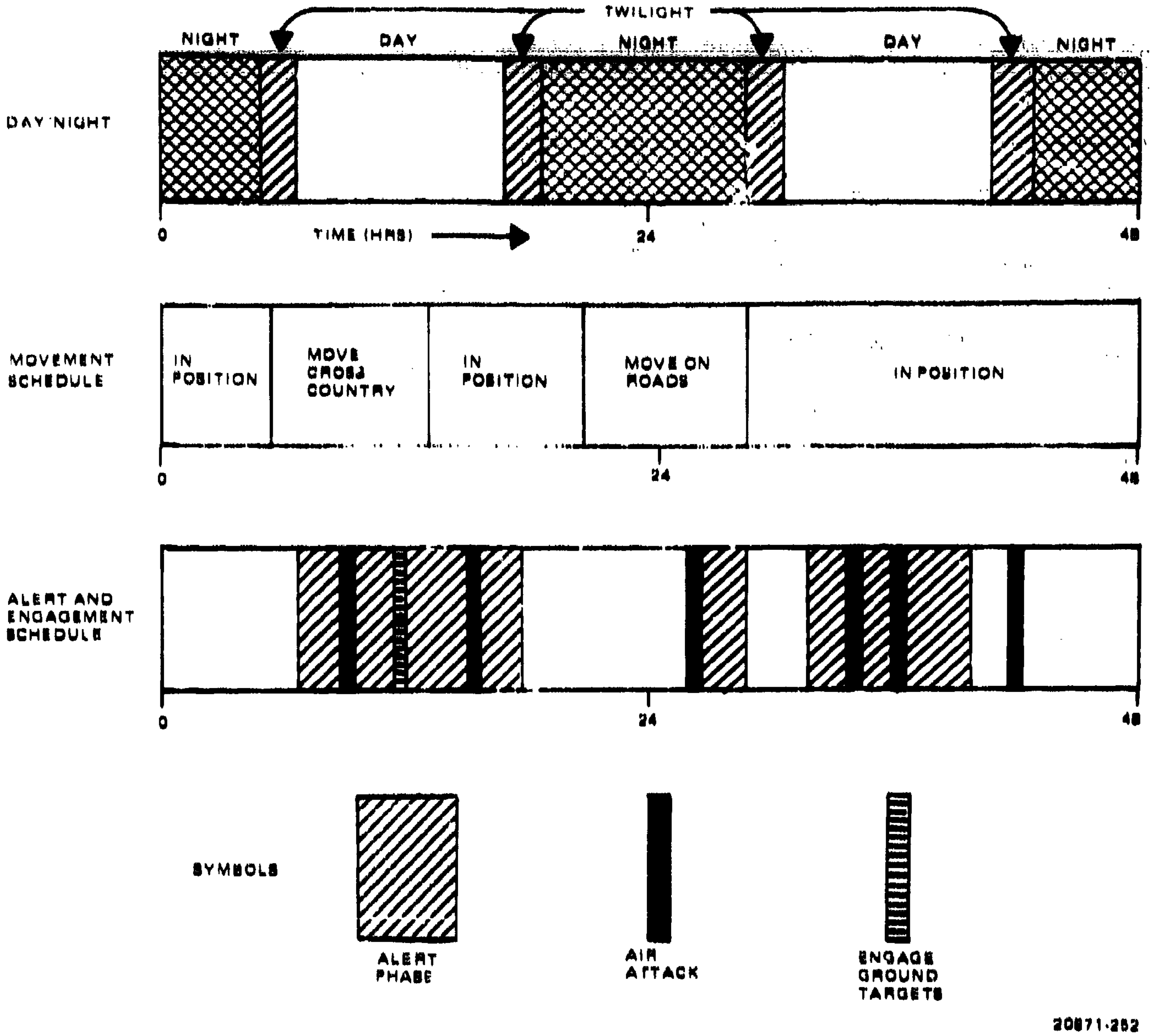


Figure 8-1. Elements of a Battlefield Day

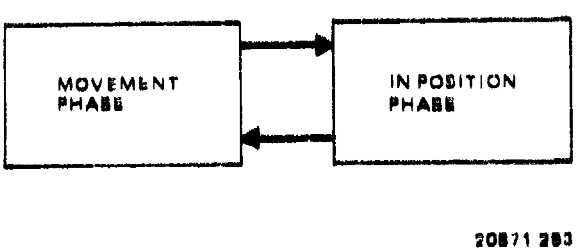


Figure 8-2. System Movement States

mode malfunction repair might be limited by the desire to keep the system ready for combat in at least the highest mode available at the initiation of alert.

In some situations the system may be under enemy artillery fire which would limit the repair activity that could be carried out in any of the above states.

Experience indicates that the combat state will constitute a small fraction of the Battlefield Day, and within the combat state an even smaller fraction will be represented by actual firing.

For example, in the defense of the Remagen Bridges in World War II a massive barrage type of defense was set up. On the three nights of heaviest action, the

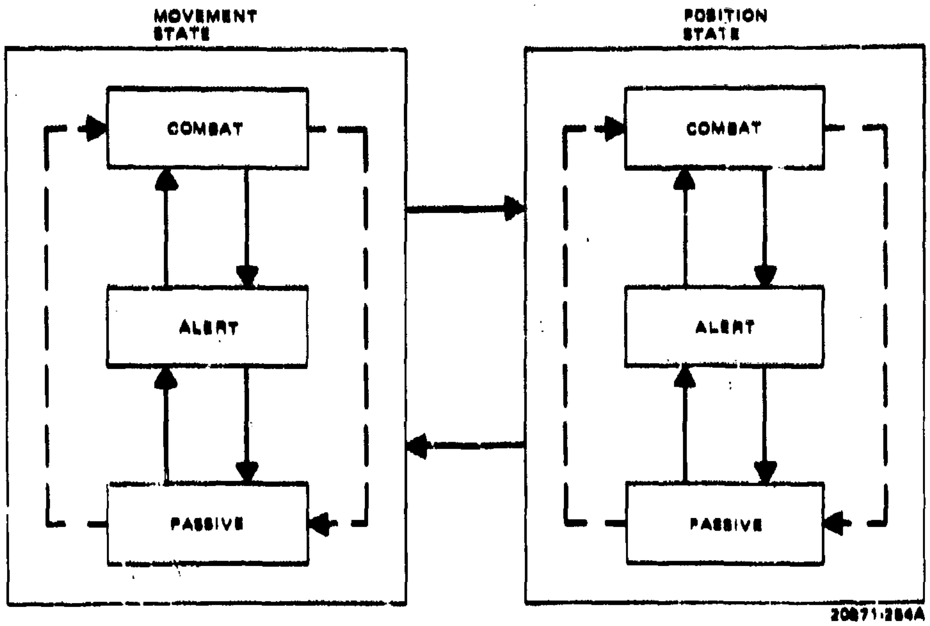


Figure 8-3. Tactical Activity States

barrage was fired three times on each night, each time for 10 seconds. The corresponding firing time for each 40-mm Bofors weapon in the defense was 30 seconds, or 60 rounds per gun.

The island of Malta was subjected to repeated attacks over a period of months[6], during which some 14,000 tons of bombs were dropped on the 143 square mile areas of Malta and Gozo. Antiaircraft destroyed 236 of the attacking aircraft. In the month of April 1942 alone, 6728 tons of bombs were dropped. 'On an average there were 170 bombers over every day, coming in waves of 12 to 15 at a few minutes interval from a variety of directions...there were usually three raids a day...each raid lasted for about one hour. The total time spent under raids during the month came to twelve days ten hours and twenty minutes'. In the month antiaircraft destroyed 102 enemy aircraft, thirty in one week.

But 'In the course of that week they achieved their record of ammunition expenditure. In one day an average of sixty-nine rounds were fired for every heavy anti-aircraft gun and fifty-six rounds for every Bofors gun.'[6]

This works out to an average firing time for each heavy gun over about seven minutes per gun per day, and for the 40-mm Bofors, about 1/2 minute of firing time per gun per day.

Of course some guns must have substantially exceeded the average. But it seems reasonable to base the analysis on the assumption that firing time will be a very small fraction of total time, and 'red alert' only a moderate fraction.

Within each of the sub-states shown in Figure 8-3, the transition rates between states vertically will differ in the movement phase from those in the position phase. For example, the towed Twin 35-mm Oerlikon fire unit requires 1 1/2 minutes to convert from travelling to firing mode, but the Vulcan, and other self-propelled fire units can fire on the move.

## 8.3 SYSTEM OPERATIONAL STATES

Each sub-set of states in Figure 8-3 is next further subdivided according to the operational modes, or states of the system. Considering a single fire unit, for example, those states in which the system has some capability to perform its mission are determined and identified as operational states. These include the 'all-up' state with all subsystems functioning properly, and the set of 'fail' states, in which the system has no capability for performing its mission. These are indicated in Figure 8-4. The possible transitions and their probabilities depend on which activity state the system as a whole is in. For example failure of the servo drive for the gun in the combat state may not be repaired until the system as a whole transitions to an alert or passive state.

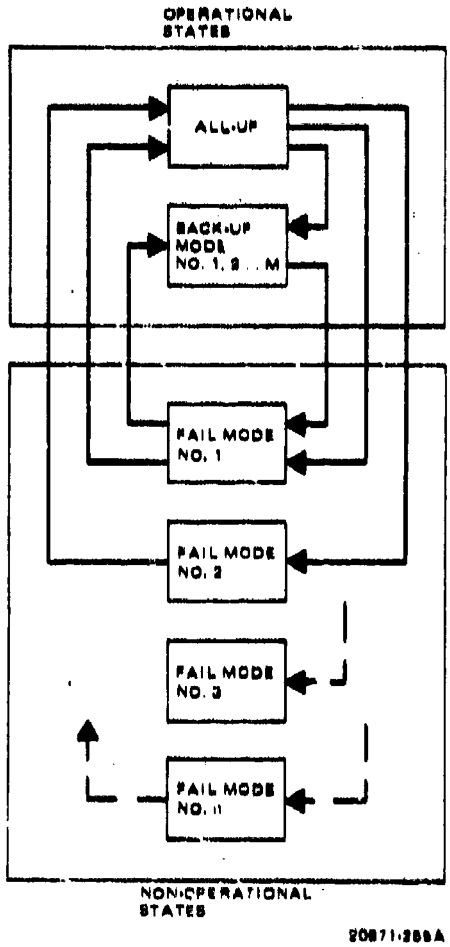


Figure 8-4. Operational Availability States

# SECTION 9
# SYSTEM COMPONENTS AND STATES

Emphasis in this report is on the defense system consisting of a number of fire units, their immediately supporting equipment, such as a common alerting radar, and the organic communications which control and coordinate the defense. These elements are shown in Figures 9-1 and 9-2.

Principal emphasis is on the fire units as opposed to organic but separately located radars, and other general support equipment.

A natural initial subdivision of fire unit elements is into 'mobility' and 'firepower' subsystems. In the case of a self-propelled fire unit, the mobility subsystem consists of the vehicle exclusive of the armament and fire power package. In the case of a towed mount the mobility subsystem consists of the wheel carriage structure and the prime mover vehicle. Some of the smaller automatic weapons fire units may be transported by a vehicle and manually unloaded and emplaced for firing.

The firepower subsystem includes the weapon, ammunition, tracking sensors, computer, sensor and gun servos and related components.

A few components may be common to both the mobility and firepower subsystems, depending in the fire unit design. These may include power and electrical components, crew functions, and communications and other components to be identified in the case of specific fire unit evaluations.

These two primary subsystems are illustrated in Figure 9-3.

## 9.1 MOBILITY SUBSYSTEM

The mobility subsystem may be further subdivided into components. A representative list is given in Table IX-1. This list is essentially the categorization used in the Army Maintenance Management System (TAMMS) which maintains a record of Army equipment reliability and maintenance data under the Army Equipment Record Procedures System (TAERS). TAERS records will be a major source of data in estimating availability of the mobility subsystems associated with an air defense system evaluation.

During the movement phase, the mobility subsystem may be in one of a set of sub states as shown in Figure 9-4.

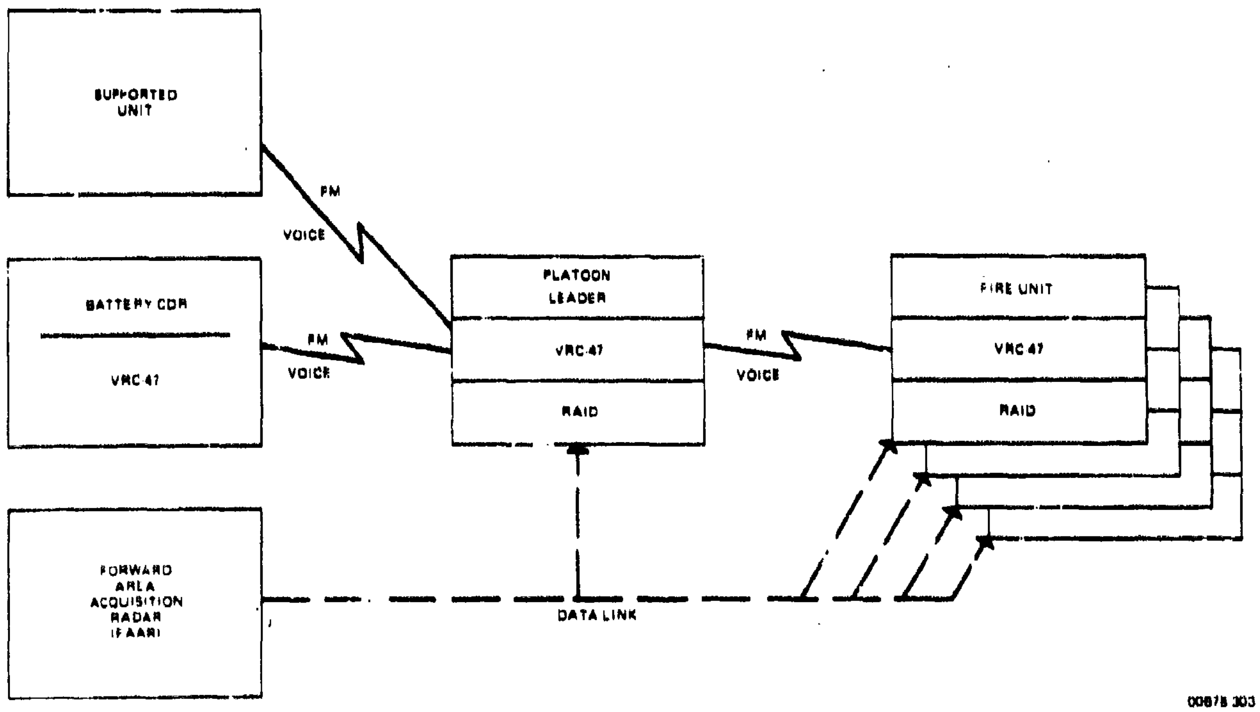


Figure 9-1. Flow of Command and Alerting Information to Fire Units

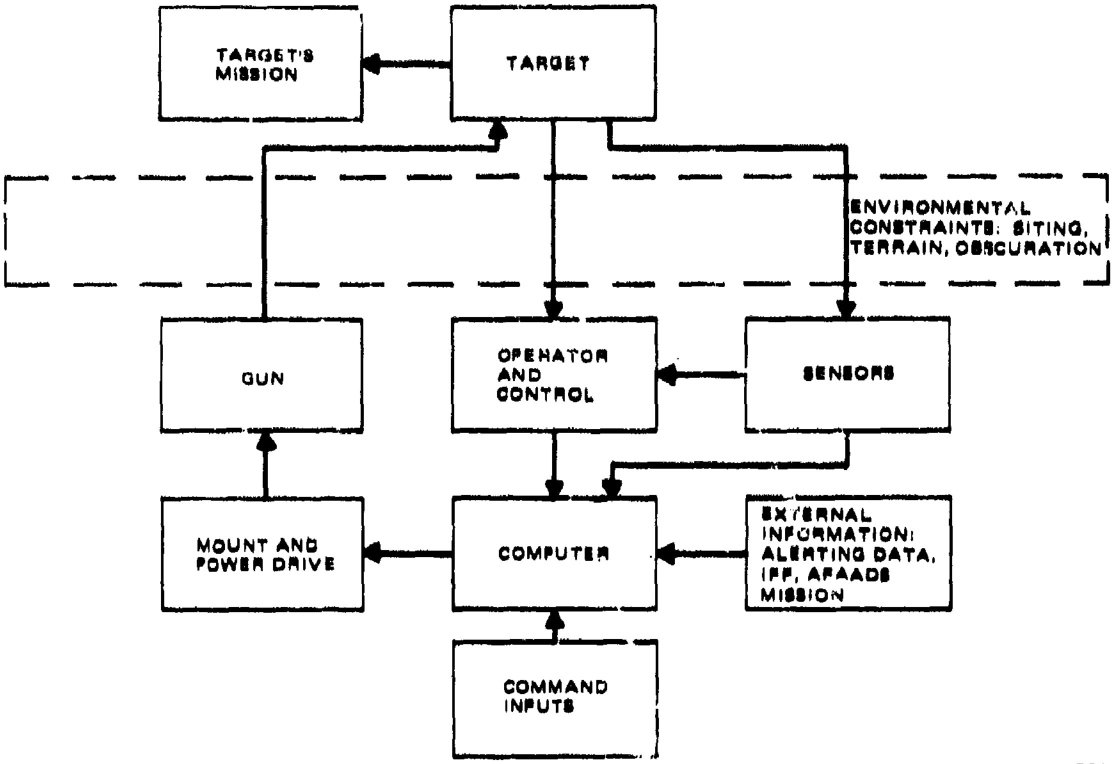


Figure 9-2. Fire Unit Components

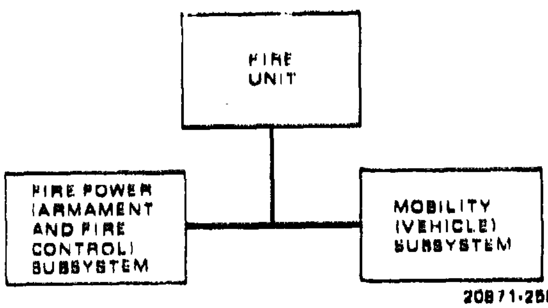


Figure 9-3. Primary Subsystems

No extensive analysis of the mobility subsystem is contemplated for this report since its evaluation is relatively straightforward as compared with the firepower subsystem.

However, we note briefly the availability figures for a few vehicle types.

Trucks have averaged about 0.40 maintenance manhours per hour of operation, with % of time available 80-90%. Under proving ground conditions, (all supply facilities on hand) the ratio might be about 0.2 maintenance manhours per hour, with an availability for continuous test of about 85%.

For tracked APC and tanks, TAERS indicated about 1.5-2.0 maintenance manhours per hour of operation with the vehicles available about 80% of the time. A proving ground test of an early APC indicated only 0.2 maintenance manhours per hour, again with an availability for test of about 85%.

## 9.2 FIREPOWER SUBSYSTEM

The functions performed by the firepower subsystem are related to alternate modes of operation, and to the sub-subsystems or components providing each function. For simplicity we continue to refer to sub-subsystems as simply subsystems. The relationships among functions and subsystems are indicated in Figure 9-5.

### 9.2.1 Alternate Operational Modes

One step in the availability computation is the determination of those system modes which allow engagement of the enemy. These include the completely operational state (all-up) and various levels of degraded operation, and alternate modes of operations in the all-up state.

The system may operate in a degraded mode if

a. The combat phase occurs with a subsystem essential to the all-up mode malfunctioned, but with a back-up mode available. For example a fire unit may operate with estimated range if the ranging device is inoperative. If the computer has mal-

Table IX-1. Probability of Operating Vehicular Components Without a Failure Requiring Support Maintenance

| Item Nomenclature | Tracked - 2,000 miles | | | Wheeled - 10,000 miles | |
|---|---|---|---|---|---|
| | M60 % | M4842 % | M113 % | M151 % | M35 % |
| Engine | 97 | 99 | 96 | 99 | 99 |
| Clutch | NA | NA | NA | 99 | 100 |
| Fuel system | 100 | 98 | 98 | 100 | 100 |
| Exhaust system | 100 | 99 | 98 | 100 | 100 |
| Cooling system | 100 | 99 | 97 | 99 | 100 |
| Electrical system | 97 | 96 | 97 | 99 | 100 |
| Transmission | 97 | 99 | 98 | 99 | 99 |
| Transfer case | NA | NA | 99 | 100 | 99 |
| Propeller shaft | NA | NA | NA | 100 | 100 |
| Front axle or final drive | 100 | 99 | 99 | 98 | 100 |
| Rear axle | NA | NA | NA | 100 | 100 |
| Brakes | 100 | 100 | 100 | 100 | 100 |
| Wheel and tracks | 100 | 98 | 98 | 99 | 100 |
| Controls | 97 | 97 | 98 | 100 | 100 |
| Frame, brackets | 100 | 100 | 100 | 100 | 100 |
| Springs, shock absorbers | 100 | 99 | 100 | 100 | 100 |
| Hood, sheet metal | NA | NA | NA | 100 | 100 |
| Cab, body or hull | 100 | 96 | 99 | 100 | 100 |
| Turret | 63 | 77 | NA | NA | NA |
| Winch | NA | NA | NA | NA | 100 |
| Bumper guards | NA | NA | NA | 100 | 100 |
| Miscellaneous accessories | 100 | 100 | 100 | 100 | 100 |
| Fire extinguisher system | 100 | 100 | 100 | NA | NA |
| Armament | 93 | 91 | 99 | NA | NA |
| Sighting & fire control | 88 | 91 | NA | NA | NA |
| Auxiliary generator | NA | 99 | NA | NA | NA |

20871-604

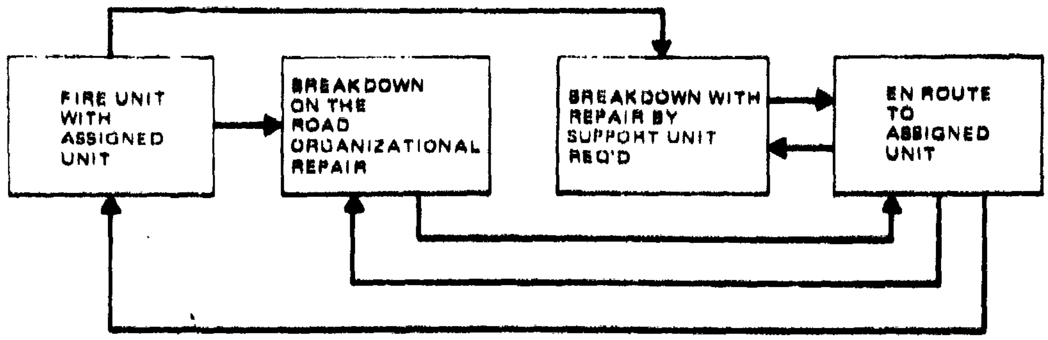


20871-259

Figure 9-4. Mobility Failure States

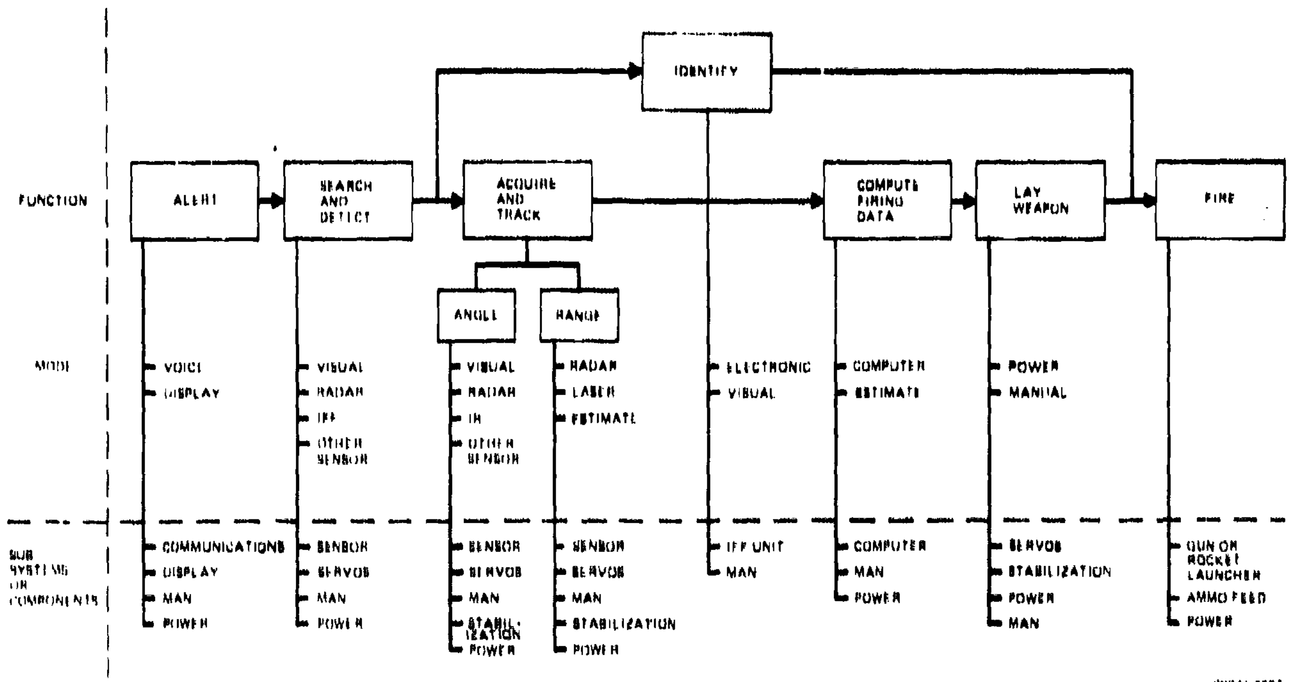


20871-260A

Figure 9-5. System Functions, Modes and Subsystems

functioned the gunner may fire with estimated lead or by tracer observation. The Matador system is planned to have a primary digital computer and a backup analog computer. Considering the defense system as a whole, malfunctioning of a common surveillance radar may deprive the fire units of early warning information, but they may operate with local surveillance (such as visual).

b. Enemy countermeasures may neutralize one or more of the sensors, but a backup mode may be available. For example if the radar range unit is jammed out, range may be estimated.

c. Weather may negate the available tracking sensors. With all tracking and computing data denied the system, a vital area defense can still be performed by barrage fire.

In general, if the system is properly designed for reliability and maintainability, the occurrence of degraded modes because of component failure will be infrequent.

Degradation caused by enemy countermeasures is difficult to anticipate because not all technical options open to the enemy can be foreseen for the operational life of the defense system.

Degradation caused by night or bad weather can be computed, but the evaluation of its importance is directly dependent on the assumed enemy capability to attack effectively under the same conditions. Hence judgement of future enemy capability is a dominating factor in this assessment.

The system may operate in one of several available alternate modes, in an all-up state depending on the tactical situation parameters. For example, if the radar is unable to cope with multipath errors at very low elevation angles, elevation angular data may be obtained by human operator tracking, with the radar continuing to provide range and azimuth.

### 9.2.2 Qualitative Comparison of Two Fire Units

To further illustrate the kinds of alternate operational modes that may be considered, the characteristics of two towed fire units, Vulcan, and the Rheinmetall twin 20-mm have been abstracted from the summary Table VII-5 and are repeated in Table IX-2.

If the engine generator set is inoperative, Vulcan can operate with full capability on its storage batteries for a limited period. The Rheinmetall mount can be laid by handwheels, with some, but markedly lessened capability. The estimation of the probability that Vulcan will become completely inert because of battery drain before the generator can be repaired is an interesting sub-problem.

The Rheinmetall mount uses estimated range input. The fire control algorithms are unknown at this time to this writer. Vulcan can operate if the radar is inoperative, with range estimated by the gunner or by another operator off-mount.

Both systems can fire by estimated lead or by tracer observation if the computers are inoperative.

The Rheinmetall mount can probably continue to fire with one gun if the other jams.

For fixed aim in surface fire, Vulcan is positioned by the drive controller, then the power is turned off. The Rheinmetall mount can be laid by the handwheels.

## 9.3 DEFINITION OF SYSTEM STATES

A general procedure for defining the system states for analysis is as follows:

It is assumed that a level of organization has been chosen, below which the analysis is to be performed. This may be, for example, an Air Defense Artillery Battalion. It is also assumed that emphasis is to be on the effectiveness evaluation of the predicted-fire units.

From the point of view of the fire units, there are functions performed within the battalion which support and affect the performance of the individual fire units. These include:

a. Tactical Functions

   (1) Warning.

   (2) Surveillance.

   (3) Communications, command and control.

   (4) Effect of missile fire units on the threat tactics.

b. Support Functions

   (1) Maintenance.

   (2) Supply.

The warning and alerting information affects the combat performance of the fire units. The maintenance and supply function affect the availability and dependability of the fire units. The command and control function improves the effectiveness of the defense by coordinating the action of the individual fire units.

### 9.3.1 States of Supporting Functions

These are developed as inputs to the fire unit state analysis, and by methods similar to those to be discussed for the fire units. For example, of the battalion uses a number of FAAR radars, the availability and dependability computations would be similar to those of radars on the fire units. Maintenance support is an input to the fire unit maintainability estimates.

### 9.3.2 Fire Unit State Definition

From the functional flow diagrams of the fire unit, and the system description, identify the subsystems which perform each function. Begin with the highest level of function and subsystem which can be developed in the following categories.

a. Functions with alternate modes of performance.

   Primary modes (for example radar or visual tracking).

   Degraded Modes (for example range estimation).

   Note that the mode designated as 'primary' may vary with the environment. A system may be 'all-up' yet use only the preferred option of its primary modes. A degraded mode is defined as one which is inferior to a primary mode, but provides some capability, but would not be used if the primary mode were available.

b. Functions without alternate modes of performance, whose loss incapacitates the system, (for example, power supply or gun drive servomechanisms for a mount which cannot be laid manually).

Next identify a set of operational states which are mutually exclusive and complete, described in each case by the set of subsystems which must be operative for the system to be operative in that state. Examples are given later.

Table IX-2. Characteristics of 20-mm Towed Mounts

| | Designation | Vulcan XM-167 | Rheinmetall |
|---|---|---|---|
| Weapon and Mount | Weapon | 6-bbl 20-mm Gatling | Twin 20-mm |
| | Rate of fire | 1000, 3000 rpm | 2000 rpm (2 guns) |
| | Muzzle velocity | 3400 f/s | 3540 f/s |
| | On mount ammo | 300 rounds | 270 rounds/gun (ammo box) |
| | Ammo types | HEIT/SD (AA)<br>HE (Surface) | HEIT<br>APIT |
| | Crew | 4 | 3 |
| | Carriage (tow) | 2-wheel | 2-wheel |
| | Weight in tow position | 3150 lbs | 4600 lbs |
| | Prime Mover | 1-1/4 ton truck M561 | Truck |
| Drive | Gun Laying Drive | Electric | Hydrostatic |
| | Power for Gun Lay | Storage Batteries and 1.5 KW, 28V gasoline engine generator set | Air-cooled gasoline engine |
| | Backup mode | Storage batteries | Manual handwheels |
| Fire Control | Fire Control | On carriage | On carriage |
| | Antiaircraft | Gyroscopic Lead Computing Sight | Electromechanical Lead Computing Sight |
| | Ground fire | | |
| | Direct | 6x telescope<br>Night vision sight<br>Fixed reticle in LSC with gyro caged | Telescope |
| | Indirect | Azimuth and elevation lay | |
| | Ranging information | Radar | Estimated (and regenerated?) |
| | Backup modes | Gunner estimate<br>Remote estimate | |
| | Gunner's Tracking Aid | Rate drive controller | Joystick with computer regenerated rates |
| Other | Dispersion | | |
| | AA | 6 x 18 mils | Small. No artificial dispersion. |
| | Ground | 5 x 5 mils | |
| | Other aids | TADDS | |
| | Communications | Wire<br>Radio | |

20871-605

Identify a set of 'down' states in which the system is non-operable. Each is initially defined by the subsystem or component whose malfunctioning identifies the state. In the analysis an attempt is made to aggregate these states where possible to simplify the analysis.

Develop a flow diagram showing possible transitions among the states defined above. How one defines the state transition probabilities with time depends on whether a computer simulation is intended, or whether an analytical solution is to be attempted. In the case of a computer simulation more freedom in incorporating a variety of probability density functions appropriate to each state transition is possible. For analytic purposes, with even moderately complex systems, one can hardly do more than describe the state transitions as a set of linear differential equations with constant coefficients.

In the present report the view is taken that the state transition probabilities (in this case mean rate of fail and mean rate of repair) for a specific subsystem will, in many cases, vary significantly depending on whether the fire unit is in a movement phase and opposed to a position phase, and within these phases, whether it is engaging a target or whether it is simply on alert. Movement across rough terrain may cause failures even of inoperative subsystems. In addition, the repair possibilities will be much more limited in a movement phase as compared with a position phase.

A method is indicated in the report for including these 'tactical state' transitions in the general state transition description.

Having developed the complete state transition diagram, the necessary fail and repair coefficients are inserted, and the differential equations are solved for the steady state solution (fixed point probability vector).

The elements of the fixed point probability vector are the desired availability and dependability estimates for each operational state and are extracted for combination with the system capability matrix for the effectiveness computation.

For each system evaluated it is probably desirable to develop the state transition diagram in considerable detail before attempting simplifications, to insure that all essential states and transitions are included.

Having made initial estimates at the subsystem level of aggregation described above, those subsystems principally responsible for loss of availability and dependability may be identified, and a more detailed development of the subsystems to component level would follow, to further identify sources of difficulty.

# SECTION 10
# DEVELOPMENT OF AVAILABILITY AND DEPENDABILITY MATRICES

## 10.1 DATA ELEMENT REQUIREMENTS

Data requirements to follow the WSEAIC type of analytical structure up to the determination of the capability vector are listed in Table X-1 as given in a WSEAIC report.[27]

The identification of system, subsystem and component elements has been described in a prior section. The time information as it is related to operational and tactical activity states is derived, as discussed earlier from the 'Battlefield Day'. A more detailed definition of event sequencing is required for the capability vector and will be developed in a later section.

The levels to which reliability and maintainability data are developed depends on the position of the system under analysis in its life cycle, and is outlined in Table V-1.

**Table X-1. Typical Data Element Requirements**

a. General identification information (nomenclature, etc.)

b. Time information (chronological time and sequence of events).
    (1) Operating Times
        (a) mission time and phases
        (b) non mission time
            1) checkout and test time
            2) full on standby
            3) partial on standby
    (2) Non-operating Times
        (a) off, no demand
            1) storage
            2) free time
        (b) downtime (when in demand)
            1) repair time
            2) logistic time (spares, transportation, queuing, other support-oriented items)
            3) administrative time (training, other cause of personnel non-availability)
            4) effect of emergency procedures

c. Event information
    (1) Failure events
        (a) identification of failure
        (b) effect on mission capability
            1) critical
            2) non-critical
        (c) repairable during mission
        (d) how detected
        (e) failure classification
            1) primary
            2) secondary
        (f) cause classification
            1) design
            2) operational environment
                a) controlled
                b) uncontrolled
            3) personnel induced
                a) supplier
                b) user
            4) time-dependent
    (2) Maintenance events
        (a) classes of maintenance (includes monitoring and system exercising)
            1) corrective maintenance
                a) scheduled
                b) unscheduled
        (b) event information
            1) type of action
                a) replacement
                b) adjustment
                c) repairs
                    1. in place
                    2. other location
            2) manhours expended (minimum number of personnel required)
            3) level of personnel
            4) adequacy of equipment and tools
            5) availability and quality of spares
            6) adequacy of facilities
            7) adequacy of technical data
            8) adequacy of maintenance action

20871-606A

In general, in the conceptual stage the simplest possible approximations to the failure and repair process would be used. As the system progresses to development, more detailed information becomes available and more accurate analyses are required. In the concept stage adequate estimates of availability and dependability may be made analytically. When the system is detailed in depth and accurate representations of the probability density functions are desired, it is probably most economical and feasible to use computer simulation.

Some of the levels of approximation and their validity are discussed in the following paragraphs.

## 10.2 GENERAL APPROACH

The presentation of the methodology for determining the availability-dependability parameters for a system is arranged as follows:

a. The discussion is initially limited to 'inherent' availability (to be defined) without regard for tactical states. Methods of simplifying the computation for complex systems are illustrated by a series of examples.

b. The analysis is then extended to include tactical states of the system. It is indicated that this provides an additional measure of realism, and that the extension is feasible. Approximation methods are illustrated by examples.

Most of the literature on reliability, maintainability and availability theory describes how to solve exactly, relatively simple cases. The solution of complex cases is easily written concisely but with the implied inversion of large matrices for the determination of the fixed point probability vector, and the solution by eigenvalues and eigenvectors of the transient solution. These methods are time-consuming for the analyst, and so at the expense of space, and perhaps, the reader's patience, a number of devices for obtaining useful approximations are developed with examples in the following sections.

## 10.3 DEFINITION OF AVAILABILITY

Consider a system or subsystem which has only two states, (1) fully operational and available for use, and (2) inoperative. The system may be inoperative because of a failure which has not yet been repaired or because it is down for preventive maintenance. In the field the down time would include not only the active repair time when the system is being worked on, but also the time waiting for spares, for maintenance personnel, etc.

Over a very long period of time, the fraction of time that the system is in an operational state is defined as 'availability'. The computation of this value does not usually require identification of the probability density functions of the time durations of the operative state or of each separate contributing action to the down state.

Insight into what factors contribute most to reduction in availability is provided by computing availability under several assumptions of support and environmental conditions, and standard definitions of availability recognize several categories depending on how many of the elements constituting total downtime are included in the measure. The standard definitions are reproduced in a following paragraph.

The highest value is that of 'inherent' availability, which is measured by running the system continuously to failure, then repairing promptly with all required resources on hand, then running to the next failure, etc.

'Achieved' availability is a similar computation, in an 'ideal' support environment, but includes downtime from both preventive and corrective maintenance actions.

'Operational' availability includes lost time because of delays in supply and administrative action.

TAERS data from 1963[21] showing the percentage of downtime in direct support maintenance in the categories of (1) in transit, (2) awaiting repair, (3) shop time and (4) MWO, indicates shop time is only about 27% for the M113 vehicle, 32% for radio set AN/GRC-19 and 55% for the UH-1B helicopter, as fractions of total downtime.

If the support system is not improved, one might reasonably apply a multiplying factor of 2 to 5 on the mean active repair time associated with any particular subsystem of AFAADS, for example.

### 10.3.1 Standard Categories of Availability Estimates[22]

availability (achieved).* The probability that a system or equipment when used under stated conditions in an ideal support environment (i.e., available tools, parts, manpower, manuals, etc.) shall operate satisfactorily at any given time. $A_a$ excludes supply downtime and waiting or administrative downtime. It may be expressed as:

$$A_a = \frac{MTBM}{MTBM + M}$$

20871-800

where

MTBM = Mean-time-between-maintenance.

M = Mean active maintenance downtime re-

*Terms identified by an asterisk taken from MIL-STD-778, Maintainability Terms and Definitions.

*sulting from both* preventive and corrective maintenance actions.

availability (inherent).* The probability that a system or equipment when used under stated conditions, without consideration for any scheduled or preventive maintenance, in an ideal support environment (i.e., available tools, parts, manpower, manuals, etc.), shall operate satisfactorily at any given time. $A_i$ excludes ready time, preventive maintenance downtime, supply downtime, and waiting or administrative downtime. It may be expressed as:

$$A_i = \frac{MTBF}{MTBF + MTTR}$$

20871-801A

where

MTBF = Mean-time-between failure.

MTTR = Mean-time-to-repair.

availability (operational).* The probability that a system or equipment when used under stated conditions and in an actual supply environment shall operate satisfactorily at any given time. It may be expressed as:

$$A_0 = \frac{MTBM}{MTBM + MDT}$$

20871-802

where

MTBM = Mean-time-between-maintenance and ready time during the same time interval, and

MDT = Mean downtime including supply downtime and administrative downtime during the same time interval. When preventive maintenance downtime is zero or not considered, MTBM becomes MTBF.

*Terms identified by an asterisk taken from MIL-STD-778, Maintainability Terms and Definitions.*

## 10.4 INHERENT AND ACHIEVED AVAILABILITY

To illustrate the approach and the kind of assumptions we propose to make in this report, consider the simple case of the system which has only two states (1) all up, and (2) inoperative.

Let:

$X_1(t)$ = the probability that the system is 'up' at time t.

$X_2(t)$ = the probability that the system is inoperative at time t.

$$X_1(t) + X_2(t) = 1.0 \qquad (10.1)$$

The transition rates across the two states may be written in general form as

$$dX_1(t)/dt = f_1[X_1, X_2, \lambda, \mu, t] \qquad (10.2)$$

$$dX_2(t)/dt = f_2[X_1, X_2, \lambda, \mu, t] \qquad (10.3)$$

where

$\lambda(t)$ is a failure related function of time

$\mu(T)$ is a repair related function of time

and the general formulation admits consideration of the fact that the system may be more likely to fail as it gets older, the likelihood of failure depends on the elapsed time since the last repair, etc.

In a computer simulation we would have a good deal of freedom in defining these relationships in complex form.

However for a first approximation we make the following simplification:

a. The probability that a failure occurs in dt given that the system is operating, is independent of t, and is equal to $\lambda dt$.

b. The probability that a repair action is completed in dt, given that the system is down for repair, is independent of t and is equal to $\mu dt$.

Then

$$\dot{X}_1 = -\lambda X_1 + \mu X_2$$

$$\dot{X}_2 = \lambda X_1 - \mu X_2 \qquad (10.4)$$

Assume that at an initial time $t = 0$ the system is operating. Then solving the differential equations

$$X_1(t) = \frac{\mu}{\lambda+\mu} + \frac{\lambda}{\lambda+\mu} e^{-(\lambda+\mu)t}$$

$$X_2(t) = \frac{\lambda}{\lambda+\mu} - \frac{\lambda}{\lambda+\mu} e^{-(\lambda+\mu)t} \qquad (10.5)$$

The system approaches a 'steady state' as defined by the exponential

$$e^{-(\lambda+\mu)t} \qquad (10.6)$$

and if either the fail rate $\lambda$ or the repair rate $\mu$, or both are large, the steady state is quickly achieved.

The steady state solution for $X_1$

$$X_1(\infty) = \frac{\mu}{\lambda+\mu} \qquad (10.7)$$

This is the probability that the system will be in an operable state if it is observed at an arbitrary time after it has been operating for a long time. It is also, the fraction of the total time that it is operable, for very long observation times.

$X_1(\infty)$ is defined as availability.

The steady state solutions could have been obtained directly by setting the derivatives equal to zero in the differential equations and solving for $X_1$ and $X_2$, using $X_1 + X_2 = 1.0$.

If there is no repair, and the system begins operation at $t=0$ in an operable state

$$X_1(t) = e^{-\lambda t} \qquad (10.8)$$

and this expression is a definition of 'dependability' during a no-repair interval.

Notation can be simplified when the number of system modes becomes large by using matrix notation. The differential equations can be written

$$\dot{X} = A X \qquad (10.9)$$

where

$$X = \begin{bmatrix} X_1 \\ X_2 \end{bmatrix} \quad ; \quad A = \begin{bmatrix} -\lambda & \mu \\ \lambda & -\mu \end{bmatrix} \qquad (10.10)$$

The mean time between recurrence of a state when $\dot{X} = 0$, is the inverse of the state probability multiplied by average rate of departure from the state. For this simple model, the mean time between failures MTBF and the mean time between repairs MTBR (the system cycle time) are equal

$$\text{MTBF} = \text{MTBR} = (1/\lambda)\left[(\lambda+\mu)/\mu\right]$$

$$= (1/\mu)\left[(\lambda+\mu)/\lambda\right] \qquad (10.11)$$

The mean up time (MUT) is the mean time that the system remains in an operational state and is the inverse of the rate of leaving the state

$$\text{MUT} = 1/\lambda \qquad (10.12)$$

Similarly the mean down time (MDT) is

$$\text{MDT} = 1/\mu \qquad (10.13)$$

and

$$\text{MTBF} = \text{MTBR} = (\text{MUT}) + (\text{MDT})$$

These separate measures allow one to discriminate between a system that fails frequently but can be repaired quickly, and a system that fails rarely, but takes a long time to repair both systems having the same availability.

The assumptions of constant transition rates with time is easier to justify as an adequate approximation in the fail mode than in the repair mode. Probability density functions of maintenance times (especially in computing achieved availability) are not simple exponentials, and most maintenance analysts prefer to describe them by lognormal functions. We show how to handle this apparent difficulty in a later section, but note at this time that the effect appears principally in the transient solution of Equation (10.9). Its effect on

the steady state solution, which is basic to the availability concept, is much smaller.

### 10.4.1 Multiple Failure Modes

When there are many components to be considered, solution along the above lines can be tedious. Usually, however, we are interested only in determining the steady state probabilities of a small number of operational states and have no interest in the relative probabilities of the down states.

In many cases the following approach can be used, or imbedded in a larger problem to reduce its complexity.

Consider a system which has n components, all of which must be operable for the system to be in an operable state. Assume that component failures occur only when the system is operating, that repair begins immediately, that the fail and repair actions are 'Poisson' streams of events, with $\lambda_j$, $\mu_j$ the fail and repair rates of the j'th component. Let $X_o$ = probability that the system is operational and $X_j$ the probability it is down because of failure of the j'th component.

The differential equations are

$$\dot{X}_0 = -\sum_{j=1}^{n} \lambda_j X_0 + \sum_{j=1}^{n} \mu_j X_j \qquad (10.14)$$

$$\dot{X}_j = \lambda_j X_0 - \mu_j X_j \qquad (10.15)$$

These expressions are easily solved for the steady state

$$X_j = (\lambda_j/\mu_j) X_0 \quad j = 1,2,\ldots n \qquad (10.16)$$

and since

$$\sum_{j=0}^{n} X_j = 1.0 \qquad (10.17)$$

$$X_0 + \sum_{j=1}^{n} X_j = 1.0 \qquad (10.18)$$

$$X_0 = \frac{1}{1+\sum_{j=1}^{n}(\lambda_j/\mu_j)} \quad ; \quad X_0 = A_v = \text{availability} \qquad (10.19)$$

The original expression could have been written in matrix form

$$\dot{X} = A X \qquad 10.20)$$

$$A = \begin{bmatrix} -\sum_{j=1}^{n}\lambda_j & \mu_1 & \mu_2 \cdots & \mu_n \\ \lambda_1 & -\mu_1 & 0 \cdots & 0 \\ \lambda_2 & 0 & -\mu_2 \cdots & 0 \\ \vdots & \vdots & \vdots & \vdots \\ \lambda_n & 0 & 0 \cdots & -\mu_n \end{bmatrix}$$

(10.21)

$$\text{MTBF} = \frac{1}{X_0 \sum_{j=1}^{n} \lambda_j} \quad (10.22)$$

$$\text{MTBF} = \frac{1 + \sum_{j=1}^{n} (\lambda_j/\mu_j)}{\sum_{j=1}^{n} \lambda_j} \quad (10.23)$$

$$\text{MUT} = A_V(\text{MTBF}) = X_0(\text{MTBF}) \quad (10.24)$$

$$\text{MUT} = \frac{1}{\sum_{j=1}^{n} \lambda_j} \quad (10.25)$$

$$\text{MDT} = (1 - A_V)\text{MTBF} = \text{MTBF} - \text{MUT} \quad (10.26)$$

$$\text{MDT} = \frac{\sum_{j=1}^{n} (\lambda_j/\mu_j)}{\sum_{j=1}^{n} \lambda_j} \quad (10.27)$$

To be more specific, suppose that we have ten components with identical fail and repair rates. Then

$$\text{MTBF} = \frac{1}{10\lambda} + \frac{1}{\mu}$$

$$\text{MUT} = \frac{1}{10\lambda}$$

$$\text{MDT} = \frac{1}{\mu}$$

$$X_0 = A_V = \frac{1}{1 + 10(\lambda/\mu)} \quad (10.28)$$

### 10.4.2 Approximate Computation

For the case of this system with n components, all of which must be operational in order that the system operate, and with the repair action on each component independent of that on all others, we now consider what error would be introduced by computing the system availability as the product of the availabilities of the n components. This is equivalent to the assumption that the failure probability of each component is independent of whether the system as a whole is operating.

For the j'th component, the steady state probability of operation is

$$Y_j = \frac{1}{1 + (\lambda_j/\mu_j)} \quad (10.29)$$

and for the system we approximate

$$X_0 = \prod_{j=1}^{n} Y_j = \prod_{j=1}^{n} \frac{1}{1 + (\lambda_j/\mu_j)} \quad (10.30)$$

expanding the product

$$X_0 = \frac{1}{1 + \sum_{j=1}^{n} (\lambda_j/\mu_j) + \sum_{j=1}^{n} \sum_{\substack{k=1 \\ j \neq k}}^{n} (\lambda_j/\mu_j)(\lambda_k/\mu_k) + \cdots} \quad (10.31)$$

and if all the $\lambda_i/\mu_i << 1.0$ the two methods give the same results.

### 10.4.3 System with Alternate Operational Modes

The complexity of the full analysis increases rapidly as the number of alternate operational modes is increased. We illustrate this by a simple example, and show how to obtain an adequate approximate solution simply.

The system states and transitions are shown in Figure 10-1. The system is assumed to have a primary operational mode depending on an Infra-red tracker. If the IR sensor is inoperative, the system can be employed with visual tracking. In addition, a set of elements (here aggregated into one and called 'servo')

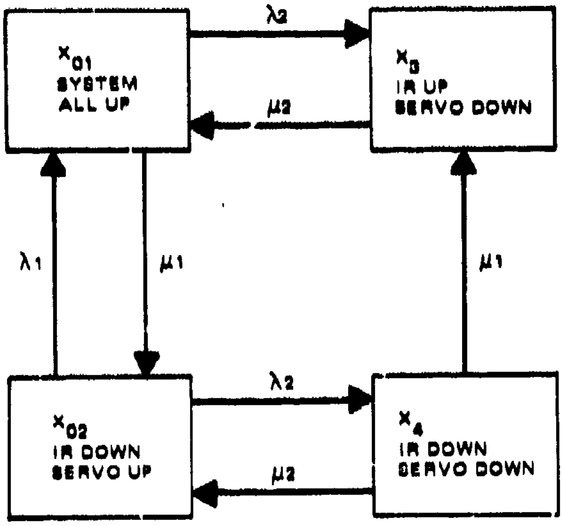


20871-261

Figure 10-1. State Transition Diagram for System with Two Operational Modes

is essential to operation in either mode. The states are defined by the probabilities (all at time t).

$X_{01}$ = probability the system is 'all up'.

$X_{02}$ = probability that the system is operable in the visual mode with the IR unit down and under repair.

$X_3$ = probability that the system is inoperative with the IR unit up, servos down and under repair.

$X_4$ = probability that the system is inoperative with both IR unit and servos down and under repair.

Note that some assumption must be made as to repair doctrine when both the IR unit and the servos are down. Depending on maintenance support and the type of malfunction, they may be repaired in sequence, or simultaneously. We use the latter assumption, with different repair rates for the two units.

The state transitions are developed in Figure 10-1.

In matrix form, the differential equations for state transition rates are given by

$$\begin{bmatrix} \dot{X}_{01} \\ \dot{X}_{02} \\ \dot{X}_3 \\ \dot{X}_4 \end{bmatrix} = \begin{bmatrix} -(\lambda_1+\lambda_2) & \mu_1 & \mu_2 & 0 \\ \lambda_1 & -(\mu_1+\lambda_2) & 0 & \mu_2 \\ \lambda_2 & 0 & -\mu_2 & \mu_1 \\ 0 & \lambda_2 & 0 & -(\mu_1+\mu_2) \end{bmatrix} \begin{bmatrix} X_{01} \\ X_{02} \\ X_3 \\ X_4 \end{bmatrix} \tag{10.32}$$

To determine the steady state solution (the corresponding set of $X_i$ is known as the 'fixed point probability vector'), set the $dX_i/dt = 0$.

Since the sum of the $X_i$ must equal unity one line of the resulting expression is redundant and we choose to replace the top row by (1,...,1) whence

$$\begin{bmatrix} 1 & 1 & 1 & 1 \\ \lambda_1 & -(\mu_1+\lambda_2) & 0 & \mu_2 \\ \lambda_2 & 0 & -\mu_2 & \mu_1 \\ 0 & \lambda_2 & 0 & -(\mu_1+\mu_2) \end{bmatrix} \begin{bmatrix} X_{01} \\ X_{02} \\ X_3 \\ X_4 \end{bmatrix} = \begin{bmatrix} 1 \\ 0 \\ 0 \\ 0 \end{bmatrix} \tag{10.33}$$

This equation may be solved 1) by inverting the matrix of transition probabilities, 2) expanding and solving the resulting set of equations.

The process is tedious, even for this simple example, but following it through we obtain

$$X_{01} = (1 + R_2 S)/D$$

$$X_{02} = R_1/D$$

$$X_3 = R_2 [(1 + R_2 S) + R_1 (1 - S)]/D$$

$$X_4 = R_1 R_2 S / D \tag{10.34}$$

where

$$R_1 = \lambda_1/\mu_1, \; R_2 = \lambda_2/\mu_2; \; S = \mu_1/(\mu_1 + \mu_2)$$

$$D = (1 + R_1 + R_2 + R_1 R_2) + SR_2 (1 + R_2) \tag{10.35}$$

### 10.4.4 Approximate Solution

In the case of any real system we shall be interested only in systems with high availability (perhaps over 0.80) in the primary all-up state. Systems with low availability need not be evaluated closely, since a rough indication of low availability at this point in the analysis is enough to send the designers back to the drawing board.

This suggests that we expand the availability fixed point probability vector as a Taylor's series in terms of the $\lambda_i$. For almost all (perhaps all) practical purposes, the series need only be carried to terms in $\lambda_i$.

In matrix form, the fixed point probability vector is defined by

$$A\,X = 0 \tag{10.36}$$

Take partial derivatives with respect to each $\lambda_i$, and then set all of the $\lambda_i = 0$ in the resulting expression. The resulting matrices are greatly simplified, are usually easily invertable, oftem by inspection, and in many cases the solution can be written by inspection without resorting to matrix inversion.

The operation is symbolically,

$$A(\lambda)\,X(\lambda) = 0 \tag{10.37}$$

$$[\partial A(0)/\partial\lambda_j]\,X(0) + A(0)\,[\partial X(0)/\partial\lambda_j] = 0 \tag{10.38}$$

and the solution desired to two terms is

$$X(\lambda) = X(0) + \sum_j \lambda_j\, \partial X(0)/\partial\lambda_j \tag{10.39}$$

For the previous example, we obtain from this operation

$$\begin{bmatrix} 1 & 1 & 1 & 1 \\ 0 & -\mu_1 & 0 & \mu_2 \\ 0 & 0 & \mu_2 & 1 \\ 0 & 0 & 0 & -(\mu_1 + \mu_2) \end{bmatrix} \begin{bmatrix} \partial X_{01}/\partial\lambda_j \\ \partial X_{02}/\partial\lambda_j \\ \partial X_3/\partial\lambda_j \\ \partial X_4/\partial\lambda_j \end{bmatrix} = -\partial/\partial\lambda_j \begin{bmatrix} -(\lambda_1 + \lambda_2) \\ \lambda_1 \\ \lambda_2 \\ 0 \end{bmatrix} \tag{10.40}$$

The matrix is triangular and relatively easy to invert, but in this case we can obtain the solution by inspection. Since

$$X_{01}(0) = [1 \;\; 0 \;\; 0 \;\; 0]^T \tag{10.41}$$

we have

$$X_{01} = 1 - R_1 - R_2$$

$$X_{02} = R_1$$

$$X_3 = R_2$$

$$X_4 = 0 \tag{10.42}$$

For this first order approximation, state $X_4$ drops out since it involves two subsystems inoperative at the same time.

Referring back to the exact solution, it is apparent that when $R_1, R_2 << 1.0$, the exact solution reduces to the simple approximation.

### 10.4.5 Generalization and Example

If, as alleged earlier, we are interested in going forward with the analysis of only systems having high availabilities, it follows that failure states resulting

Table X-2. Subsystem Fail and Repair Parameters

| Subsystem | Data Elements | Failure Rate $\lambda_j$ | Repair Rate $\mu_j$ | $\lambda_j/\mu_j$ |
|---|---|---|---|---|
| Radar | Range, Angle | 0.02 | 1.0 | 0.02 |
| Infrared Tracker | Angle | 0.015 | 1.0 | 0.015 |
| Laser Tracker | Range, Angle | 0.01 | 1.0 | 0.01 |
| Supporting Subsystem | | 0.02 | 1.0 | 0.02 |

20871-607

from more than one subsystem or component being simultaneously inoperative will have a very low probability of occurrence compared with those involving only one failure. Hence we should be able, almost always, to neglect them in systems of interest.

This rationale can be employed at the level of the state transition diagram, where multiple failure mode states can be eliminated by inspection, or by the series expansion method described above. Infrequently, one may be interested in double failure modes. In this case the Taylor series expansion can be extended one term, at the expense of complexity.

For an example of the validity of the single component failure assumption we use a system analysed in a paper by Ebenfelt and Holmqvist.[23] In their paper, the authors carefully worked out the availability by mode, of an antiaircraft defense system which had twenty-two possible states, of which eight were operational states.

In the referenced paper, a fire control system is assumed having the following characteristics (Table X-2).

The fire control system is operational if any set of sensors is operational which provides both angle and range. The system is non-operational if either range or angle is not available, or if the supporting subsystem is down.

The 'all-up' availability of the system computed exactly in the referenced paper is 0.9363. Our approximate method gives

$$a_1 = 1 - \sum(\lambda_j/\mu_j) = 0.935 \qquad (10.43)$$

more exactly

$$a_1 = \frac{1}{1 + \sum(\lambda_j/\mu_j)} = 0.9367 \qquad (10.44)$$

However the 'all-up' case is the simplest to compute in any event.

There are eight possible operational states according to the definition given above of an operational state. We compare two levels of approximation against the exact figures computed in the reference. These are

a. When only one subsystem is down, the availability in the corresponding state equals the ratio $\lambda_i/\mu_i$ for the down system. If the state has two subsystems down, its probability is zero.

b. Same as the above, but for the two subsystem down case, the availability is the product of the $\lambda_i/\mu_i$ of the two down subsystems.

As in the reference, the state is identified by indicating the down subsystems after the state number in the order of their failure (Table X-3). (The reference gives an order-of-repair doctrine which is needed to work out the exact solution.)

Since the exact solution has some 64 elements in the state transition matrix, it is clear that the simple approximation suggested above has much to recommend it for the initial evaluation of any system.

## 10.5 OPERATIONAL AVAILABILITY AND DEPENDABILITY

We now superimpose the considerations of tactical states on the availability models developed in the preceding section. A moderate amount of algebra is

Table X-3. Comparison of Computational Methods

| Operational States | Availability | | |
|---|---|---|---|
| | Exact | Approximation 1 | Approximation 2 |
| 1. All up | 0.9363 | 0.935 | 0.935 |
| 2. Radar down | 0.0140 | 0.02 | 0.02 |
| 3. Radar, IR, down | 0.0002 | 0 | 0.0003 |
| 4. IR down | 0.0168 | 0.015 | 0.015 |
| 5. IR Radar down | 0.0003 | 0 | 0.0003 |
| 6 IR, Laser down | 0.0002 | 0 | 0.0002 |
| 7. Laser down | 0.0112 | 0.01 | 0.01 |
| 8. Laser, IR, down | 0.0002 | 0 | 0.0002 |

20871-608

involved, but as will be seen, this needs to be gone through only once for a specified stochastic 'battlefield day' after which the determination of availability-dependability for specific systems is relatively simple. The method also has the advantage that it gives the probabilities of state availability in the combat states directly.

### 10.5.1 Method of Analysis

Referring back to the description of the battlefield day, it will be noted that two movement states were identified, and three tactical activity states were identified within each movement state. In the following, to conserve space, we delete the 'passive' state in each movement state. However, separate analysis indicates that there is only moderate additional work in including it.

The method is to work down from 'top level' state aggregates by matrix partitioning until the system operational states are reached. This has the advantage that state transition rates which are common to subsets of states can be manipulated economically.

The procedures are best described by example. The process is outlined in Figure 10-2. Beginning with the top level states, the system is progressively detailed to lower levels. At each level, the steady state solution is 'normalized' by matrix manipulation, so that by the time one has worked down through the second level, the resulting matrix to be inverted, or otherwise solved, is only n x n, if the system has n 'operational' states, where 'operational' states are distinguished from movement and tactical activity states.

The top level expression is

$$A\,X = 0 \qquad (10.45)$$

Expand the matrix and vector to describe transitions between the movement and non-movement states.

$$\begin{bmatrix} N_1 \cdot aI & bI \\ aI & N_2 \cdot bI \end{bmatrix} \begin{bmatrix} X_1 \\ X_2 \end{bmatrix} = 0 \qquad (10.46)$$

where $N_1, N_2$ describe transitions that occur only *within* $X_1, X_2$ respectively.

The fractions of time spent in $X_1, X_2$ (designated as $F_1$, $F_2$, $F_1 + F_2 = 1$) are obtained by setting $N_1, N_2 = 0$ and solving the above expressions, obtaining

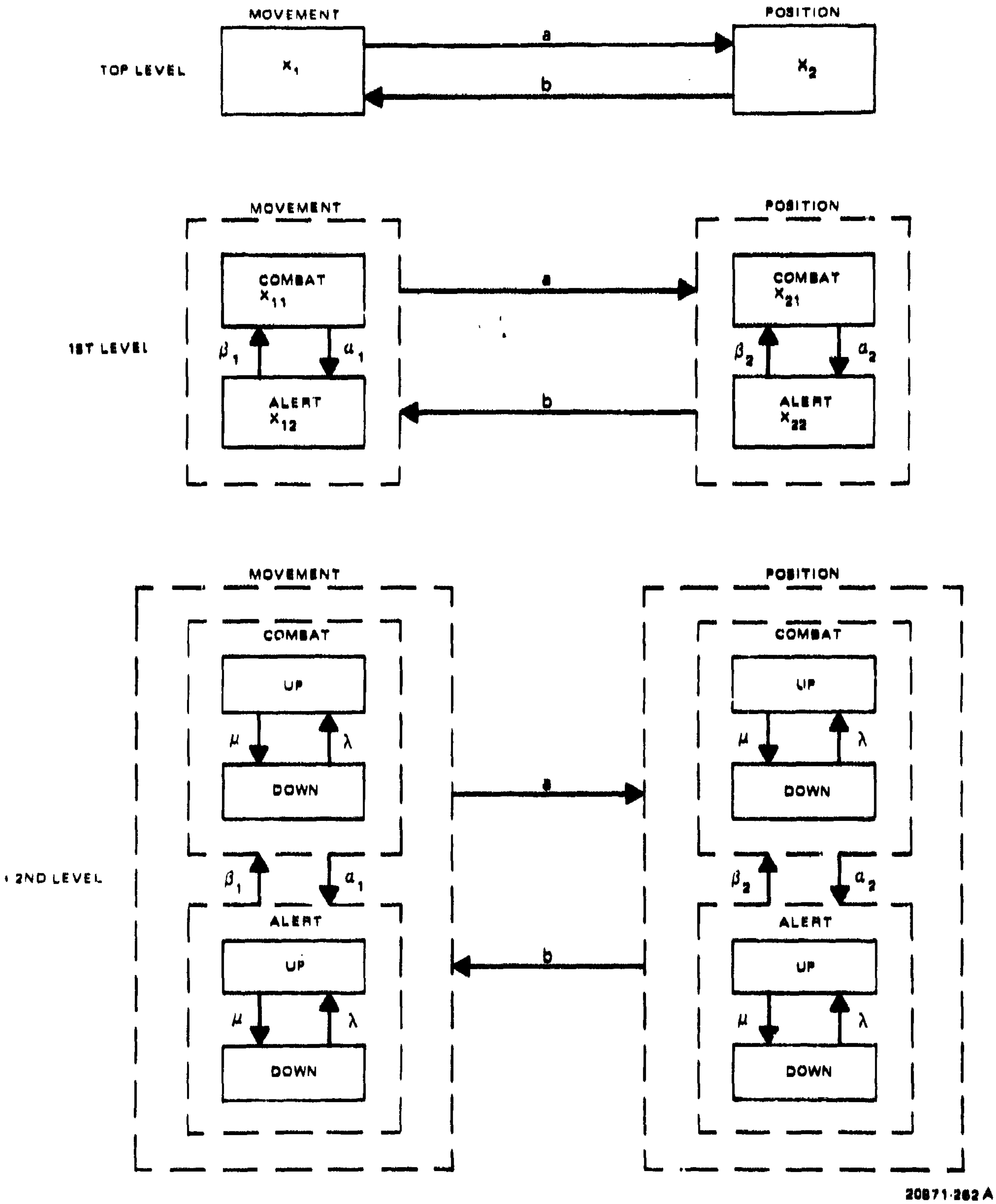


Figure 10-2. Progressive Development of Sub-states

$$F_1 = \frac{b}{a+b} \; ; F_2 = \frac{a}{a+b} \qquad (10.47)$$

normalize the matrix equation as follows

$$\begin{bmatrix} F_1 [N_1 - aI] & F_2 bI \\ F_1 aI & F_2 [N_2 - bI] \end{bmatrix} \begin{bmatrix} X_1/F_1 \\ X_2/F_2 \end{bmatrix} = 0$$

(10.48)

Substitute the values for F within the matrix and write Y = X/F

$$\begin{bmatrix} N_{1a} - I & I \\ I & N_{2b} - I \end{bmatrix} \begin{bmatrix} Y_1 \\ Y_2 \end{bmatrix} = 0 \qquad (10.49)$$

where

$$N_{1a} = a^{-1} N_1 \; ; \; N_{2b} = b^{-1} N_2 \qquad (10.50)$$

Since the normalization makes all elements of $Y_1$ sum to unity and all elements of $Y_2$ sum to unity, the problem can be separated into two parts by solving for $Y_1, Y_2$ from the above expression.

$$[N_{1a} + N_{2b} - N_{2b} N_{1a}] Y_1 = 0$$

(10.51)

$$[N_{1a} + N_{2b} - N_{1a} N_{2b}] \; Y_2 = 0$$

(10.52)

Next expand the matrices and vectors to identify the separate alert and combat states within each movement state. We need work only with $Y_1$ since the expressions are symmetrical and we can write each by inspection from the solution to the other.

The transition rates between combat and alert need not be the same in the movement and position states. At this level we also explicity show the system operational state transition matrix M. M will be different in each of the four substates. The $N_1, N_2$ matrices expanded before normalization are, where the $\alpha$, $\beta$ are transitions between combat and alert.

$$N_1 = \begin{bmatrix} M_1 - \alpha_1 I & \beta_1 I \\ \alpha_1 I & M_2 - \beta_1 I \end{bmatrix} \qquad (10.53)$$

$$N_2 = \begin{bmatrix} M_3 - \alpha_2 I & \beta_2 I \\ \alpha_2 I & M_4 - \beta_2 I \end{bmatrix} \qquad (10.54)$$

These are divided by a, b respectively

$$N_{1a} = \begin{bmatrix} M_{1a} - \alpha_{1a} I & \beta_{1a} I \\ \alpha_{1a} I & M_{2a} - \beta_{1a} I \end{bmatrix} \qquad (10.55)$$

$$N_{2b} = \begin{bmatrix} M_{3a} - \alpha_{2b} I & \beta_{2b} I \\ \alpha_{2b} I & M_{4b} - \beta_{2b} I \end{bmatrix} \qquad (10.56)$$

Substituting these expressions into the relation for $Y_1$ and expanding,

$$\begin{bmatrix} B_{11} - c_1 I & B_{12} + c_2 I \\ B_{21} + c_1 I & B_{22} - c_2 I \end{bmatrix} \begin{bmatrix} Y_{11} \\ Y_{12} \end{bmatrix} = 0 \qquad (10.57)$$

where

$$c_1 = \alpha_{2b} + \alpha_{1a} (1 + \alpha_{2b} + \beta_{2b})$$

$$c_2 = \beta_{2b} + \beta_{1a} (1 + \alpha_{2b} + \beta_{2b}) \qquad (10.58)$$

and

$$B_{11} = M_{1a} + M_{3b} - M_{1a} M_{3b} + M_{1a} \alpha_{2b} + M_{3b} \alpha_{1a}$$

$$B_{22} = M_{2a} + M_{4b} - M_{2a} M_{4b} + M_{2a} \beta_{2b} + M_{4b} \beta_{1a}$$

$$B_{12} = -M_{2a} \beta_{2b} - M_{3b} \beta_{1a}$$

$$B_{21} = -M_{1a} \alpha_{2b} - M_{4b} \alpha_{1a} \qquad (10.59)$$

As before, we can determine the way in which the time spent in $Y_1$ divides between $Y_{11}$ and $Y_{12}$ by setting the $B_{jk} = 0$ and solving to obtain

$$F_{11} = \frac{c_2}{c_1 + c_2} \; ; \; F_{12} = \frac{c_1}{c_1 + c_2} \qquad (10.60)$$

Again normalizing, with $Z = Y/F$

$$\begin{bmatrix} C_{11} - 1 & C_{12} + 1 \\ C_{21} + 1 & C_{22} - 1 \end{bmatrix} \begin{bmatrix} Z_{11} \\ Z_{12} \end{bmatrix} = 0 \qquad (10.61)$$

where

$$C_{11} = B_{11}/c \; ; \; C_{12} = B_{12}/c \; ;$$

$$C_{21} = B_{21}/c \; ; \; C_{22} = B_{22}/c \qquad (10.62)$$

On solving for $Z_{11}, Z_{22}$ in matrix form we now find that we must invert at least one of the matrices including a $C_{jk}$. Now each of the $C_{jk}$ turns out to be Markovian, however, for the most general form of the constituent M (system operational matrix) the inversion is tedious, but possible. There are two ways of circumventing this problem.

a. Choose a 'worst case' and allow no repairs during movement, and no repairs during the combat substate of the position state. This leaves only $M_4$ as the matrix with both fail and repair states, and inversion of the other matrices is simple.

b. Apply the Taylor's series expansion described earlier, in which case all of the required matrices are easy to invert.

For reference we show the matrix inversion for matrices containing only failure transition probabilities or only repair transition probabilities.

First consider

$$[I - L]^{-1} \qquad (10.63)$$

where L is a matrix containing only failure transition probabilities.

$$[I - L]^{-1} = \begin{bmatrix} 1 + \Sigma L_j & 0 & 0 & \cdot \\ -L_1 & 1 & 0 & \cdot \\ -L_2 & 0 & 1 & \cdot \\ \cdot & \cdot & \cdot & \cdot \end{bmatrix}^{-1} = \begin{bmatrix} \frac{1}{1 + \Sigma L_j} & 0 & 0 & \cdot \\ \frac{L_1}{1 + \Sigma L_j} & 1 & 0 & \cdot \\ \frac{L_2}{1 + \Sigma L_j} & 0 & 1 & \cdot \\ \cdot & \cdot & \cdot & \cdot \end{bmatrix} \qquad (10.64)$$

so that

$$[I - L]^{-1} = I + (1 + \Sigma L_j)^{-1} [L] \qquad (10.65)$$

Next consider

$$[I - M]^{-1} \qquad (10.66)$$

where M is a matrix containing only repair transition probabilities.

$$[I - M]^{-1} = \begin{bmatrix} 1 & -m_1 & -m_2 & \cdot \\ 0 & 1 + m_1 & 0 & \cdot \\ 0 & 0 & 1 + m_2 & \cdot \\ \cdot & \cdot & \cdot & \cdot \end{bmatrix}^{-1} = \begin{bmatrix} 1 & \frac{m_1}{1 + m_1} & \frac{m_2}{1 + m_2} & \cdot \\ 0 & \frac{1}{1 + m_1} & 0 & \cdot \\ 0 & 0 & \frac{1}{1 + m_2} & \cdot \\ \cdot & \cdot & \cdot & \cdot \end{bmatrix} \qquad (10.67)$$

whence

$$[I - M]^{-1} = I + [M] \begin{bmatrix} 1 & 0 & 0 & . \\ 0 & \frac{1}{1+m_1} & 0 & . \\ 0 & 0 & \frac{1}{1+m_2} & . \\ . & . & . & . \end{bmatrix} \qquad (10.68)$$

Note, however, that if one wishes to compare a variety of systems for a specified set of movement and tactical activity states, the progression of analysis through the second level needs to be done only once, since only the M matrices will differ across systems.

### 10.5.2 Explicit Solution of Particular Case

To relate the foregoing algebra to reality, we choose an abbreviated example, in which there are only two tactical states, with fail and repair possible in each state, but at different rates. In accordance with our prior conclusion regarding multiple simultaneous failure modes, we consider only single fail modes for the system.

The matrix equation for one of the tactical states is

$$[N_{1a} + N_{2b} - N_{2b}N_{1a}]\, Y_1 = 0 \qquad (10.69)$$

where the N are now the system operational state transition matrices which we expand as follows, in terms of fail and repair rates.

$$N_{1a} = \begin{bmatrix} -\Sigma\lambda_{a1} & \mu_{a1} & \mu_{a2} & . & . \\ \lambda_{a1} & -\mu_{a1} & 0 & . & . \\ \lambda_{a1} & 0 & -\mu_{a2} & . & . \\ . & . & . & . & . \end{bmatrix} \qquad (10.70)$$

$$N_{2b} = \begin{bmatrix} -\Sigma\lambda_{b1} & \mu_{b1} & \mu_{b2} & . & . \\ \lambda_{b1} & -\mu_{b1} & 0 & . & . \\ \lambda_{b2} & 0 & -\mu_{b2} & . & . \\ . & . & . & . & . \end{bmatrix} \qquad (10.71)$$

Although we could multiply the matrices and solve the resulting expression for the $Y_{ij}$ the algebra becomes tedious. Instead we use the ruse of expanding $Y_i$ in a series in the $\lambda$.

Writing the original expression as

$$A\,Y = 0 \qquad (10.72)$$

take the partial derivative with respect to $\lambda_{a1}$, then set all $\lambda = 0$

$$A_o\,[\partial Y/\partial\lambda_{a1}] + [\partial A_o/\partial\lambda_{a1}]\, Y_o = 0 \qquad (10.73)$$

where the subscript (o) indicates that the $\lambda = 0$. Also, if there are no failures

$$Y_o^T = [1\ \ 0\ \ 0\ \ .\ \ .] \qquad (10.74)$$

Performing the operations

$$\begin{bmatrix} 0 & \mu_{b1}+\mu_{a1}+\mu_{b1}\mu_{a1} & \mu_{b2}+\mu_{a2}+\mu_{b2}\mu_{a2} & . \\ 0 & -\mu_{b1}-\mu_{a1}-\mu_{b1}\mu_{a1} & 0 & . \\ 0 & 0 & -\mu_{b2}-\mu_{a2}-\mu_{b2}\mu_{a2} & . \\ . & . & . & . \end{bmatrix} \begin{bmatrix} \partial Y_{10}/\partial\lambda_{a1} \\ \partial Y_{11}/\partial\lambda_{a1} \\ \partial Y_{12}/\partial\lambda_{a1} \\ . \end{bmatrix} = \begin{bmatrix} 1+\mu_{b1} \\ -(1+\mu_{b1}) \\ 0 \\ . \end{bmatrix} \qquad (10.75)$$

The solution of the above is easily obtained by inspection and it can at once be generalized to all of the other $\lambda_a$.

It is

$$\frac{\partial Y_{10}}{\partial\lambda_{aj}} = \frac{-(1+\mu_{bj})}{\mu_{bj}+\mu_{aj}+\mu_{bj}\mu_{aj}}$$

$$\frac{\partial Y_{1j}}{\partial\lambda_{aj}} = -\frac{\partial Y_{10}}{\partial\lambda_{aj}}$$

$$\frac{\partial Y}{\partial\lambda_{aj}} = 0\ ;\ k \neq 0, j \qquad (10.76)$$

Repeating the above operations, but differentiating with respect to the $\mu_{bj}$ we obtain

$$M_o\,\partial Y/\partial\mu_{bj} = \begin{bmatrix} 1 \\ -1 \\ 0 \end{bmatrix} \qquad (10.77)$$

where $M_o$ is the same $\mu$ matrix previously derived

We can now write the full solution as

$$Y_{1j} = \frac{\lambda_{aj}(1+\mu_{bj})+\lambda_{bj}}{\mu_{aj}+\mu_{bj}+\mu_{aj}\mu_{bj}} \tag{10.78}$$

$$Y_{10} = 1-\sum_j Y_{1j} \tag{10.79}$$

The solution for the complementary state $Y_2$ and its sub-states is obtained by simply interchanging the a,b subscripts in the above expression.

We can now make the effect of relative system time in the 1,2 top level states explicit by remembering that the mean time in state 1 in $T_a = 1/a$ and the mean stay in state 2 is $T_b = 1/b$. In the first normalization operation each $\lambda$ and $\mu$ was divided by a or b as appropriate. Writing $L_{aj}$ = failure rate before dividing by a, so that

$$L_{aj} = a\lambda_{aj}$$

and

$$M_{aj} = a\mu_{aj} \tag{10.80}$$

with similar expressions for b,

$$Y_{1j} = \frac{L_{aj}T_a(1+M_{bj}T_b)+L_{bj}T_b}{M_{aj}T_a+M_{bj}T_b+(M_{aj}T_a)(M_{bj}T_b)} \tag{10.81}$$

$$Y_{10} = 1-\sum_j Y_{1j} \tag{10.82}$$

To clarify the meaning of the expression consider a case in which failures occur only in state (1), and repairs only are made in state (2). For the j'th state (component j down),

$$Y_{1j} = L_{aj}T_a + \frac{L_{aj}T_a}{M_{bj}T_b} \tag{10.83}$$

The first term represents failures which occur during state (1) when no repair is allowed. The second term represents the recycling of prior failures for which repair was not completed in state (2).

If we observe component j in state 2 we find

$$Y_{2j} = \frac{L_{aj}T_a}{M_{bj}T_b} \tag{10.84}$$

which represents the residue of uncorrected failures in state (2).

Next, to be even more explicit, we consider the application of the methodology to a specific system configuration.

### 10.5.3 Evaluation of Specific Fire Unit Configuration

Consider a fire unit with the following characteristics, which display a multitude of possible operational modes:

The fire unit mounts both a surveillance and a tracking radar. Each radar has its own servo system and is independently driven. An optical sight is normally slaved to the tracking radar, but can be independently controlled by a human operator with a drive controller.

In the human operator tracking mode the angular tracking data is normally processed by the fire control computer but if the computer is out, it can be bypassed, in which case the operator lays the gun directly and estimates lead on a fixed reticle in his sight.

With the computer functioning the gun is laid automatically to the computer generated firing data.

If either the surveillance radar or the IFF unit is out, the corresponding function is performed visually.

If all system power is off the gun can still be laid manually by handwheels, but the possible tracking rates are so low that this mode can be used only against fixed targets or for barrage fire.

The various operational modes are indicated in the diagram of Figure 10-3. Considering all combinations yielding a possible operational state one finds 25 operational states. Even without considering the many down states that must be considered, this makes for an impressive matrix of state transition probabilities.

If, however, one assumes that no system will be acceptable in which any single subsystem has less than about 0.80 availability, it is possible to ignore all operational states containing more than one failed subsystem.

For the hypothetical system the number of operational states to be considered then reduces from 25 to 6, as follows

a. System all up.

b. Surveillance radar only down.

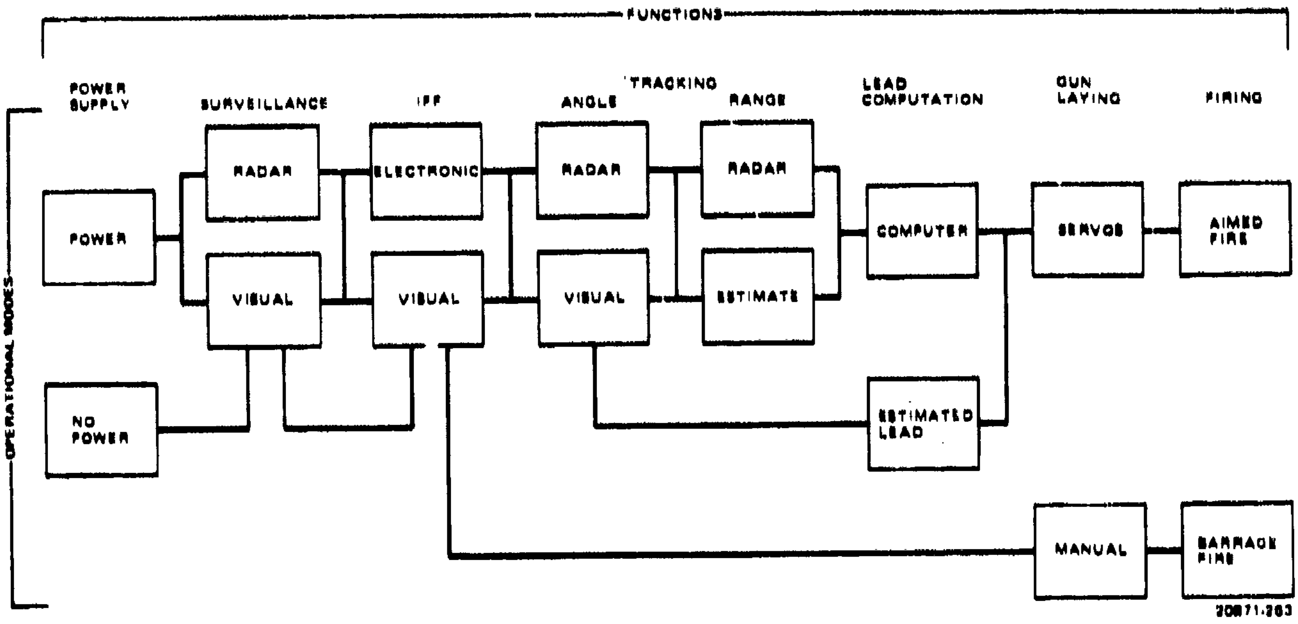


Figure 10-3. Operational Modes of a Hypothetical Fire Unit

c. IFF unit only down.

d. Tracking radar only down.

e. Computer and associated input-output devices only down.

f. Gun servos or power supply only down.

This is a manageable number.

The subsystems identified above are next developed in Table X-4 showing the mean time to failure from an operational state and the mean time to repair, for each component.

The table shows these parameters for each movement phase, and each tactical activity state within a movement phase.

All of the fail and repair rates listed in the table are fictitious. They are intended to indicate the following assumptions.

a. During movement any subsystem may fail even though it is not activated. This is the result of shock and vibration of travel.

b. In the alert state components requiring warm-up have power applied, but only the surveillance radar is fully active. However an occasional false 'red alert' will result in full system activation, although the guns may not be fired.

c. In the combat state the system is fully activated, but only a small fraction of the time represents active firing.

Other decisions are required as to the amount of repair permitted in each state. A worst case is to assume no repair during a movement phase, and no repair during a combat state of a position phase. An alert state of a position phase allows repairs, but the system will of course be down during repairs.

We now abstract the parameters for the position phase, assuming that there is no movement phase, omit the passive phase, and determine how the system availability-dependability depends on the interaction of the tactical and operational states.

We make the following explicit assumptions

a. Only a position phase is involved.

b. Alert is continuous unless interrupted by a combat state.

c. There are no repairs during a combat state.

d. Attacks occur at a mean rate of 0.10 per hour and each corresponding combat state has a mean duration of 1.0 hour. The corresponding mean duration of an alert, non-combat state is 10 hours.

Table X-4. Assumed Failure and Repair Parameters

| | Movement Phase | | | | Position Phase | | | |
|---|---|---|---|---|---|---|---|---|
| | Mean Time to Fail (Hrs) | | | Mean Time to Repair | Mean Time to Fail (Hrs) | | | Mean Active Time to Repair (Non Combat) |
| | Combat | Alert | Passive | | Combat | Alert | Passive | |
| Surveillance Radar Subsystem | 60 | 300 | 500 | No Repair Assumed During Movement Phase | 100 | 500 | – | 3.0 |
| Tracking Radar Subsystem | 30 | 100 | 800 | | 40 | 200 | – | 4.0 |
| IFF Equipment | 80 | 180 | 1000 | | 100 | 200 | – | 1.0 |
| Computer and Input-Output Units | 40 | 800 | 1500 | | 50 | 1250 | – | 3.0 |
| Gun Laying Servo System | 60 | 400 | 800 | | 100 | 800 | – | 4.0 |
| Power Supply | 500 | 1600 | 3000 | | 1000 | 2000 | – | 1.0 |
| All Other Essential Subsystems and Components | 30 | 160 | 1000 | | 50 | 500 | – | 3.0 |

20871-609

From the previously developed Equation 10.81, the probability that the system is 'all up' during the combat state is

$$Y_{oc} = 1 - \sum_j \left\{ \frac{\lambda_{aj}}{\mu_{aj}} + \lambda_{cj} T_c [1 + (\mu_{aj} T_p)^{-1}] \right\} \quad (10.85)$$

The first term within the braces represents the unrepaired failures that occurred during the alert state. The second term has two elements: the first represents new failures during the combat phase; the second represents failures that occurred during prior combat phases on which repair was not completed during prior alert phases.

The corresponding expression for the probability that the system is 'all-up' during the alert phase is

$$Y_{oa} = 1 - \sum_j \left\{ \frac{\lambda_{aj}}{\mu_{aj}} + \frac{\lambda_{cj} T_c}{\mu_{aj} T_a} \right\} \quad (10.86)$$

The probability that the system is not 'all up' but is in a state defined by non-operability of the j'th subsystem is simply the corresponding j'th term in each of the respective braces.

The state probabilities have been worked out numerically for the fail and repair rates given in Table X-4 and are shown in Table X-5.

The probabilities given for the combat state in the table are the equivalent of the availability x dependability operation in the WSEAIC format.[27]

The degradation from unity for the all-up probability in the combat state has the following components

| | |
|---|---|
| Unrepaired failures from the alert state | 0.045 |
| New failures during the combat state | 0.096 |
| Unrepaired failures from prior combat states | 0.030 |
| | 0.126 |

The degradation from unity for the all-up probability in the alert state has the following components

| | |
|---|---|
| Unrepaired failures from prior combat states | 0.030 |
| Unrepaired failures in the alert state | 0.045 |
| | 0.075 |

Table X-5. System State Probabilities

| | Operational State | Tactical State | | Remarks |
|---|---|---|---|---|
| | | Combat | Alert | |
| Up | All Up | 0.829 | 0.925 | Fully Operational |
| Inoperative Subsystem | Surveillance Radar | 0.019 | 0.009 | Operation Possible in an alternate or degraded mode |
| | Tracking Radar | 0.055 | 0.030 | |
| | IFF Equipt | 0.016 | 0.006 | |
| | Computer and Ancillaries | 0.029 | 0.009 | |
| | Gun-laying Servos | 0.019 | 0.009 | |
| | Power Supply | 0.001 | 0.000 | |
| | All other subsystems and Components | 0.032 | 0.012 | No Operation Possible without repair |

20871-610

The foregoing computations required only a few minutes with a slide rule. It seems evident that if one admits the assumptions and approximations involved, the more general case of two movement states with three tactical substates in each, and any number of single failure modes and alternate operational states of the system being evaluated can be worked with an acceptable amount of effort.

The possibility should not be excluded that the approximations may have reduced the problem to one for which a simpler path to the solution can be found by going back to first principles, and introducing the approximations ab initio.

## 10.6 RELIABILITY ESTIMATES

Estimation, measurement, and verification of the reliability of a military system constitute a specialized area of activity which is usually defined explicitly in requirements documents and contractural agreements. Reliability analysis is usually carried out by specialists using data banks of reliability data on past and existing systems, subsystems, components and elements. It is far beyond the scope of the present report to cover this field adequately. Here we note only briefly the nature of the activity as a system proceeds from concept to use.

### 10.6.1 Estimation and Acquisition of Reliability Data

When the system is in the conceptual stage, reliability estimates are made by first determining those system elements which are similar to elements already in use and those which are new. Reliability of the former is estimated on existing data, reliability of the latter requires estimates based on a study of the design, and a general knowledge of 'reliability physics.' As the concept moves into design, special reliability tests may be made on a continuing basis of new components for which no data exists. Records kept on operating and repair performance of subsystems of a prototype as they are assembled provide progressive improvement of the original reliability estimates. During acceptance tests, a formal reliability validation effort determines whether the system meets requirements. Once it is in the field, TAERS records provide a pool of information which can be applied to new systems.

There are numerous official documents which establish design standards to help to avoid some of the known causes of unreliability that have been encountered in the past. However achievement of excellent reliability always begins with the equipment designer: it is designed into the equipment, not added after design.

A survey of published U.S., and some Soviet reliability data are included in the text by Polovko.[15] This and other reliability texts will not make the reader a reliability expert, but they do illustrate how reliability measurements on generic parts types vary with the source and differences in measurement techniques and conditions. Polovko cites a method for applying a set of component reliability estimates taken under one consistent set of conditions to a new environment, in which the reliability of only one member of the set is known.

A survey and comparison of methods predicting reliability has been given by Dworkin.[16] This includes methods which correlate reliability against many other component characteristics in addition to the original active element and piece count methods.

The opinion of a non-expert in reliability is that as in all systems analysis problems, estimates of reliability of the same equipment by separate skilled groups will differ, sometimes widely. The reliability assurance process then consists of initial estimates, refined and improved by continued and progressive part, component, subsystem and system testing as a new system is assembled and produced.

### 10.6.2 Validity of the Exponential Failure Assumption

For the models used in this report the dependability, the probability that a system will operate without failure for a time t, is assumed to be

$$X_0(t) = e^{-\sum_{j=1}^{n} \lambda_j t} \qquad (10.87)$$

How closely does this approximate real life?

Many studies indicate that it is an excellent approximation for systems dominated by electronic components, such as radars. We digress briefly to cite some measurements taken on a fire control system and reported by Bredemann.[30] The measurements were taken early in the system life, between the assembly line and delivery to the user. The system itself was an active tail defense system for a strategic bomber.

The system under examination, exclusive of the armament (guns) consisted of a radar transmitter and receiver, stabilized platform, computer, radar signal processing circuitry, weapon control circuits and radar antenna control circuits. Primary electric power was supplied from the aircraft electrical system. Hydraulic power, special electric power and regulation of primary power was provided by the defense system. The system had simultaneous search and track capability, using dual radar and antenna systems.

The data was taken on 11,168 hours of system operation (33 systems) between assembly and installation in aircraft.

The mean operating time between failures (MUT) was 4.87 hours with a standard deviation of 5.90 hours.

Defining R(t) = probability of operating without failure for t hours, it was found that R(t) could be expressed as

$$R(t) = e^{-(1/a)t^c}; \text{ (Weibull distribution)} \qquad (10.88)$$

with $a = 3.36$; $c = 0.822$

For "exponential" failure, $c = 1.0$

For the Weibull distribution

$$MUT = \Gamma\left[(1+c)/c\right](1/a)^{-1/c} = \Gamma\left[(1+c)/c\right]a^{1/c} \qquad (10.89)$$

The following Weibull Parameters were found for failure cause sub-populations (Table X-6).

The report states, 'The Weibull shape parameter c, is less than one for each failure cause. These results

**Table X-6. Weibull Parameters For Failure Cause Sub-Populations**

| Failure Cause Sub-population | Weibull Parameters a | Weibull Parameters c |
|---|---|---|
| Fabrication Defects | 15.5 | .780 |
| Marginal Equipment Design | 21.3 | .748 |
| Part Design Deficiencies | 42.1 | .837 |
| Potentiometers | 31.2 | .778 |
| Relays | 83.1 | .939 |
| Semiconductors | 65.4 | .947 |
| Transformers, Chokes, and Motors | 49.9 | .828 |
| Tubes | 32.1 | .803 |

20871-611

emphasize the strong effect that turn-on transients have in inducing failures.[7]

It is interesting that failures attributable to the maintenance activity were so frequent that when they were removed from the data the mean time to failure for other causes was about doubled.

It may be concluded that:

a. The simple exponential model ($c = 1.0$) is a fair approximation for initial system reliability estimates until test data on actual components becomes available.

b. As the system development moves forward, the evaluation model can be improved by more accurate representation of the failure probability, such as by use of the Weibull distribution. This will complicate the analysis.

c. Beware of maintenance.

## 10.7 MAINTENANCE AND REPAIR CONSIDERATIONS

Table X-7 from AMCP 706-134[22] describes categories of maintenance. Organizational maintenance and repair is limited to relatively simple activities, however, by proper equipment design the scope of the repair activity can be increased by simple means for malfunction location and component removal and replacement.

Direct support maintenance has greater capability, it is in the same organization as the units supported, and although time delays will be greater than for organizational repairs (when possible) they are less than those associated with general support maintenance. There may be delays associated with competition for support services and limited crews.

Capability and time delays are still greater for general support maintenance. Depot maintenance essentially removes the equipment from the tactical environment, involves much larger delays, and should probably be paired with the probability that a replacement piece of equipment will be supplied the user while his equipment after repair goes into the supply pool.

These activities as defining maintenance and repair states for the system are configured in Figure 10-4.

Like reliability, maintainability analysis is a specialized field in itself, and is properly done by groups skilled in the field. Numerous trade-offs can be made involving manpower skills available at each echelon of maintenance, automatic checkout and fault location, repair versus discard options at each subsystem and component level, the number of spare parts carried at each organizational level, the number of maintenance personnel assigned and the numbers and types of systems they service, and so on. Since the cost of maintenance usually exceeds the initial cost of complex

Table X-7. Categories of Maintenance in a Theater of Operations

| Category | Organizational Maintenance | | Direct Support Maintenance | General Support Maintenance | Depot Maintenance |
|---|---|---|---|---|---|
| Former Echelon | First | Second | Third | Fourth | Fifth |
| Done Where | Wherever the Equipment is | In Unit | In Mobile and/or Semi-Fixed Shops | | In Base Depot Shop |
| Done by Whom | Operator | Using Unit | Division/Corps/Army | | Theater Commander Zone and/or Z/I |
| On Whose Equipment | Own Equipment | | Other People's Equipment | | |
| Basis | Repair and Keep it | | Repair and Return to User | | Repair for Stock |
| Type of Work Done | Inspection<br>Servicing<br>Adjustment<br>Minor Repairs and Modification | | Inspection<br>Complicated Adjustment<br>Major Repairs and Modification<br>Major Replacement<br>Overload from Lower Echelons | | Inspection<br>Most Complicated Adjustments<br>Repairs and Replacement Including Complete Overhaul and Rebuild<br>Overload from Lower Echelons |

20871-612

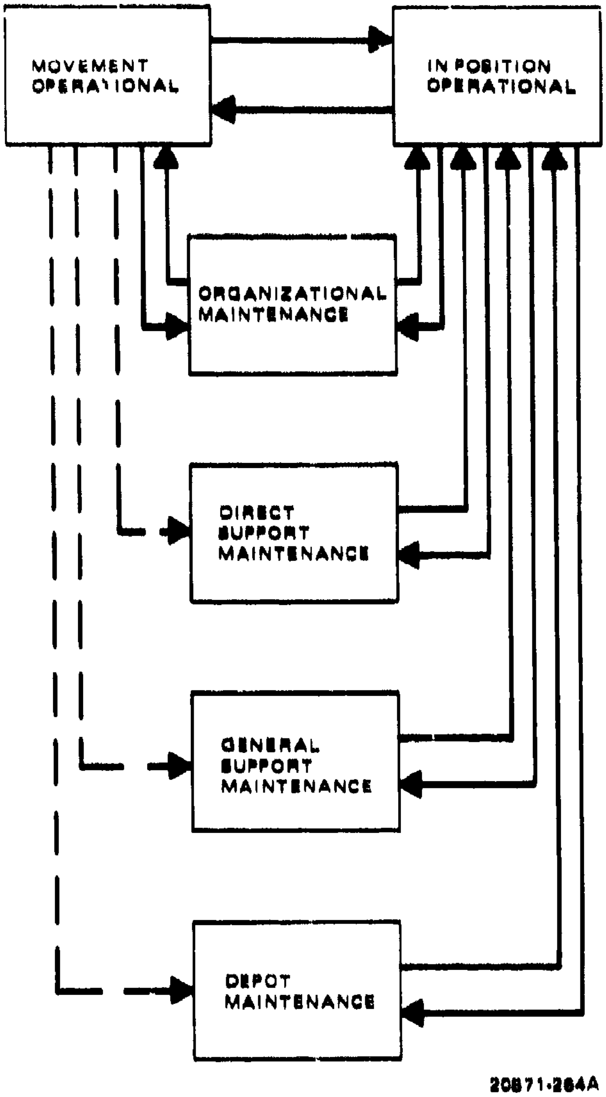


Figure 10-4. Operational and Maintenance States

military equipment over its life cycle, these and many other options are fertile topics for cost reduction and overall system optimization.

From a military operations point of view, however, neither reliability nor maintainability is a proper trade-off against system performance (i.e., effectiveness in its proper operational state). A system that has high effectiveness when it is working, but is often inoperable is not a good military choice over a system of moderate effectiveness that is almost always operational even though both have the same 'average' effectiveness. To this writer, the proper attitude to take on reliability and maintainability is to set levels of the triad, reliability, maintainability and availability that are consistent with the simple fact that the military requires materiel that will work when it is needed and can be maintained in the field. For a particular system, the life cycle cost of meeting these requirements is then compared with the system performance estimates to determine whether the system should be procured.

This in no way reduces the critical importance of reliability and maintainability, but it excludes from consideration system configurations with low availability, regardless of their effectiveness when they are working.

### 10.7.1 Sources of Maintainability Data

Most of the comments made with regard to reliability data apply to maintainability data. For a new system the estimation of the maintainability parameters is a combination of extrapolation from data on existing systems and estimation for new components and subsystems. As in the case of reliability, there are groups of specialists in maintainability, usually as a part of the same organization, or the same group.

Since maintainability as an analytical field is somewhat more recent than reliability, the data bank is not as large. However it is growing. A review of maintainability analysis is given by Slattery.[14]

Just as in the case of reliability, maintainability begins with the system designer. Maintainability guides for design will be found on AMCP 706-134[n] and related handbooks of the Army and the other services.

The need to measure maintainability early in system prototype development where changes can be most easily made is perhaps less recognized than in the case of reliability. It is common knowledge that maintenance actions can introduce new failures (as all automobile owners know). A partial cure is easy accessibility of components with the higher fail rates.

On the whole, since reliability can be designed into a system at the manufacturer's plant and maintainability must be done in the field by available personnel of varying skills and experience, it is best to achieve high availability by high reliability and simple maintenance.

### 10.7.2 Validity of the Exponential Repair Assumption

The analytical methods for combining reliability and maintainability thus far have used a simple exponential approximation for the holding time of the system in the repair and maintenance state. Although this is usually satisfactory as long as one works with expected values, the approximation deviates greatly from reality in many cases if one is interested in probability density functions for various state durations.

Many analyses of probability density functions of repair operations have indicated that the time to re-

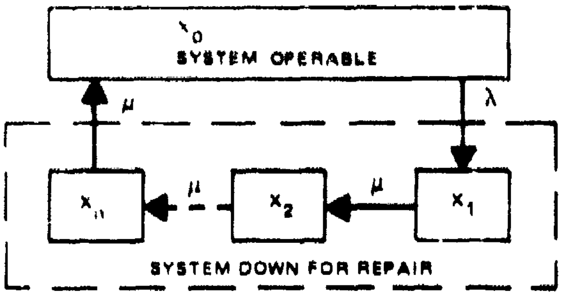


20871-265

Figure 10-5. Sequential Substate Repair Model

store to service tends to have a log-normal distribution, and there are some a-priori grounds based on sequential selection among alternatives that lead to such a distribution. The log-normal function does not fit easily, if at all, into the state space formulation. However, the Erlang distribution, which is compounded of a number of simple exponential delays has nearly the same shape and does fit the state space model. We review briefly how this comes about.

A simple method for replacing the simple exponential holding time in a state (maintenance and repair, for example) by a probability density function approximating the lognormal, yet still retaining the linear constant coefficient form of the state differential equations is the following:[17]

Consider the simple system configuration of Figure 10-5. The repair state has been subdivided into a number of sequential substates. For this example the mean stay in each state $(\mu)^{1}$ is assumed to be the same for each substate, but different stay times could be used

The matrix equation is

$$\begin{bmatrix} \dot{X}_0 \\ \dot{X}_1 \\ \dot{X}_2 \\ \cdot \\ \cdot \\ \dot{X}_n \end{bmatrix} = \begin{bmatrix} -\lambda & 0 & 0 & \cdot & \cdot & \mu \\ \lambda & -\mu & 0 & \cdot & \cdot & 0 \\ 0 & \mu & -\mu & \cdot & \cdot & 0 \\ & \cdot & \cdot & \cdot & \cdot & 0 \\ & \cdot & \cdot & \cdot & \cdot & 0 \\ & \cdot & \cdot & \cdot & \cdot & -\mu \end{bmatrix} \begin{bmatrix} X_0 \\ X_1 \\ X_2 \\ \cdot \\ \cdot \\ X_n \end{bmatrix} \qquad (10.90)$$

If we solve for the steady state solution by setting the derivatives equal to zero we find that availability is

$$A = \frac{(\mu/n)}{\lambda + (\mu/n)} \qquad (10.91)$$

and so the repair state subdivision has no effect on the steady state availability, and we could as well have assumed a single state with mean stay in the state $(n/\mu)$.

However, if we examine the probability density function for the duration of stay in the repair state we find that it is no longer a simple exponential. To observe this assume that at $t = 0$, the system enters the repair state, so that $X_1(0) = 1.0$. We determine the probability that it emerges from repair as a function of time, by solving for $X_0(t)$, assuming no new reentries to the repair state. By Laplace transforms

$$X_0(s) = 1/s\,[\mu/(s+\mu)]^n \qquad (10.92)$$

$$dX_0(t)/dt = \frac{\mu}{(n-1)!}(\mu t)^n e^{-\mu t} \qquad (10.93)$$

The mean stay in repair, $T_r$, may be obtained from the Laplace Transform as

$$T_r = \lim_{s \to 0} -(\partial/\partial s)\left[s\,X_0(s)\right] \qquad (10.94)$$

and the variance of the holding time $\sigma^2$ is

$$\sigma^2 = \lim_{s \to 0} \frac{\partial^2 X(s)}{\partial s^2} - T_r^2 \qquad (10.95)$$

Then

$$T_r = n/\mu$$

$$\sigma^2 = n/\mu^2 \qquad (10.96)$$

If we hold $T_r$ constant, varying the number of substates $n$, $\mu = n/T_r$

$$\sigma^2 = T_r^2/n \qquad (10.97)$$

For constant $T_r$, Figure 10-6 shows how the probability of remaining in the repair state as a function of time varies with n. When n becomes very large, we approach a constant holding time. Figure 10-7 shows the corresponding probability density function of holding times. Clearly, one can obtain a probability density function closely approximating a log-normal function, usually as close as the available data justifies.

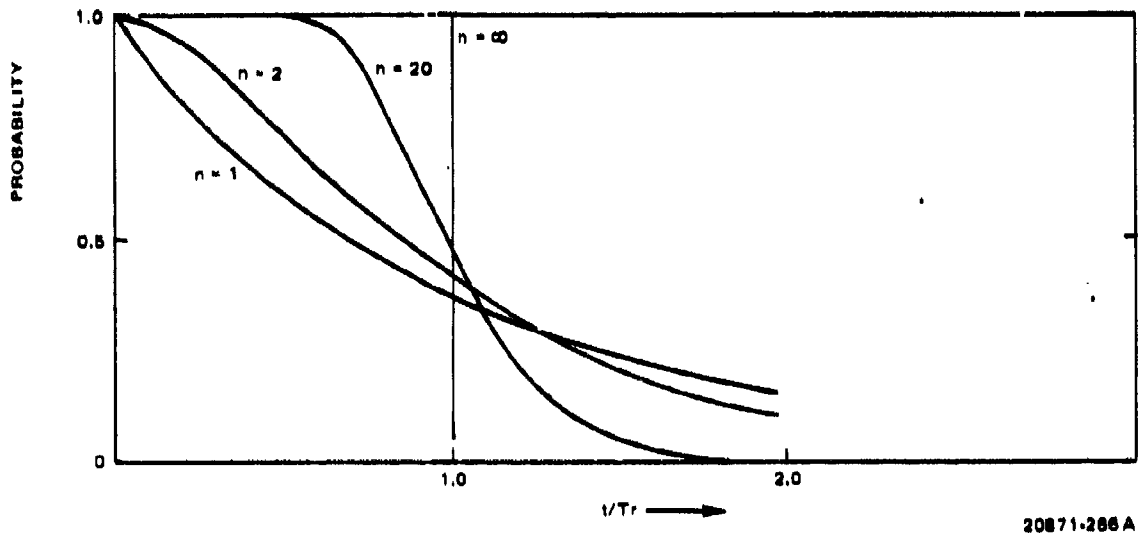


Figure 10-6. Probability That Repair Time Exceeds Specified Value

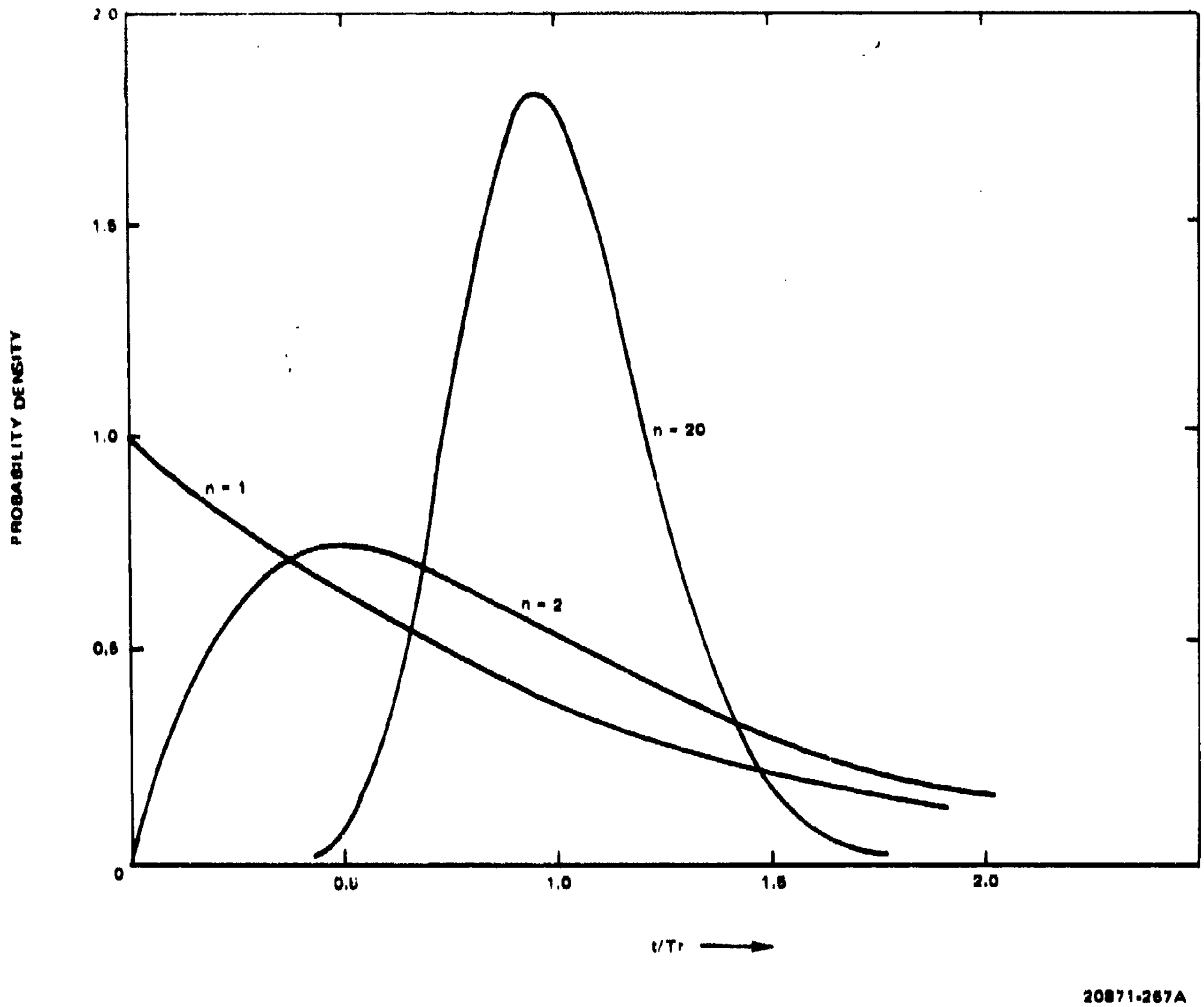


Figure 10-7. Probability Density Function of Repair Time

### 10.7.3 Extended Models of Maintenance

The model previously developed for availability as it is affected by the various tactical states may be extended by introducing the maintenance sub-states indicated in Figure 10-4, after which the analysis proceeds as before. In addition, by further partitioning each maintenance sub-state to lower levels of detail one can account for transit time, administrative delay, delays waiting for spares, as well as active repair time. For initial rough estimates the average time in all of these states for each identified failure type may be estimated and the simpler model used. Down time for scheduled maintenance to that level of approximation might be included as an equivalent failure type, even though it is scheduled. Since 'scheduled' maintenance allows some latitude in when it is done, it could be located as a 'failure' to occur only during a 'passive' tactical state in the simple model.

## 10.8 AVAILABILITY WITH MULTIPLE FIRE UNITS AND MAINTENANCE CREWS

The relationships among the number of fire units serviced and the number of maintenance crews available is discussed briefly in this section.

It is assumed that the system contains N fire units and m maintenance crews. Each fire unit is either operable or inoperable and being repaired. Failure rates and repair rates are assumed to be 'Poisson streams' of events.

The 'steady state' probability that n out of N units are operational is determined. The problem and its solution are classical, and this paper simply reproduces well known results.

Extensions are required of the analysis when the fire units have more than one operational state each, of differing effectiveness, and when distinctions must be made among failures according to the maintenance skill required for repair and the availability of each skill.

Let

$P_n$ = probability that n units are operational at time t.

The probability that a fire unit fails in dt is taken to be $\lambda_n\,dt$, that is the failures occur as a 'Poisson stream'. The subscript of $\lambda_n$ allows $\lambda$ to be a function of the number of systems operating.

The probability that a repair is completed in dt is also described by a Poisson stream with a mean rate $\mu_n$.

The following differential equations can be written at once:

$$\dot{P}_N = -\lambda_N P_N + \mu_{N-1}P_{N-1}$$

$$\dot{P}_n = -(\lambda_n + \mu_n)P_n + \lambda_{n+1}P_{n+1} + \mu_{n-1}P_{n-1}$$

$$\dot{P}_0 = -\mu_0 P_0 + \lambda_1 P_1 \tag{10.98}$$

If, as is usual, we are only interested in the steady state solution, set $\dot{P}_n = 0$.

The solution is easily obtained, following Gnedenko[18] by defining

$$z_n = -\mu_n P_n + \lambda_{n+1} P_{n+1} \tag{10.99}$$

substituting into the original equations and observing that

$$z_0 = 0$$

$$z_n - z_{n-1} = 0 \tag{10.100}$$

hence

$$z_n = 0 \text{ for all n.}$$

Hence

$$P_{n+1} = P_n(\mu_n/\lambda_{n+1}) \tag{10.101}$$

whence

$$P_n = P_0 \prod_{n=1}^{n} \frac{\mu_{k-1}}{\lambda_k} \tag{10.102}$$

and since

$$\sum_{n=0}^{N} P_n = 1.0 \tag{10.103}$$

$P_0$ can be determined.

There is a priori no reason to assume that the fire units will fail individually at different rates. Hence

$$\lambda_n = \lambda = \text{constant}$$

20871-803

It is assumed that only one crew works on a down fire unit. Hence as long as crews are available,

$$\mu_n = \mu(N - n); \tag{10.104}$$

since N - n units are down and all are

being worked on.

If there are more fire units than crews

$$\mu_n = \mu(N\text{-}n)\ ;\ N\text{-}n \le m$$

$$\mu_n = \mu m\ ;\ N\text{-}n \ge m \tag{10.105}$$

in which case the $P_n$ are obtained from

$$P_n = \frac{N!}{n!(N\text{-}n)!} R^{(N\text{-}n)} P_0\ ;\ 1 \le N\text{-}n \le m \tag{10.106}$$

$$P_n = \frac{N!}{m^n m!\, n!} R^{(N\text{-}n)} P_0\ ;\ m \le N\text{-}n \le N \tag{10.107}$$

$$P_0 \left[ \sum_{N\text{-}m}^{N} \frac{N!}{n!(N\text{-}n)!} R^{(N\text{-}n)} + \sum_{0}^{N\text{-}m\text{-}1} \frac{N!}{m^n m!\, n!} R^{(N\text{-}n)} \right] = 1.0 \tag{10.108}$$

### 10.8.1 Example

Assume that there is one maintenance crew which can only work on one down fire unit at a time. Then

$$\mu_n = \mu. \tag{10.109}$$

Then

$$P_n = P_0 R^n/n!\ ;\ R = \mu/\lambda. \tag{10.110}$$

$$P_0 \sum_{n=0}^{N} R^n/n! = 1.0 \tag{10.111}$$

$$P_n = \frac{R^n/n!}{\sum_{0}^{N} R^n/n!} \tag{10.112}$$

Let R = 10; i.e. if there were only one fire unit, the crew could keep it operable 91% of the time. Assume that there are 4 fire units. Then

$P_4$ = 0.65

$P_3$ = 0.26

$P_2$ = 0.07

$P_1$ = 0.02

$P_0$ = 0.00

If there were one maintenance crew on each fire unit,

$$P_4 = (.91)^4 = 0.66$$

20871-804

and so for this case there is no appreciable degradation in having one crew service four units. This results of course from the fact that R is assumed to be 10.

However this is a poor showing for the 4-unit defense, since the expected number of fire units operational is only 3.54 or 88% of the total. Adding crews does not raise this percentage, the availability of the individual fire units must be increased.

### 10.8.2 Approximate Solution

It is doubtful that any system will be acceptable in which $P_N$ for the set of fire units comprising it is not above 80%. Then $P_{N-1}$ will be very small, and other $P_i$ negligible. In this case only one crew is required, and

$$P_n = \mu/(N\lambda + \mu) \tag{10.113}$$

$$= \frac{1}{1 + N(\lambda/\mu)} \tag{10.114}$$

$$\cong 1 - N(\lambda/\mu) \tag{10.115}$$

since the availability of a single fire unit serviced by a single crew is

$$A = \frac{1}{1 + (\lambda/\mu)} \tag{10.116}$$

the above expression is equivalent to

$$P_N = A^N \tag{10.117}$$

and the average number of fire units available is

$$E = NA \tag{10.118}$$

which furnishes an easy transition from the availability computations of individual fire units to the expected number operable for combination with capability estimates in determining system effectiveness.

## 10.9 CONCLUSION AND RECOMMENDATIONS

Beginning with the premise that a military system must work reliably in its operational environment, high levels of reliability, maintainability and availability should be set as objectives and must be met by candidate systems to survive the evaluation.

Availability and its component elements should not be considered as unconstrained trade-offs against capability (performance in full operational state). Instead the cost of keeping the system at the specified levels should be determined and included in life cycle costs for the full cost versus effectiveness comparison. A system which cannot reach the specified 'RAM' levels, regardless of the amount of support should be dropped from consideration.

For a system with high availability, multiple component failure modes will have very low probability compared with single component failure modes. This greatly simplifies the availability analysis.

For a defense system comprised of a number of fire units each with very high availability, the analysis of maintenance crew and logistics requirements is also simplified.

To insure high availability a great deal of analysis, testing, and attention to good design procedures is required.

Although not discussed in this paper the difficulty of maintenance under combat conditions emphasizes the achievement of high availability by high reliability and minimal maintenance far more than vould be revealed in paper studies.

## SECTION 11
## RELATIONSHIP OF RATE OF FIRE, AMMUNITION LOAD, RELOAD TIME AND THE TACTICAL SITUATION

As the tabulated data on weapon characteristics indicates, very high maximum rates of fire are possible with modern automatic weapons. This characteristic interacts with the number of rounds of ammunition charged in the automatic loading system, the time to recharge the loader, the available firing time against each target, and the time interval between targets.

These interrelationships may be analyzed by methods similar to those discussed in the previous section on Availability. It was noted there that to compute operational availability, one must include causes of system down time in addition to immediate repair of failures under ideal conditions, and on the other hand, changes in the tactical situation offer opportunities to repair in non-combat states those failures which occurred in combat states.

One may similarly define an 'inherent' rate of fire of the gun/ammunition system assuming a requirement for continuous target engagement over very long periods of time. This provides maximum exposure of the reload time, but is a poor indicator of the average firing rate attainable in a long series of engagements broken by non-combat intervals between targets. On this basis, if the gun has a maximum on-mount load of N rounds, and fires at a rate $\nu_0$, it can fire for $T_f = N/\nu_0$ minutes, then is down for a reload time $T_r$. Over a long period of time it is firing for a fraction of time

$$A = \frac{T_f}{T_f + T_r} \qquad (11.1)$$

How the time to reload varies with the number of rounds loaded is a function of the particular mechanical design of the ammunition feeding system. For a first approximation, we can define a 'reload rate' $\rho_0$ as

$$\rho_0 = N/T_r \qquad (11.2)$$

Then

$$A = \frac{\rho_0}{\rho_0 + \nu_0} \qquad (11.3)$$

and the average rate of fire is

$$\nu_{eff} = \frac{\nu_0 \rho_0}{\nu_0 + \rho_0} \qquad (11.4)$$

But this is a poor estimate because it assumes continuous combat. We now develop an improved model.

### 11.1 STOCHASTIC APPROXIMATION TO FIRING AND RELOAD STATES

In order to combine the firing and reload states with the tactical states we introduce a stochastic representation of the fire and reload process along the following lines:

As the gun engages successive targets the number of rounds fired against each will vary from none to very large numbers, depending on variations in acquisition range, target breakaway range, and individual gunner differences. Depending on whether there has been time to reload before a prior target, the available ammunition to engage a new target may vary from a few rounds to the maximum N. In complete ignorance of what the real probability density functions are of the variables involved, we choose the simplest assumption, which we state as follows:

Let

$X_a$ = probability that the gun is in a firing state

$X_r$ = probability that the gun is in a reload state.

$$\begin{aligned} \dot{X}_a &= -\nu X_a + \rho X_r \\ \dot{X}_r &= \nu X_a - \rho X_r \\ \nu &= \nu_0/N \,;\, \rho = \rho_0/N \end{aligned} \qquad (11.5)$$

If we solve these equations for the simple case of a gun beginning to fire fully loaded, with no reload, we find that the probability that it is still able to fire at time t is

$$X_a(t) = e^{-\nu t} = e^{-\nu_0 t/N} \qquad (11.6)$$

whereas if we computed the deterministic solution we would find

$$X_a(t) = 1 - (\nu_0 t/N) \; ; \; \nu_0 t/N \leq 1.0$$
$$= 0 \qquad ; \; \nu_0 t/N \geq 1.0 \tag{11.7}$$

and so the stochastic approximation is not unrealistic.

We are now able to combine the stochastic representation with a description of the defense against sequential targets with tactical state transitions.

## 11.2 STATE TRANSITION RELATIONS FOR DEFENSE VS SEQUENTIAL ATTACKS

The tactical situation is defined in extended terms using as a basis the description of Luftwaffe attacks on Malta during the month of heaviest attacks. This situation has enough generality so that by changing parameters, one may represent most tactical situations to the same level of realism. It might, for example, be preferable to adjust the model to describe U.S. Air Force tactical operations in Vietnam, given the availability of the appropriate descriptive and quantitative material.

The situation considered is the following: There are three 'raids' per day on the average. Each raid has a mean duration of about one hour.

Each 'raid' is carried out on the average by 60 aircraft, which execute the attack in a series of waves of 12 aircraft per wave. On the average there are 5 waves per raid. The raid breaks down into waves to provide control and coordination of the attacking aircraft during the attack. Each wave is further subdivided into attack elements (section, flights) of 3 aircraft each; each attack element of 3 aircraft makes a firing pass as a unit. The attack elements attack sequentially with close spacing.

For a general comparison with Vietnam, a newspaper report stated, 'American aircraft flew 426 strikes in Quang Tri Province in the 24 hours ended at noon today. It was the heaviest in a single province in four years.'[10] Of course these strikes were distributed over many targets.

Depending on the distribution of defended vital areas and the distribution of the low altitude defense fire units, each defensive fire unit may not be able to fire at each attack element before bomb release, because of limitations in the range at which the fire units can deliver effective fire.

For a standard defense of a small vital area by four fire units, for example, the fire unit on the target side away from the attack may be able to open fire only after the attacker has dropped his bombs. In a 'cloverleaf' attack pattern by successive attack elements, the defense units will on the average, all be able to engage targets.

For simplicity in the present analysis, and without detailing the geometry, we assume that against each attack element of three aircraft, three fire units will be in a position to engage, and each will fire at one aircraft. Repeated attacks are assumed to be from the same direction, so that the reload rates of the three active fire units are more highly stressed than if attacks came from different quandrants in successive strikes.

For the present section, we do not consider the effect of immediately observable kills by the defense on ammunition expenditure.

The state transitions are developed in Figure 11-1, where the tactical states are related to the fire/reload states of a single fire unit. The definition of each symbol is apparent from the Figure.

To conserve space here we work the solution omitting the $X_3$ state (which has a minimal effect on the results) but give the results for the complete set of states as well. The methods in both cases are identical.

Initially, the time to acquire targets is not made explicit. The model is then expanded to include detection and acquisition.

It will be observed that for simplicity the model assumes that reloading does not take place until the full load on the mount has been exhausted, and that reload then continues until a full load is on board. A real system might obtain better performance than indicated by the model if the operators take advantage of topping off partly depleted ammunition loads when possible, or engaging with partly reloaded mounts when enough ammunition is on board to make this effective. To include these options would require establishment of a doctrine, and more detail in the model.

Following the transitions of Figure 11-1, write the state transition matrix in aggregated form as

$$\begin{bmatrix} \dot{X}_{11} \\ \dot{X}_{12} \\ \dot{X}_2 \end{bmatrix} = \begin{bmatrix} -(b+\lambda)I + G & \mu I & aI \\ \lambda I & -\mu I + R & 0 \\ bI & 0 & -aI + R \end{bmatrix} \begin{bmatrix} X_{11} \\ X_{12} \\ X_2 \end{bmatrix} \tag{11.8}$$

Set the derivatives equal to zero. Then the steady state solution (fixed point probability vector) can be determined.[25] However, the process of determining the solution can be simplified as follows:

First determine the fraction of time that the system spends in each of the aggregated states by setting G = R = 0. These matrices are the gun ammunition consumption and reload matrices

$$G = \begin{bmatrix} -\nu & \rho \\ \nu & -\rho \end{bmatrix}$$

$$R = \begin{bmatrix} 0 & \rho \\ 0 & -\rho \end{bmatrix} \qquad (11.9)$$

Writing F for the fraction of time spent in each of the three states we easily determine that

$$F_{11} = 1/D \qquad \text{where } D = 1 + (b/a) + (\lambda/\mu)$$

$$F_{12} = (\lambda/\mu)/D$$

$$F_2 = (b/a)/D \qquad (11.10)$$

Then normalize the matrix equation by setting $Y = X/F$. The expressions simplify to

$$\begin{bmatrix} -(b+\lambda)I + G & \lambda I & bI \\ \lambda I & -\lambda + (\lambda/\mu)R & 0 \\ bI & 0 & -bI + (b/a)R \end{bmatrix} \begin{bmatrix} Y_{11} \\ Y_{12} \\ Y_2 \end{bmatrix} = 0 \qquad (11.11)$$

We are only interested in $Y_{11}$. Its components sum to 1.0 as a result of the normalization.

Solving for $Y_{11}$ we easily obtain

$$\left\{[-(b+\lambda)I + G] + \lambda[I - \mu^{-1}R]^{-1} + b[I - a^{-1}R]^{-1}\right\} Y_{11} = 0 \qquad (11.12)$$

The inverse matrices are easily determined to be

$$[I - \mu^{-1}R]^{-1} = I + (\mu + \rho)^{-1}R \qquad (11.13)$$

$$[I - a^{-1}R]^{-1} = I + (a + \rho)^{-1}R \qquad (11.14)$$

So that

$$[G + sR]Y_{11} = 0 \; ; \; s = \frac{\lambda}{\mu + \rho} + \frac{b}{a + \rho} \qquad (11.15)$$

Expanding $Y_{11}$ and solving for $Y_{11a}$

$$Y_{11a} = \frac{\rho_e}{\nu + \rho_e} \qquad (11.16)$$

where

$$\rho_e = \rho(1 + s) = \rho\left[1 + \frac{\lambda}{\mu + \rho} + \frac{b}{a + \rho}\right] \qquad (11.17)$$

Identical procedures, with a bit more algebra, yield the result for the complete eight state system of Figure 11-1 as

$$Y_{11a} = \frac{\rho_e}{\nu + \rho_e} \qquad (11.18)$$

where

$$\rho_e = \rho\left[1 + \frac{\lambda}{\mu + \rho} + \frac{b(\alpha + \beta + \rho)}{a(\alpha + \rho) + \rho(\alpha + \beta + \rho)}\right] \qquad (11.19)$$

$Y_{11a}$ is the 'availability' of the gun in the firing mode during an attack pass, and the effective or average rate of fire

$$\upsilon_e = \upsilon_0 Y_{11a} \qquad (11.20)$$

The mean duration of an attack pass, from the flow diagram is

$$T_p = \frac{1}{b+\lambda} \qquad (11.21)$$

And so the average number of rounds fired per firing pass is

$$N_{up} = \upsilon_c T_p \qquad (11.22)$$

Note that if $\lambda = b = 0$, the model degenerates to a single firing pass of unbounded duration and $\nu_e$ reduces to

$$\nu_e = \nu_o \frac{\rho_o}{\rho_o + \nu_o} \qquad (11.23)$$

We note for reference that the fraction of time that the system spends in the four tactical states in the average, is

$$F_{11} = 1/D$$
$$F_{12} = (\lambda/\mu)/D$$
$$F_2 = (b/a)/D$$
$$F_3 = (b/a)(\beta/\alpha)/D$$

where

$$D = 1 + (\lambda/u) + (b/a)[1 + (\beta/a)] \qquad (11.24)$$

## 11.3 DETERMINATION OF COEFFICIENTS

To determine the necessary coefficients of the tactical state transitions from the description of the situation, we recall the following characteristics of a system with Markov type transitions between states:[28]

a. The mean duration of a specified state is $1/\Sigma\ a_i$, where the $a_i$ are the departure rates from that state to other states. b. The mean recurrence rate of a state is $F\ \Sigma\ a_i$, where F is the fixed point probability (steady state, average fraction of time spent in the state) of that state.

From the description of the Malta attacks we specify

$$F3 = 7/8$$
$$F_2 = 1/16$$
$$F_{11} + F_{12} = 1/16 \qquad (11.25)$$

We specify only the sum of the $F_{1i}$ states at this time to allow parametric variation of the fraction of time that an attack element is within the defensive fire zone during each pass. This will vary to some degree with the weapon capability as well as with the attacker's tactics.

We also assume that on the average there are 3 raids per day, 5 waves per raid, or 15 waves per day, and 4 attack passes (of 3-element units) per wave, or 60 attack passes per day. Then

$$F_3\alpha = 3\ ;\ \alpha = 24/7 \text{ per day}$$
$$F_3/F_2 = (\beta/\alpha)\ ;\ \beta = 48 \text{ per day}$$
$$F_2(a+\beta) = 15$$
$$a = 192 \text{ per day}$$
$$F_{11}(b+\lambda) = 60 \qquad (11.26)$$

The mean duration of an attack pass is $(b+\lambda)^{-1}$; if we wish to make a parametric study of the effect of duration of the attack pass, on system performance, we compute for a range of $(b+\lambda)^{-1}$. For the present example, we choose the duration of an attack pass as 24 seconds, so that

$$(b+\lambda) = 3600 \text{ per day}.$$

Then

$$F_{11} = 1/60$$

But

$$F_{11} + F_{12} = 1/16$$

so

$$F_{12} = 11/240$$

Now

$$b/a = F_2/F_{11} = 15/4$$
$$b = 720/\text{day}$$

and

$$\lambda = 2880/\text{day}$$

Finally,

$$F_{11} + F_{12} = F_{11}[1 + (\lambda/\mu)] = 1/16$$

whence

$$\mu = (4/11)\lambda\ . \qquad (11.27)$$

The coefficients are summarized in Table XI-1.

## 11.4 EXAMPLE FOR SPECIFIC WEAPONS

To see what the above relations mean, in terms of the effect of maximum rate of fire, reload rate, number of rounds on mount and the tactical descriptors on the average number of rounds that a fire unit gets off

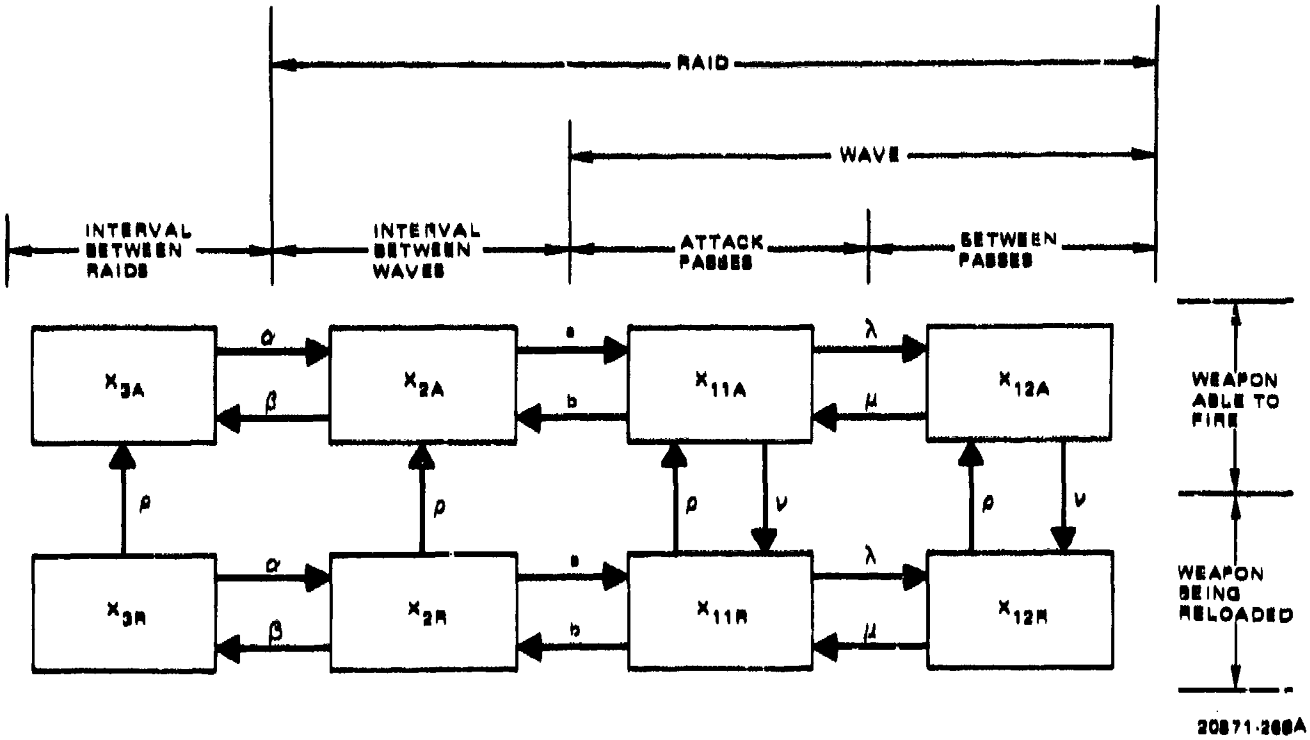


Figure 11-1. Engagement and Reload Substates

Table XI-1. Tactical State Transition Rates

| Coefficient | Value (per hour) |
|---|---|
| $\alpha$ | 1/7 |
| $\beta$ | 2 |
| a | 8 |
| b | 30 |
| $\lambda$ | 120 |
| $\mu$ | 480/11 |

20871-613

against each attack pass over a long series of raids, some computations have been made based on limited data on hand on specific weapons. The data and associated descriptive material extracted from Field Manuals and various issues of the International Defense Review and Janes Weapons Systems, are given below.

In this example, the time to acquire and generate firing data is not subtracted from the duration of the attack pass. The computation therefore stresses the weapon reload capability excessively, but not as heavily as the simple Equation (11.3).

### 11.4.1 Fire Unit Characteristics

*Vulcan*

Vulcan can be fired at 3000 or 1000 rpm. In the high rate of fire mode rounds are fired in bursts with options of 10,30,60 and 100 rounds per burst. Burst duration in the slow mode is gunner's choice.

The towed version uses linked ammunition with a capacity of 300 rounds per load. The basic load is 4,000 rounds; 300 are carried on the mount, 3,700 on the towing vehicle and battery ammunition carriers.

Reload time is about 1 minute per 100 rounds of ammunition.

The SP version uses linkless feed with a capacity of 1200 rounds per load. The basic load of ammunition is 6000 rounds per weapon of which 1800 rounds are carried on the weapon carrier, the remainder on battery ammunition vehicles. Each weapon also carries 200 rounds which remain in the feed system to prevent malfunctioning.

The linkless feed system consists of a drum and conveyor. There are 1000 rounds in the drum. 800 rounds are stored in the carrier.

800 rounds can be loaded in the drum in about 7 minutes. The estimated time to reload the drum is 3 minutes plus one half minute for each 100 rounds loaded.

*Oerlikon 5 PFZ -B.C*[31]

The PFZ (SP) mounts twin 35mm guns with rate of fire of 550 rpm each. Either anti-aircraft or anti-tank ammunition, belted, can be fired with changeover by remote control from within the turret. Ammunition carried on the vehicle totals 660 rounds of AA and 40 rounds of AP. AA ammunition is stored in the turret cage. 'Replenishment of the ammunition containers can be carried out by the crew in about 20 minutes, the linked ammunition belts being fed in from the exterior via the feeder channel and into the ammunition container'. Twenty minutes to reload, if true, would penalize this weapon system rather heavily in an evaluation based on an extended series of attacks with short intervals between attack passes.

*Vigilante*[29]

The Vigilante was designed for two rates of fire, 3000 rpm and 120 rpm. In the high rate of fire, firing was in bursts of 48 rounds each. There was a 2 second delay between bursts to recharge the drum. Normal magazine load was 144 rounds (3 bursts) with optional 192 rounds (4 bursts) by hand loading. The magazine reload time was 2.5 minutes.

*Falcon*

Falcon (SP) mounts two HSS 831L 30mm guns with 650 rpm each. Ammunition is fed to the guns from two 310 round ammunition boxes in the base of the turret. Reloading is achieved by replacing the ammunition boxes via a rear loading door with the turret reversed. The last few rounds from the empty boxes are automatically held in the ammunition chutes and the linked belts of fresh ammunition are clipped directly onto there. Time to reload is unavailable, (but may be as short as 30 seconds).

An illustration of the operation is provided as Figure 11-2.

*Duster*

Duster (M42 SP) mounts two WW II vintage 40mm guns. Rate of fire is only 120 rpm for each gun, but the guns are manually clip-loaded in 4 round clips which are easily manhandled and inserted sequentially, without interrupting the firing. Hence reload time may be assumed to be zero. Barrel heating under continuous fire can interrupt the firing. After 60 rounds of continuous fire the barrels must be changed, requiring 3 minutes each. 240 rounds are carried on the mount. Additional stowage for another 240 rounds is provided in compartments on the vehicle fenders.

### 11.4.2 Results of Computations

A general observation is that for light, towed mounts, reloading is simple and should take very little time. For the self-propelled installations, considerable design ingenuity is required to keep reloading time short.

Table XI-2 compares the weapons described in the context of the assumed tactical situation. Since the source data may be erroneous or erroneously interpreted, the comparisons should be considered illustrative only.

It has been assumed that ammunition at the battery level is unlimited, hence the only parameters affecting the comparison are rate of fire, reload time, rounds per reload, and the tactical parameters. Since Vigilante is indicated to be able to fire only one second out of three, its base rate of fire in the high mode is taken as 1000 rpm. It is not known whether Vulcan has a similar delay between bursts, hence none is assumed.

It must be remembered that the tactical situation assumed represents an intense attack, and that it was assumed that each gun must attempt to fire at each section of three aircraft as it carries out its attack pass.

However, the inhibiting effect of reload time is clearly indicated, and under the assumptions used, the elderly Duster makes a fine showing in average number of rounds fired per pass. However this simple model does not account for gun heating limits, and according to the Field Manual Duster could not be fired continuously for more than 60 rounds per barrel without changing tubes.

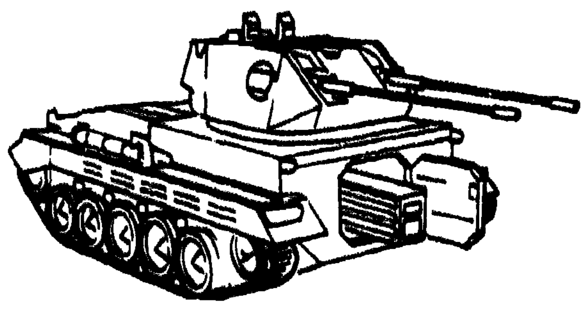

Reloading of the guns is achieved by replacing the ammunition boxes in the base of the turret via the rear loading door with the turret reversed. The last few rounds from the empty boxes are automatically held in the ammunition chutes and the linked belts of fresh ammunition are clipped directly onto these.

20871-269A

Figure 11-2. Falcon System Reload Method

**Table XI-2. Comparison of Average Firing Rates and Rounds per Pass**

| Weapon | Per Gun | | | Complete Fire Unit | | |
|---|---|---|---|---|---|---|
| | Rate of Fire (rpm) | Rounds per load | Assumed Reload Rate (rpm) | Rate of Fire Availability | Effective (Average) Rate of Fire (rpm) | Average No. of rounds fired per pass |
| Vulcan (towed) 20-mm | 3000 | 300 | 100 | 0.11 | 330 | 132 |
| Vulcan (SP) 20-mm | 3000 | 800 | 116 | 0.17 | 510 | 203 |
| Falcon (SP) Twin 30-mm | 650 | 310 | 310 | 0.55 | 720 | 290 |
| Oerlikon (SP) Twin 35-mm | 550 | 330 | 33 | 0.26 | 285 | 114 |
| Vigilante (High) 37-mm | 1000 | 144 | 58 | 0.18 | 180 | 72 |
| (Low) | 120 | 144 | 58 | 0.65 | 78 | 32 |
| Duster Twin 40-mm | 120 | (Continuous manual loading assumed) | | 1.00 | 240 | 96 |

20871-614A

## 11.5 PARAMETRIC STUDY

A brief set of computations was performed for the assumed tactical situation, but with the duration of each firing pass a variable parameter, all other tactical parameters held constant except those derived from the duration of the firing pass. The results are shown in Figures 11-3 through 11-6. They are not exactly comparable to the weapons table since the tactical parameters differed slightly.

For short durations of attack passes, with attack rate held constant, the average rate of fire achieved approaches the maximum rate of fire. For medium duration of attack passes, the average rate of fire and the average number of rounds fired per pass are more sensitive to reload rate than to number of rounds per load, over the parametric ranges considered. All other factors held constant, increasing the rate of fire is advantageous but the gain is less than proportional to the increase in rate of fire.

It may be noted that the results shown are only slightly affected by the presence of state $X_3$, and for all practical purposes in additional computations the simpler solution resulting by setting $\alpha = \beta = 0$ can be used.

As developed in later sections, the potential firing time per pass depends on the target exposure time, and the time to detect, identify, acquire, and generate firing data. As their 'reaction times' encroach on available firing time, the value of high maximum rate of fire increases.

In considering the implications of Figures 11-3 through 11-6, the term 'attack pass' can be equally well interpreted as 'potential firing time per pass' in which case it would represent exposure time less the time to detect, acquire, identify, generate firing data and open fire.

## 11.6 SIMPLE APPROXIMATE CASE

A simple solution, intermediate between the forms developed in preceding paragraphs and Equation (11.3) can be obtained by making the following assumptions:

a. Attack passes continue indefinitely at a regular rate.

b. Each pass is of duration $T_a$, and the interval between passes is $T_d$.

c. $T_a$ is small compared with the reload time of the fire unit, and it is small compared with $T_d$.

Then on the average, the gun will be able to fire for a time

$$T_w = \frac{T_a}{1 + (\nu/\rho)(T_a/T_d)} \qquad (11.28)$$

against each attack pass, and the average number of rounds fired per pass will be

$$n = \frac{\nu_0 T_a}{1 + (\nu/\rho)(T_a/T_d)} \qquad (11.29)$$

*Model for Gun Barrel Heating*

There has been insufficient time in the present contractual effort to complete a model of gun barrel heating. However an approach to such a model is sketched below.

Define

$\theta(t)$ = temperature of the gun tube at e time t after a single round is fired

$\theta$ is measured above ambient temperature.

Cooling is assumed to occur as a simple exponential decay, with a time constant T which is long compared with the time of heat input of a single round.

Then the temperature at time t caused by single round fired at time zero is approximately

$$\theta(t) = \theta_0 e^{-t/T} \qquad (11.30)$$

If rounds are fired at time $t_1,...,t_n$, the temperature at time $t \geq t_n$ is

$$\theta(t) = \theta_0 \sum_{j=1}^{n} e^{-(t-t_j)/T} \qquad (11.31)$$

Let n rounds be fired in a burst, with uniform spacing in time $\Delta$, and $\Delta << T$. The first round is fired at t = 0. Then the temperature at time t is

$$\theta_0 e^{-t/T} \left[\frac{e^{n\Delta/T} - 1}{e^{\Delta/T} - 1}\right] \qquad (11.32)$$

The last round is fired at

$t_n = (n-1)$, and measuring time from $t_n$

$t_1 = t - t_n$

$$\theta(t_1) = \theta_0 e^{-t_1/T} \left[\frac{1 - e^{-n\Delta/T}}{1 - e^{-\Delta/T}}\right] \qquad (11.33)$$

$$\cong n\theta_0 e^{-t_1/T} \left[(1 - e^{-n\Delta/T})/(n\Delta/T)\right] \qquad (11.34)$$

$$\cong n\theta_0 e^{-t_1/T} e^{-n\Delta/2T} \qquad (11.35)$$

In terms of the above parameters, we can also write a state space expression for the temperature

$$T\, d\theta/dt + \theta = \theta_0 \nu S \qquad (11.36)$$

where

$\nu$ = rate of fire when the gun is firing

S = 1.0 when the gun is in a firing "state" (11.37)

= 0 when the gun is not firing

If $\theta$ reaches a value $\theta_{max}$, there is an additional constraint: the state S = 0 is entered and maintained at least until temperature has dropped to some value $\theta_c$, or the gun barrel has been changed. Both these conditions can be included as a constant delay time of availability to fire imposed subsequent to attainment of $\theta_{max}$.

The remaining problem is to combine these considerations with the state transitions between firing and nonfiring states obtained from the tactical engagement models.

We note for further analysis that Equation (11.36) can be solved to obtain the probability density function for $\theta$, by the Feller-Kolmogorov partial differential equations, but that the introduction of the $\theta_{max}$, boundary complicates the analysis.

An empirical/heuristic approach is to compute the temperature rise during the firing interval determined from the tactical model without consideration of temperature. If the temperature exceeds $\theta_{max}$, the average firing time is reduced, arbitrarily, so that the probability of attaining $\theta_{max}$ is substantially less than unity. The average firing and nonfiring times are then analysed to determine whether additional reduction in firing time is necessary, so that the heat/cool cycle does not lead to progressively increasing maximum temperatures.

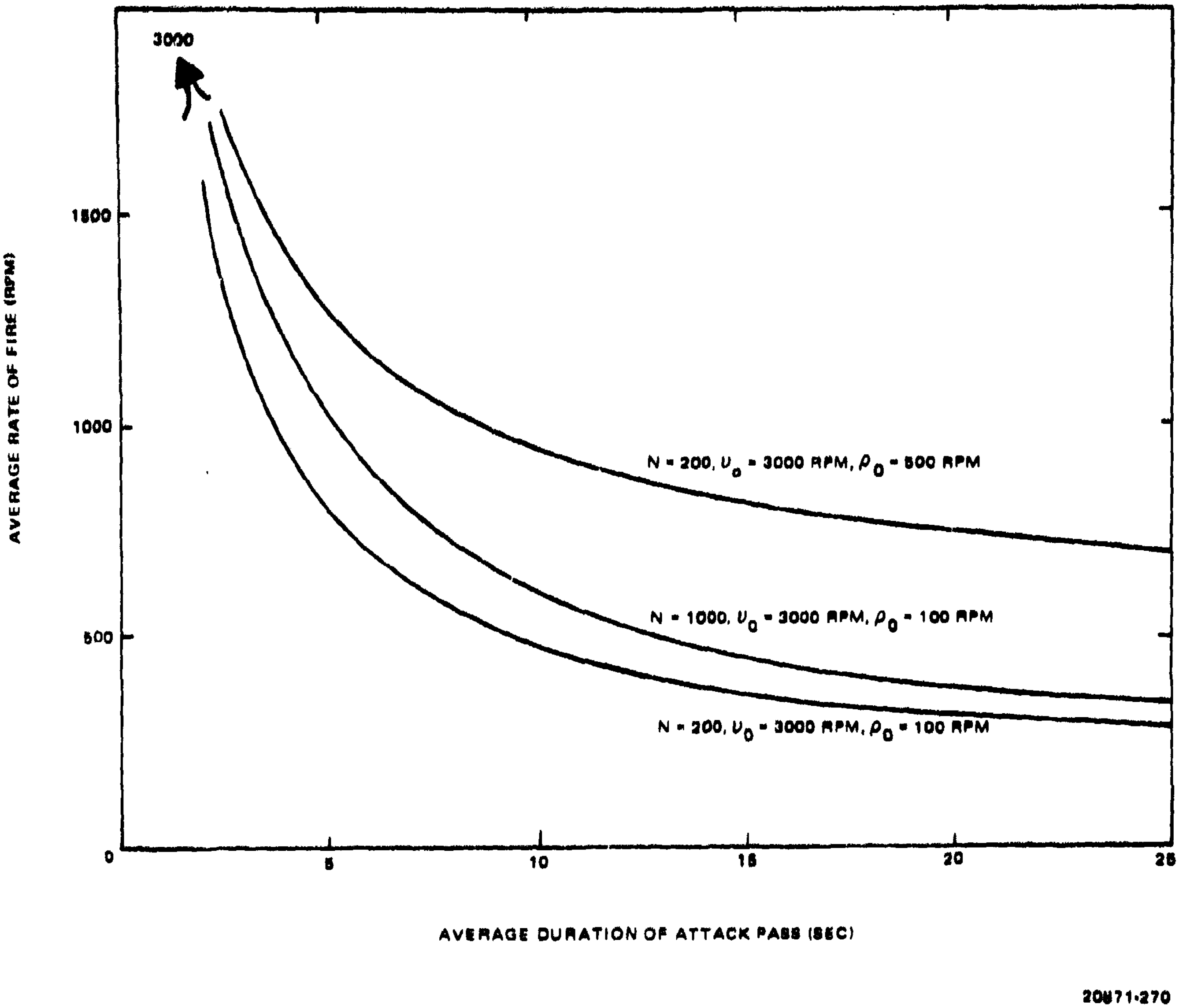


Figure 11-3. Effect of Number of Rounds per Load and Reload Rate on Average Rate of Fire

Note that the same kind of analysis is required to evaluate the probability that the battery-operated mode of Vulcan will not fail during periods of generator inoperability.

## 11.7 FURTHER DEFINITION OF ENGAGEMENT DETAILS

The simple model described in Section 11.2 for a preliminary examination of the interactions of rate of fire and loading time with the attack characteristics can be extended as far as one wishes to include a more detailed description of the details of the engagement. A moderate expansion is described below, which now separates the combat (engagement) state into three sequential activities consisting of

a. Target detection and identification.

b. Acquisition and computation of firing data.

c. Firing.

The load/reload elements are retained. Since we had previously concluded that the interval between raids had only a minor effect on the load/reload results, the interval between raids is omitted from the subset of attack states, in the following model but the description of the attack as a series of waves, each wave subdivided into firing passes, is retained.

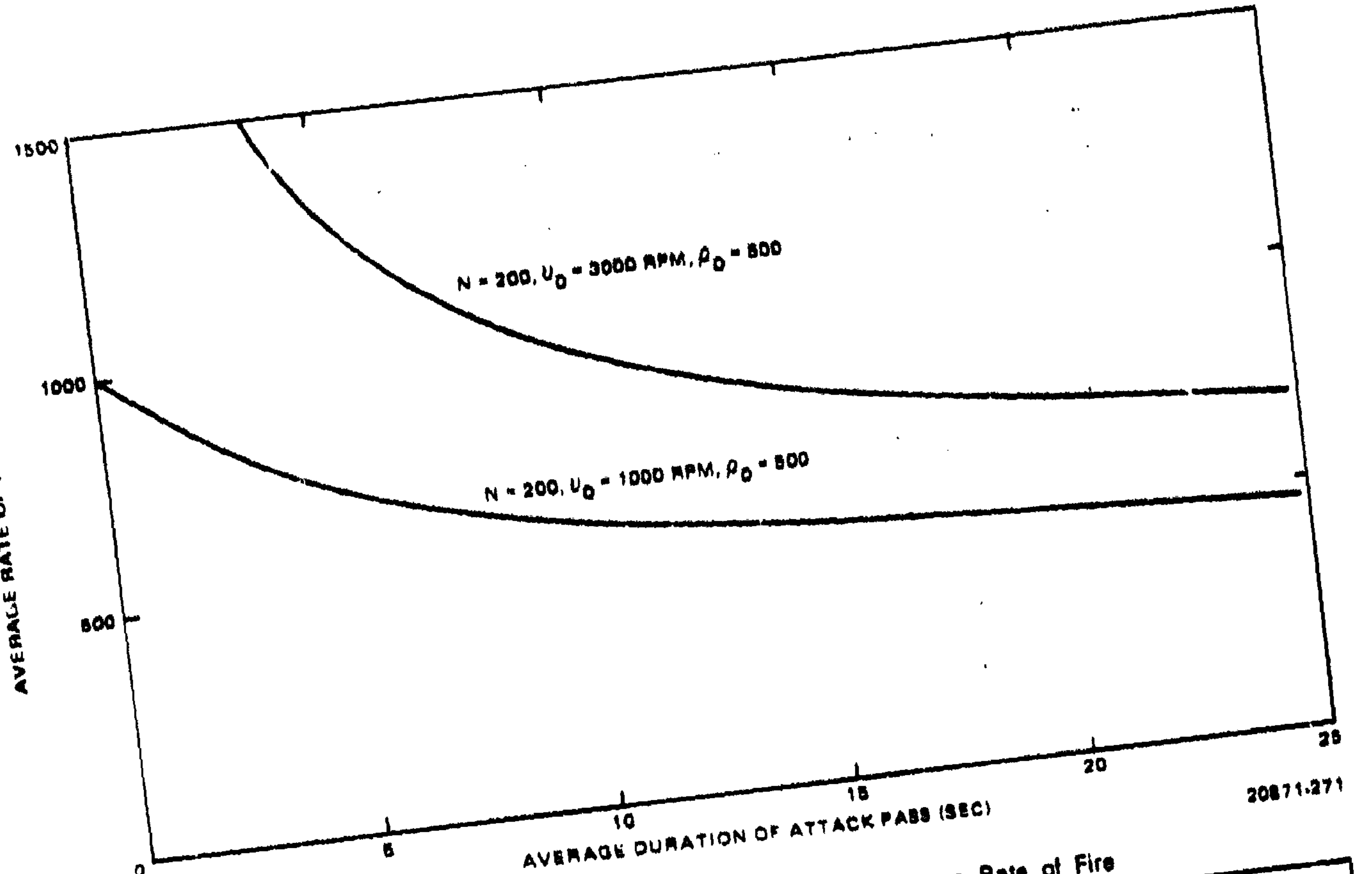


Figure 11-4. Effect of Maximum Rate of Fire on Average Rate of Fire

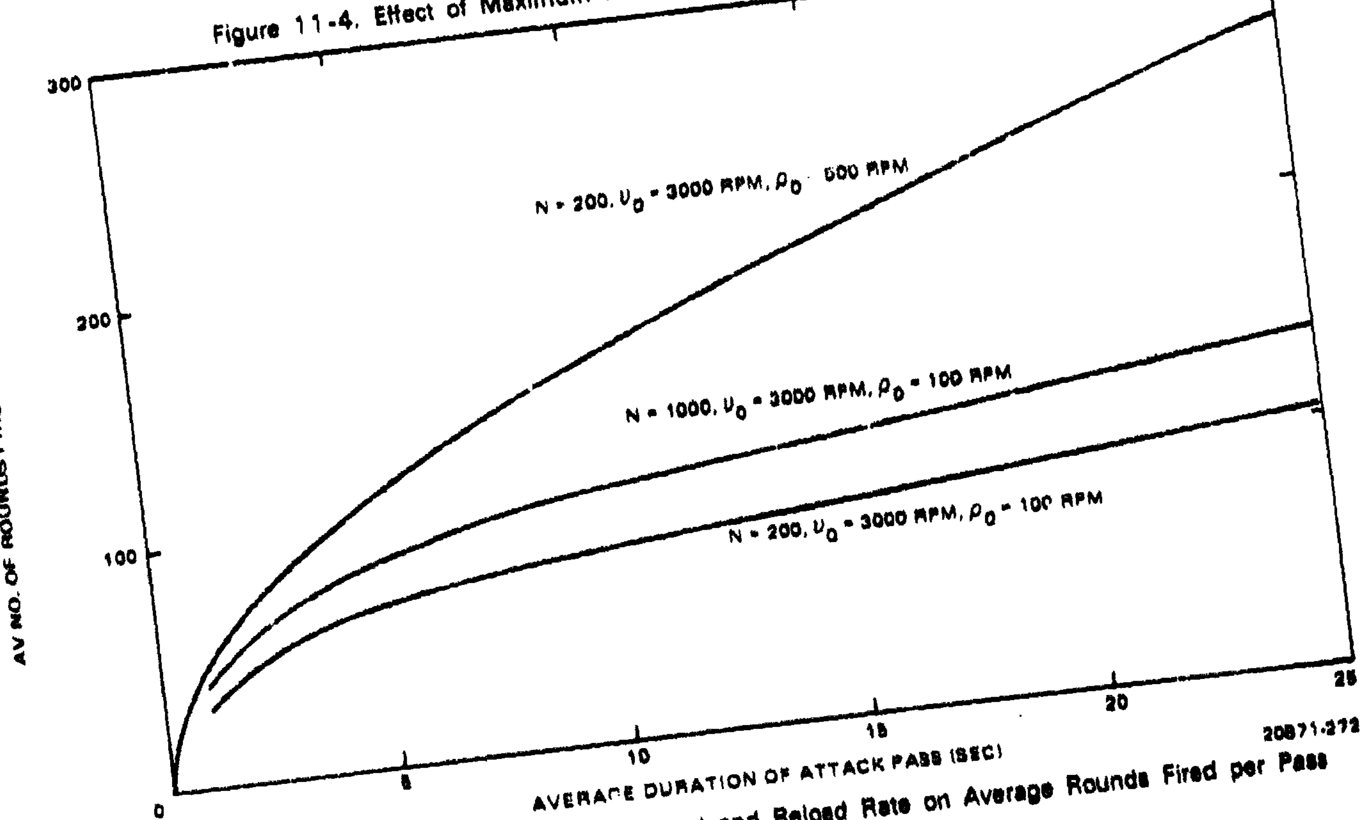


Figure 11-5. Effect of Number of Rounds per Load and Reload Rate on Average Rounds Fired per Pass

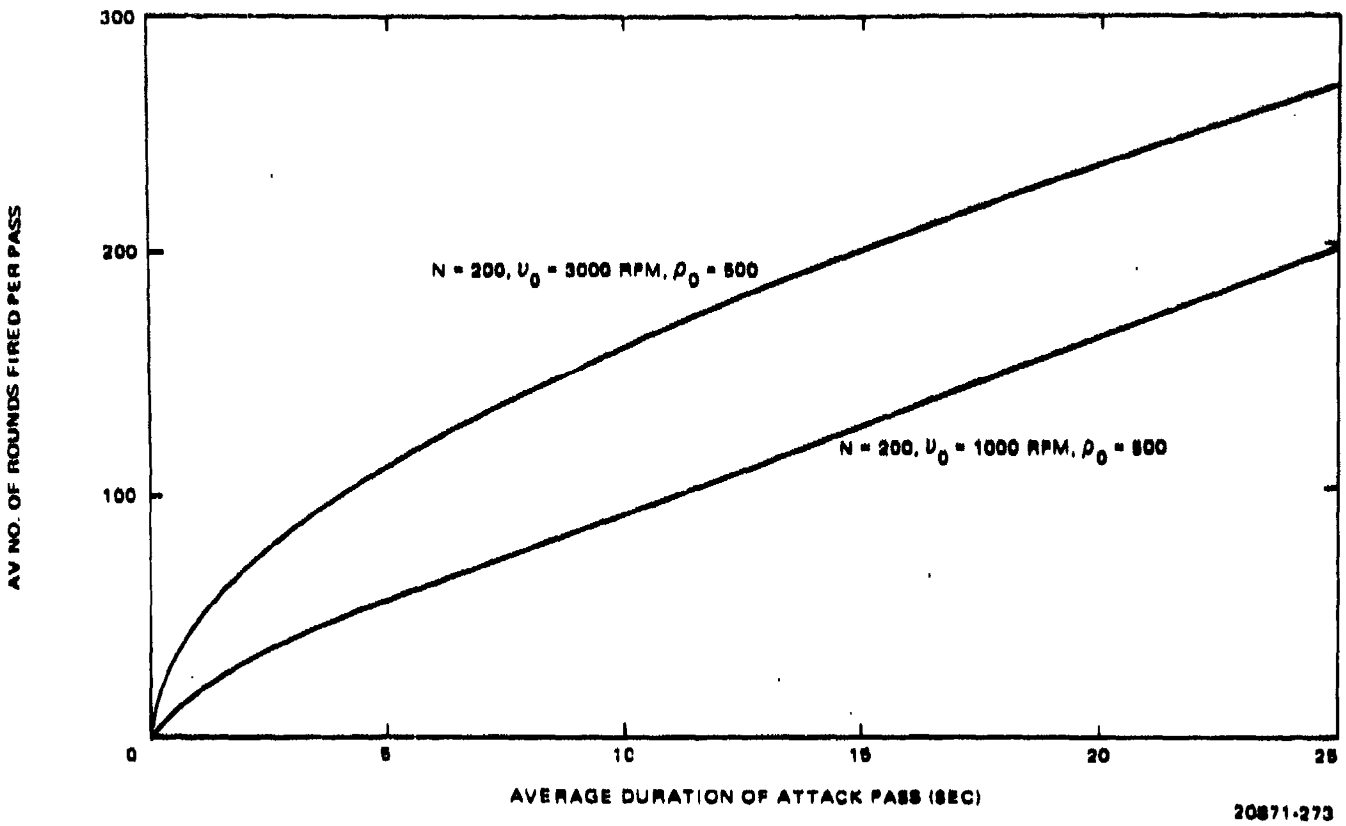


Figure 11-6. Effect of Maximum Rate of Fire on Average Number of Rounds Fired per Pass

### 11.7.1 Model Development

The flow diagram is shown in Figure 11-7. At this point we still consider only one fire unit per target. Note that the fire unit can run out of ammunition only as a transition from the firing substate, and if reloading is completed during an attack pass, the fire unit must go back through the detection and acquisition substates before it can open fire again.

Targets enter the fire unit set of substates only via the detection substate, but they can leave the defense zone from any of the fire unit states. The departure rate could be chosen to have a different value at each fire unit substate level but for this example we use the same coefficients.

Proceeding as before, we write the matrix expression of state transitions in aggregated form as

$$\begin{bmatrix}\dot{X}_1\\ \hline \dot{X}_2\\ \hline \dot{X}_3\end{bmatrix} = \left[\begin{array}{c|c|c} -(b+\lambda)I+G & A & M\\ \hline B & -aI+R & O\\ \hline L & O & -\mu I+R\end{array}\right]\begin{bmatrix}X_1\\ \hline X_2\\ \hline X_3\end{bmatrix} \tag{11.38}$$

where

$$G = \begin{bmatrix} -a_{12} & 0 & 0 & \rho\\ a_{12} & -a_{2c} & 0 & 0\\ 0 & a_{2c} & -\nu & 0\\ 0 & 0 & \nu & -\rho \end{bmatrix} \tag{11.39}$$

$$R = \begin{bmatrix} 0 & \rho \\ 0 & -\rho \end{bmatrix}$$

$$L = \begin{bmatrix} \lambda & \lambda & \lambda & 0 \\ 0 & 0 & 0 & \lambda \end{bmatrix}$$

$$B = \begin{bmatrix} b & b & b & 0 \\ 0 & 0 & 0 & b \end{bmatrix} \qquad (11.40)$$

$$M^T = \begin{bmatrix} \mu & 0 & 0 & 0 \\ 0 & 0 & 0 & \mu \end{bmatrix}$$

$$A^T = \begin{bmatrix} a & 0 & 0 & 0 \\ 0 & 0 & 0 & a \end{bmatrix}$$

We solve for the steady state (fixed point probability vector) by setting the derivatives equal to zero. As before we normalize to expressions in terms of the fraction of total time that the target spends in the three sets of states, $F_1, F_2, F_3$. To find these values set $G, R = 0$ (this is not really necessary, since the method causes them to drop out), and solve for $X_{1,2,3}$.

Typically

$$[X_4] = (1/\mu)\ L[X_1] \qquad (11.41)$$

Since

$F_4$ is the sum of the substate probabilities in $X_4$.

$$F_4 = [1 \quad 1]\ [X_4] \qquad (11.42)$$

and carrying through the operation

$$F_4 = (1/\mu)[1 \quad 1]\, L\, [X_1] \qquad (11.43)$$

we obtain

$$F_4 = (\lambda/\mu)\, F_1$$
$$F_2 = (b/a)\, F_1 \qquad (11.44)$$

since

$$F_1+F_2+F_4 = 1.0$$
$$F_1 = 1/D \qquad \text{where } D = 1 + (a/b) + (\lambda/\mu)$$
$$F_2 = (b/a)/D$$
$$F_4 = (\lambda/\mu)/D \qquad (11.45)$$

As before, we normalize the matrix equation by setting $Y = X/F$.

We then have

$$\begin{bmatrix} -(b+\lambda)\, I + G & (b/a)A & (\lambda/\mu)M \\ B & -bI + (b/a)\, R & 0 \\ L & 0 & -\lambda I + (\lambda/\mu)R \end{bmatrix} \begin{bmatrix} Y_1 \\ Y_2 \\ Y_4 \end{bmatrix} = 0 \qquad (11.46)$$

and as a result of the normalization, all of the subset probabilities within each Y sums to unity. Since we are only interested in $Y_1$, we solve the above set of matrix equations by expanding and eliminating all Y except $Y_1$. As in the load/reload model, all matrix inversions involved are simple.

The result is the following matrix equation for $Y_1$

$$\left\{ \cdot (b+\lambda) I + G + [(b/a)A + (\lambda/\mu)M + (b/a)(a+\rho)^{-1} AR + (\lambda/\mu)(\mu+\rho)^{-1} MR] U_2 \right\} Y_1 = 0 \tag{11.47}$$

where

$$U_2 = \begin{bmatrix} 1 & 1 & 1 & 0 \\ 0 & 0 & 0 & 1 \end{bmatrix}$$

No doubt one could postpone the final extraction of the four subsets of probabilities within $Y_1$ by additional matrix manipulation, but the solution is simple, when Equation (11.47) is expanded directly. It is

$$Y_{11} = 1/D$$

$$Y_{12} = k_1/D$$

$$Y_{1c} = k_1 k_2/D$$

$$Y_{1r} = k_1 k_2 k_3/D$$

where

$$k_1 = \alpha_{12}/(b + \lambda + \alpha_{2c})$$

$$k_2 = \alpha_{2c}/(b + \lambda + \nu)$$

$$k_3 = (\nu/\rho)/\left[1 + \left(\frac{\lambda}{\mu+\rho}\right) + \left(\frac{b}{a+\rho}\right)\right]$$

$$D = 1 + k_1 + k_1 k_2 + k_1 k_2 k_3 \tag{11.48}$$

In the above expressions, if $\alpha_{12}$, $\alpha_{2c}$ are very large, corresponding to no delay in detection, identification and acquisition, the expression for $Y_{1c}$, the fraction of the attack pass over which firing is conducted on the average, reduces to

$$Y_{1c} = 1/(1 + k_3) \tag{11.49}$$

and this is the expression obtained earlier.

Since $\nu$ is defined by $\nu = \nu_0/N$, where $\nu_0$ is the maximum rate of fire on the gun, and N is the number of rounds per load, if we set $\nu = 0$ in the above expressions, we obtain the mean firing time per attack pass, without the load/reload limitation, as it depends on the tactical parameters, and the mean time to detect, identify, acquire, etc.

### 11.7.2 Example of Weapon Evaluation

To observe the implications of the relations developed in the previous section, we consider a sustained attack consisting of a series of waves, each wave consisting of a number of attack passes. Attacks are assumed to be at low level, with the targets exposed at about 7500 meters, with target speed about 300 m/s, so that the average time to weapon release is 24 seconds.

The evaluation is conducted from the point of view of the loading experienced by a single fire unit, on the assumption that all available fire units fire at the 3-plane element of each attack pass.

We assume

$$F_2 = 1/2$$

$$(F_1 + F_4) = 1/2$$

Each wave has an average duration of 6 minutes, the average interval between waves is 6 minutes, and there are 4 attack passes per wave, each duration 0.40 minutes. Then

$$F_2 a = 1/12 \text{ per minute}$$

$$a = 1/6 \text{ per minute}$$

On the average there are 4 attack passes per cycle, or 4/12 per minute

$$F_1(b + \lambda) = 1/3 \text{ per minute}$$

$$F_1(b = \lambda) = 2.5 \text{ per minute}$$

$$F_1 = 2/15$$

$$b/a = F_2/F_1 = 15/4$$

$$b = 5/8 \text{ per minute}$$

$$= 15/8$$

$$b/a = 1 + (\lambda/\mu)$$

$$= 15/22 \text{ per minute}$$

The tactical coefficient set is shown in Table XI-3.

For a hypothetical weapon comparison, we use three generic weapons roughly similar to existing weapons. These are

a. 'Duster-type': visual detection, identification and acquisition.

b. 'Vulcan type': visual detection and acquisition, electronic IFF.

c. 'Oerlikon-type': radar detection and tracking, electronic IFF, automatic track radar put on.

The coefficients describing these characteristics are

$(\alpha_{12})^{1}$ = mean time for detection and identification

$(\alpha_{2c})^{1}$ = mean time for acquisition and firing data computation

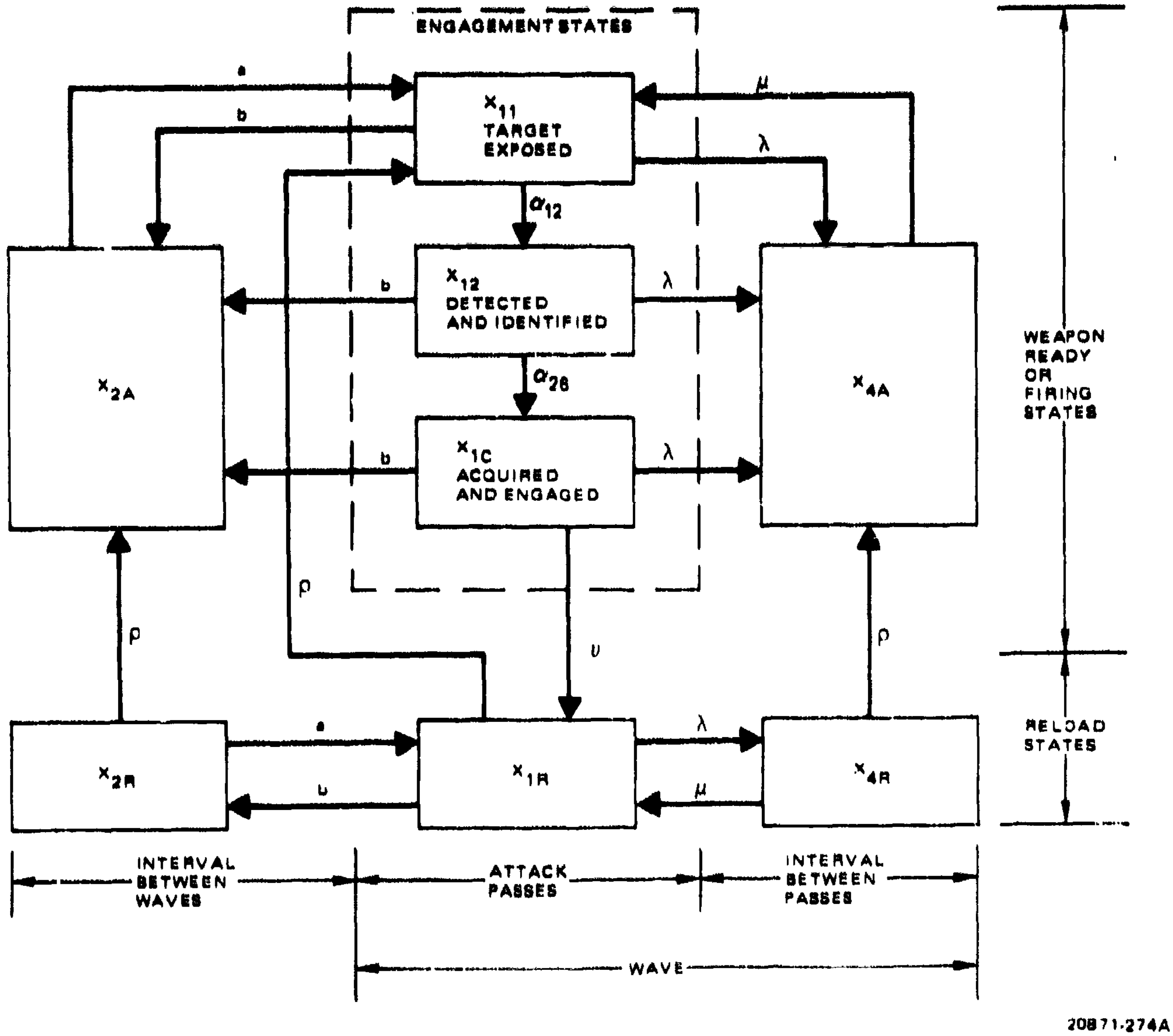


Figure 11-7. Flow Diagram for Attack and Engagement

In a real weapon evaluation these coefficients would be determined by separate analyses. Here we *assume* values for illustration. The maximum rate of fire, rounds on mount and reload rate are those listed in Table XI-2. The set of weapon parameters is then as shown in Table XI-4.

On working through Equation (11.48), we obtain the following results, shown in Table XI-5.

The assumed attack pattern with its frequent waves and passes within waves stresses the reload capability of the weapons.

Rather than drop the example at this point, we anticipate later considerations and introduce a rough comparison of effectiveness including terminal effect and probability of hitting.

Duster has a simple course and speed sight, requiring human estimates of target course and speed. Vulcan has a computing sight, manual tracking, radar range, (and 6 x 12 mils artificial dispersion). The Oerlikon system has radar tracking and a 'complete' fire control solution. We estimate for the example (again, simulation and/or separate analysis are required to properly evaluate real systems) that the equivalent standard deviation of projectile miss distance for the three systems is in the ratio 15 mils, 10 mils, 5 mils. Then the expected number of lethal hits per firing pass is as given in Table XI-6.

Table XI-3. Tactical State Transition Rates for Engagement Analysis

| Coefficient | Value (per minute) |
|---|---|
| a | 1/6 |
| b | 5/8 |
| $\lambda$ | 15/8 |
| $\mu$ | 15/22 |

20871-615

The last column has been normalized to unity for the Duster-type weapon.

Fire control performance dominates this hypothetical comparison, and it is clear that evaluation of fire control system performance will be the critical (as well as the most difficult) element of an evaluation.

## 11.8 MODEL EXTENSIONS

The model developed in Section 11.8 may be extended and further detailed along the following lines.

### 11.8.1 Simultaneous Presence of Several Attack Elements in Defense Envelope

As developed thus far, the model does not recognize the number of attack elements which may be simultaneously present within the defense envelope. In effect, it bases the engagement computation on the assumption that only one element (of n closely spaced aircraft) is present on each activation of a 'combat state'. Since successive attack elements may be spaced by about 2 kilometers in reality, so that each element is not exposed to bomb fragments from the preceding element, this is probably an acceptable assumption, and in fact, the probability that two elements are simultaneously present is negligibly small for the tactical arrival and departure rates assumed in the examples.

There is no difficulty in extending the flow diagram by adding states and substates in which two attack elements are within the defense envelope. It is doubtful that more than two elements need ever be considered for short range weapons. However the total number of substates to be considered is more than doubled, and the increased complication is not considered advantageous in view of the other approximations in describing the situation.

### 11.8.2 Advantage of Early Kill Recognition

The model does not explicitly recognize the ammunition savings possible if a fire unit can stop firing when it obtains a recognizable kill. This effect can be easily included by augmenting the target departure rate from the defense envelope by an average kill rate.

### 11.8.3 Variation of Coefficients During an Attack Pass

The detection rate, identification rate, kill rate and other parameters change as the target range decreases, passes through a minimum, and again increases. The probability that the target will drop its munitions and begin evasive breakaway varies with range. There are several approaches to including these variations, as follows

a. *Computer Simulation.* If the Army maintains an evaluation effort devoted to short range air defense systems, a computer simulation containing all of the sub-models of this report and others as well will no doubt come into being.

b. *Division of Attack Pass into Substates.* The attact state can be subdivided into several sequential sub-states, during each of which each of the state transition coefficients is assumed constant, although they may differ across states. This approach is feasible, does not require a computer, and the matrix algebra is feasible, but tedious. However it needs to be done only once, after which the resulting expressions can be worked on a slide rule for system evaluation, or programmed on a desk size minicomputer.

c. *State Space Solution with Time Varying Coefficients.* The differential equations of state can be written either in linear form, with time varying coefficients, or in non-linear form. One would then attempt to find reasonable forms for the equations which would admit relatively simple determination of the steady state values. This approach requires as much art and ingenuity as mathematical skill.

d. *Separate Sub-model Analysis of the Engagement.* Engagements may be separately modelled and analysed, and from these analyses average coefficients may be determined to use in the model of Section 11.9. This is probably the best way to obtain good estimates of fire unit effectiveness per engagement, and to understand how each of the performance parameters influences effectiveness. Fewer Procrustean approximations are required to describe system performance, and causes and effects can be better resolved than at the macroscopic level of overall system performance. It is this approach which is developed in subsequent sections of this report.

Table XI-4. Weapon Parameters

| Weapon | Per Gun | | | Mean Time (sec) for | |
|---|---|---|---|---|---|
| | Max rate of fire (rpm) | Rounds on mount | Assumed Reload rate (rpm) | Detection and IFF | Acquisition and Computing |
| Duster-type (two guns) | 120 | Not applicable | | 15 | 8 |
| Vulcan-type (Gatling) | 3000 | 800 | 116 | 8 | 7 |
| Oerlikon-type (two guns) | 550 | 330 | 33 | 4 | 5 |

20871-616

Table XI-5. Comparison of Potential Firing Time and Average Number of Rounds Fired per Pass

| Weapon | Mean Firing Time (sec) | | Average Number of Rounds per Pass with Reload Constraint |
|---|---|---|---|
| | Without Reload Constraint | With Reload Constraint | |
| Duster-type | 11 | 11 | 44 |
| Vulcan-type | 14 | 3.1 | 155 |
| Oerlikon-type | 17 | 5.2 | 96 |

20871-617

Table XI-6. Expected Number of Lethal Hits per Firing Pass

| Weapon | Number of Rounds (N) | Probability of Kill, Given a Hit ($p_c$) | $Np_c$ | Relative Number of Lethal Hits $Np_cp_h$ |
|---|---|---|---|---|
| Duster-type | 44 | 0.48 | 21 | 1.0 |
| Vulcan-type | 155 | 0.15 | 23 | 2.4 |
| Oerlikon-type | 96 | 0.50 | 48 | 20.0 |

20871-618A

# SECTION 12
# ANALYSIS OF THE ENGAGEMENT

The most critical part of a system evaluation of a predicted fire system is the analysis of possible engagements. It is this element of the evaluation that is most likely to be averaged over in top level defense simulations, but only at the engagement level can one determine the best values of the many trade-offs possible in system design which cumulate to make a difference of 10/1 in overall effectiveness between excellent systems and good systems.

To fully define the system capability, one requires engagement computations for a large number of combinations of

a. Illumination (day/night).

b. Weather.

c. System operational modes.

d. Threat magnitude and attack scheduling.

e. Target type, munition, and attack mode.

## 12.1 ENGAGEMENT SUBSTATES

The principal substates into which the engagement may be subdivided are shown in Figure 12-1 for an engagement with prior target identification, and in Figure 12-2 for an engagement without prior target identification.

The transition rates between states depend on the target position relative to the defense site, and hence on time, as well as on environmental parameters, target tactics and system design characteristics.

Subject to the availability of the information required to quantify the model, the event sequences of Figures 12-1 and 12-2 can be developed in a simulation. In the present section, however, sub-models are developed which allow preliminary analysis and comparisons of systems, prior to the availability of a complete engagement simulation.

The Litton simulation allows the portion of the engagement beginning with target acquisition and continuing through kill or departure of the target to be evaluated quickly. This simulation has an extremely versatile capability for evaluating a wide range of sensor characteristics, weapon characteristics, prediction and smoothing algorithms, and target path types.

To complete the present section, however, some simple analytical models of the firing state are presented. The approximations used have been determined, by comparison with more exact results from the simulation, to be adequate for rough estimates. They permit an initial sizing of the problem prior to laying out simulation runs.

One is not necessarily limited to simulation for a complete engagement analysis. Given the probability distributions required in any case to properly design a simulation for this non-linear, time varying set of event transitions, it is possible to work through the successive convolutions of probability density functions to obtain the desired probabilities of aircraft destruction and destruction of the defended target. This requires some skill in choosing integrable forms to approximate the individual functions, and if a computer is available, and continued analyses of this kind are planned, it may be more economical to use simulation.

Target tactics are a principal determinant of the outcomes. Note from the flow diagrams that the target can exit from each event state by releasing its munitions and breaking away. The time at which this occurs, or, more generally, the probability density function of release ranges, is an option open to the attacker. By delaying munitions release, he improves his chances of destroying the defended target, in general, but lessens his own survival probability.

The defender, on the other hand, would prefer to do most of his shooting at relatively short ranges to conserve ammunition for given effect, provided that he is clever enough to get in his shooting before the aircraft releases its munitions.

A proper engagement analysis should therefore consider the interaction between attacker's weapon release doctrine, and defender's firing doctrine.

In the following sections a series of sub-models is presented which allow a preliminary exploration of each state of the engagement.

## 12.2 INITIAL EXPOSURE RANGE OF TARGET

The range at which a target is first exposed to possible detection depends on its altitude, terrain characteristics, and on whether the target is flying level or following terrain contours.

The variability with terrain, for low flying aircraft, is very large, and the initial exposure range will vary widely for different directions of approach to a defense site in most cases, since few sites have uniform 360° coverage.

One may use digitized terrain to examine a particular site in detail. However, a substantial amount of effort is involved in doing this for a wide set of representative terrain types and site locations in a specific terrain class. For initial estimates it may be preferable to use a simpler method which employs the principal parameters defining exposure range. A possible approach, which is not yet completely satisfactory

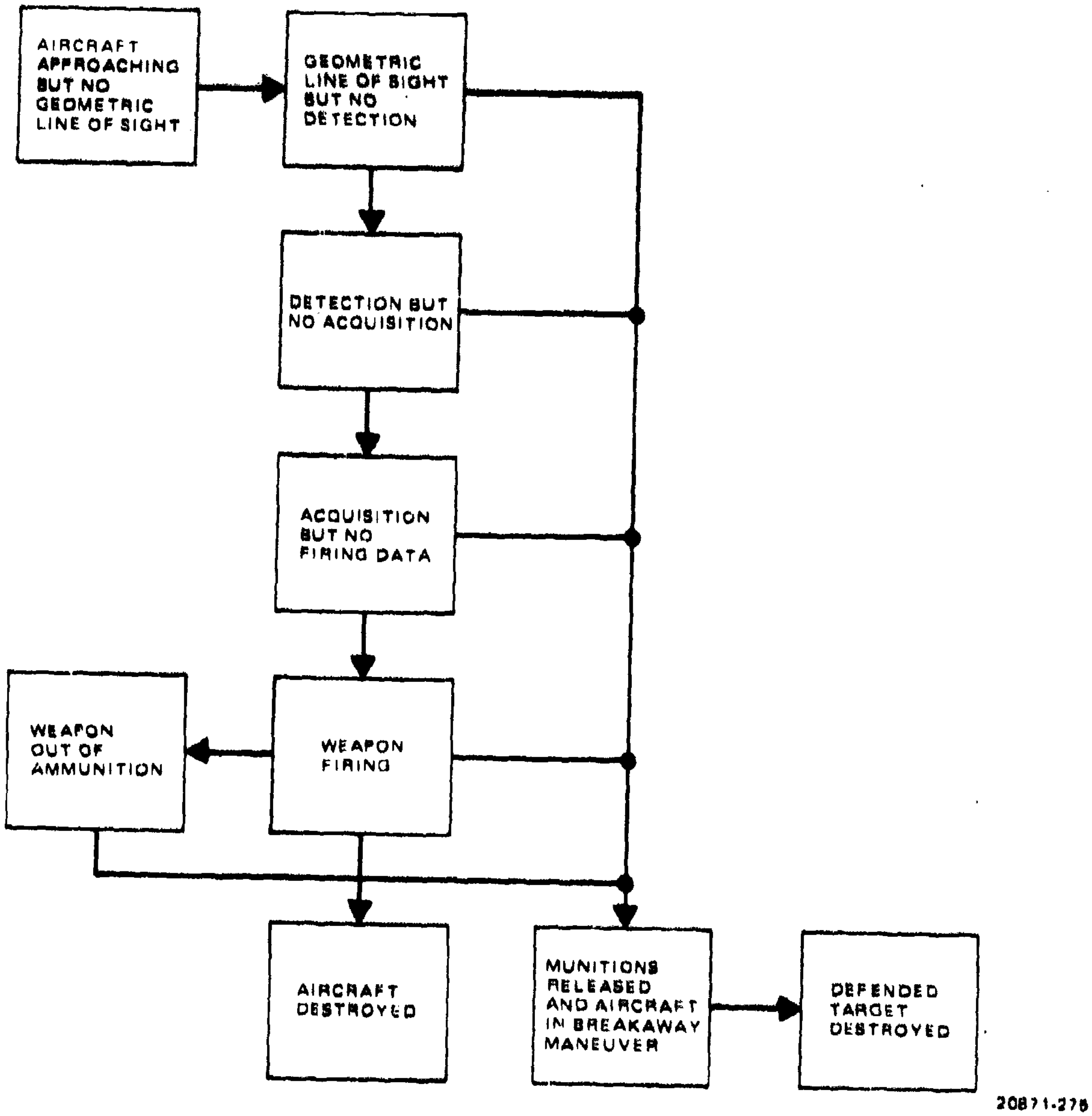


Figure 12-1. Engagement Sequence With Prior Identification

for reasons developed below, is to employ an excellent terrain model developed by Caywood-Schiller, and validated against computerized terrain.

The Caywood-Schiller model expresses the *average* range at which a low flying target can be sighted as

$$R = R_0 e^{0.21 n + 0.27 m} \qquad (12.1)$$

where

$R_o$ = characteristic range for a terrain type

n = target height above terrain contours in units of standard deviation of terrain

m = height of the site above the mean terrain elevation in units of standard deviation of terrain

$R_o$ is developed as a function of the parameter $(\beta\sigma)$ where

$\beta$ = a measure of terrain correlation (units of km$^{-1}$)

$\sigma$ = standard deviation of terrain about the mean

Terrain 'roughness' is defined in terms of the value of $(\beta\sigma)$.

This expression has been laid out in the form of a nomogram in Figure 12-3. In addition, two curves

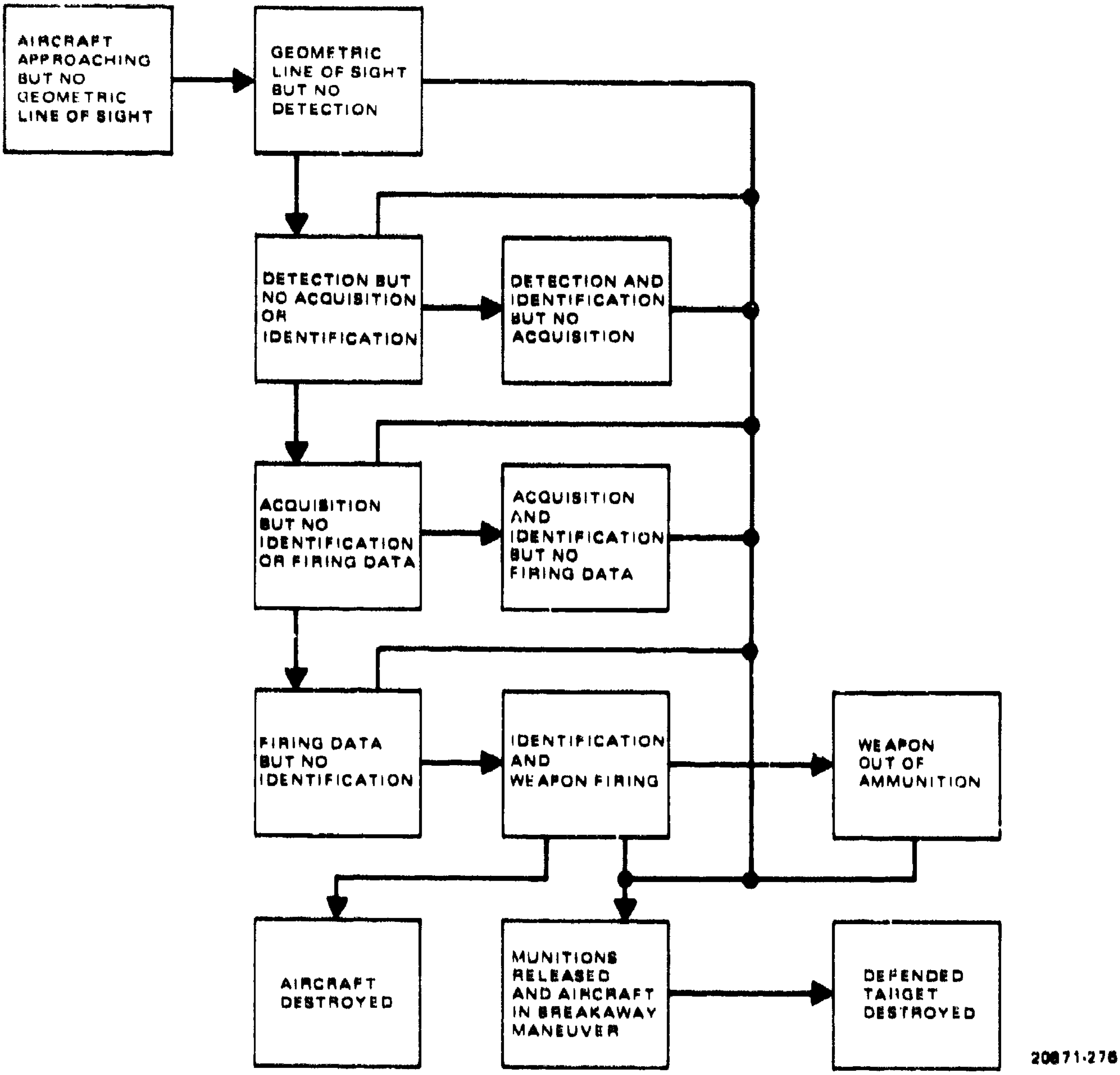


Figure 12-2. Engagement Sequence Without Prior Identification

have been sketched in to relate target velocity to average height above terrain (in units of standard deviation of terrain).

If one uses the Caywood-Schiller formula directly, one finds that the exposure ranges are high by a factor of about 2.5 over those obtained in helicopter detection experiments. This difference might be explained on the basis that the helicopters used approach paths which concealed them from the sight as long as possible, but the difference requires detailed analysis for a full explanation. However, a 'best approach' scale has been added in Figure 12-3 to reduce exposure range by a factor of 2.5.

In Figure 12-4 the experimental data on helicopter sighting ranges has been plotted as a function of target velocity and terrain roughness. Since terrain roughness was not measured in the experiments, the assumption is made that the qualitative designations can be related to the qualitative designations suggested by Caywood-Schiller.

It will be noted from Figure 12-4 that increasing terrain roughness increases exposure range. As terrain becomes increasingly flat, exposure range *must* increase again, as sketched via the dashed lines, but this was not observed in the experiments.

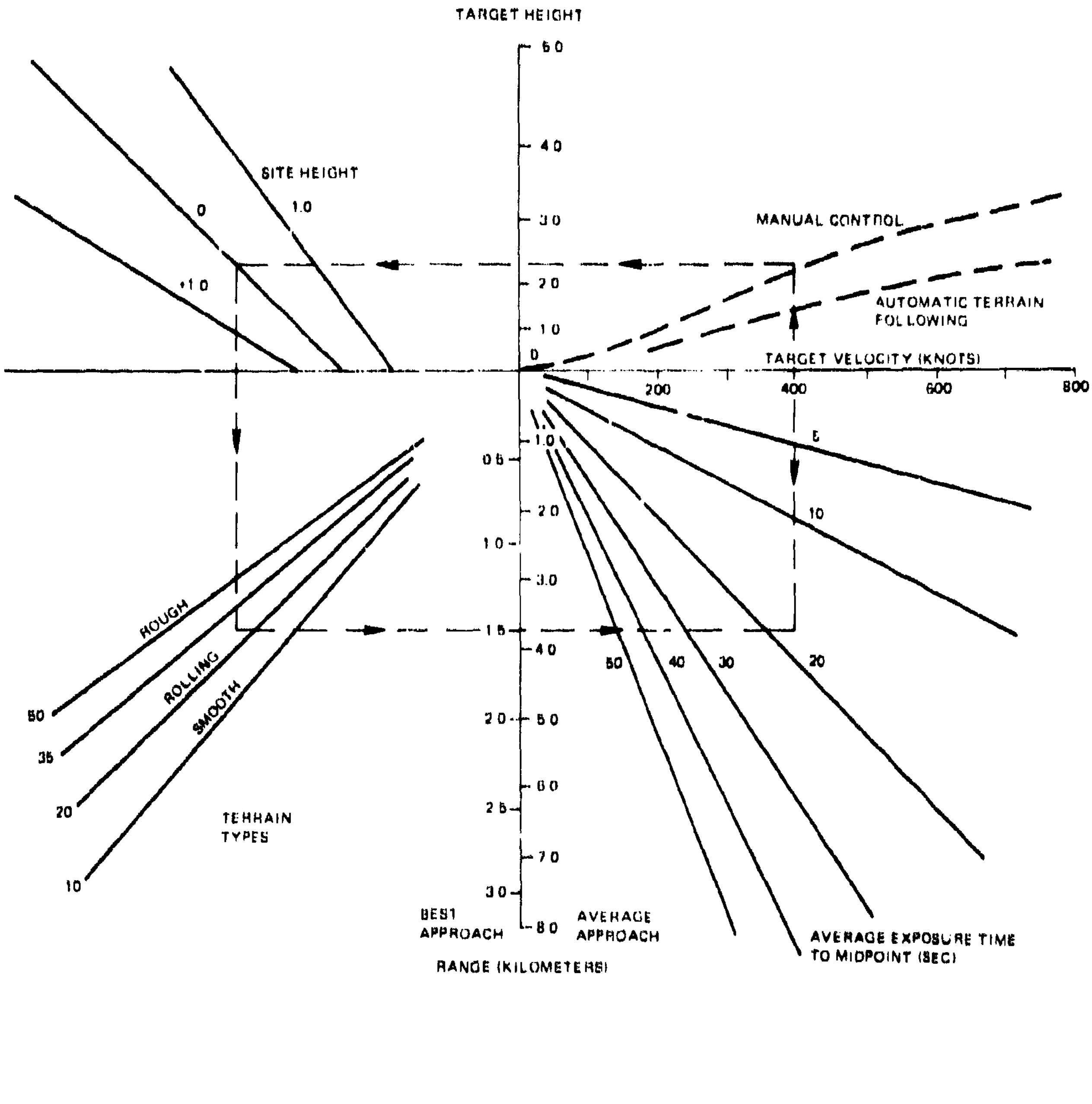


Figure 12-3. Nomogram for Estimating Target Exposure Range

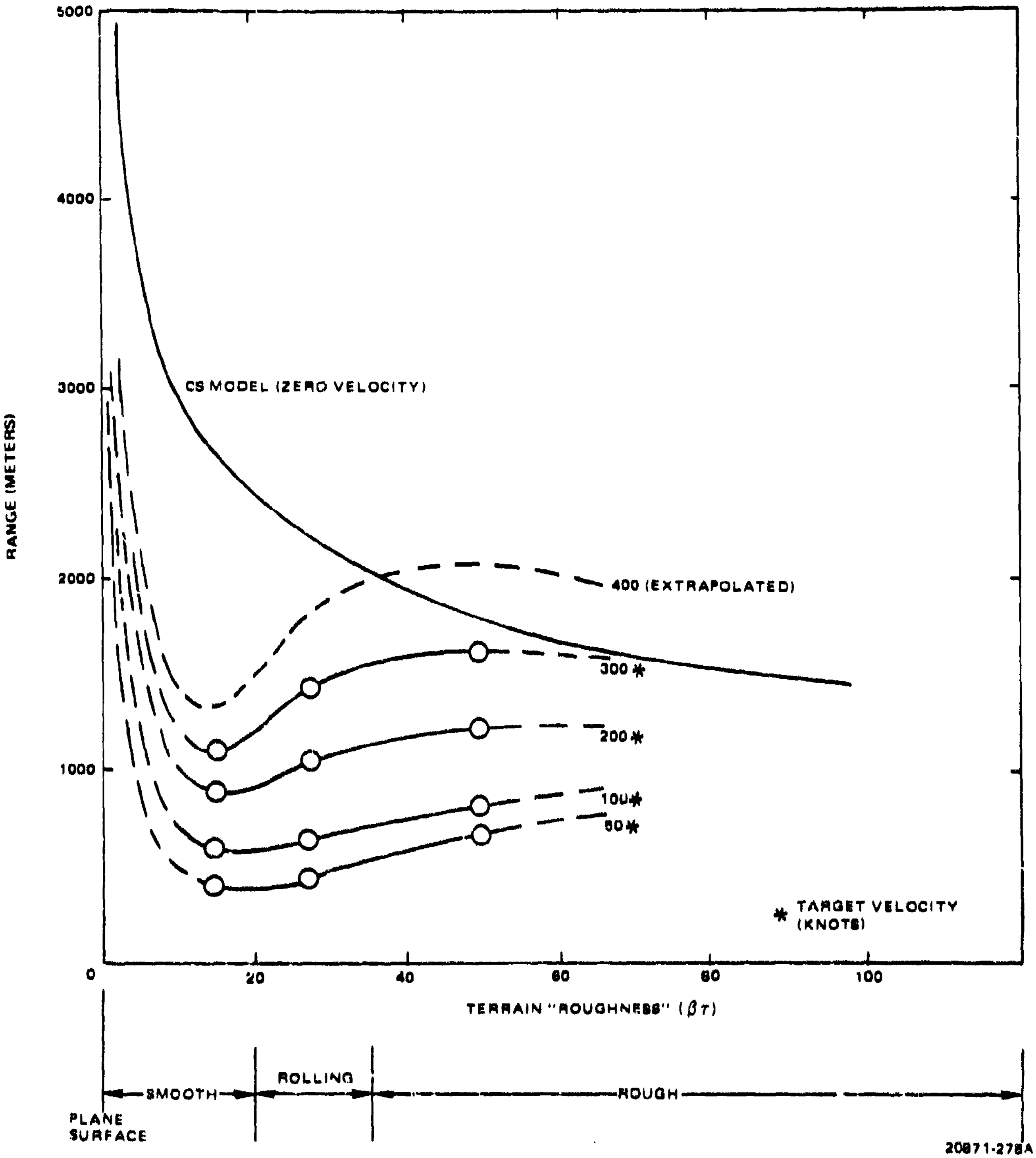


Figure 12-4. Visual Detection Range of Helicopters versus Terrain Roughness

The actual measurement in the experiments was 'exposure time' during which the observers could see the helicopters, and to construct Figure 12-4 this was multiplied by velocity and divided by a factor of 2.0, to obtain a rough estimate of initial exposure range. The experiment included the detection process, but even if one adds two or three seconds for the observer to detect the helicopter after it has been exposed (in almost all cases he had already heard the engines and was alerted to the approximate direction of approach), the difference between the model and the experiment is still not resolved.

Another complicating factor, difficult to include properly in map studies is the effect of vegetation, buildings, etc. in shielding low flying aircraft against exposure and this may help to explain the difference.

The relationship between target height above ground and speed in Figure 12-3 assumes that height/standard deviation is a simple function of velocity. In fact it is probable that for a given velocity, target height above ground increases as a higher power of standard deviation, and this may also help to explain the increase in sighting range with terrain 'roughness'.

The variation of the experimental data with even small displacements in observer position is much greater than the indicated effect of terrain roughness in Figure 12-4.

It is therefore suggested that Figure 12-3 may be acceptable for rough estimates of target exposure range, and that the usefulness of a simple chart of this type may be sufficient to encourage its improvement based on more extensive experimental data and computer analysis of terrain data.

An example of the use of the nomogram is shown by the dotted lines. A target flying at 400 knots under manual control is estimated to follow contours at about 2.2 times terrain standard deviation. For a site at the terrain mean elevation in rolling terrain, the average initial exposure range is about 3.8 kilometers, and the exposure range for a 'best' approach is 1.5 kilometers. The exposure time to midpoint is therefore about 19 seconds for an average approach and about 8 seconds for a 'best' approach.

In estimating sighting distances, one might expect that as the velocity of a helicopter is reduced in nape of the earth flying, and the height above ground approaches zero, the distribution of exposure ranges might approach that already worked for tanks in tank versus tank combat. Some data on tank sighting ranges has been published in an unclassified journal[24] and appears to be based on an exponential distribution, so that the probability that a tank is exposed beyond D kilometers is

$$p = e^{-D/D_m} \qquad (12.2)$$

where the reference indicates a values of $D_m = 1.3$ kilometers for a mid-European zone, and 1.65 kilometers for northwest Germany.

An extensive set of references on the effect of terrain on target exposure range is given in the accompanying Analysis Report on this contract, including the Caywood-Schiller analyses.

## 12.3 VISUAL DETECTION PROBABILITY

Before going into detailed computations of visual detection probability it may be helpful to have a simple method of making initial rough estimates. The nomogram of Figure 12-5 makes this possible. A detailed discussion of the factors entering the estimation of detection probability by a human observer is provided in Section 3.0 of the Analysis Report. Figure 12-5 is based on the following rationale:

a. The search rate of a human observer can be represented by a 'glimpse rate' multiplied by a function of range which depends on target relative contrast at the observer and the angle subtended by the target at the observer's eye. The relative contrast of a target against a sky background is approximated as a simple exponential function of meteorological visibility range $V_m$.

b. The probability that a target approaching the observer has been detected by range R, if it is first exposed at range $R_0$ is approximated by

$$P(R,R_0) = 1 - e^{-k/v\int_R^{R_0} R^{-2} e^{-k_2 R/V_m}} \qquad (12.3)$$

where

- v = target velocity
- R = slant range
- $V_m$ = meterological visibility (meters)
- $k_2$ = a numerical constant
- k = a coefficient depending on the solid angle scanned by the observer.

c. The function

$$Q(R,\infty) = 1 - P(R,\infty) \qquad (12.4)$$

has been computed, using Hummro and Human Engineering Laboratory experiments under conditions of excellent visibility, as a point of departure. From the curves of detection probability versus range for 45/90° search, curves for other values of $V_m$ have been estimated.

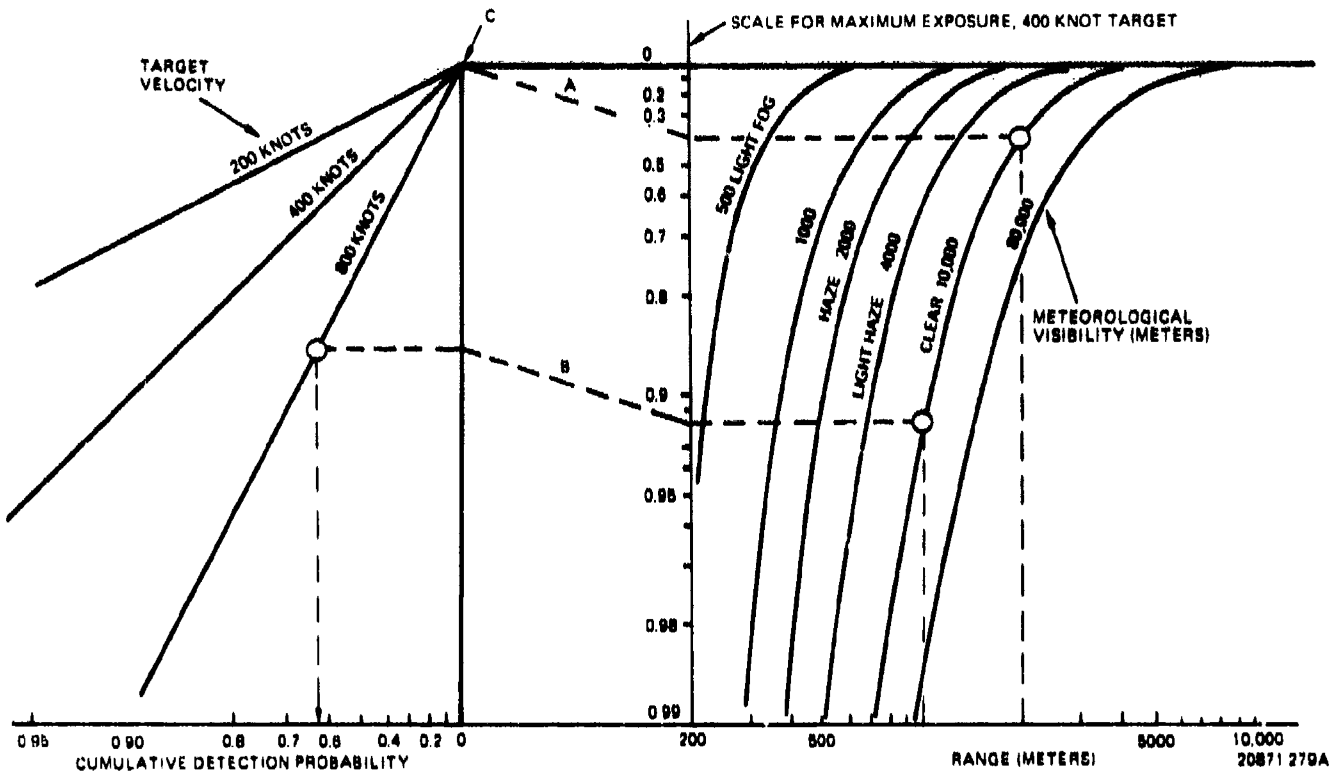


Figure 12-5. Nomogram for Estimating Cumulative Visual Detection Probability

d. From the form of Equation (12.3)

$$Q(R,R_0) = Q(R,\infty)/Q(R_0,\infty) \qquad (12.5)$$

and conversion to other target velocities v is accomplished by

$$Q(R,R_0,v) = Q(R,R_0,400)^{400/v} \qquad (12.6)$$

To use Figure 12-5 enter with the initial target exposure range $R_o$ and the range R at which the cumulative detection probability is desired. Draw a line from the higher intercept on the vertical axis to point C. This is line A. Draw line B parallel to A. Enter the target velocity section of the nomogram with the intercept of line B on the axis OC and read cumulative detection probability on the horizontal axis.

The basic data was taken against low level targets with unobstructed line to sight to very long ranges. The question of whether the basic data has been properly interpreted and extended in Figure 12-5 certainly needs to be examined very carefully. If the data have been interpreted properly, one would not consider seriously the design of a low altitude air defense system to operate beyond 2000 meters and depending on visual target detection by a human operator.

Figure 12-5 is limited to estimates of detection probability of aircraft approaching the observer on a low altitude path the ground track of which passes through the observer's position. It should not be used for paths with more than a few hundred meters crossing range, or for high altitude paths. It also does not allow for sun angle, which should be included in an accurate computation. Since the aircraft always flies over the observer at low altitude it is always detected eventually. For offset, or high altitude paths, one might perform the integration of Equation (12.3) over the corresponding range segments, in which case, final detection probability would not be unity. In this case one should probably also introduce the change in projected target area with aspect.

As an example of how one might combine the probability density functions of successive states, consider the convolution of the exposure range function with that for visual detection.

Over the range

$$500 < V_m < 10{,}000 \text{ meters} \qquad (12.7)$$

the range at which a cumulative detection probability of 50% is attained, for the conditions of Figure 12-5 by

$$(R_{50}/1000) = 16\,K\,(400/v)\,(V_m/1000)^{1/2} \quad (12.8)$$

where $R_{50}$, $V_m$ are measured in meters, v = target velocity in knots, and

$$\begin{aligned} K &= 0.5 \text{ for } 180 - 360^\circ \text{ scan} \\ &= 1.0 \text{ for } 45 - 90^\circ \text{ scan} \\ &= 2.0 \text{ for less than } 10^\circ \text{ scan} \end{aligned} \quad (12.9)$$

The probability that the target has not been detected by a range R, given initial exposure at very long range can be approximated as

$$Q(R,\infty) = e^{-.693(R_{50}/R)^2} \quad (12.10)$$

and the probability that the target has not been detected by R, given initial exposure at $R_o$ is then

$$\begin{aligned} Q(R,R_0) &= e^{-.693(R_{50}^2)(R^{-2}-R_0^{-2})} \quad ; \; R \leq R_0 \\ &= 1.0 \quad ; \; R \geq R_0 \end{aligned} \quad (12.11)$$

We now wish to combine this with the probability density function for initial exposure range. For this example, we ignore the probability that the target may drop its bombs and depart before the detection process has been completed.

To perform the convolution of the probability densities in closed form we require an approximate form for the exposure function that will integrate with Equation (12.11). The function given by Caywood-Schiller is rather complex, and we replace it by one of about the right shape, which has not, however, been checked through for accuracy of representation.

We assume that the probability that the target has not been exposed by range $R_o$ can be approximated by the function

$$F(R_0) = e^{-a/R_0^2} \quad (12.12)$$

The average exposure range (which would be obtained from Figure 12-3) defines the coefficient a, as

$$(R_0)_{av} = (\pi a)^{1/2} \quad (12.13)$$

Then the probability that the target will not have been detected by range R, averaged over the distribution of exposure ranges, works out to

$$Q(R) = \int_R^\infty Q(R,R_0)\,dF(R_0) + \int_0^R dF(R_0)$$

$$= \frac{m\,e^{-a/R^2} - a\,e^{-m/R^2}}{m-a} \quad (12.14)$$

where

$$\begin{aligned} m &= .693\,R_{50}^2 \\ a &= (R_0)_{av}^2/\pi \end{aligned} \quad (12.15)$$

For an evaluation, one needs information on the probability of having visibility ranges $V_m$ under the operational conditions being considered in the evaluation. This data exists in large quantities for all operational theaters of interest. Figure 12-6 shows typical distribution functions for Germany, for two months of the year.

The function seems to be representable in the form

$$\text{Prob}(V_m > V_m^*) = e^{-k(V_m^*)^{3/2}} \quad (12.16)$$

Equally important in assessing tactical limits on the engagement is the amount and level of cloud cover. In general visibility at low angles of sight is greater than visibility range at high angles, since cloud cover tends to lie at about 5000 ft. With extensive low cloud cover, an attacker using visual bombing is unable to acquire targets for dive bomb attacks, although he may be engaged through cloud cover by a radar directed fire unit. Data on cloud cover and its frequency of occurrence is also available from sources of meteorological statistics.

## 12.4 VISUAL IDENTIFICATION

A chart similar to that of Figure 12-5 could be developed for visual identification, but unfortunately time has not permitted this. Range for visual identification is much shorter than that for detection. References to experimental data are given in the Analysis report, and some sketches of identification contours, compared with detection contours, were provided in the AFAADS-1 report.

In general, reliance on visual identification will be even more severely limiting on a defense system than reliance on visual detection, and there is hardly any point in attempting to develop a system with extended effective range if it cannot be cleared to fire until the target is within a few hundred meters.

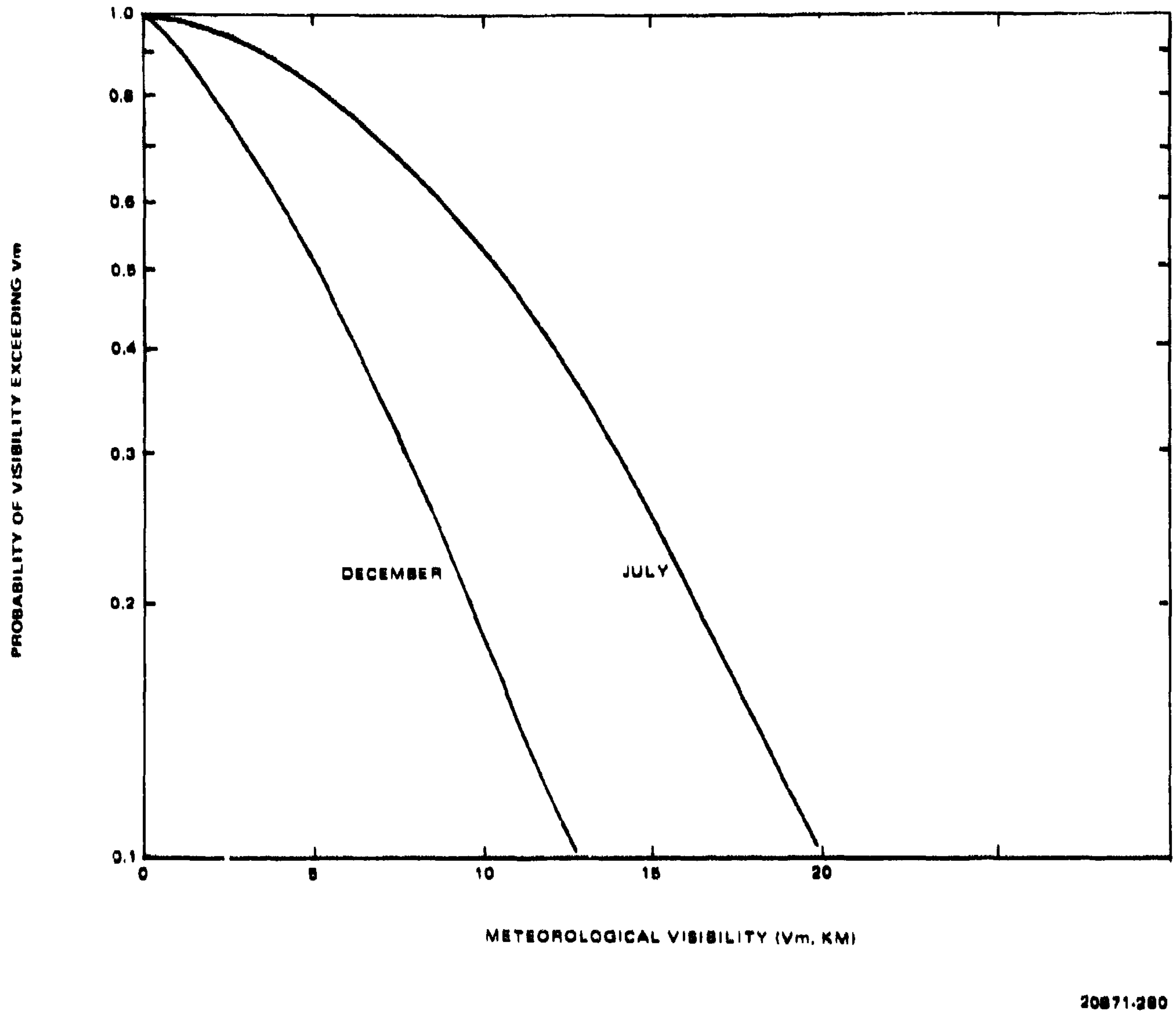


Figure 12-6. Visibility Range Distributions in Germany

## 12.5 TARGET DETECTION BY RADAR

Characteristics of a number of current radars intended for surveillance in air defense systems are listed in Table XII-1. The indicated detection ranges are all considerably in excess of those required for a predicted fire system to operate at its maximum effective range, which for a gun is not likely to exceed

$$D_{max}\,(\text{km}) = \text{Caliber (mm)}/5 \qquad (12.17)$$

with the best fire control currently possible.

Radar rotation speeds are about 1 second, and if two scans are required to confirm detection, targets emerging from terrain masks should be reliably detectable in no more than 2 seconds.

In the case of the Crotale short range surface to air missile system, which employs a surveillance and a tracking radar, an elapsed time of 5 seconds has been estimated from first target sensing by the surveillance radar to lock-on by the tracking radar. Of the 5 seconds, 2 seconds are allotted to slewing of the tracking radar to the direction designated by the surveillance radar.

Table XII-1. Characteristics of Air Defense Surveillance Radars

| Country | France | France | France | France | France | Sweden | Sweden | Sweden |
|---|---|---|---|---|---|---|---|---|
| Designation | Domino 20 | Domino 30 | Mirador | Mirador II | Oeil Noir I | Ericsson | Ericsson | Ericsson |
| Band | L | L | S | S | L | X | C | L |
| Peak Power | | 1 kw | 350 w | 270 w | 120 w | 26 kw | 14 kw | |
| Av Power | | 45 w | 33 w | 30 w | 24 w | 200 w | 250 w | 100 w |
| Az Beamwidth | $10^\circ$ | $6.5^\circ$ | | $4^\circ$ | $10^\circ$ | $1.7^\circ$ | $2^\circ$ | $8^\circ$ |
| El Pattern | $CSC^2$ | $CSC^2\ 35^\circ$ | $CSC^2\ 20^\circ$ | $CSC^2\ 20^\circ$ | $CSC^2\ 35^\circ$ | Cassegrain $35^\circ$ | $CSC^2\ 45^\circ$ | |
| Rotation Speed | | 45 RPM | 60 RPM | 60 RPM | 60 RPM | 60 RPM | 60 RPM | 60 RPM |
| Radial Speed Range | 30-450 m/s | 30-500 m/s | 30-370 m/s | 45-420 m/s | 50-160 m/s<br>160-320 m/s | 22-385 m/s | | 30-400 m/s |
| Range Resolution | | 1500 m | | | | 160/320 m | 400 m | 950 m |
| Detection Range | 17 km on 2 $m^2$ | 30 km on fighter | 18 km on 2 $m^2$ | 17 km on 1 $m^2$ | 15 km on 3 $m^2$ | 20 km | | 20 km on 3 $m^2$ |
| Azimuth Accuracy | | $1.5^\circ$ | $3^\circ$ | $0.75^\circ$ | | | | |
| Range Accuracy | | 400 m | 1000 m | 400 m (200 m TWS) | ±50 m (3800-1500 m) | | | |
| Subclutter Visibility | | 60 dB | 55 dB | 55 dB | 50 dB | 50 dB | | |
| ECCM | | CFAR REC<br>strobe on JAM | | CFAR REC<br>strobe on JAM | | CFAR REC | | |
| Weight | | 360 kg | 290 kg | | 205 kg | | | |
| Comments | Lightweight | | | Automatic Alert<br>Automatic Threat<br>Assessment | Range measurements<br>1500-3800 m<br>Regen only 500-1000 | | | |
| Application | | | | Crotale | SP-AA/AMX-30 | Skyguard | | |

NOTE: All radars listed are coherent pulse doppler types

20871-619A

## 12.6 ELAPSED TIME TO ENGAGEMENT OF TARGET

As a rough indication of a minimum elapsed time from target exposure to first possible projectile impact, Table XII-2 has been developed based on the Crotale estimates. The times indicated are for a completely automatic system. Elapsed times can, of course, be very much longer with a manual system, depending on whether the operators are alerted and at their operating stations. They might even be shortened by further improvements in automatic system design.

In the present study, no data has been acquired on the actual elapsed times of the component parts of the engagement process from which one may estimate limits and possiblities of improvement. No doubt this data exists in records of antiaircraft system tests, and it should be organized in a form suitable for use in analysis and simulation.

## 12.7 EXTERIOR AND TERMINAL BALLISTICS

Before discussing the evaluation of the prediction algorithms, approximate methods for estimating projectile time of flight and lethality are a useful preliminary, since these factors are employed in the overall engagement kill probability estimates.

Table XII-2. Event Sequence in Engaging Target

| Event | Elapsed Time (seconds) |
|---|---|
| Target Exposed | 0 |
| Target Detected (60 rpm scan) | 1 |
| Target Designated to Tracker | 2 |
| Tracker Slews | 4 |
| Tracker Lock-on | 5 |
| Firing Data Available (2-sec smoothing) | 7 |
| First Round Arrives at Target | 7 + time of flight |

20871-620

### 12.7.1 Estimating Time of Flight

The computation of exterior ballistic data is a highly sophisticated science. However, it is helpful to have a quick means of estimating time of flight to a specified range without searching through firing tables. Drawing some confidence from Figure 7-14 which indicates that simple normalization of projectile data allows time of flight to be plotted against slant range with only small scatter about a mean curve, a nomogram has been developed and is presented as Figure 12-7.

The family of curves is based on the esimated time of flight versus range relationship developed in a design study for an improved 37-mm projectile, with boattail and without rotating band. The curves for other calibers are obtained simply by scaling ordinate and abscissa in proportion to caliber.

The curves are computed for a muzzle velocity of 1100 meters/second. Again, relying on Figure 7-14, if not on theory, time of flight to a specified range is computed as a ratio to time of flight for 1100 meters per second, and the left hand portion of the nomogram allows correction to other muzzle velocities.

The dashed lines show an example. A 20-mm round at 1100 meters per second with excellent drag coefficient has a time of flight of about 5.5 seconds to 3000 meters, and at a muzzle velocity of 1000 meters per second the time of flight is determined to be approximately 6.0 seconds.

The nomogram is constructed for a projectile density

$$\rho = (w_p/C^3) \times 10^4 = 0.317 \qquad (12.18)$$

where $w_p$ = projectile weight in pounds, and $C$ = caliber in millimeters.

It can be used for other values of $\rho$ and less than optimum ballistics by entering with a value of caliber $C_t$ computed as

$$C_t = C(\rho/0.317)\,K \qquad (12.19)$$

Where

- $C$ = the caliber of the round being estimated
- $\rho$ = its computed density
- $K$ = 1.0 for 'excellent' ballistics
  - 0.8 for 'good' ballistics
  - 0.6 for 'fair' ballistics (Typical of most WW II projectiles)
- $C_t$ = value of caliber used to enter the nomogram instead of C.

The two curves of Figure 7-14 differ by a value of K = 0.6 as can be seen by sliding one along the zero drag line until they coincide.

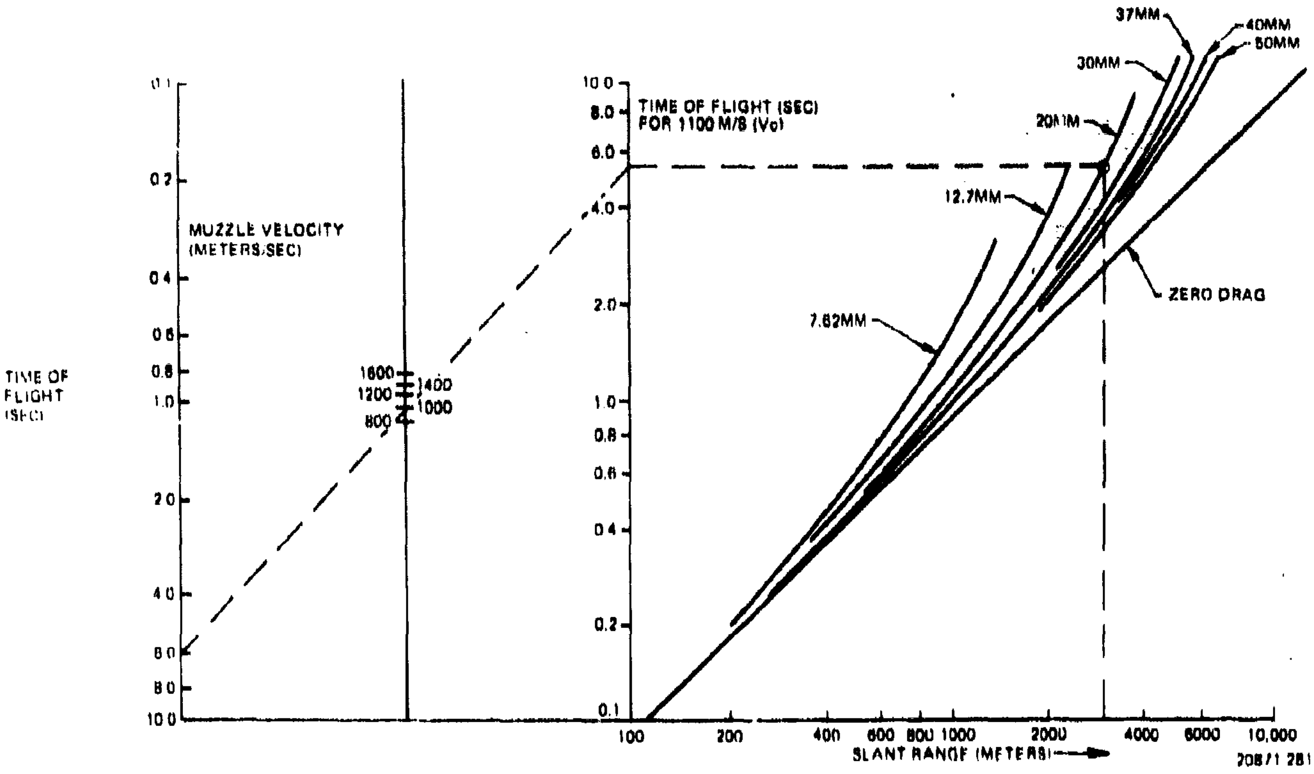


Figure 12-7. Nomogram for Estimating Time of Flight versus Slant Range With Excellent Ballistics

The nomogram might also be used inversely by entering with given time of flight versus range points for a specified projectile, reading out an equivalent caliber, and computing K to provide a basis for discussion with the ballisticians as to whether the ballistic design might be improved.

### 12.7.2 Estimation of Terminal Effectiveness

Determination of the probability that an impact on a specific target type by a specific projectile type will cause damage or destruction of the target in various categories is an advanced and sophisticated science. Such estimates for modern weapons and targets are classified and in any actual system evaluation, should be done by experts.

For initial rough estimates, however, the nomogram of Figure 12-8 may be helpful. The nomogram allows a quick estimate of the probability that a high explosive, contact fuzed projectile striking a fighter-bomber will cause destruction of the target in each of two categories (1) immediately observable, mid-air destruction, and (2) a delayed crash within observable range of the defense site. In the case of observed, mid-air destruction, the defending fire unit can cease fire at once, and attempt to engage a new target. In the case of delayed destruction, the fire unit will 'fire the course' and have a lower availability rate against a new target.

The user may improve Figure 12-8 by replacing the kill probability curves by data from classified analyses which may, or may not reveal similar functional relationships.

A similar nomogram could be devised for AP or API projectiles, as opposed to HE, but since these projectiles have an effectiveness which varies significantly with impact velocity, an additional parameter would be required.

It appears that all modern antiaircraft guns are intended to employ high explosive projectiles against aircraft targets. Evaluation of automatic weapons of less than 20 mm caliber would require consideration of other types of projectiles.

In addition, the possibility that some ground support aircraft may be heavily armored could make the 'observed crash' curve too high.

The following comments are extracted from a summary report on German antiaircraft artillery in World War II:

'The 20 mm flak gun was too light and lacked penetrating power. The 37 mm gun was good and should have been set up on multiple (three or four gun) mounts. Efforts should also have been made to develop a somewhat heavier gun, with a caliber of 40 to 50 mm, especially since tests carried out with 50

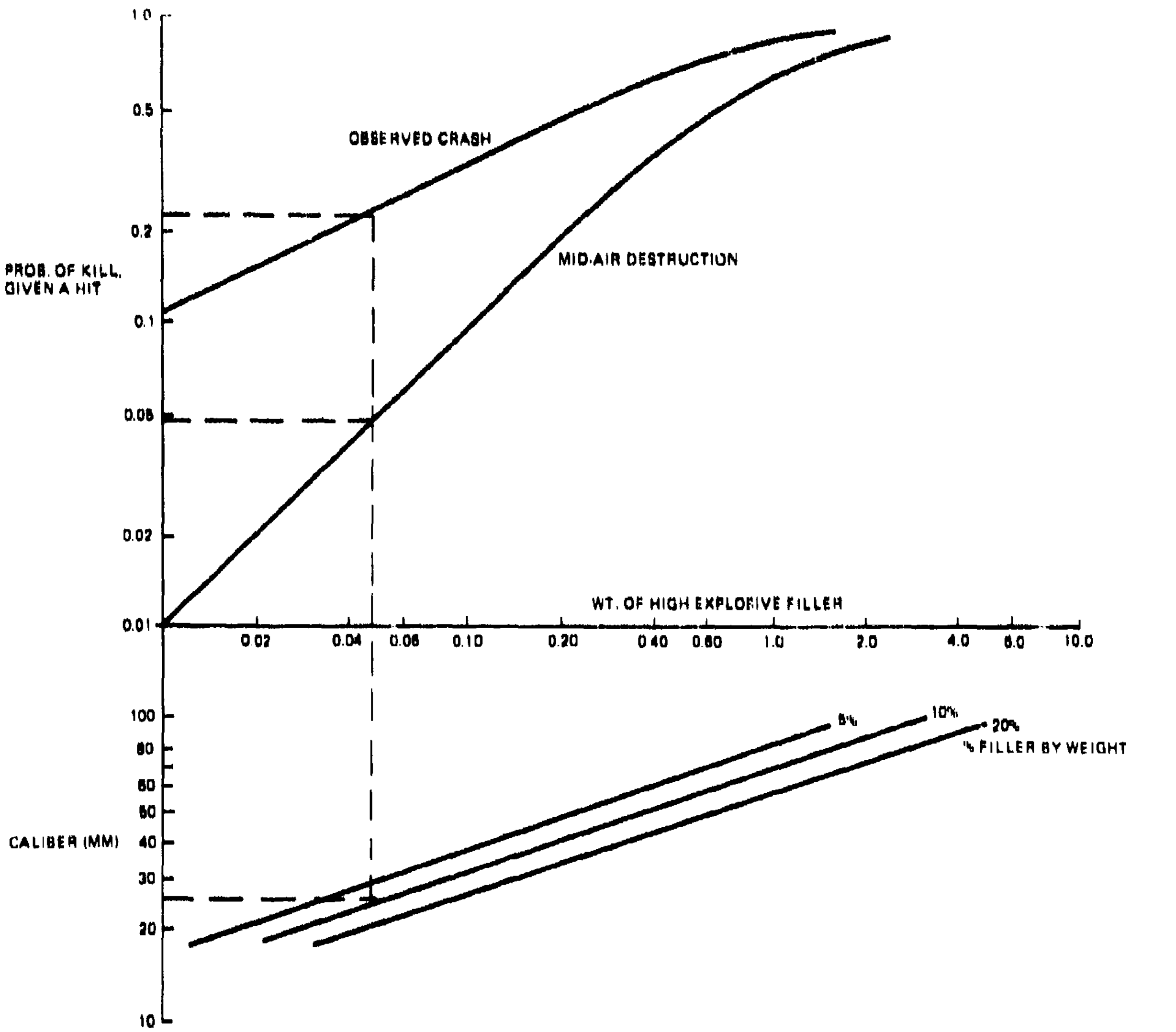


Figure 12-8. Nomogram for Estimating Probability of Kill, Given a Hit with HE, Contact Fuzed Projectiles

mm guns had produced such excellent results. The 8.8-cm and the 12.8-cm guns, which were sometimes used in defense of static installations, also proved to be satisfactory in every respect in 1943. Because of the frequent appearance of armored Soviet ground-attack aircraft it was found to be advisable to issue ammunition in mixed lots, containing both armor-piercing (shaped-charge) and regular high-explosive flak ammunition in a ratio of 1:3 or 1:4.'

'As early as the autumn of 1941 the first IL-2 (Ilyushin) 'Stormovik' ground-attack plane appeared at the front. This type, which soon became available in large numbers, was ideally suited, by virtue of its rugged construction and excellent armor protection, for air support missions. Frequently formations of Me-109s and even Fw-190s expended their entire allocations of ammunition firing at them without bringing them down. German antiaircraft commanders noted that the 'Stormoviks' could be shot down by light and medium antiaircraft artillery only if direct hits were scored and soon began to make greater use of the heavy (8.8 cm) gun against Soviet aircraft. IL-2 planes were most vulnerable when fired upon from above or from the rear by explosive ammunition. The tail and control surfaces disintegrated readily if struck by gunfire. At ranges of 900 to 1,200 feet, light antiaircraft guns had little effect upon them, although successful hits were scored by medium or larger calibre guns

which happened to strike the engines, tail assemblies, or control surfaces of these planes. The 'Stormovik' was somewhat sluggish in performance; it might have been more maneuverable except for its weak power unit.'

## 12.8 FIRE CONTROL EVALUATION

As indicated at several points in the earlier sections of this report, the principal factor determining the effectiveness of predicted fire systems is the accuracy with which the predicted target position can be computed. The difference between a 'best' set of prediction algorithms and a set of approximations justified on the basis of ease of implementation is too large to be rectified by high rate of fire and artificial dispersion.

### 12.8.1 Limiting Constraints on Well Designed Systems

With the current state of the art of digital computers, high performance servomechanisms, sensors, good mechanical design of the gun mount, excellent projectile ballistic characteristics, and effective system calibration procedures it should be possible to reduce all sources of system error to a level where performance can be described in terms of

a. Irregularities of the target path.

b. Sensor dynamics (error and power spectral density).

c. Prediction algorithms.

d. Ammunition dispersion.

e. Projectile terminal effectiveness.

f. Rate of Fire.

At the relatively short ranges of predicted fire systems, a pulse-doppler tracking radar is expected to be limited in accuracy principally by 'glint', with a linear standard deviation constant with slant range, and about equal to half the projected target dimension before data processing. Visual tracking by a human operator with regenerative aiding, and well designed control, and, possibly up to 3x magnification in optics should do at least as well. The provision of regenerative assistance should make this capability independent of target angular velocity and acceleration.

However, this performance can be improved by data smoothing, and the amount of the reduction depends on the glint, or human tracking error band width, and the corresponding filtering which is possible in data processing.

Since prediction involves differentiation, very narrow sensor error bandwidth may be as advantageous as very wide bandwidth, if associated angular lag problems can be circumvented by regenerative aids.

The sensor tracking data is processed in fire control system by various coordinate transformations, smoothing operations, differentiation and prediction. With modern computers and servomechanisms it should be possible to hold errors resulting from the computational elements to very small values, compared with the errors resulting from sensor errors.

The prediction error resulting from sensor tracking errors increases with projectile time of flight and decreases with increasing data smoothing time. It also increases with the number of derivatives used in prediction. Thus sensor noise is amplified more in a quadratic predictor than in a linear predictor.

Short smoothing time is desirable for rapid initial generation of firing data, and to minimize lag when the target changes direction or velocity. For a specified effective smoothing time, some shaping of the weighting function is possible to improve the effectiveness of smoothing. It is usually better to have a weighting function approaching a parabolic shape rather than a simple exponential, because the long tail of the exponential delays the rate at which old data disappears from the system. The best shape depends on the power spectral density of the sensor error, and some compromising between early availability of good data, and minimization of the effect of old data.

Some averaging times of past fire control systems are given in Table XII-3. The M9 computer was for use with the 90 mm and 120 mm guns out to time of flight $t_p = 30$ seconds.

It seems probable, from experiments on the Litton simulation that smoothing time should be an increasing function of time of flight, to retain short settling time against targets exposed at short ranges and effectiveness at the longer ranges against targets using pop-up tactics to deliver stand-off weapons.

To show how performance may vary with target path and the prediction algorithms used in the fire control system, Figures 12-9 and 12-10 have been obtained from runs on the Litton simulation. The simulation was for a 25 mm gun with excellent ballistics, 1100 meters/second muzzle velocity, and the target flew at an average altitude of about 400 meters at 300 meters per second.

The index shown in for probability of destroying the target with a one second burst which, for this weapon, contained 58 rounds.

The curves correspond to computations along a line of constant angle from path midpoint on paths of progressively increasing crossing range. The projected area of the target was therefore approximately constant, and the curves show the effects of range, time of flight, prediction algorithm and target maneuver. In all cases the weapon was assumed to have 3 mils angular round to round ammunition dispersion.

Table XII-3. Data Smoothing Functions

| Year | System | Weighting Function | Time Constant of Memory Time |
|---|---|---|---|
| 1930 | Wilson-Sperry T-4 | Constant | 3 sec |
| 1935-40 | M-4, M-7 Mechanical | Exponential | $t_p/13$ |
| 1940-current | Gyroscopic Lead Computing Sight | Exponential | $t_p/5$ |
| 1942-50 | M9 | Approximately Parabolic | 10 sec/20 sec options |
| 1960 | Vigilante | Approximately Bi-exponential | 3 sec |

20871-621

At short ranges the probabilities drop because of the very high rates of change of acceleration and the fact that the assumed regeneration algorithm was only effective in correcting the first two derivatives.

The systems have not been optimized. The linear prediction system would do better at the longer ranges if smoothing time had been increased with time of flight. Note that the preference order of the prediction algorithms changes across the two cases.

System optimization would project the effective range in both cases considerably beyond 3000 meters.

### 12.8.2 Possible Deficiencies of Existing Systems

Unfortunately, many fire control systems offered as candidates for selection do in fact contribute additional errors to the generation of gun data resulting from

a. Computational algorithms which are imperfect even against unaccelerated targets.

b. 'Instrumentation (mechanization) errors', resulting from scale factor limitations, gear backlash, shaft torsion, transducer errors, internal servo lags, etc.

c. Imperfect computation of projectile ballistic data.

and other causes. In addition, gun mounts may have an undesirable degree of flexibility, drive servos lag, and the computational process and the system operation as a whole may be degraded in various ways by the shock of firing.

Most important, all predicted fire systems are highly vulnerable to errors of boresighting and day to day 'calibration'.

### 12.8.3 Need for Comparative Tests and Analyses

Some of these error components may be estimated by paper studies. One may, for example, compute the magnitude of aim error resulting from approximations in various computational algorithms.

Experience indicates, however, that the performance of an existing system can only be determined with acceptable validity by actual testing. The testing must be done in a way that separates the inherent system errors from those resulting from target path irregularities. This suggests the following sequence of tests.

a. Static, or semi-dynamic test of computational accuracy with fixed position inputs, and possibly constant velocities injected at the differentiating units.

b. Dynamic test with synthetic target path inputs injected at the sensor inputs. This may include firing.

c. Dynamic test tracking a synthetic target on a specified set of paths with sensors operating.

d. Tests against real targets on simple (unaccelerated) paths, possibly firing blank ammunition.

e. Repeat of (4) with the target flying typical attack paths.

f. Firings against drone targets, with live ammunition.

## 12.9 COMPUTATION OF ENGAGEMENT KILL PROBABILITIES

The Litton simulation allows rapid computation of engagement kill probabilities for a wide variety of prediction modes, algorithms, target path types and system parameters. Considerable insight can be gained, nevertheless, on why results on the simulation turn out the way they do, by simple analytic models. These models use approximations which have been determined to be acceptable by comparison with simulation runs.

### 12.9.1 Summary of Probability Relations

This section summarizes briefly, the probability relations used in computing engagement kill probability.

Single shot hit probability is approximated as

$$p_{ss} = \frac{a^2}{a^2 + 2\sigma^2} e^{-r^2/(a^2 + 2\sigma^2)} \qquad (12.20)$$

where the projected area of the target normal to the bullet trajectory is

$$A_t = \pi a^2 \qquad (12.21)$$

and

$\sigma$ = standard deviation of the probability density function of the shot pattern (linear) measured from the center of the pattern.

$r$ = 'bias', or deviation of the center of the shot pattern from the target center.

Single shot probability will usually be very small, in which case the relative shapes of the target and the shot pattern are irrelevant. If the bias occurs principally in one dimension, a simple and obvious modification of Equation (12.20) is required. For details, see the AFAADS-I report.

To convert hit probability to kill probability either multiply $p_{ss}$ by $p_c$, the probability that a hit causes a kill, or replace the term $a^2$ by $p_c^2$. The former assumption is equivalent to assuming uniform vulnerability of the target over its surface; the latter assumes that vulnerable components are collected about the geometric center of the target. When $p_{ss}$ is small, both approaches give the same result, for all practical purposes.

All of the terms of Equation (12.20) will vary with time, but for a short burst of say one second, they can be assumed to be constant.

The term $\sigma$ contains two components: 1) the random round to round ammunition dispersion, and 2) a component of 'aim wander' of the error in aiming the weapon. For very short bursts the component resulting from aim wander tends to be constant during a burst and randomly distributed across bursts; for very long bursts, a portion of aim wander may be included in the random round to round dispersion.

The bias 'r' also includes boresight, calibration, and systematic solution errors of the fire control system. In this section, we assume an excellent fire control system, so that the only sources of 'bias' are the effect of sensor error as amplified in the prediction process, and target deviations from a predictable path.

For a short burst of n rounds, the probability that the target survives is

$$\phi = \int_0^\infty e^{-np_{ss}(y)} f(y)\, dy \qquad (12.22)$$

where f(y) is the probability density function of bias across bursts. If f(y) is assumed to be representable as a circular normal distribution with variance $\sigma_b^2$, $\phi$ can be evaluated in terms of the Incomplete Gamma Function.

Figure 12-11 shows burst kill probability $p_b$ computed from Equation (12.22) where

$$p_b = 1 - \phi \qquad (12.23)$$

In Figure 12-11

E = expected number of lethal hits

$$E = np_c \frac{a^2}{a^2 + 2\sigma^2 + 2\sigma_b^2} \qquad (12.24)$$

and

$$\lambda = 2\sigma_b^2/(a^2 + 2\sigma^2) \qquad (12.25)$$

Ammunition dispersion may be considered a disposable parameter, at least in the system concept stage, and the dashed lines show how burst kill probability varies, for a constant value of $na^2p_c/2\sigma_b^2$, as ammunition dispersion is varied.

When E is small, $p_b$ is essentially independent of $\lambda$, and is a function only of E. For large E, an adequate approximation to $p_b$ with optimum dispersion, is obtained by taking $\lambda = 1$, and for this case, Equation (12.22) yields the very simple solution

$$p_b = 1 - \frac{1 - e^{-2E}}{2E} \qquad (12.26)$$

Another simple solution is available, if the shot pattern is assumed to be adjustable to optimum shape (not necessarily Gaussian). In this case

$$p_b = 1 - \left\{1 - \left[\frac{np_c a^2}{\sigma_x \sigma_y}\right]^{1/2}\right\} e^{-\left[\frac{np_c a^2}{\sigma_x \sigma_y}\right]^{1/2}} \qquad (12.27)$$

where the form has been generalized to allow $\sigma_x$, $\sigma_y$ to assume different values.

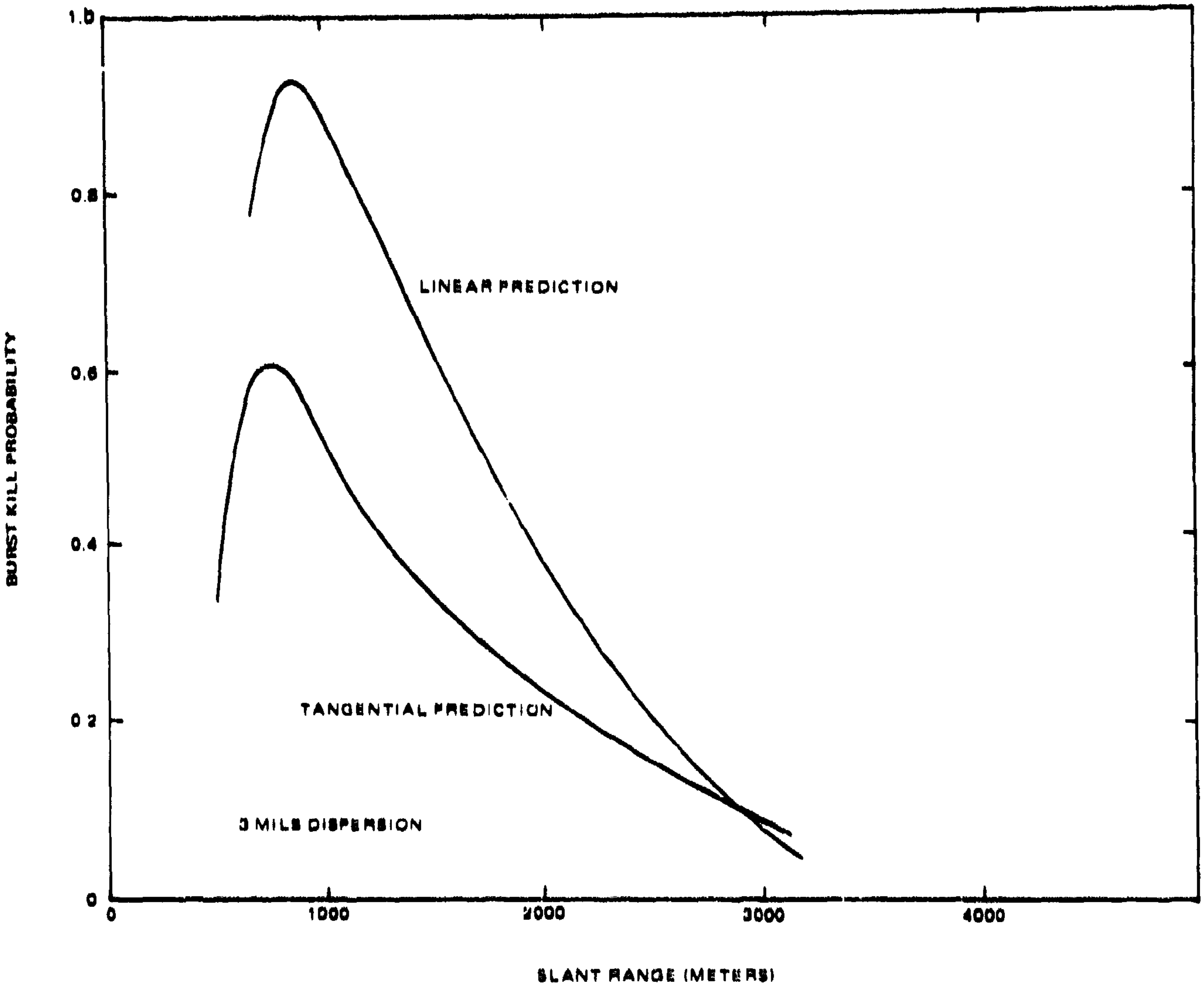


Figure 12-9. Burst Kill Probability versus Unaccelerated Target with 25 MM Gun

The variance of prediction error caused by sensor error can be written approximately, for a linear predictor, as

$$(\sigma_p/\sigma_t)^2 = c_0 + c_1\,(t_p/T_s) + c_2\,(t_p/T_s)^2 \quad (12.28)$$

where the coefficients depend on the band width of the sensor noise and

$\sigma_p^2$ = variance of prediction error

$\sigma_t^2$ = variance of sensor error

$t_p$ = time of flight

$T_s$ = smoothing time

This ignores the second order effect of errors in time of flight caused by sensor errors, and the second order effects of geometric transformations.

The function is asymptotic to unity for very narrow sensor error band width (i.e., the error approaches a constant value) and to zero for very wide band width. It should always be possible to do somewhat better than

$$(\sigma_p/\sigma_t)^2 = 1 + 2(t_p/T_s) + 2(t_p/T_s)^2 \quad (12.29)$$

however this function will be used in the present discussion.

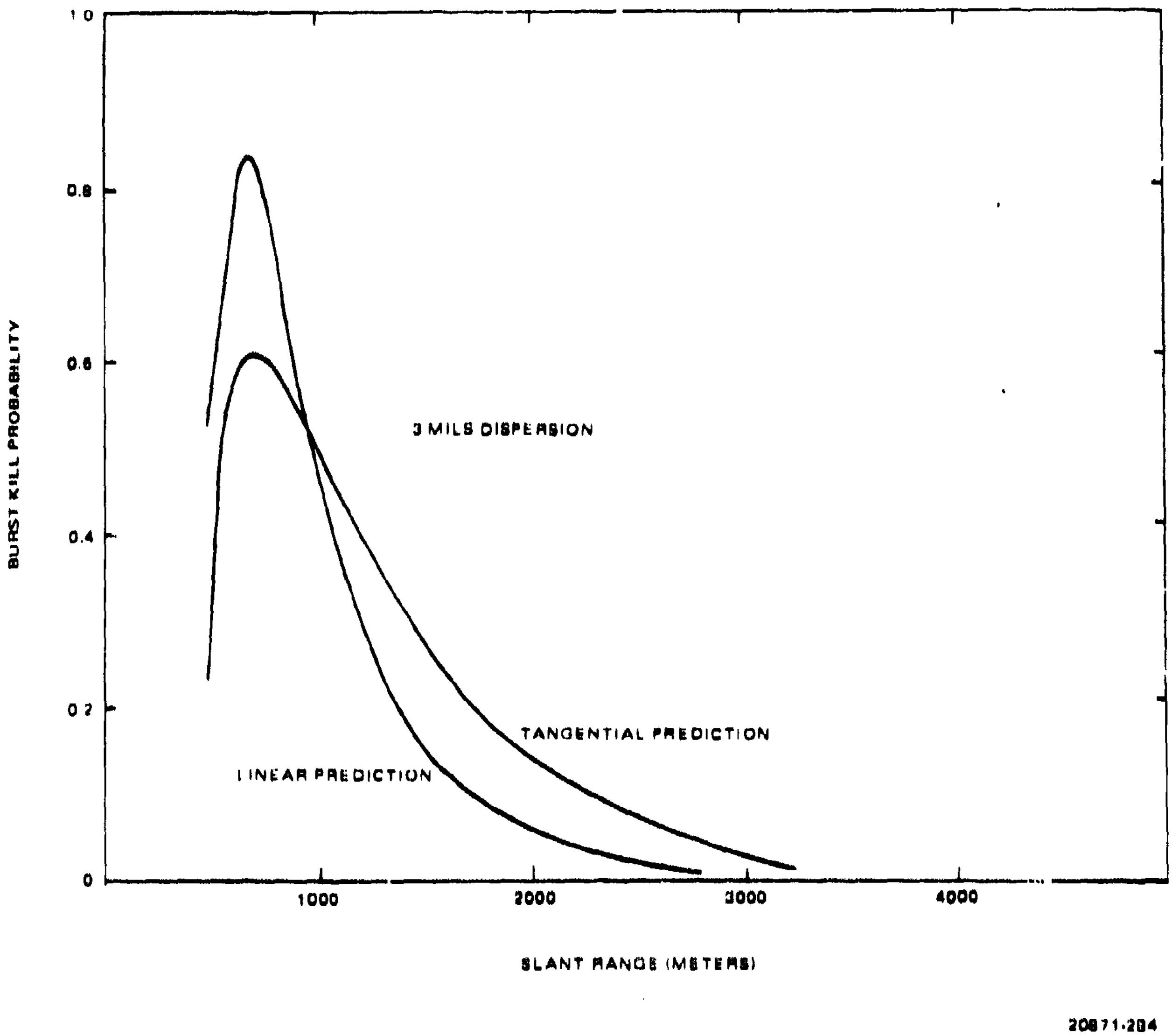


Figure 12-10. Burst Kill Probability versus Linking Target with 25 MM Gun

If quadratic prediction is used, Equation (12.28) will contain terms up to $t_0^4$. Intermediate modes between linear and quadratic include 'tangential' prediction in which the prediction is updated by an acceleration correction to correct for velocity lag caused by acceleration, but not for deviations caused by target acceleration during time of flight.

Computation of the appropriate coefficients for Equation (12.28) for linear predictors and for quadratic and partial quadratic predictors is developed in detail in the AFAADS-I report.

For a very long firing interval, it is necessary to account for the fact that all of the terms in Equation (12.22) will be time varying. Some remarkable simulation results indicate that over a wide variation of path parameters, with simulated radar tracking, the coefficient $\lambda$ may be assumed to be a constant, i.e., by a judicious choice of angular dispersion, the dispersion pattern and the aim wander pattern remain in about the same ratio.

One may then compute E from Equation (12.24) by numerical integration over the firing segment, or in closed form by analytical approximations, and finally compute engagement kill probability from Equation (12.26). Note that this process *does* account for serial correlation of miss distances.

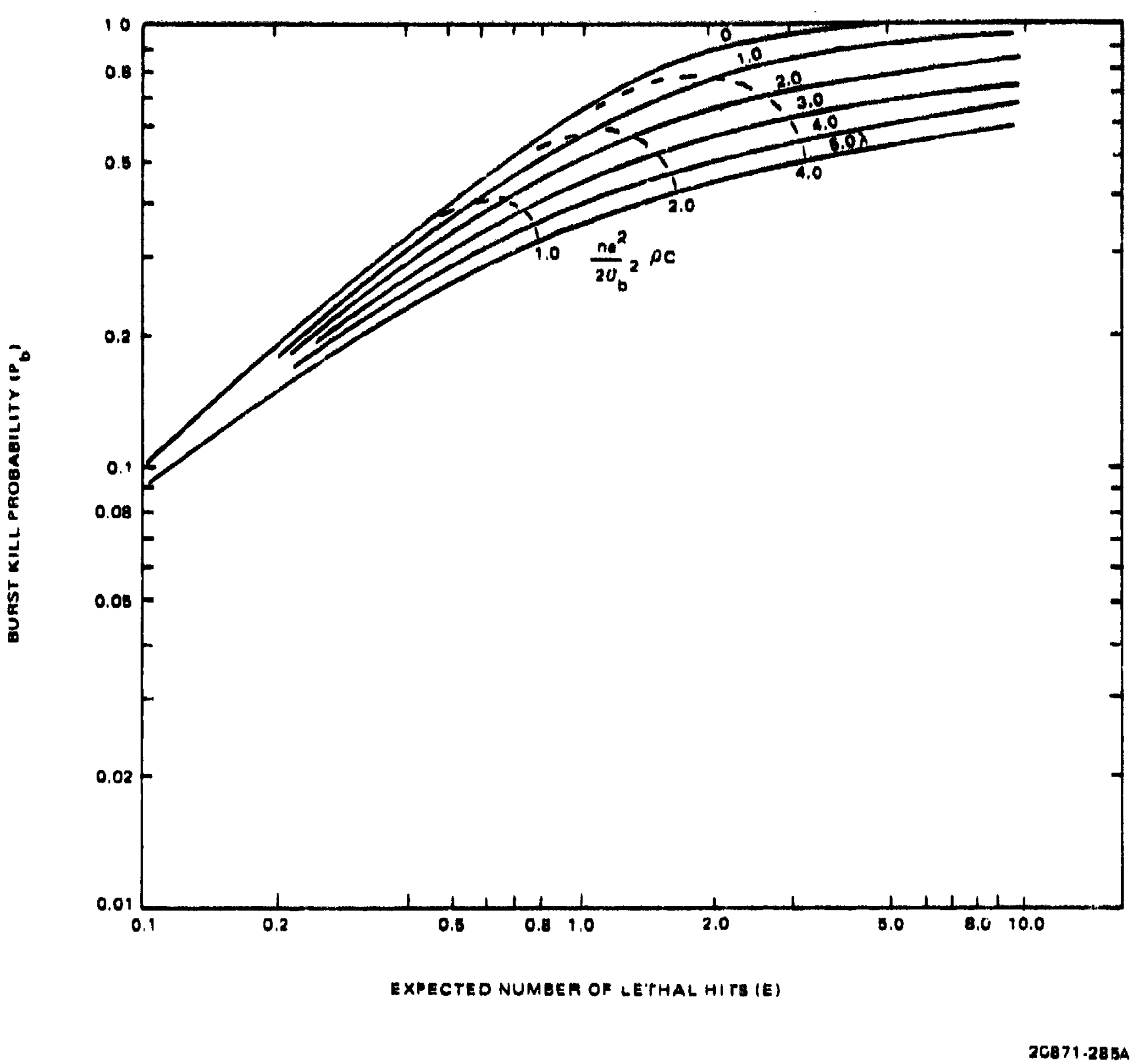


Figure 12-11. Burst Kill Probability with Aim Wander

For systems with large, slowly varying systematic errors caused by solution imperfections one needs to know how these errors vary with the engagement geometry and dynamics, and the computation is more involved. However, the difficult step is obtaining estimates of the errors. Once obtained, they can be introduced to either the simple analysis or the simulation. The simulation already contains a sub-routine for computing effectiveness of predictors using simple angular velocity times time of flight algorithms, and other approximation algorithms can be similarly programmed.

The very large aim errors possible when the target flies accelerated or jinking paths of various types are easily evaluated on the simulation, where any type of target path can be programmed. In a following section, a simple analytical model for estimating fire unit effectiveness against a jinking target is developed and compared against simulation results.

### 12.9.2 Variation of Target Projected Area with Aspect

For quick reference, Figure 12-12 shows how the projected area of an ellipsoidal target varies with its position along a straight line flight path relative to a tracking sensor or fire unit. The dimensions are approximately those of the fuselage of a fighter-bomber. In engagement kill computations, this area must be

multiplied by the probability that a hit causes a kill, which in turn is a function of the weapon caliber and projectile characteristics.

### 12.9.3 Limiting Effect of Ammunition and Gun Dispersion

The angular dispersion of a weapon and its ammunition, considered as an error which is random across successive rounds, places an upper limit to weapon effectiveness which cannot be exceeded by fire control improvements. This limit, although trivial to compute, is shown for reference in Figures 12-13 and 12-14. The target is assumed to be ellipsoidal, and the variation of its presented area with position along a passing straight line path is as depicted in Figure 12-14. The head-on area of the target is two square meters, the side-on area is 20 square meters.

Figure 12-13 shows the single shot probability of hitting the target in the head-on aspect, as a function of slant range and standard deviation of angular dispersion, and Figure 12-14 shows the probabilities for the side-on aspect.

As an example consider the 6 x 18 mil dispersion pattern which may be used with Vulcan. In the head-on target aspect the elliptical pattern shape can be represented as an equivalent circular dispersion pattern of about 10 mils. At 1000 meters, about 300 rounds

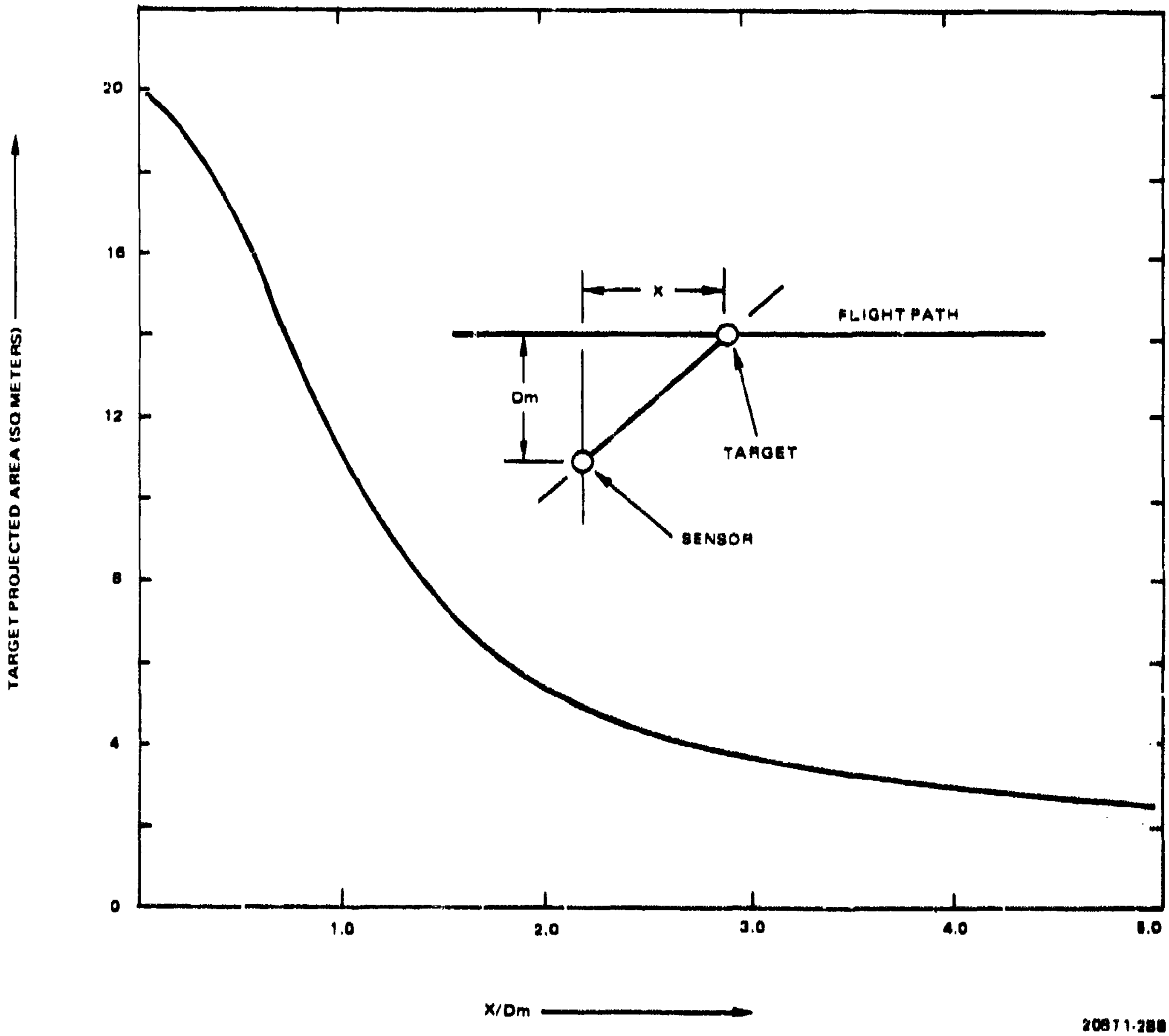


Figure 12-12. Variation of Projected Area of Ellipsoidal Target With Position on Flight Path

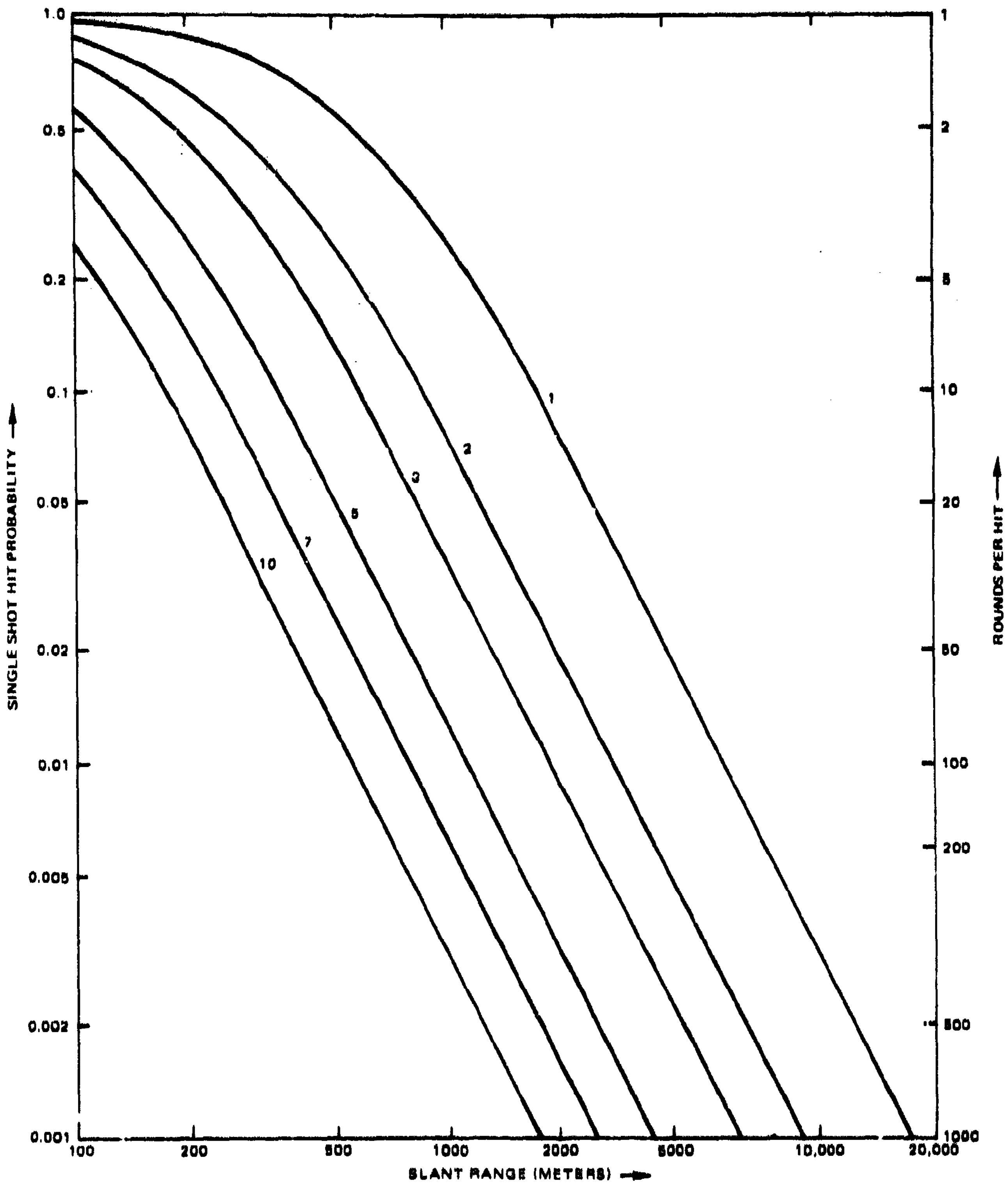


20971-289

Figure 12-13. Single Shot Hit Probability on 2 Meter$^2$ Circular Target as Limited by Dispersion

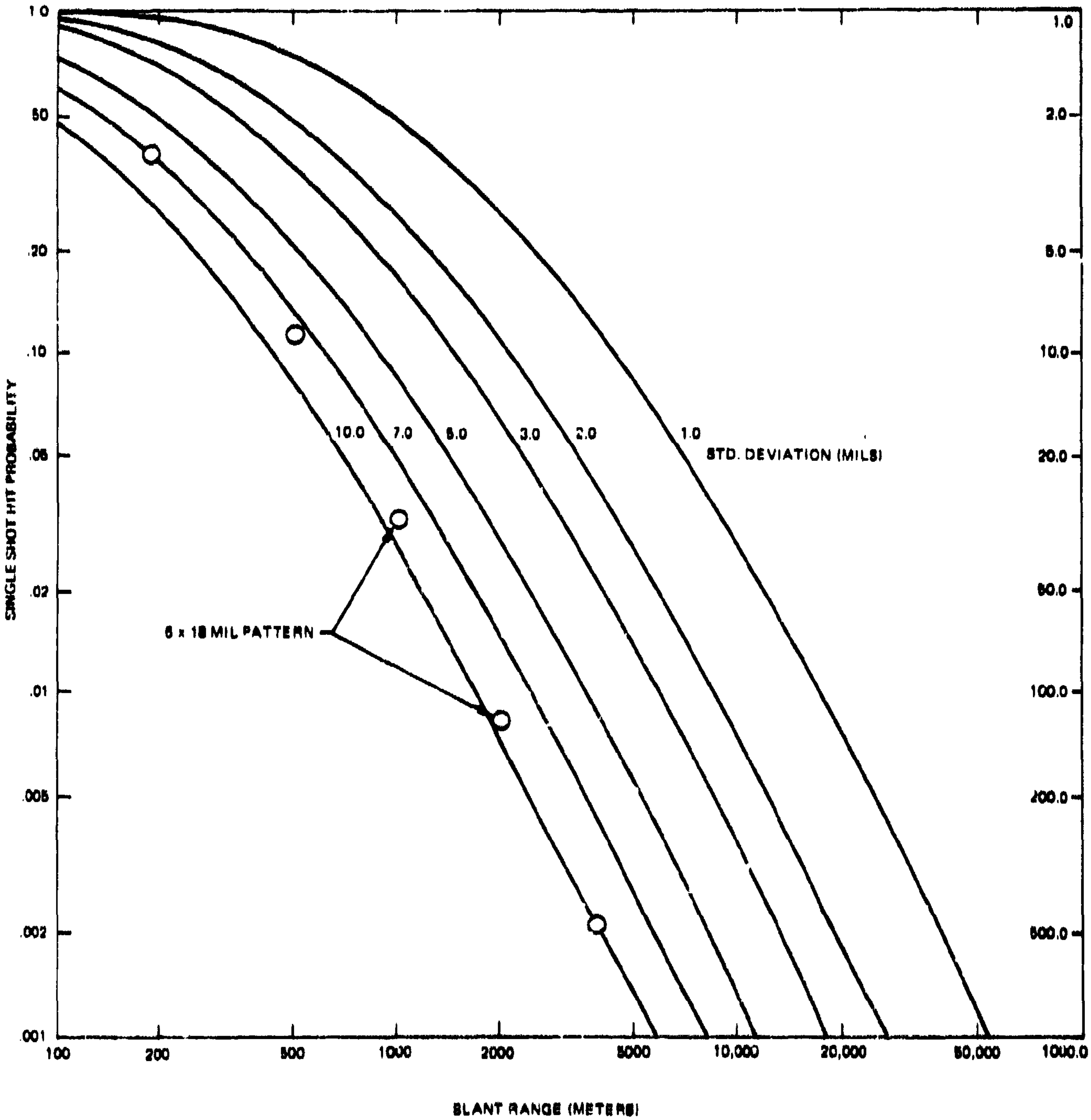


Figure 12-14. Single Shot Probability on 20 Meter² Elliptical Target as Limited by Dispersion

per hit are required, and if the probability that a hit produces a kill is about 0.20, the weapon would exhibit about 1500 rounds per kill, with no other sources of error present.

In the side on aspect, the elliptical shapes of the dispersion pattern and the target interact, so that the Vulcan pattern is equivalent to a 6 mil circular pattern at short ranges, approaching a 10 mil circular pattern at very long ranges. A few computations are indicated as circles to indicate this effect. At 1000 meters in this aspect only about 30 rounds per hit, or 150 rounds per kill are required, with the Vulcan pattern.

To re-emphasize, however, Figures 12-13 and 12-14 represent upper limits of effectiveness, depending only on angular dispersion, and effectiveness will always be below these values in the presence of errors in the center of aim caused by prediction errors, and other error sources.

The design objective, of course, is to match angular round to round dispersion of a system to the other errors resulting from the computation of gun orders, so that system effectiveness is optimized. Hence in conceptual analysis, dispersion should be considered initially as a disposable, rather than a limiting parameter.

On the other hand, when the dispersion is known for an existing system it can be used for quick estimates of performance limits which cannot be exceeded by the system. In most cases performance will be substantially below these limits.

### 12.9.4 Engagement of a Dive Bombing Aircraft

This section applies the simple expressions developed in Section 12.9.3 to the evaluation of the defense against an aircraft performing a dive or glide bombing attack. The aircraft is assumed to approach at low level, then to 'pop up' to an altitude from which it can acquire the defended ground target, and then to make an attack pass which contains a short straight segment during which the attacker lines up his bomb sight, and develops a solution to his bombing problem.

A simple model is employed in which it is assumed that

a. The target path during its firing pass is a straight line which can be approximated as a radial line through the defense site.

b. The defense has a significant probability of hitting the aircraft only while it is on the straight line segment.

c. The computer uses an algorithm which corrects for the target acceleration along the straight line segment.

d. The attacker's munition effectiveness depends on the munition release range. This may be approximately as the inverse of release range squared.

Under these assumptions, there will be some release range beyond which none of the rounds fired by the defense will be effective, since settling time of the computer plus time of flight of the first effective round will exceed the duration of the straight line segment. This range is an inverse function of the average projectile velocity.

A simple analytical model quantifying these relationships is now developed.

The sequence of events is shown in Figure 12-15. The aircraft, after preliminary maneuvers to get into position for an attack pass, reaches a point A, at which it begins a straight line 'down the chute' run, which requires $T_a$ seconds. It is assumed that the defense sensor has acquired the target, by this time, hence good firing data is available after settling time $T_s$, at which point the defense opens fire. The first round arrives after a time of flight $t_{p1}$.

The target releases its munitions at time $T_a$ from the beginning of its run at point B, and begins its breakaway maneuver. It is assumed that the breakaway is at high enough acceleration so that hit probability after this point is negligible. The last effective round, therefore is the one that reaches the target at $T_a$, at a range $D_b$, and this was fired at a time $T_a$-$t_{pb}$. Table XII-4 summarizes these events.

It can be observed at once that the effective firing time of the defense is

$$T_d = T_a - T_s - t_{pb} \qquad (12.30)$$

Consider the boundary condition, which according to the assumptions states that to deliver effective fire, at least one round must arrive at the target based on firing data computed after the target has settled to a straight line path.

The requirement is that time of flight be less than $T_a$-$T_s$. If the airplane is able to perform its firing run in six seconds, and the computer requires two seconds to settle, the maximum time of flight will be four seconds. That is, if the aircraft begins its breakaway beyond a range corresponding to 4 seconds time of flight, accurate aimed fire will not be possible.

More sophisticated prediction modes are possible. For example, the algorithm for 'defense of a known point' developed in the AFAADS-I report requires *zero* settling time.

Simulation runs also indicate that at the expense of accuracy on the straight line segment, effective fire can be delivered during the last segment of the turn in to attack, and the initial portion of the breakaway.

However, for the straight line segment only, Figure 12-16 shows the 'safe' breakaway range for the aircraft as a function of weapon muzzle velocity and

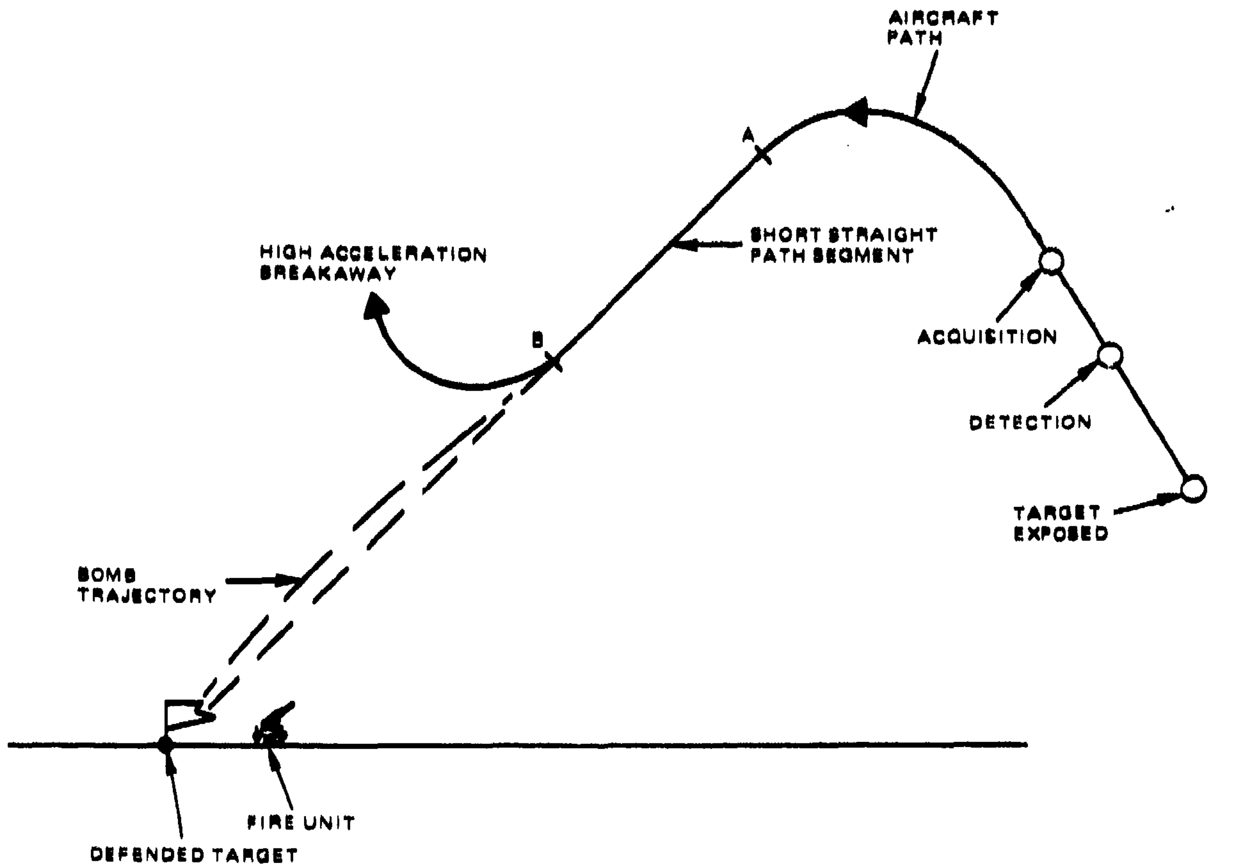


Figure 12-15. Geometry of Dive Bombing Attack

caliber. These ranges are all so large so that the aircraft will have difficulty in locating its target in the first place, and will be unable to secure satisfactory accuracy with unguided bombs. It seems probable therefore, that except when the attacker uses smart munitions of one sort or another, he will in fact have to penetrate the defense to a release range such that effective fire can be delivered only a portion of the straight attack segment.

To obtain an estimate of defense effectiveness when breakaway is within the limit defined by Equation (12.30) assume that single shot probability can be written in the form

$$p_{ss} = \frac{a^2 p_c}{a^2 + 2\sigma^2 D^2 + 2\sigma_0^2 [1 + 2(t_p/T_s) + 2(t_p/T_s)^2]} \tag{12.31}$$

where

- $a$ = target effective radius
- $\sigma$ = angular round to round ammunition standard deviation
- $\sigma_0$ = standard deviation of tracking error
- $p_c$ = probability that a hit produces a kill

For excellent radar or optical tracking one can hope to attain

$$\sigma_0 \cong a \tag{12.32}$$

Next take advantage of Equation (12.24) and (12.26) and estimate E by

$$E = \int p_{ss}(t)\, dt \tag{12.33}$$

It is convenient to change the variable of integration to slant range D, using

$$dD/dt = -v[1 + (dt_p/dt)] \quad ; \; v = \text{target velocity} \tag{12.34}$$

Then expand the integrand as a series in $D^i$, using the following approximate expressions as a basis for obtaining series in $D^i$ for the time of flight and projectile velocity terms

$$dD/dt_p = v_0 e^{-k_1 D} \tag{12.35}$$

$$t_p = (D/v_0)\, e^{k_1 D/2} \tag{12.36}$$

where the coefficient $k_1$ may be estimated from Section 12.7.1.

It is not necessary to retain terms in the expansion beyond $D^2$, or possibly $D^3$, and the integral is then readily obtained in closed form.

Having E, one obtains the kill probability over the engagement from Equation (12.26).

For a simple case to indicate the form of the result, assume that the engagement occurs at a range where the $D^2$ terms dominate $p_{ss}$, and assume a constant shell velocity during the engagement. Then

$$E = (\nu p_c/D_a)\left[\frac{a^2 T_s^2 (v/v_a)}{4\sigma_0^2 + 2\sigma^2 v_a^2 T_s^2}\right]\left[\frac{v_a(T_a - T_s) - D_a}{v(T_a - T_s) + D_a}\right] \tag{12.37}$$

Some observations on the optimum value of $T_s$ for this case can be made by inspection. If the ammunition dispersion is small, the optimum value of $T_s$ will be approximately

$$T_s = (2/3)[T_a - (D_a/v_a)] \tag{12.38}$$

that is, reduction of error resulting from tracking error is so important in this case, that 2/3 of the possible firing time is allocated to data averaging, and 1/3 to shooting. However, this is an upper limit; if the optimum $T_s$ is computed from the full form of Equation (12.31) the best smoothing time will always be found to be less than that given by Equation (12.37).

The value of average shell velocity is seen to lie between the first and second power of velocity. If angular dispersion of the ammunition is small, E increases about as $v_s$ squared.

This simple model indicates therefore, as would be expected, that system effectiveness at the longer ranges with a well designed system against a non-jinking target increases as about the square of average projectile speed, all other parameters held constant.

As a further example of what one can do with these simple relations, assume a dive bomb attack in which the attacker has a 6 second straight line segment just prior to weapon release. Assume that the defending fire unit requires 2 seconds to compute accurate firing data. Assume that the defender will accept 20% attrition, and that he chooses his weapons release range accordingly. Then compute this weapons release range, which is designated 'standoff range'.

A series of fire unit characteristics is abstracted from Table VII-6. It is assumed that the fire control systems in each case have been replaced by a fire control system of modern design, for which the single shot probability can be described by Equation (12.31). The variance of ammunition dispersion is assumed to have been adjusted to equal that of the amplification of sensor noise, and to be conservative, some serial correlation of successive rounds is assumed, such that the variance of burst to burst aim error equals the variance of round to round error.

The total firing time cannot exceed $4 - t_{pa}$, where $t_{pa}$ is the time of flight of the last round to reach the target. Some rough computations indicate that an average

**Table XII-4. Sequence of Events in Defense Against Dive Bombing**

| Event | Elapsed Time | Range to Target |
|---|---|---|
| Begin Attack Pass | 0 | $D_0$ |
| Computer Settled, Fire First Round | $T_s$ | $D_0 - vT_s$ |
| First Round Reaches Target | $T_s + t_{pl}$ | $D_{pl} = D_0 - vT_s - vt_{pl}$ |
| Last Effective Round Fired | $T_u - t_{pn}$ | $D_u + vt_{pn}$ |
| Last Effective Round Reaches Target | $T_u$ | $D_u = D_0 - vT_u$ |

20871-622

time of flight over the firing interval will be about 1.5 $t_{pa}$. The variance of sensor error is assumed to equal one half the target linear extent in each dimension. Then the expected number of lethal hits is given by

$$E = \nu p_c \left[ \frac{(4 - t_{pa})}{(5 + 6t_{pa} + 4.5t_{pa}^2)} \right] \qquad (12.39)$$

where

- $\nu$ = rate of fire of the fire unit (which may mount several guns)
- $p_c$ = probability that a hit causes a kill.

Burst kill probability is computed from

$$p_b = 1 - \frac{1 - e^{-2E}}{2E} \qquad (12.40)$$

Setting $p_b$ = .20, these relations allow $t_{pa}$ to be computed. Then assuming *excellent* ballistics for each weapon, time of flight can be converted to slant range.

Results are shown in Table XII-5. One weapon was added to those abstracted from Table VII-6, a hypothetical 37 mm weapon having the same rate of fire as Vigilante, but firing a sub-caliber 25 mm round at about 5000 f/s muzzle velocity. Rough computations indicate that this combination might be achieved at a complete round weight (projectile plus discarding sabot plus propellant plus case) about equal to that of the 3600 f/s full caliber Vigilante round.

This hyper-velocity weapon shows the best performance in the comparison, followed by the full caliber Vigilante. A weapon with 'Duster' muzzle velocity and rate of fire cannot attain 20% kill probability at all in this situation.

The provision of this excellent fire control in all cases except the low performance 40 mm gun, forces the attacker to release his munitions at ranges from which iron bombing will be relatively ineffective. If, instead of 20% attrition, the attacker will accept only 5% attrition he is forced out to still greater ranges, approaching those of Figure 12-18.

The fire control system assumed is still not the optimum that can be conceived. More efficient sensor noise filtering is possible, and this brief analysis did not consider the trade between firing time and settling time. A full 2-seconds of firing time against this attack path may possibly be gained by the algorithm designated in the AFAADS-1 report as 'defense of a known point'.

It seems to be a reasonable conclusion that a modern predicted fire defense system with well conceived and implemented fire control algorithms can inflict losses on dive/glide bombing aircraft delivering iron bombs that will cause him to abandon this type of attack.

The standoff ranges of Table XII-5 are most sensitive to weapon exterior ballistics. For example, if one assumes not one, but four 20 mm fire units, and approximates their effect by multiplying the rate of fire given in the table by 4.0, the standoff range against a 20 mm defense of four fire units is only increased to 2020 meters, as compared with 1620 meters for one fire unit.

This suggests that the weapon caliber and muzzle velocity preferred for the defense are determined by the standoff range which it is desired to achieve, and the number of fire units comprising the defense should then be chosen to match the maximum number of aircraft expected to be simultaneously within the defense envelope.

#### 12.9.5 Engagement of Passing, Jinking Aircraft

Maneuvering at the maximum acceleration of which it is capable, a target is unlikely to be hit by predicted fire weapons. However, any real flight path is a compromise between the need to execute a tactical mission,

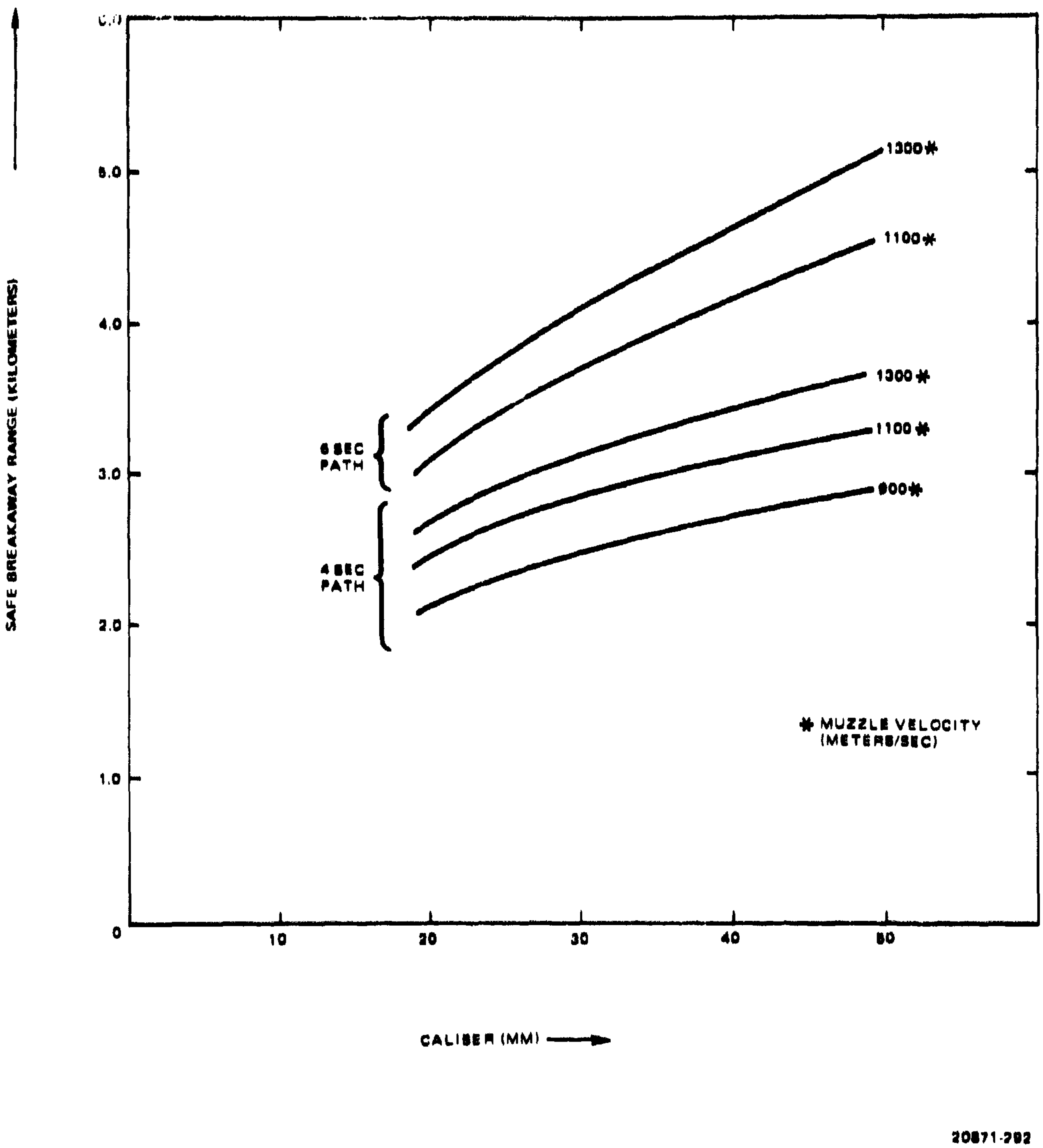


Figure 12-16. Safe Breakaway Range versus Caliber and Muzzle Velocity

Table XII-5. Comparison of Fire Units Against Dive Bombing Attack

| Caliber (mm) | Rate of Fire (rpm) | Muzzle Velocity (meters/sec) | Assumed Terminal Effect ($r_0$) | Standoff Range(1) (meters) |
|---|---|---|---|---|
| 20 | 3000 | 990 | 0.15 | 1620 |
| 23 | 4000 | 900 | 0.20 | 1720 |
| 30 | 1300 | 1080 | 0.28 | 1870 |
| 35 | 1100 | 1175 | 0.50 | 2140 |
| 37 | 3000 | 1100 | 0.50 | 2650 |
| 40 | 240 | 875 | 0.50 | 676(2) |
| 40 | 650 | 1000 | 0.50 | 1910 |
| 57 | 240 | 1000 | 0.65 | 1545 |
| 37/25(3) | 3000 | 1525 | 0.22 | 2910 |

Notes: (1) Standoff range is the range at which the defense has 20% probability of destroying the target
(2) This weapon cannot achieve 20%, the value is for 15%
(3) This is a 37-mm gun firing a 25-mm subcaliber projectile

20871-623

the desire of the pilot to minimize the time he spends within a defense envelope, and the possible degradation of aim of predicted fire weapons by deliberate jinking.

A terrain following aircraft will 'jink' because of the variation in terrain contours, and some irregularities of flight will be caused by air turbulence.

This section develops a simple model for computing engagement outcome against a passing, jinking, aircraft, and compares the model results with more accurate simulation results.

Consider a target jinking in a direction perpendicular to its average flight direction according to the expression

$$y(t) = A_0 e^{st} \quad ; \quad s = j\omega \qquad (12.41)$$

The transfer function of the prediction and smoothing algorithm is

$$F_p(s, T_s, t_p) \qquad (12.42)$$

Then the prediction error will be

$$e_p(t) = A_0 e^{st} \left[ e^{st_p} - F_p(s, T_s, t_p) \right] \qquad (12.43)$$

That is, it will vary sinusoidally as

$$e_p(t) = A_0 \mu e^{j(\omega t - \phi)} \qquad (12.44)$$

where

$$\mu^2 = \left| e^{st_p} - F_p(s, T_s, t_p) \right|^2 \qquad (12.45)$$

For a simple example, consider noiseless tracking and prediction according to

$$F_p = 1 + st_p + (k/2)s^2 t_p^2 \qquad (12.46)$$

where

k = 0; corresponds to linear prediction

k = 1; corresponds to quadratic prediction

Now the maximum target acceleration is

$$\ddot{y}_{max} = A_0\omega^2 = ng \qquad (12.47)$$

where

n = the number of gravities of acceleration.

We have

$$\mu^2 = [\cos\theta - 1 + (k/2)\theta^2]^2 + [\theta - \sin\theta]^2 \quad ;$$

$$\theta = \omega t_p \qquad (12.48)$$

The defender wishes to minimize this expression, which he can do for a given value of $\theta$ by setting

$$k = (1 - \cos\theta)/(\theta^2/2) \qquad (12.49)$$

The square of the maximum amplitude of the sine wave representing the prediction error is

$$s^2 = A_0^2\mu^2 = 4G^2\mu^2/\theta^4 \qquad (12.50)$$

where

$$G = (1/2)\,ngt_p^2 \qquad (12.51)$$

The attacker wishes to maximize this value, by choosing $\theta$, recognizing that the defender will then choose a minimizing value of k. That is, the attacker chooses $\theta$ to maximize (for given maximum ng),

$$s^2 = 4G^2\,[\theta - \sin\theta]^2/\theta^4 \qquad (12.52)$$

and this occurs at $\theta = \pi$, so that

$$s(\max) = (2/\pi)G \qquad (12.53)$$

If the period of weave of the aircraft is $T_W$

$$T_W = (2\pi)/\omega = (2\pi)t_p/\theta \qquad (12.54)$$

and so the best period of weave for the aircraft is

$$T_W = 2t_p \qquad (12.55)$$

Figure 12-17 shows the maximum error amplitude in terms of G as a function of $t_p/T_w$ for several values of k, and for the best k for each value of $t_p/T_w$.

Since the aircraft is unlikely to be able to match its period of weave to time of flight, one can see from Figure 12-17 that for the case considered, the predictor should use an increasing proportion of quadratic prediction as range shortens. For very short ranges, however, the effect of target maneuver is small, and there is little advantage in attempting to correct for it.

It would therefore appear that there is a time of flight interval within which significant advantage in hit probability can be obtained by using a correction based on target acceleration, but this correction should not be used at long ranges, and need not be used at short ranges.

In any real system, $F_s$ will be more complicated than Equation (12.46) because of the inclusion of the terms to express the data smoothing process. For example, one might consider

$$F_p = \frac{1 + s(t_p + T_s)}{[1 + s(T_s/2)]^2} + \frac{s^2(k_1 + k_2 t_p + k_3 t_p^2)}{[1 + s(T_s/2)]^4} \qquad (12.56)$$

One can then go through the same process as demonstrated for Equation (12.46), but optimizing $k_1, k_2, k_3$. One would expect that the end result would work out in about the same way, but with time of flight increased by half the smoothing time, since the effect of smoothing is to delay all measurements by about this amount.

In fact, some advantageous optimization is possible, since for the simpler case of no smoothing, the error amplitude 's' does not increase with $t_p^2$ indefinitely, but approaches a mean value

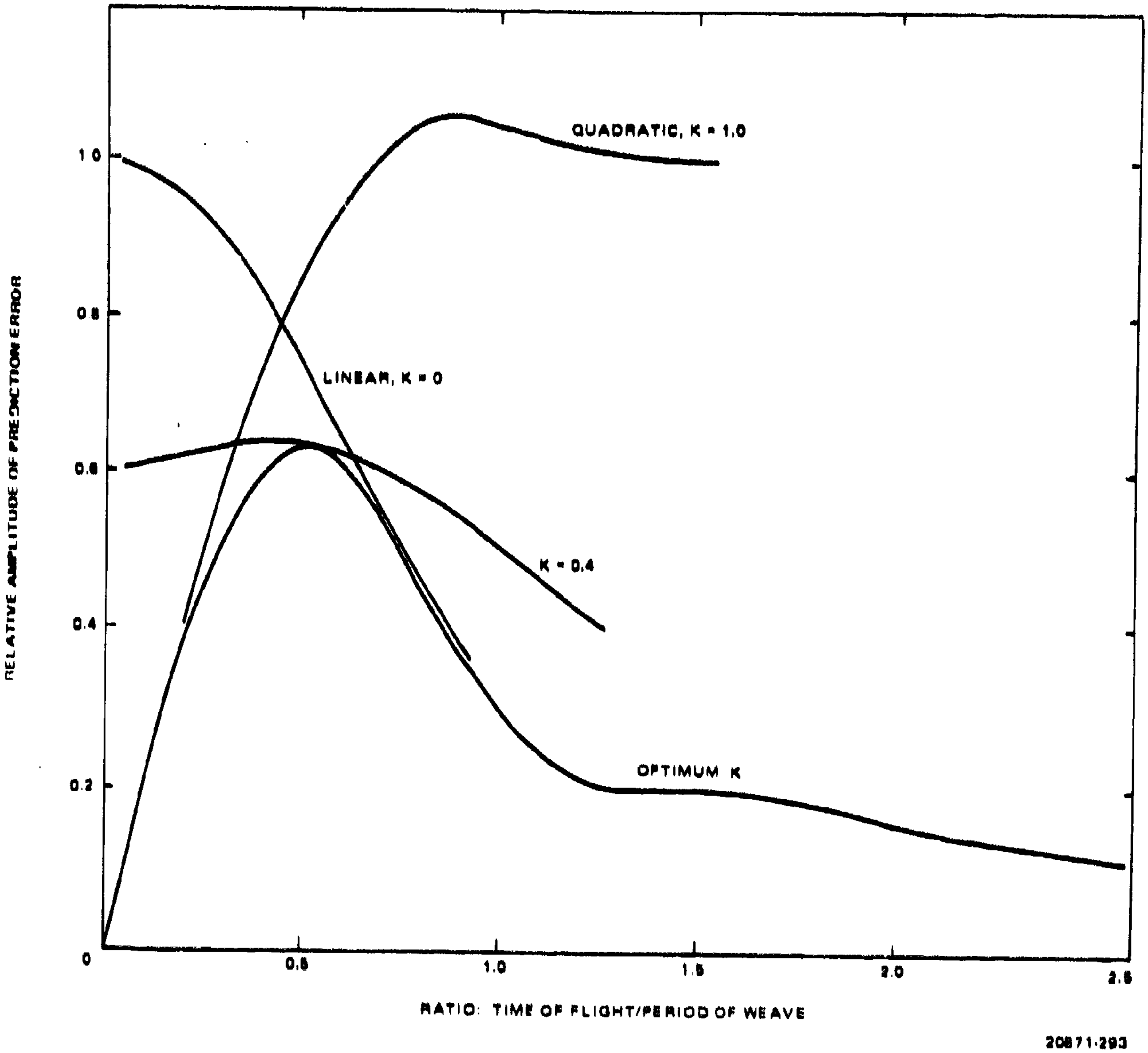


Figure 12-17. Relative Prediction Error versus Weaving Target

$$s = ngt_p/\omega \qquad (12.57)$$

for very large $t_p$, and this value can be further reduced by smoothing which would average against high frequency weaves.

To obtain a rough idea of how system effectiveness may be degraded by a weaving target, a simple analysis is worked through below, and then compared with a few simulation results.

The single shot probability is expressed as

$$p_{ss} = p_c \frac{a^2}{a_t^2 + 2\sigma^2} e^{-r^2/(a^2+2\sigma^2)} \qquad (12.58)$$

where

- $a$ = average target radius
- $p_c$ = probability that a hit produces a kill
- $r$ = radial error in aim
- $\sigma$ = linear standard deviation of random error.

For a burst of about one second, the error in aim caused by a weaving target can be assumed to be constant during the burst. The error in aim caused by tracking error can be described statistically in terms of two components, one which can be associated with the random round to round dispersion of the weapon, and one which can be assumed to be constant during a burst and random across bursts.

Simulation runs with radar tracking and linear prediction indicate that for all practical purposes, one can treat this component in a one second burst as random round to round. A particular prediction algorithm run on the simulation with acceleration correction to update the velocity measurement to present time in the presence of acceleration indicated that the two components of error were about equal. In the present analysis, however, it is intended to consider cases where the error caused by target acceleration is relatively large, and then to add artificial random round to round dispersion for optimum kill probability. In this case, the systematic component of prediction error caused by sensor error (excellent tracking) will be submerged in the added artificial dispersion.

It is next assumed that the target acceleration results from a weave in a vertical plane through the flight path, so that

$$r = G\beta \cos\omega t = G\beta \cos\theta \,;\, \theta = \omega t \qquad (12.59)$$

where

$$G = 1/2\,(ng)\,[(t_p + T_s/2)]^2 \qquad (12.60)$$

and

$\beta$ is obtained from Figure 12-19.

If n, rounds are fired, the average survival probability of the target, since the burst may be fired at any point during the weave, is

$$\phi = \frac{2}{\pi}\int_0^{\pi/2} e^{-E\, e^{-A\cos^2\theta}}\, d\theta \qquad (12.61)$$

where

$$E = np_c\, A_t/(A_t + 2\pi\sigma^2)$$

$$A = \pi\beta^2 G^2/(A_t + 2\pi\sigma^2)$$

$$A_t = \pi a^2 \qquad (12.62)$$

Note that if the weapon fired not a one-second burst, but continuously for exactly one quarter cycle of target weave, we should have

$$\phi = e^{-E\frac{2}{\pi}\int_0^{\pi/2} e^{-A\cos^2\theta}\, d\theta} = e^{-Ee^{-A/2} I_0(A/2)}$$

$$(12.63)$$

and for the same number of rounds, effectiveness would be much higher. Hence Equation (12.61) is conservative.

For a directly incoming target with vertical and lateral weave a more complicated expression results, since the effectiveness depends on the phasing of the two components. This can be worked, but will not be analysed here.

To evaluate $\phi$ we now obtain an exact solution, then an approximation which is asymptotically correct for small and large A, but the errors of which have not yet been determined.

Consider the integral

$$\phi = (2/\pi)\int_0^{\pi/2} e^{-E\, e^{-A\cos^2\theta}}\, d\theta \qquad (12.64)$$

This can be expressed as the series

$$\phi = (2/\pi)\sum_0^{\infty} \frac{(-E)^j}{j!}\int_0^{\pi/2} e^{-jA\cos^2\theta}\, d\theta$$

$$\phi = \sum_0^{\infty} \frac{(-E)^j}{j!}\, e^{-(jA/2)}\, I_0(jA/2) \qquad (12.65)$$

However the evaluation of the series is tedious.

An alternate approach is to approximate I as follows:

$$\phi = (2/\pi)\int_0^{\pi/2} e^{-M e^{A\sin^2\theta}}\, d\theta \,;\, M = Ee^{-A}$$

$$\phi \cong (2/\pi)\int_0^{\pi/2} e^{-M(1+A\theta^2)}\, d\theta$$

$$\phi \cong e^{-M}\left[\frac{1 - e^{-2AM}}{2AM}\right]^{1/2} \qquad (12.66)$$

Probability of killing the target with the burst of n rounds is $p_b$

$$p_b = 1 - \phi \qquad (12.67)$$

and $p_b$ has been plotted in Figure 12-18, using Equation (12.66), and the parameters E and R = E/A. It will be remembered that

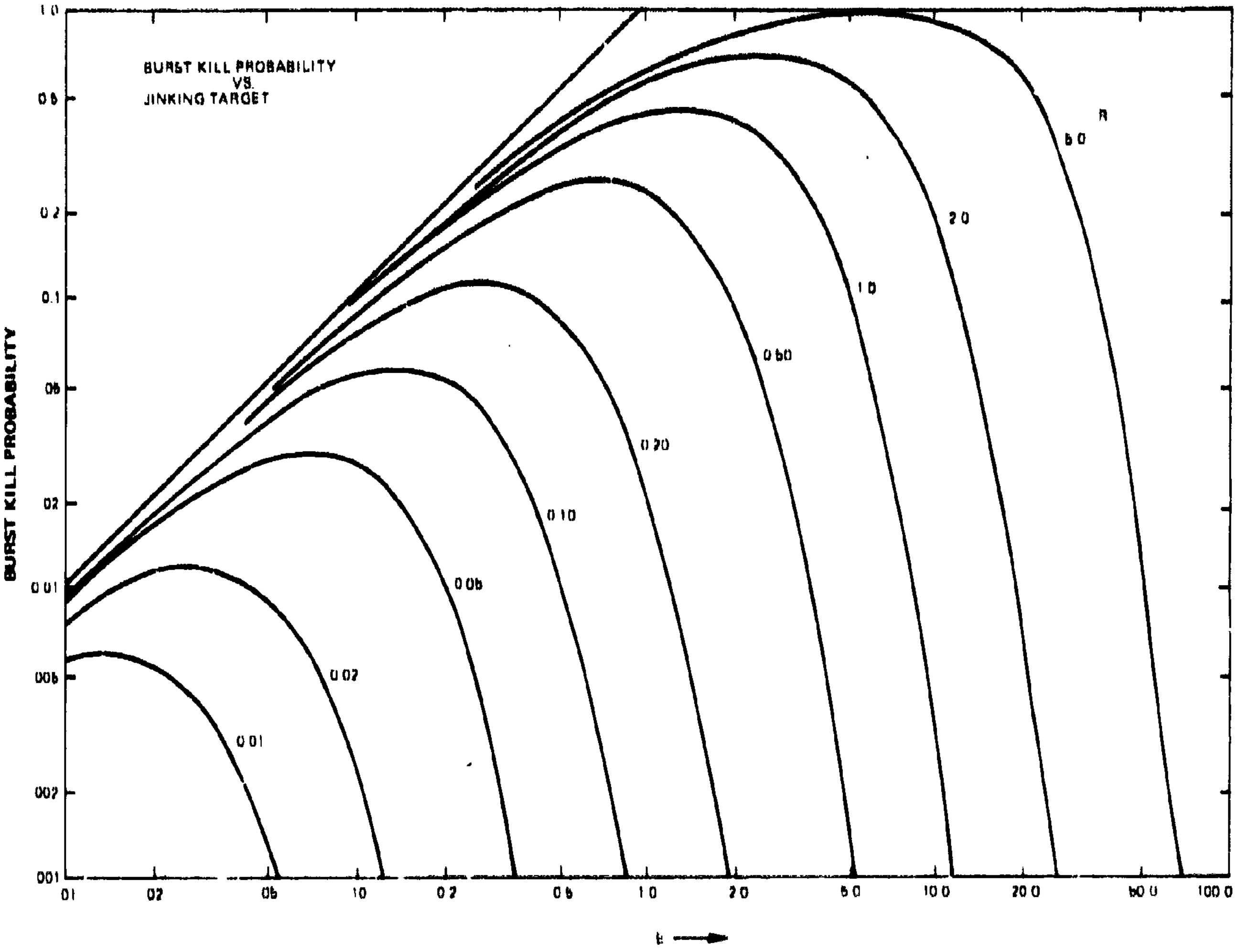


20871 294A

Figure 12-18. Burst Kill Probability versus Jinking Target

$$E = np_cA_t/(A_t + 2\pi\sigma^2)$$

$$A = \pi\beta^2G^2/(A_t + 2\pi\sigma^2)$$

and so

$$R = np_cA_t/(\pi\rho^2G^2) \qquad (12.68)$$

For constant R, A is the only parameter varying with dispersion, hence the maximum of the constant R curves correspond to burst kill probabilities for optimum dispersion, in the case where the dispersion pattern is circular.

The maxima of Figure 12-18 can be observed to occur at approximately

$$A^* = E^*/R = (2)^{1/2} \qquad (12.69)$$

This can also be obtained from Equation (12.26) via the assumption, justified by Figure 12-18 that except for $p_b$ close to unity, the maxima occur for values of AM small enough so that Equation (12.26) can be approximated by

$$\phi = e^{-M[1 + (A/2)]}$$
$$= e^{-RA[1 + (A/2)]e^{-A}} \quad (12.70)$$

differentiating with respect to A, the optimum A* for constant R is found to be

$$A^* = (2)^{1/2} \quad (12.71)$$

Then kill probability for optimum dispersion, $p_b^*$ is

$$p_b^* = 1 - e^{-0.587\, R} \quad (12.72)$$

If the target is jinking in one dimension, it is relatively inefficient to increase the dispersion pattern equally in two dimensions. The results already obtained can be used to obtain an estimate of the best dispersion in the direction of the jinking and the resulting burst kill probability.

Assuming the target to be circular (the shape is irrelevant when single shot probability is small),

$$E = np_c \frac{A_t}{\left[(A_t + 2\pi\sigma_x^2)(A_t + 2\pi\sigma_y^2)\right]^{1/2}} \quad (12.73)$$

and assuming that the target jinks in the x direction only

$$A = \frac{G_x}{A_t + 2\pi\sigma_x^2} \ ; \ G_x = \pi\beta G \quad (12.74)$$

Define

$$R_1 = np_c (A_t/G_x)^{1/2} \left[A_t/(A_t + 2\pi\sigma_y^2)\right]^{1/2} \quad (12.75)$$

Then

$$E = R_1 A^{1/2} \quad (12.76)$$

Using the approximation of Eq. (12.70)

$$\phi = e^{-R_1 A^{1/2}[1 + (A/2)] e^{-A}} \quad (12.77)$$

The optimum A* is

$$A^* = 0.618 \quad (12.78)$$

and

$$p_b^* = 1 - e^{-0.555\, R_1} \quad (12.79)$$

Comparing the two cases, we see that with optimum dispersion, for a circular dispersion pattern the burst probability falls off as $G^{-1}$ but if dispersion is optimized in the direction of a one-dimensional jinking, burst probability falls off only as $G^{-1/2}$. The potential gain is therefore seen to be very large.

Equation (12.72) is compared with simulation results in Figure 12-19. The simulation used a 'tangential' prediction algorithm, which together with three mils round to round ammunition dispersion appears to have developed a fortuitously good match of random and bias errors against this jinking target. The jinking path simulated was more complex than that used in the analysis: the aircraft executed a ±0.5g lateral weave, out of phase with a +0.4g, -0.2g vertical weave. The analytical computation assumed a maximum 0.3g acceleration in one dimension. The computation is for a one-second burst of 64 rounds, target presented area of 4.0 square meters, and conditional probability that a hit causes a kill of 0.24.

Having obtained some confidence in the simple expression of Equation (12.72) by this means, it has been applied to the weapons set already employed in Table XII-5, with results shown in Table XII-6.

Again, the assumption is that the fire control systems actually associated with each weapon were replaced by an 'excellent' system using tangential prediction, and a good match of dispersion against aim error caused by target maneuver.

It was also assumed that each weapon had 'excellent' exterior ballistic characteristics.

In this comparison an 'effective range' was defined as that range at which, for this target aspect, the defense could secure a 5% kill probability with a one-second burst. For a passing course of this type, the weapons would probably be able to fire for much longer than one second per pass, and in fact effectiveness might be expected to rise more rapidly with duration of fire than given by Equation (12.72), tending to be better represented by Equation (12.63).

The oscillatory nature of kill probability against a jinking target is shown by the simulation results of Figure 12-20, which shows one-second burst kill probabilities along a specific path for two muzzle velocities, and a 20 mm weapon at 6000 rpm.

The results of the one-second burst computations using Equation (12.72) are given in Table XII-6. Note that the order of preference of weapons is almost identical with that of Table XII-5.

The comparison against a jinking target tends to weight time of flight as the fourth power, whereas the comparison against the dive bombing target tends to weight time of flight as the square.

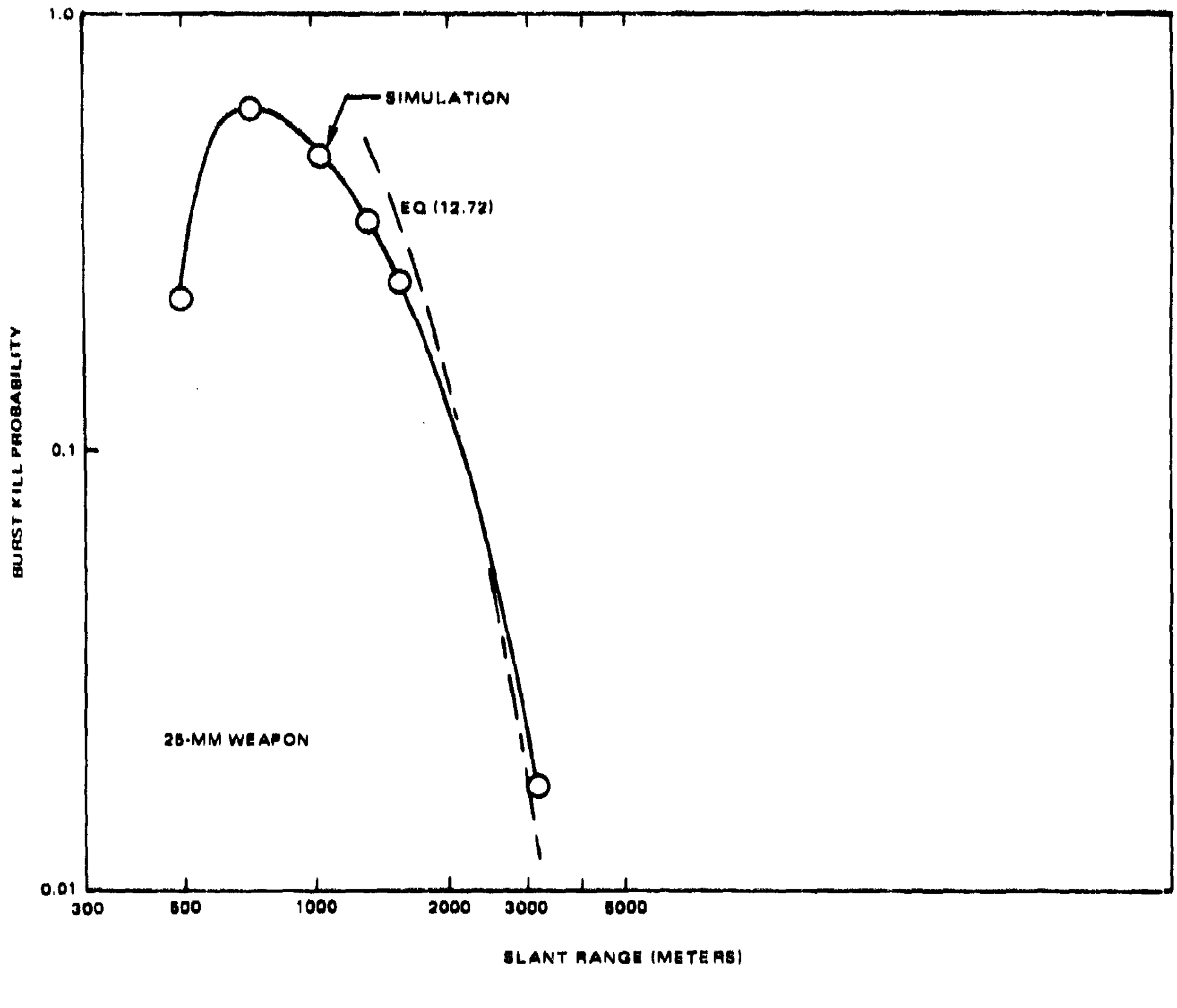


Figure 12-19. Comparison of Analytical and Simulation Estimations of Burst Kill Probability versus Jinking Target

It will, of course, be obvious that the two simple models can be written in parametric form, including simple trade-off functions for weapon characteristics so that some preliminary and approximate weapon design optimization can be done before making extensive overall systems comparisons.

### 12.9.6 Graphical Estimates of System Performance Limits

The essential elements of the two simple engagement models can be shown approximately but simply in graphical form in the following way:

If the weapon fires n rounds against a target with projected area $A_0$ and radius a, it may be considered to have a useful coverage area $nA_0$, or radius $n^{1/2}$ a. For the moment we consider hit probability rather than kill probability.

For an unaccelerated target, considering only the aim error resulting from prediction error, the aim point may be considered to lie in a circle of area $2\sigma_p^2$, or radius $2^{1/2}\sigma_p$. Now the simple expression Equation (12.28) makes $\sigma_p$ a function of time of flight only.

For about a 20% probability that the coverage area will overlap the area of uncertainty of the aim error, we may plot $2^{1/2}\sigma_p$ against time of flight, and on the same graph, plot $[(5n)^{1/2}$ a] as a horizontal line and observe the time of flight at which they intersect.

**Table XII-6. Comparison of Fire Units Against Jinking Target With 'Optimum' Fire Control**

| Caliber (mm) | Rate of Fire (rpm) | Muzzle Velocity (meters per second) | Effective Range (meters) |
|---|---|---|---|
| 20 | 3000 | 990 | 1800 |
| 23 | 4000 | 900 | 2000 |
| 30 | 1300 | 1080 | 2200 |
| 35 | 1100 | 1175 | 2600 |
| 37 | 3000 | 1100 | 3000 |
| 40 | 240 | 875 | 1000 |
| 40 | 650 | 1000 | 2200 |
| 57 | 240 | 1000 | 1900 |
| 37/25 | 3000 | 1525 | 3200 |

Maximum target acceleration: 0.3 g

Target projected area: 4.8 square meters

Effective Range is defined as that range at which the fire unit obtains 5% kill probability with a one-second burst.

20871-624

This has been done for n = 50 in Figure 12-21, for a one meter radius target, two-seconds smoothing, and simple, nonoptimum forms of the expressions for $\sigma_p$ for linear and tangential prediction.

We observe that we might expect to attain 20% burst hit probability out to about four sec time of flight with tangential prediction and to about 15 seconds time of flight with linear prediction. For a particular weapon, burst hit probability is converted to kill probability by multiplying by the appropriate terminal effect probability, and time of flight is converted to range by the appropriate exterior ballistic relation.

One can easily sketch in other curves for other smoothing times and prediction algorithms.

The same process can be followed for a jinking target, as shown in Figure 12-22. We now have an additional curve: the set of three includes (1) the target coverage radius $[(5n)^{1/2}\ a]$, (2) the noise amplification error radius caused by the prediction algorithm operating on sensor noise, and (3) the prediction error caused by the target acceleration (shown for 0.3g maximum).

With linear prediction (effect of sensor noise not shown, but identical with that of Figure 12-21), the prediction error caused by target acceleration is slightly increased by the lag introduced by smoothing time. With quadratic prediction, the effect of target maneuver is essentially zero at less than three seconds time of flight, but the noise amplification is so great that it causes an even earlier intersection of the coverage radius.

The use of tangential prediction produces a slight reduction in the error caused by target acceleration, and the sensor noise amplification radius is slightly smaller than that of the target acceleration error. Hence this prediction mode appears as a good match to the requirements of the problem, which could be further improved by using a small portion of additional acceleration correction so that all three curves would intersect at about the same time of flight point.

For this magnitude of target maneuver, the curves sketched indicate that 20% hit probability with 50 rounds could only be maintained out to about three seconds time of flight.

These sketches cannot be used to substitute for more accurate computations, but they do serve to indicate what is involved in attempting to extend system effective range. In the presence of target jinking the dominant role of time of flight is clear.

Varying the weapon dispersion only allows the indications of these curves to be approached, but not exceeded.

## 12.10 NEED FOR VALIDATION OF MODELS BY EXPERIMENT AND COMBAT DATA

Complex and useful simulations are available for evaluating predicted fire systems, in addition to the simple models presented in previous sections. The major deficiency of the evaluation process appears to be in the absence of valid data with which to load them. Data requirements include the following:

### 12.10.1 Target Path Statistics

Even the simple analytic models of this report indicate how sensitive the evaluation of system performance is to assumptions about how long an attack aircraft is likely to fly a straight line path in weapons delivery, and what kind of irregular flight paths may result from terrain following, deliberate jinking, weapons release with 'free-maneuver' bomb sights, etc. This information is a basic requirement for any definitive weapons evaluation and comparison.

### 12.10.2 Engagement Statistics

In addition to target path data, experimental information is required on the times required to perform the many functions associated with target detections, acquisition, and system operation. These can be estimated, but estimates have low validity until they are confirmed by operational measurements, with particu-

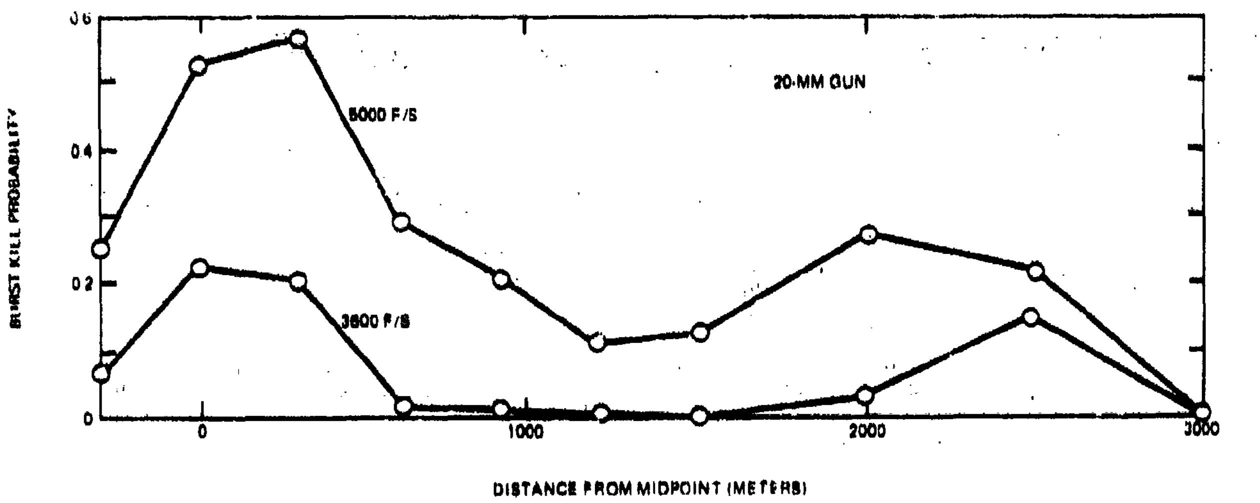


Figure 12-20. Simulation Demonstration of Effect of Muzzle Velocity on Burst Kill Probability versus Jinking Target

lar attention given to probable degradation in a combat environment.

### 12.10.3 Overall Performance Validation

It has been noted frequently in this report that estimates of the effectiveness of the prediction algorithms of a predicted fire air defense system tend to dominate the comparison. A number of different sets of algorithms are used in existing predicted fire systems, several of these systems have been tested in the United States and NATO, and presumably overall effectiveness data exists which could, with some effort, be put into a common form to observe whether in real life there is any observable difference resulting from the process of computation, or whether the effectiveness of all systems is dominated by the characteristics of the target path.

A partial list of current predicted fire systems is given in Table XII-7. It is recognized that test conditions will vary widely. The possibility that direct comparison will not be possible should not, however, prevent an effort to assemble the data and compare it. One will at least obtain some idea of parametric ranges and capabilities to be exceeded in new systems.

The off-carriage systems are included, not because it is recommended that the U.S. consider off-carriage solutions, but because a wider variety of prediction algorithms and methodologies for their realization can be sampled by their inclusion.

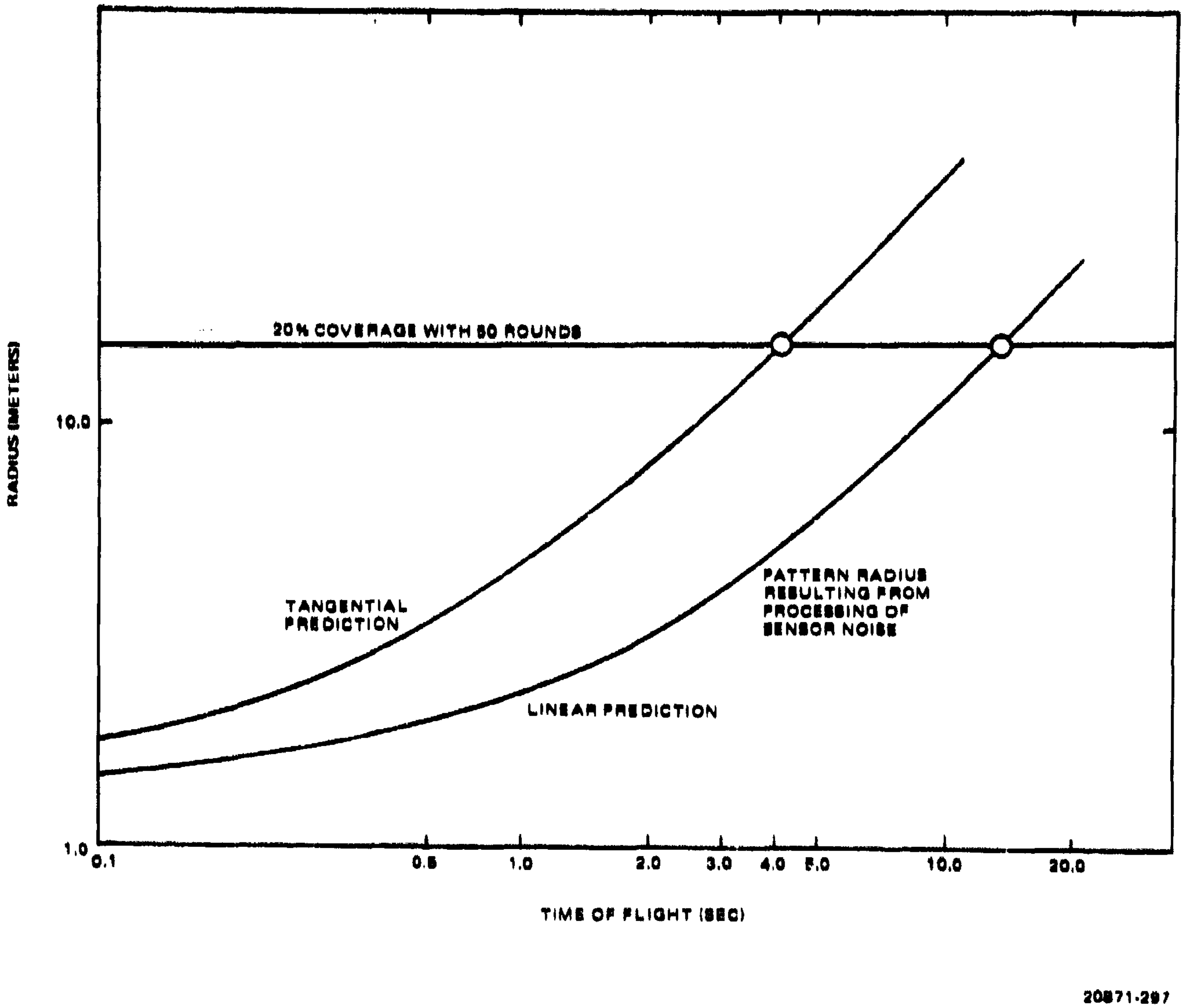


Figure 12-21. Graphical Estimation of Performance Limit Against Unaccelerated Target

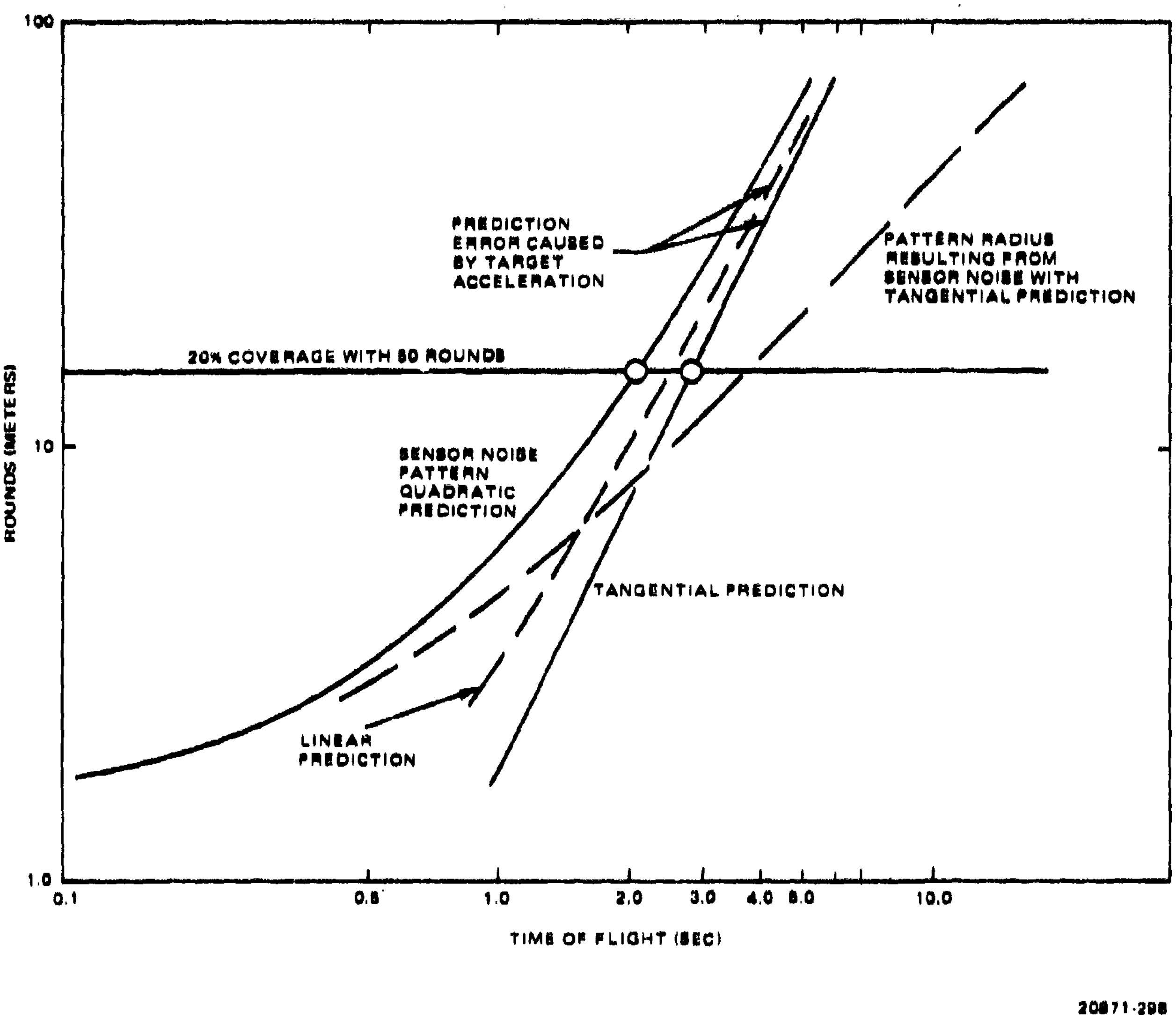


Figure 12-22. Graphical Estimation of Performance Limitation Against Jinking Target

Table XII-7. Partial List of Suggested Fire Control Systems for Comparative Analysis and Evaluation

| On-Carriage Systems | Off-Carriage Systems |
|---|---|
| Vulcan Gyrosight | Oerlikon Skyguard |
| Vigilante | French TPC Type 40 and later versions |
| Oerlikon | |
| French SAMM on AMX 30 | Netherlands L4/5 |
| Galileo P36 and P56 | Italian NA9 |

20871-625

# SECTION 13
# ESTIMATION OF SYSTEM EFFECTIVENESS

In comparing predicted fire air defense systems on an overall systems basis, two considerations deserve special attention. These are:

a. The predicted fire system operates as a part of a larger air defense system. The complete air defense system includes surface to air missiles, each fire unit of which provides defense over a large area. The purpose of the short range predicted fire systems is to fill in low altitude gaps in the defense and to strengthen the overall defense of vital areas. Hence the maximum altitude coverage required of the predicted fire defense is roughly defined by the minimum altitude capability of the area missile defense. Its maximum effective range objective is related to the intersection of the local terrain mask angle projected, with the low altitude coverage limit of the missiles.

b. There is a strong (first order effect) interaction between defense effectiveness and tactics and munitions used by the attacker. A strong local defense forces the attacker to compromise between his desire to close with his target for high delivery accuracy, and the aircraft loss rate that he is willing to accept.

We next consider the measures of mission success in view of this second factor.

## 13.1 MEASURES OF MISSION SUCCESS

In its air defense role the measure of success of an air defense system is the degree of protection it provides for the vital areas and friendly units under its protection. There are many historical examples of antiaircraft gun defenses having sufficient effectiveness so that enemy attacks were held off to ranges at which enemy weapons were relatively ineffective, and cases were antiaircraft defenses caused the termination of enemy attacks on the defended targets.

In World War II British merchant vessels in the Mediterranean were armed with antiaircraft guns. The guns shot down only 4% of the attacking aircraft. However, in terms of merchant vessels subjected to low level attacks, antiaircraft fire had the effect shown in Table XIII-1.

The payoff was in survival of the defended target.

In Korea, the anti-rail interdiction campaign of the UN was curtailed by antiaircraft guns placed along the track. Although losses rates per sorties were low by WW-II standards they exceeded the capability of the UN forces to maintain the campaign with the limited number of available tactical bombers.

In World War-II operations of the 9th Air Force it was found that in B-26 attacks on bridges, only 2% of the bridges attacked were destroyed when defended by flak, compared with 20% when flak was not present. Moreover 28% of all bridges attacked were missed completely when defended by flak, compared with 3% being completely missed in the absence of flak. About 25% of the aircraft exposed to flak were damaged by it and 70 to 90% of the damage occurred in the target area.

An effective air defense against day dive or glide bombing may be countered by night attacks or by the use of stand-off missiles. Both of these enemy responses are more costly to him. Even though the immediate defense effectiveness measured in aircraft destroyed may have been reduced, the reduction in enemy force capability (not all tactical bombers and fighter-bombers will have night and all weather capability; the payload in terms of warhead weight is less for two standoff missiles than for an equal weight of iron bombs) may be comparable to that which would have been achieved in terms of destroyed aircraft if the enemy had not resorted to the more expensive option.

These considerations are difficult to introduce without complicating the analysis. They must, however be included in the measures of mission success.

One method of exposing the relationship between the effectiveness of the defense in protecting the defended target and the losses inflicted on the attacker is to include terms in the capability vector which extract these measures separately. They can then be compared and a judgement made. Iterations of the computation can be made, changing tactics of attacker and defender to observe the degree to which the comparison may vary with such tactical options as the number and sequence of enemy attacks, the munitions release

**Table XIII-1. Effect of Antiaircraft Defense of Ships**

| Outcomes | Situation | |
|---|---|---|
| | AA Guns Fired | AA Guns not Fired |
| % of bombs dropped which hit ship | 8% | 13% |
| % of ships sunk of those attacked | 10% | 25% |

20871-626

ranges, etc. and the number of fire units and rounds fired at varying ranges by the defense.

In the case of low level fly-by enemy passes with laydown or retro weapon delivery, the attacker's options may be more limited than in the case of dive bombing (where release range is optional, as are the approach tactics prior to weapon release).

To obtain a rough idea of what attrition rates may cause an enemy to change his mode of attack, we consider some historical data.

## 13.2 ACCEPTABLE LOSS RATES[43]

Materiel, tactical, and psychological considerations affect the sustained attrition rates that a tactical air force commander is willing to accept. One consideration is the rate at which lost aircraft are being replaced. In World War II, the 8th Air Force accepted a sustained loss rate of bombers of 5-7% per sortie for month after month when the resupply rate of new aircraft was 1.7 times the loss rate. However when losses exceeded about 10% per sortie, missions were curtailed until fighter escort could be provided.

The Luftwaffe attacks on England in the Battle of Britain were halted by a loss rate of less than 5%, with a resupply/loss rate ratio of less than 1.0, but the RAF was able to maintain its defense with a loss rate of about 4% per sortie, and a resupply/loss ratio of slightly over 1.0. The British Bomber Command curtailed operations against Germany when it experienced a loss rate of about 9% per sortie with a resupply/loss ratio of slightly over 1.0.

In the Korean War, a short term loss rate of 2.6% experienced by the B-26 aircraft with negligible replacement prospect (the production line had been phased out) caused this aircraft to be taken off operations until new tactics could be devised.

It was determined by the British that high sustained loss rates had severely degrading effects on crew morale and combat effectiveness, regardless of replacement rates. At 10% losses per sortie, the missing places at the Squadron mess have an understandable effect on the survivors.

Aside from morale, for a force with F aircraft, a sortie rate of S sorties per aircraft per day, a loss rate of $\lambda$ aircraft per sortie, and a replacement rate of $\mu$ aircraft per aircraft lost, the force size changes at a rate

$$dF/dt = FS\lambda(\mu - 1) \qquad (13.1)$$

When $\mu < 1.0$ the commander is forced to consider how long he can sustain operations. He is more likely to project his current loss and replacement rates linearly than to integrate Equation (13.1), and so he can look forward to a total of about

$$S_{cum} = [\lambda(\mu - 1)]^{-1} \text{ sorties per aircraft} \qquad (13.2)$$

In Figure 13-1 a boundary has been drawn for $S_{cum}$ = 200 sorties, a second boundary has been sketched estimating performance degradation resulting from the psychological effect of losses, and the estimated data points for combat operations cited have been indicated.

## 13.3 SOME COST CONSIDERATIONS OF TACTICAL AIR OPERATIONS

At one time U.S. defense planning was popularly credited with attempting to get 'more bang per buck'. Presumeably the other side is attempting to produce 'more rubble per ruble' and this involves a consideration of what tactics to use to obtain a favorable trade of resource consumption against military effectiveness.

It has been noted that almost all means for overcoming an air defense system, or reducing its effectiveness impose additional costs on the attacker. One might work out a set of states describing the condition of the enemy air force as indicated in Figure 13-2, and combine it with the complementary states of the air defense system to achieve an overall defense/attack analysis. This is beyond the scope of the present study, especially since to be done properly, it would require that all components of the air defense system be included.

We note, however, a few measures of cost to the attacker, as a basis of reference. Costs are expressed in U.S. dollars and drawn from U.S. experience for obvious reasons.

Consider aircraft lost and damage to aircraft which survive. Given a hit on an aircraft, damage or loss may occur in various categories, as sketched in Figure 13-3, which indicates roughly how these might vary with the caliber of the impacting weapon.

The two loss categories are important to the defense analysis, since immediately observed kills allow conservation of ammunition. Considering the damage category 'replacement of a major component', one might estimate that on this average the associated cost would not exceed about 0.3 times the cost of a new aircraft. Lesser degrees of damage would incur relatively small cost increments. The cost of a lost aircraft might therefore be multiplied by about 1.5 for an upper limit to the total cost associated with a hit. The reduction in force effectiveness caused by time lost in damage repair depends on the resupply rate of new aircraft, and replacement parts for damaged aircraft. In general, it is doubtful that this is of first order significance.

Similarly, the non-availability of personnel because of injuries probably is probably a second order effect, compared with the personnel losses in crashed aircraft. Figure 13-4 shows the time lost from duty by Air

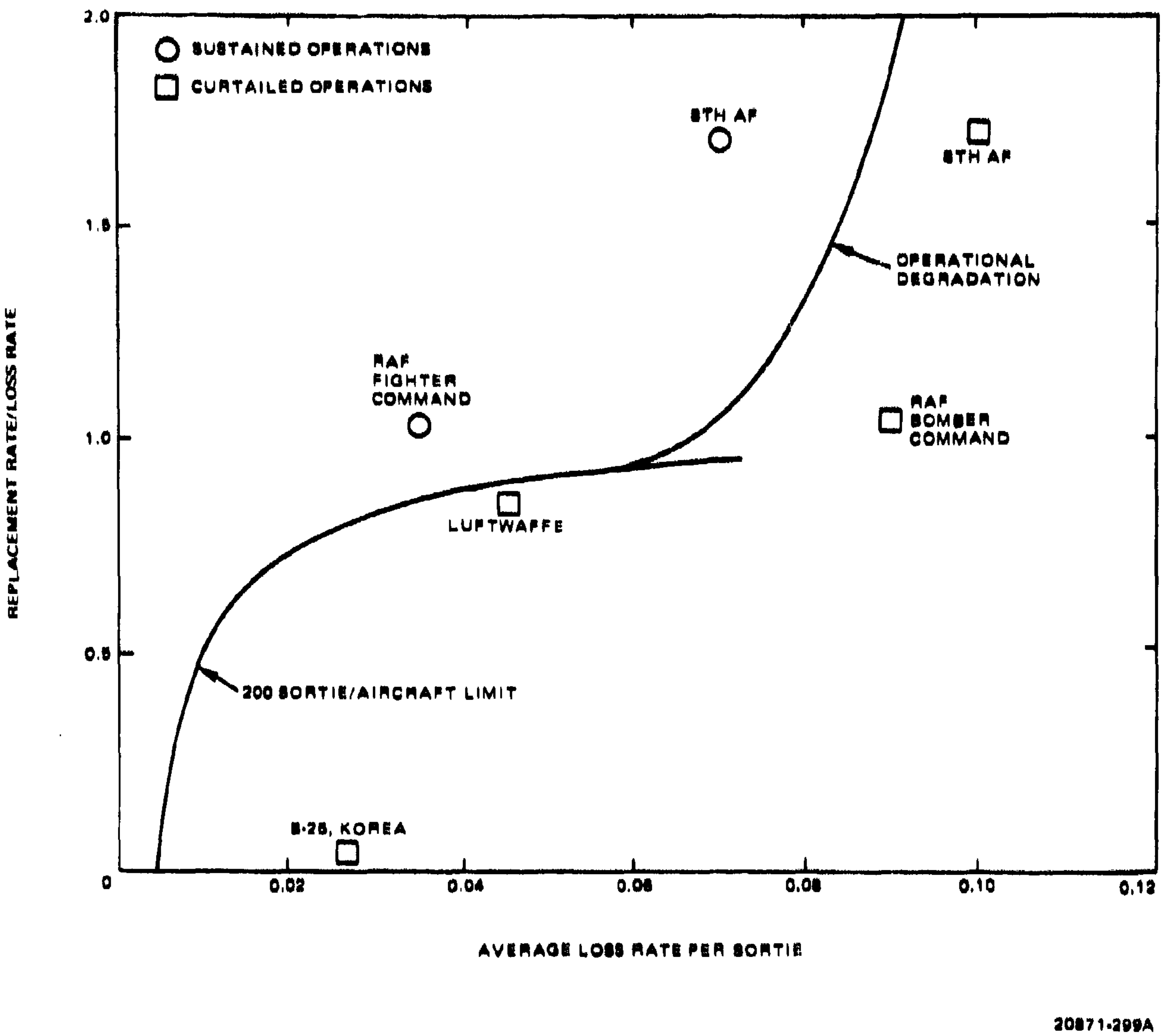


Figure 13-1. Loss Rates in Sustained Operations

Force bomber personnel in World War-II, as a result of strikes by antiaircraft shell fragments.

Operational costs of U.S. aircraft per sortie in Southeast Asia, derived from unclassified sources, are indicated in Table XIII-2.[41]

For fighter-bombers (averaged over all types), the munitions cost (iron bombs) works out at about 50 cents per pound and is a small part of the sortie cost. However, in Table XIII-3 an attempt has been made to guess how this cost might increase with the provision of more sophisticated munitions. With more time, this comparison could be done accurately, but the present purpose is to suggest that sortie costs could escalate by a factor of 10/1 over iron bombs, if only sophisticated air to surface missiles were carried.

It is doubtful that an intermediate range standoff missile can be built for as little as $15 per pound. However, the delivery aircraft would presumeably carry less total payload in missiles than if it were carrying iron bombs.

The AX aircraft, for example (A-9A version) is reported[42] to have the capability of carrying 18 Mk82 500 lb bombs or 6 to 8 Maverick missiles. The cost of the simple Bullpup missile has been worked down from $4,000 each to about $2,000 each over many years of production,[39] but at the other extreme of

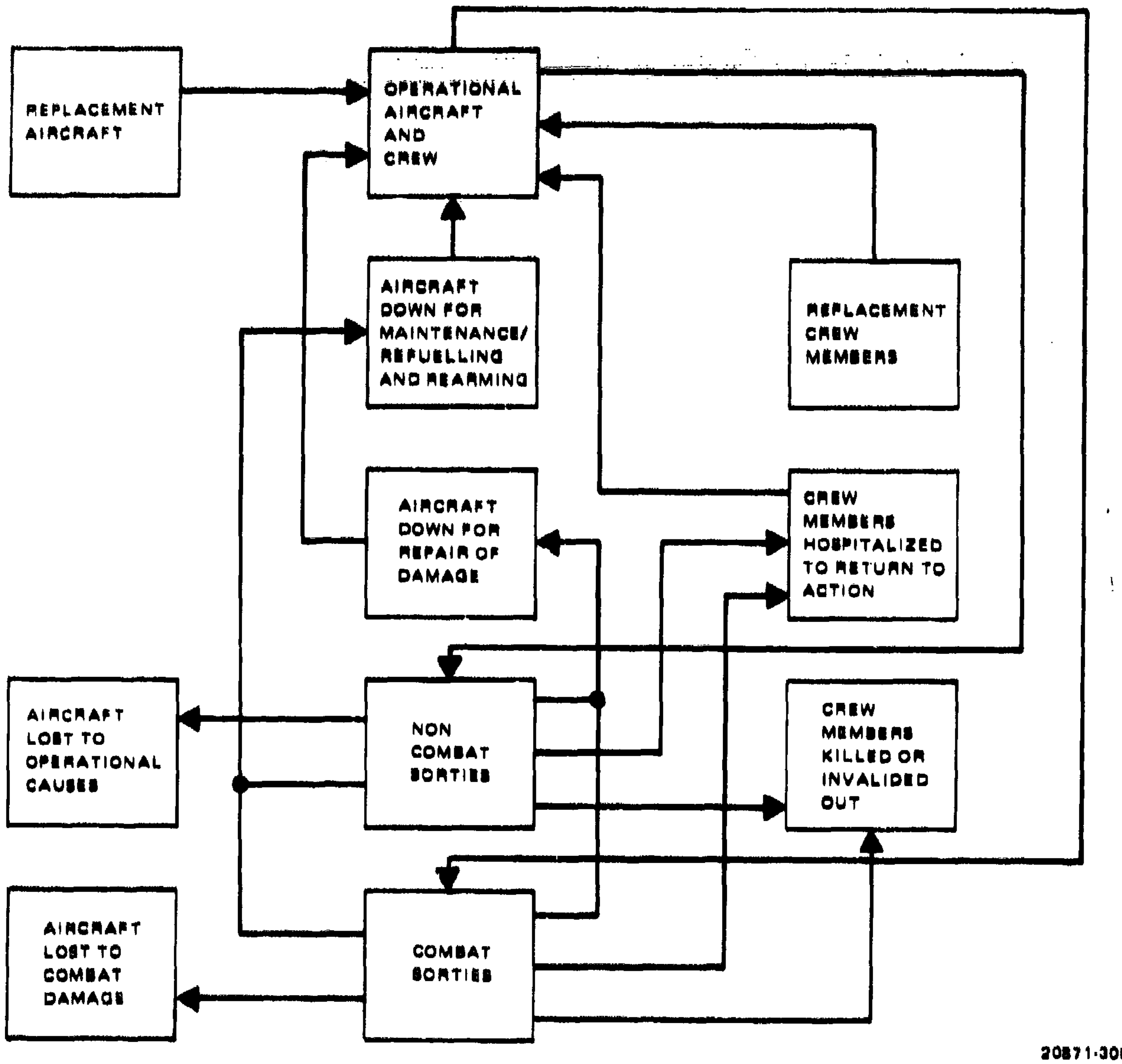


Figure 13-2. Aircraft and Crew Operational States

sophistication[40], open sources have indicated a price of over $200,000 per missile in early production for the long range Condor air to surface missile.

## 13.4 COMBINING SUB-MODEL ESTIMATES

Most of the components of the complete system effectiveness estimation have now been developed in prior sections. The methods of Section 10 lead to estimates of the availability/dependability product of the WSEAIC structure, i.e., the probability that the system will be in one of its possible operational, or non-operational states at and during the brief combat states.

From Section 11, one can obtain an estimate of the fraction of available targets that each fire unit will be able to engage as limited by its rate of ammunition expenditure and its reload rate.

From Section 12, one can develop the probability that each fire unit will destroy a target, once it engages it, provided that the environmental parameters are defined, and the target tactics made specific.

The number of combinations of environmental and tactical parameters that can be laid out as important for evaluation is extremely large, and results are so critically dependent on judgemental assumptions that it seems to be unnecessarily misleading to attempt to take

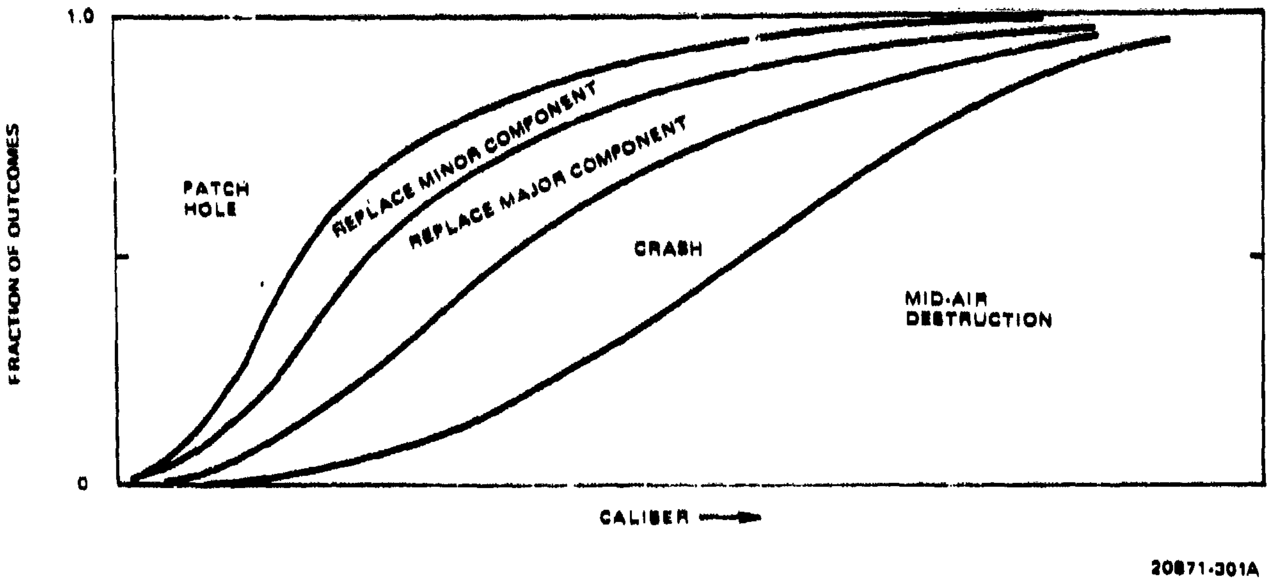


Figure 13-3. Relative Damage and Destruction From Projectile Impact

some kind of weighted average of system effectiveness over all sets of parameters.

It is suggested that a more reasonable procedure is the following:

a. Estimate the most likely and effective modes of enemy attack if there were no AFAADS defense.

b. Estimate AFAADS effectiveness against these modes of attack, and attempt to raise the defense effectiveness to a level where the enemy must resort to a more costly attack mode.

c. Estimate AFAADS effectiveness against this next level of enemy options and attempt to force him to a still more costly attack means, still maintaining the capability against the least expensive mode.

In fact, once one has gone through the availability (RAM) estimation, assessed the interaction of reload rate and rate of fire against plausible strike patterns, and computed a set of engagement results for a representative set of combinations of enemy attack modes and visibility/weather conditions, the set of candidate systems will have been markedly reduced, and perhaps the preferred system choice will already be evident.

It remains, however, to arrange the results in an orderly fashion, and this is facilitated by combining the results of the sub-model computations.

Before outlining how this might be done, we first digress to deal with the matrix computation of effectiveness by the WSEAIC model (for each tactical situation), and indicate why further matrix multiplication of availability and dependability across a capability vector is probably an unnecessary refinement.

## 13.5 SIMPLIFICATION OF COMPUTATION

The WSEAIC scheme suggests that one may compute effectiveness E as

$$E = ADC \qquad (13.3)$$

where AD is the probability vector that the system will be available and continue to operate in each of its possible operational modes, including modes of degraded operation, in the combat state and C is a vector describing system capability in each mode.

As an example of how this works out, the probabilities of various operational and inoperative states for the combat phase of an operation have been extracted from Table X-5, and are listed in Table XIII-4. Also shown are some estimated capability figures. These might be considered to be, for example, 'probability of destroying an aircraft in a specified attack mode and operational environment' in each of the system operational modes.

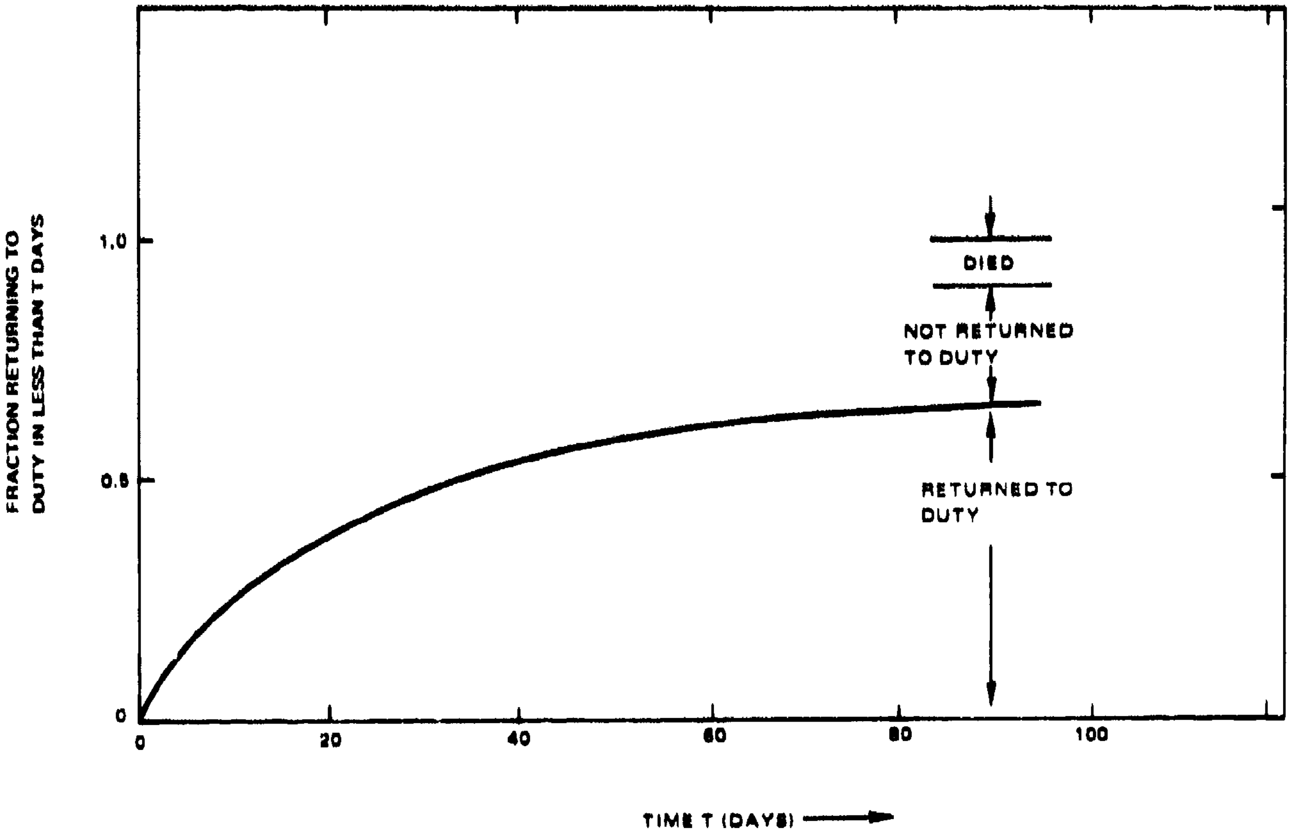


Figure 13-4. Casualties and Time Lost From Duty Due to Flak Injuries

These two columns are the AD and C vectors of the WSEIAC type of effectiveness computation, and one obtains an overall effectiveness estimate by multiplying corresponding terms and summing.

The first thing to note is that one gets almost all of the final result from the 'all-up state'. The other possible degraded modes contribute a total of only .03 out of a total 'effectiveness' of .44. In view of the many uncertainties and unknowns in estimating both availability and capability, it hardly seems worth while to devote time to computing the contribution to average effectiveness of performance in degraded modes of operation.

This conclusion would be different if the all-up mode had a lower probability of occurrence than one or more of the degraded operational modes. But this would be an unsatisfactory system from a military point of view and should probably not be accepted regardless of its effectiveness when operational. If, in fact, the system developed most of its effectiveness from degraded mode operation, and its acquisition was required because there was no alternative, one might be better off to remove the high failure rate subsystem entirely and plan on making the previous secondary mode a primary mode. In World War II, 40-mm antiaircraft gun units left their off-carriage fire control

Table XIII-2. Estimated Costs per U.S. Sortie in Vietnam

| | Aircraft Type | |
|---|---|---|
| | B-52 | Fighter-Bomber |
| Munitions Cost per Sortie | $24,000 | $3,200 |
| Tons per Sortie | 28 | 3.2 |
| Munitions Cost per Ton | $850 | $1,000 |
| Other Costs per Sortie | $20,000 | $8,400 |
| Total Costs per Sortie | $44,000 | $11,600 |
| Average A/C Unit Cost | | $3,000,000. |

20871-627

systems at the docks and went into action with simple on-carriage open sights.

A second observation from Table XIII-4 is that capability is not assumed to degrade more than 25% on loss of the surveillance radar, on the assumption that the tracking radar can partly fill in for it. If these numbers were obtained from analysis instead of assumption, one would then have to inquire very carefully into the question of whether the cost of the surveillance radar justified the 25% increase in capability associated with it.

It is suggested that the availability/dependability analysis should be done with some care to insure that a system being evaluated does in fact have a high probability of operating in an 'all-up' state. In addition, the ability to operate in degraded modes should be designed into the system to a reasonable extent. Once these requirements have been met, however, systems may reasonably be compared against each other in terms of the single elements of the ADC matrices corresponding to the fully operational mode.

We next consider what combinations of tactical/operational parameters should be evaluated.

## 13.5 DISCUSSION OF TACTICAL/OPERATIONAL PARAMETERS

This section discusses some of the tactical and environmental parameters and variables which should properly be considered in a system evaluation. Any analytical or simulation model which includes all of these considerations is likely, in the present state of the art of simulation fabrication, to cost almost as much to develop as the construction of a prototype fire unit. Hence the object of the initial survey is to attempt to devise a judgemental basis for ordering situations in priority of consideration, and to indicate, if possible, how much of the evaluation can be usefully performed by economical simulations and analyses, and how much by common sense.

### 13.5.1 Nature's Options

Visibility state space transitions between day and night occur with predictable reliability. A brief survey of the unclassified descriptions of Soviet and U.S. tactical aircraft capabilities indicates that Soviet fighter-bombers and possibly light bombers as well, possess only limited night attack capability at present, but that U.S. aircraft (and helicopters) have sophisticated and expensive fire control systems for acquiring and attacking targets at night. The U.S. development has of course been accelerated by combat requirements in Korea and Vietnam. Soviet acquisition of an equivalent operational capability is a matter of priorities rather than technology, however the immediate threat from Communist Bloc strike aircraft is of major magnitude by day, and currently, may be of substantially reduced magnitude in tactical operations by night.

This probable disparity in effectiveness of equipment of U.S. and communist tactical aircraft extends into adverse weather operations both by day and night. Even with the sophisticated equipment on board U.S. aircraft, the frequent references to weather problems noted in press reports, and cited in the accompanying Analysis volume on this contract indicates that weather is a major problem for the U.S. as well.

Table XIII-5 indicates combinations of visibility and weather which might be considered in an analysis, in four categories of priority A,B,C,D, with A representing highest priority.

Day/Clear Weather represents the highest priority, and the provision of an effective defense for this state denies an enemy the use of his most numerous, least expensive, and most effective (in the absence of air defense) aircraft.

### 13.5.2 Enemy Options: Aircraft, Munitions, and Delivery Tactics

Table XIII-6 indicates some of the enemy options with regard to aircraft, munitions types, and delivery

**Table XIII-3. Estimates of Costs per Sortie by Monitor Type**

| Costs | Munitions Types | | | |
|---|---|---|---|---|
| | Iron Bombs | Smart Bombs | Short Range Missiles | Intermediate Long Range Missiles |
| Munitions Cost per Pound | $0.50 | $1.50 | $5.00 | $15.00 |
| Munitions Cost per Sortie | $3,200 | $9,600 | $32,000 | $96,000 |
| Other Costs per Sortie | $8,400 | $8,400 | $8,400 | $8,400 |
| Total Cost per Sortie | $11,600 | $18,000 | $40,400 | $104,400 |

20871-628

means. Only non-nuclear munitions are considered in the present study.

All of the munitions types and delivery modes can be employed by either day fighter/bombers or all weather aircraft. However, the comments regarding the comparative numbers and costs of the two aircraft types made in the prior section apply here. The major difference in evaluation is in the requirement for night and all weather capability of the defense sensors to deal with the 'all weather' aircraft, and aircraft with night operational capability.

Priorities for analysis are based on the assumption that the first objective is to deny the enemy the use of his lowest cost munitions and most accurate delivery means. Until the last few months, stand-off missiles were a second priority on a cost-effectiveness argument, but it now appears that laser directed and image-homing missiles have attained an operational capability against small, vital targets which make them a first priority attack mode even against undefended targets.

There has been no opportunity to observe a Communist block capability with stand-off missiles in actual combat, and the assessment of the Intelligence community regarding existence or development of such a capability must be relied upon to establish a time-phasing of this threat.

It appears therefore, that each of the first priority options in Table XIII-6 must be considered in a defense analysis, with the ground rule that the attacker will use whatever munitions and delivery mode will give him the highest probability of destroying the targets he attacks at acceptable cost to him.

### 13.5.3 Enemy Tactics and Strike Size

One way of penetrating a defense effectively is to saturate it. The Eight Air Force was able to carry out daylight bombing over Germany by putting so many bombers in a raid that percent losses were acceptable even though German fighters shot down the same number of bombers whenever weather permitted them to intercept a raid. Even though antiaircraft guns inflicted about a constant percent attrition regardless of raid size, it was possible to bomb from such a high altitude that losses to antiaircraft were acceptable.

Air defense missiles may counter high altitude bombing, but the effect of saturation attacks against low altitude defenses can still be significant. The sensitive interaction between low altitude defense effectiveness and fire unit reload time has already been noted. It may be expected that enemy raids will be sized and spaced in time and space to minimize the ability of the low altitude defenses to recover and reload between attack passes of raid elements.

Table XIII-4. Computation of System Effectiveness

| | System State | Availability-Dependability AD | Assumed Capability C | ADC Element |
|---|---|---|---|---|
| Operable, Degraded Modes | All up | 0.829 | 0.50 | 0.415 |
| | Surveillance Radar | 0.019 | 0.40 | 0.008 |
| | Tracking Radar | 0.055 | 0.30 | 0.016 |
| | IFF Equipment | 0.016 | 0.10 | 0.002 |
| | Computer and Ancillaries | 0.029 | 0.04 | 0.001 |
| | Gun-laying Servos | 0.019 | 0.01 | 0.000 |
| | Power Supply | 0.001 | 0.01 | 0.000 |
| | System Inoperative | 0.032 | 0 | 0.000 |
| | Sum | | | 0.442 |

20871-629

Table XIII-5. Nature's Options

| | Clear | Low Cloud Cover | Haze | Fog | Precipitation |
|---|---|---|---|---|---|
| Day | A | A | B | D | C |
| Night | A | B | C | D | D |

20871-630

A related consideration is the size of the defended vital area, the disposition of the defending fire units, and the number of fire units comprising the defense, and the effective range of the defending weapons.

A raid may consist of a series of elements, each element consisting of two or three aircraft, with elements closely spaced in time. Considering the attacker's problem of maintaining a reasonably safe spacing of aircraft in each attack element to avoid collisions during the pass and breakaway, there is some limit to the number of aircraft which can attack simultaneously, and this limit depends somewhat on the size of the area being attacked. However, the total number of aircraft assigned to a raid is limited only by availability of aircraft and the attacker's estimate of the value of the target under attack.

A proper evaluation of defense effectiveness therefore requires a fairly extensive determination of how the effectiveness varies with the number of aircraft thrown against the defense, and their time and space sequencing.

It is suggested that the relatively limited size of the local defense envelope will make it unlikely that more than one attack element will be in it at a given time, although each element may consist of several aircraft attacking simultaneously. This simplifies the 'M on N problem' of analysis. It is also suggested that since the radius of the defense envelope is more sensitive to time of flight than to rate of fire, individual fire units should be sized to match the lower altitude boundary of the area missile defense, at lowest individual cost, and then employed in numbers allowing a one on one match of the defense against the most probable size of attack element.

### 13.5.6 Enemy Countermeasures

To minimize his losses, it can be expected that an enemy will use countermeasures of various kinds against an effective defense. These can include electronic and optical countermeasures, and direct attack

**Table XIII-6. Enemy Munitions/Attack Mode Options**

| Aircraft/Weather \ Attack Mode | Strafing | Level(2) | Bombing Glide/Dive | Laydown | Toss(1) | Missile Delivery: Guided or Image Homing | Missile Delivery: Radiation Homing |
|---|---|---|---|---|---|---|---|
| Fighter Bombers | | | | | | | |
| Day, Clear Weather | A | C | A | A | D | A | A |
| Night, Clear Weather | A | B | A | B | D | A | A |
| Inclement Weather | A | A | A | B | D | B | A |
| Helicopters | | | | | | | |
| Day, Clear Weather | A | – | | – | – | A | – |
| Night, Clear Weather | A | – | | – | – | A | |

Notes: (1) Toss Bombing is given a low priority because of its relatively low effectiveness.

(2) Level Bombing is given a relatively low priority for local defense because the aircraft is vulnerable to the area missile defenses.

20871-631

on the defense by artillery fire and aircraft launched weapons. All foreign antiaircraft, self-propelled vehicles employ some degree of armoring against artillery fragments and small arms fire. By comparison, both Vulcan and Chaparral would appear to require modifications to allow them to accompany troops to forward areas of the battlefield, and to perform their air defense function under enemy artillery fire.

Electronic and optical countermeasures have not been analyzed in the present effort, but these factors must be considered in system evaluation. It would appear from brief examination of the problem that countermeasure resistance can be more easily provided for predicted fire systems than for surface to air missile systems, but possible system degradation and means for avoiding it must be determined by analysis. The ECM evaluations should be considered as a separate set of results, and not averaged with non-ECM results via a probability estimate of how often the attacker will employ ECM.

## 13.6 DEVELOPMENT OF EFFECTIVENESS RESULTS

It is suggested that the basic defense situation might be a one-on-one engagement, in which an attack element of N aircraft attacks a vital area defended by F fire units, with $F = N$. If $N > F$, N-F aircraft are unopposed; if $N < F$, one could assume that on the average each aircraft receives fire from F/N fire units, or one could assume a one-on-one engagement with the fire units taking the advantage in the fire-reload cycle. Excursions about one-on-one can thus be done as sub-studies.

Define:

$A$ = the availability of a fire unit in the combat state.

$R$ = the average rate of fire availability, from the fire/reload model. This is the probability that a fire unit will be loaded and ready in the steady state.

$K_a$ = the probability that the attacking aircraft is destroyed before it can release its munitions.

$c_i$ = a multiplying factor on $K_a$ to account for cost to the enemy of aircraft lost from delayed damage, and for the cost to repair damage to returning aircraft.

$K_d$ = the probability that the defended vital area sustains some specified level of damage if the attack is not defeated.

For some types of attack, such a dive bombing, both $K_a$ and $K_d$ will depend on the attacker's choice of weapon release range, and the variation of outcome with this and similar attack options should be considered. With iron bombs, $K_d$ probably decreases at least as the inverse of release range squared.

Then the aircraft destroyed in each attack element before munitions release is

$$L_a = NARK_{u u_a}$$

and the effective cost to the attacker is (in equivalent aircraft numbers)

$$C_a = NARK_{u u_a C_a}.$$

The damage sustained by the defender is

$$D_d = NK_d (1 - ARK_a).$$

The result of working through a set of munitions release ranges might appear as shown in Figure 13-5, for a particular tactical/environmental set of parameters. If one assumes some maximum acceptable attrition rate for the attacker, the effect of the defense in saving ground targets is at once obtained.

Since attack modes depend on weather, it is possible to work out $C_a$ and $D_d$ for a range of weather and visibility conditions, and then average over their frequency of occurrence. However, this reduces the visibility of the results and implies that one can estimate how the attacker will weight his attack distribution with environmental conditions.

It is probably better to work out a number of curves of the type of Figure 13-5, and then exercise judgement in making a consolidated estimate. Presentation of the results might be simplified by extracting the ground target damage estimates for some specified level of enemy attrition. A brief outline of how major categories of outcomes might be organized is sketched in the following section.

## 13.7 INTERACTION OF ENEMY OPTIONS VERSUS DEFENSE CAPABILITIES

Rather than attempt to model a portion of the evaluation which depends entirely on the judgemental estimates that are made to define the tactical situation, we outline a form in which these judgemental estimates may be arranged for comparison.

We assume for this example that the attacker employs weapons, the effectiveness of which decreases with an increase in the range from which they are released. This would include iron bombs, and the simpler types of air to surface missiles. From engagement analyses, one could develop a curve of trade-offs of the probability that an aircraft is destroyed in attacking a defended site versus the probability that it will succeed in destroying the defended target. This curve might take the form shown in Figure 13-5.

Next we assume for this example that the attacker is willing to accept 5 percent attrition, and that if he releases his weapons from a corresponding range analysis indicates that they have 1/5 the capability against the ground target that they would have if he could make an unopposed attack.

The attacker is assumed to have a mixed force, consisting of aircraft depending on visual sighting, with only limited night attack capability, a smaller number of aircraft which can carry out attacks by night, and a still smaller number of expensive aircraft which can attack under all conditions of weather and visibility. It is assumed that each aircraft makes one sortie per day.

Table XIII-7 shows the assumed strike capabilities of the aircraft and Table XIII-8 shows the assumed costs and numbers.

When the defense has a night capability, it is assumed that this is as good as that of the day defense, and the same assumption is made for the all weather defense.

The assumed 5 percent attrition is, of course high, since not all targets can be defended. Similarly the attack aircraft target destruction rate is high, since not all attack aircraft will be able to find targets. However, the numbers can be considered in a relative sense, and could be replaced by good estimates after some analysis.

Results of an analysis may be arranged as in Table XIII-9.

The provision of a day defense only, according to these assumptions, saves 2/3 of the defended targets, even though the defense is never fired. The provision of a day/night defense saves 80 percent of the defended targets, and costs the attacker 75 aircraft. As Table XIII-10 indicates, the attacker might prefer to accept still lower effectiveness, and risk only his least expensive aircraft.

If the attacker restricts his operations to unfavorable weather, with greatly reduced capability, he experiences an even more unfavorable cost/effectiveness penalty if the defense also has an all weather capability.

The total number of aircraft assumed is about the same order of magnitude as the number of Soviet tactical fighter-bombers and light bombers. If only iron bombs were delivered, the munitions cost per day might be the equivalent of about \$10Xx $10^6$. However, if the attacker used standoff missiles to avoid the defenses, the munitions cost might approach

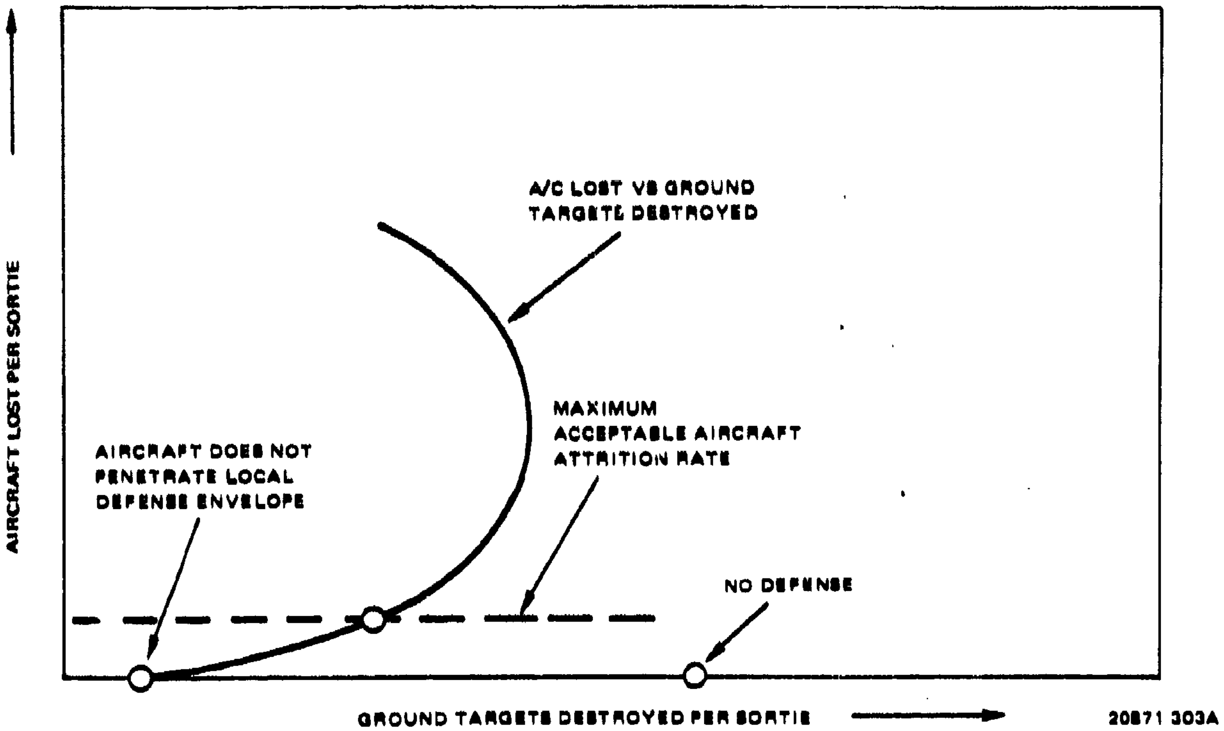


Figure 13-5. Effect of Varying Munition Release Range

\$100 x $10^6$ per day, roughly the indicated cost of lost aircraft.

Obviously, one can change the results obtained from this example widely by changing the assumptions of numbers and the estimates of capabilities. Two observations seem likely to be supportable however, even with wide changes in the assumptions. These are:

a. A defense can be effective, even though the enemy finds a way of avoiding it at reduced capability.

b. A defense can inflict an increased cost on an enemy, if he can avoid it only by using more costly weapons.

Table XIII-7. Assumed Attack Effectiveness in Kills/Sortie

| Aircraft Capability | Operational Environment | | |
|---|---|---|---|
| | Day | Night | "Inclement Weather" |
| Day+Ltd/Night | 0.5 | 0.1 | 0 |
| Night | 0.5 | 0.3 | 0 |
| All Weather | 0.5 | 0.3 | 0.2 |

20871-632

Table XIII-8. Assumed Force

| Aircraft Type | Approx Unit Cost | Assumed Number | Assumed Sorties/Day |
|---|---|---|---|
| Day+Ltd Night | $\$1 \times 10^6$ | 1000 | 1000 |
| Night | $2 \times 10^6$ | 400 | 400 |
| All Weather | $5 \times 10^6$ | 100 | 100 |

20871-633

## Table XIII-9. Interaction of Defense/Offense Options

| Defense | None | Day Defense | Day and Night Defense | | All Weather Defense |
|---|---|---|---|---|---|
| Enemy Tactics / Outcomes | Only Day Attacks | Attack by Night Only | Attack by Day or Night (1) | Attack Only in Inclement Weather | Attack Only in Inclement Weather |
| Day Aircraft | | | | | |
| Targets Destroyed | 500 | 100 | 100 | 0 | 0 |
| A/C Lost | 0 | 0 | 50 | 0 | 0 |
| Night Aircraft | | | | | |
| Targets Destroyed | 200 | 120 | 40 | 0 | 0 |
| A/C Lost | 0 | 0 | 20 | 0 | 0 |
| All Weather Aircraft | | | | | |
| Targets Destroyed | 50 | 30 | 10 | 20 | 20 |
| A/C Lost | 0 | 0 | 5 | 0 | 5 |
| Totals | | | | | |
| Targets Destroyed | 750 | 250 | 150 | 20 | 20 |
| A/C Lost | 0 | 0 | 75 | 0 | 5 |
| Cost of A/C Lost | 0 | 0 | $\$115 \times 10^6$ | 0 | $\$25 \times 10^6$ |

(1) Since attrition is the same by day or night, day attacks are assumed because of higher enemy weapons effectiveness.

20871-634

## Table XIII-10. Enemy Options Versus Day/Night Defense

| Option / Outcomes | Use Only Dayfighters | Use Day and Night Fighters | Use Whole Force |
|---|---|---|---|
| Ground Targets Destroyed | 100 | 140 | 150 |
| Aircraft Lost | 50 | 70 | 75 |
| Cost of Aircraft Lost | $\$50 \times 10^6$ | $\$90 \times 10^6$ | $\$115 \times 10^6$ |

20871-635

# SECTION 14
# USE OF PREDICTED FIRE WEAPONS AGAINST GROUND TARGETS

Air defense weapons have a secondary role in the engagement of ground targets. However, the requirements of the air defense role are so stringent that the design for air defense should not be compromised in favor of the ground role.

Once the design has been laid out for air defense, however, the requirements for ground fire may be examined, and provision made for use of the weapon in this role.

Since guns tend to have a good inherent capability against ground targets, these provisions consist principally of the provision of appropriate sighting and laying means for the weapon.

No effectiveness models are provided for ground fire in this report, since it is felt that the air defense role should be the primary determinant in weapon selection. Instead, to illustrate the kinds of situations in which the employment of antiaircraft weapons against ground targets have been important, extracts from a summary report on the operations of German flak artillery on the Russian front are provided below. Two conclusions of this summary are noteworthy: 1) the observation that air defense was weakened by diversion of flak to the ground role, and 2) the emphasis on the need to train flak troops in self defense against ground forces.

## 14.1 GERMAN EXPERIENCE ON THE EASTERN FRONT[36,37]

'During 1943, the main emphasis of the flak artillery mission in the Eastern Theater constantly fluctuated between air defense and ground operations. In 1941 and 1942, when there was little Soviet air activity, German flak units were often employed with outstanding success in direct-fire ground support, mainly against tanks. In fact, the results achieved against armored units by the flak artillery equalled, and in many cases exceeded, its achievements in air defense missions.'

'According to General Pickert, the 9th Flak Division had destroyed 600 aircraft and 826 tanks by 1 January 1943. In the Kuban bridgehead and in the Crimea this division reported 165 aircraft shot down and 189 tanks destroyed between 8 April and 10 May 1943.

'Owing to the steadily increasing Soviet armored strength, and the corresponding decline in the number of armor-piercing weapons available to the German ground forces, the Army demanded more and more flak artillery to make up for the shortage and to stave off powerful enemy attacks. But, this employment of antiaircraft artillery was really the policy of 'the poor man,' since flak batteries were taken away from their natural mission (air defense) at the very time when increasing protection against Soviet air attacks was needed by the ground forces because of the resurgence of enemy airpower. Moreover, increased protection became necessary for many vital installations not theretofore endangered which were exposed to aerial attack, especially airfields and supply depots, supply routes, bridges, and rail junctions.

'Until the winter of 1942-43 Soviet air activities had still been relatively light. Thus, astonishing as it seems, the Russian air units did nothing to interfere with traffic on the Don River at Rostov and on the only available main highway from Bataysk to Rostov during January 1943 when the German First Panzer Army and the Fourth Army were threading their way to the west from the Caucasus and the Kalmyk plains. This was a serious omission on the part of the Soviet Command.

'From the summer of 1943 on, however, the air situation changed radically. Soviet air units then began for the first time with sizeable units to attack airfields, important rail junctions in the German rear areas, and concentration areas. Flak forces in the front then tried to fulfill both their air defense mission and the direct-fire ground support mission. The main enemy was the Soviet air forces, especially the ever-dangerous ground attack units. This mission was all the more important because Soviet air units had become ever bolder in their support of the Red Army as a result of the continual decline in German fighter strength. With the decline in fighter strength the need for protection by flak units was greatly increased.

'Light and medium flak units were committed near the front, from the foremost lines back as far as artillery firing areas, while heavy flak batteries, also mobile, were placed in artillery firing areas and farther to the rear. The heavy batteries actually had a triple mission: 1) air defense, 2) supporting and augmenting regular artillery and providing air defense for it, and 3) direct-fire ground support against tanks which might break through the forward defenses. This illustrates the German efforts to compensate for their numerical weaknesses in antiaircraft artillery in the vast Soviet regions by achieving enough flexibility to make it possible to develop main areas of fire in critical defense sectors.

'Maneuverability was not absolutely essential for the performance of the second mission, which included protecting targets in the rear areas against air attack. Here it was sufficient to move flak batteries in by means of flak transport batteries.

These were units in which prime movers were consolidated specifically for the movement of artillery pieces. However, it was impossible to activate enough of these transport batteries, and because of insufficient advance knowledge about the development of situations, or in case of sudden enemy breakthroughs, the time was frequently too short to include the antiaircraft pieces in the hasty withdrawals. It was then necessary to demolish the guns and all fire control instruments and devices to prevent their capture intact. Because of inadequate available transportation space, much valuable materiel had been lost during retrograde movements, most of which had to be carried out under heavy Soviet pressure.

'The inadequate output of motor vehicles by German industry compelled a separation of the flak forces into motorized, and truck-drawn units in order to insure at least some degree of mobility, thereby also enhancing the chances for a quick concentration of forces in the front areas. As a rule, motorized units were committed in the front areas and truck-drawn units in the rear areas for the protection of static targets.

'One basic requirement for motorized flak units was all-terrain mobility. For the light and medium guns, self-propelled mounts with protective armor similar to armored personnel carriers had proven to be the most practical, for which reason they were in great demand. For the heavy (8.8-cm.) guns, the prime movers designed from them continued to be satisfactory.

'Lack of forces were the one factor which made it difficult to develop power concentrations in the air, and the necessity for a wide distribution of German air units, brought about by the increasing frequency and size of Soviet attacks against installations in rear areas, resulted in an even wider distribution of available flak batteries. In the past the rule had been to have at least one heavy flak battalion assigned for the protection of important static targets. In 1943 the number of installations requiring protection made this impossible. Thus, truck-drawn batteries in the East were reinforced with additional guns and organized into what were called twin or oversize batteries.

'Flak units lacked adequate signal facilities, which, in the course of time, had made it necessary to situate all command posts interested in the air defense of airfields in close proximity. Often it was even necessary to combine a command post.

'Heavy (motorized) flak batteries should have been issued special radio instruments so that they could have maintained contact between the battery firing positions and the artillery observers in order to keep them ready for firing at all times. An urgent need for all batteries was the issue of close-defense weapons, such as Panzerfaust antitank rockets.

'Flak trains should also have been created in order to permit a speedier shift of main emphasis in air defense. The individual air fleets did what they could to provide for this missing element by improvising flak trains with the means at their disposal. These were committed not only in the defense of static targets, but also frequently with great success in action against large partisan groups. In this connection it should be mentioned that it became absolutely essential to give flak units special training in close combat and ground defense in order to avoid heavy losses.

'By September 1943 the armies of the southern front in Russia were being withdrawn and established in their new main line of resistancee behind the Dnepr River. Strong flak and fighter forces were assigned to protect the new positions, while ground force units reorganized and reestablished their forces.

'The evacuation of airfields were particularly difficult because of the dual requirement that airfields were to be destroyed as thoroughly as possible but would be kept in operational use up to the last possible moment. For this reason, sheds, billets, shelters, signal communication and command post installations, and similar structures were demolished first. The airfields were plowed up and mined, and only one take-off and landing runway was maintained until the moment when the planes took off to transfer to another field. Frequently this last runway was not blasted until after the last aircraft had taken off and the first shells from Soviet tanks or artillery had begun to fall in the area.

'Often these last-minute demolition tasks were only possible because of defensive action by flak units which were committed to protect the airfields. After the flying units had evacuated the field, these flak units assumed a ground-defense (direct-fire) role, and maintained effective fire to halt the Russians until all demolitions were completed.'

## BIBLIOGRAPHY/REFERENCES LIST


1. Marriott, John, *Tactical Air to Surface Weapons*, International Defense Review, Vol. 3, No. 2, June 1970, p. 165.
2. Foskett, R.J., et al, *A Review of the Literature on Use of Tracer Observation as an Antiaircraft Firing Technique*, HumRRO Tech Report 68-11, September 1968, AD 675 581.
3. Weiss, H.K., *The Importance of Target Speed and Projectile Time of Flight in Antiaircraft Fire*, Ballistic Research Laboratories Report No. 716, March 1950, AD 376 933.
4. Kent, R.H., *The Probability of Hitting an Airplane as Dependent upon Errors in the Height Finder and the Director*, Ballistic Research Laboratories Report No. 127, December 1938, AD 701 865.
5. Weiss, H.K., *Analysis of World War II Air Combat Records*, BRL Report No. 727, July 1950, ATI-170 220.
6. *The Air Battle of Malta*, His Majesty's Stationery Office, London, 1944.
7. Rankine, R.R., Jr., *The Effects of Aircraft Dynamics and Pilot Performance on Tactical Weapon Delivery Accuracy*, University of California, UCLA-ENG-7085, November 1970, AD 728 324 (AFOSR TR 71/2262).
8. International Defense Review, (all issues).
9. Janes Weapons Systems, Annual, last three volumes.
10. Los Angeles Herald Examiner, Tuesday, 2 May 1972.
11. Barlow, R.E., and Proschan, F., *Mathematical Theory of Reliability*, Wiley, 1967.
12. Shooman, M.L., *Probabilistic Reliability: an Engineering Approach*, McGraw-Hill, 1968.
13. Sandler, G.H., *System Reliability Engineering*, Prentice Hall, 1963.
14. Goldman, A.S., and Slattery, T.B., *Maintainability*, Wiley, 1964.
15. Polovko, A.M., *Fundamentals of Reliability Theory*, Academic Press, 1968.
16. Dworkin, E.J., *New Methods for Predicting Electronic Reliability*, 1966, Annual Symposium on Reliability, 25-27 January 1966, IEEE Catalog No. 7, C 26, pp 552-569.
17. Morse, P.M., *Queues, Inventories and Maintenance*, Wiley, 1958.
18. Gnedenko, B.V., *The Theory of Probability*, Chelsea, 1968.
19. De Russo, P.M., Roy, R. J., Close, C.M., *State Variables for Engineers*, Wiley, New York, 1967.
20. Gantmachher, F.R., *Matrix Theory*, Vols. I and II, Chelsea, New York, 1960.
21. Andre, W., *Analytical Maintainability Models Costed and Uncosted which Consider Maintenance Ratios in Optimizing System Availability and Effectiveness*, Report MA-71-1, June 1971, Maintenance Directorate, U.S. Army Weapons Conmmand, Rock Island, Illinois, AD 726 904.
22. Engineering Design Handbook, *Maintainability Guide for Design*, HQ U.S. Army Materiel Command, July 1970, AMCP 706-134.
23. Ebenfelt, H.I., and Holmquist, Robert H., *Effectiveness Model of an Antiaircraft Fire Control System*, Proceedings of the 1970 Annual Symposium on Reliability, 3, 4, 5 February 1970, IEEE Catalog Number 70 C 2-R. Note: This is an excellent paper which contains a great deal of relevant material in addition to the availability computation extracted here.
24. Schreier, F., *The Modern Battle Tank, Part 2: Firepower*, International Defense Review, Vol. 5, No. 1, February 1972.
25. Heenan, N.I., *The State Variable Approach to System Effectiveness*, IEEE Transactions on Reliability, Vol. R-19, No. 1, February 1970, pp 24-32.
26. Engineering Design Handbook, Systems Analysis and Cost Effectiveness, AMCP 706-191, April 1971.
27. WSEIAC Reports, U.S. Air Force Systems Command, AFSC-TR-64-1, 2, 3, 4, 5, 6, January 1965.
28. Department of the Army Pamphlet No. 70-5, *Mathematics of Military Action*, Operations, and Systems.
29. Final Report, A Parametric Study of the Advanced Forward Area Air Defense Weapon System (AFAADS), Contract DAAG05-70-C-0328, submitted by Data Systems Division, Litton Systems, Inc., to U.S. Army Frankford Arsenal, 2 October 1970.

30. Bredemann, R.V., *Reliability Model of a Complex System*, Proceedings of the Tenth National Symposium on Reliability and Quality Control, Washington D.C., 7-9 January 1964, pp 156-165.

31. *Procedures and Drills for Twin 40 mm Self-Propelled Gun M42 and M42A1*, Department of Army Field Manual, FM 44-61, 25 January 1968.

32. *Air Defense Artillery Employment, Chaparrel/Vulcan*, Department of Army Field Manual, FM 44-3, 9 April 1968.

33. *Vulcan Weapon System*, Department of Army Field Manual, 44-100.

34. Scrivenor, Desmond, *Down to a Gunless Sea?*, International Defense Review, Vol. 5, No. 3, June 1972, pp 254-257.

35. Rossi, L.C., *The NA 9 Fire Control System*, Interavia 12, 1965, pp 1824-1825.

36. Plocher, Hermann, Generalleutnant, *The German Air Force vs. Russia*, 1943,; U.S.A.F Historical Division, Aerospace Studies Institute, Air University, U.S.A.F. Historical Studies No. 155, Arno Press, New York, 1968.

37. Uebe, A.D. Klaus, Generalleutnant, *Russian Reactions to German Airpower in World War II*, U.S.A.F. Historical Studies, No. 176, Arno Press, New York, 1968.

38. International Defense Review, Vol. 3, No. 1, March 1970, pp 72-74 (Description of Oerlikon Fire Units).

39. Missiles and Rockets, 22 June 1963, p. 16.

40. International Defense Review, Vol. 3, No. 3, September 1970, p. 317.

41. Littauer, R., et al, (editors), *The Air War in Indochina*, Beacon Press, Boston, 1972. This report collects a large amount of unclassified information from Congressional Hearings and other sources. The accompanying commentary is controversial.

42. Geddes, J.P., *The A-9A-Northrop's AX Entry*, Interavia, August 1972, pp 866-868.

43. Weiss, H.K., *Systems Analysis Problems of Limited War*, Annals of Reliability and Maintainability, Vol. 5, Achieving Systems Effectiveness, AIAA, New York, 18 July 1966.